Strathclyde Institute of Pharmacy and Biomedical Sciences

NOVEL GENE DELIVERY SYSTEMS

FOR BRAIN TARGETING

By

Sukrut Somani

A thesis presented in fulfilment of the requirements for the degree of Doctor of Philosophy

2015

This thesis is the result of the author's original research. It has been composed by the author and has not been previously submitted for examination which has led to the award of a degree.

Signed:

Date:

Acknowledgements

My deepest gratitude goes first to my supervisor Dr Christine Dufès whose expert guidance and support at all the stages of the PhD have made the research and learning experience a joyful journey. Her unwavering enthusiasm towards research in the field of drug delivery has inspired me to work more enthusiastically towards my research project.

I would like to thank my second supervisor Prof Gail McConnell, Dr Owain Millington, Mr David Blatchford and Ms Gillian Robb from the Centre of Biophotonics for their guidance in the epifluorescence microscopy and flow cytometry studies. I am thankful to M. Lynn Stevenson from University of Glasgow and Dr Ben Pickard for their help in the *in vivo* microscopy studies. I am pleased by the amazing people in the Lab 224, Joan, Majed, Najla, Reatul, and Stephen towards their contribution to good atmosphere in the lab.

What would be life without friends? I would like to express my gratitude to Sajjad, Serge and Molly for enriching my Glasgow experience by their warm friendship. I am thankful to Louise, Dima, Roua, Charitra and Bill in the Write Up room for an amazing working atmosphere and timely celebrations.

I would like to dedicate this thesis to my parents, grandparents, brother and members of my family for believing in me, supporting all my dreams and ambitions and for their selfless love.

Finally, I would like to express my gratitude to The Cunningham Trust for financially supporting the project, without which this thesis would not have been possible.

On a lighter note,

If we knew what it was we were doing, it would not be called research, would it? – Albert Einstein

Contents

Chapter 1 Introduction

List of Figures

Chapter 1

Chapter 3

Chapter 4

List of Tables

List of Abbreviations

AchR	Acetylcholine Receptors
ACP	Activatable Cell-penetrating Peptide
AMT	Adsorptive-Mediated Transcytosis
AJ	*Adherens* Junctions
BBB	Blood-Brain Barrier
BBMEC	Bovine Brain Microvessel Endothelial Cells
BDNF	Brain-Derived Neurotrophic Factor
bEnd.3	Murine brain endothelial cell line
bFGF	Basic Fibroblast Growth Factor
bLfc	Bovine Lactoferricin
BMVEC	Brain Microvascular Endothelial Cells
cAMP	Cyclic Adenosine Monophosphate
CMC	Critical Micelle Concentration
CNS	Central Nervous System
Colch	Colchicine
CPP	Cell-Penetrating Peptide
CTX	Chlorotoxin
D_2O	Deuterated water
DAB	Generation 3-Diaminobutyric polypropylenimine dendrimer
DAB-Ang	Angiopep-2- bearing generation 3-diaminobutyric polypropylenimine dendrimer
DAB-Lf	Lactoferrin-bearing generation 3-diaminobutyric polypropylenimine dendrimer

DAB-Lfc	Lactoferricin-bearing generation 3-diaminobutyric polypropylenimine dendrimer
DAB-Tf	Transferrin-bearing generation 3-diaminobutyric polypropylenimine dendrimer
DAPI	4’,6-diamidino-2-phenylindole
DDAO	7-hydroxy-9H-(1,3-dichloro-9,9-dimethylacridin-2-one)
DDAO-Gal	9H-(1,3-dichloro-9,9-dimethylacridin-2-one-7-yl) β-D-galactopyranoside
DMEM	Dulbecco’s Modified Eagle Medium
DMSI	Dimethylsuberimidate
DMSO	Dimethyl Sulfoxide
DNA	Deoxyribonucleic acid
DTR	Diphtheria Toxin Receptor
EDTA	Ethylenediaminetetraacetic acid,
EGF	Epidermal Growth Factor
EO	Ethylene Oxide
FACS	Fluorescence-Activated Cell Sorting
FBS	Foetal Bovine Serum
FDA	Food and Drug Administration
Fil	Filipin
GDNF	Glial-Derived Neurotrophic Factor
GFP	Green Fluorescent protein
GLUT 1	Glucose transporter 1
HIV	Human Immuno-deficiency Virus
hLfc	Human Lactoferricin
HTT	Huntingtin (Gene or protein)

JAM	Junctional Adhesion Molecules
LAT 1	L-type Amino acid Transporter
LED	Light-Emitting Diode
Lf	Lactoferrin
Lfc	Lactoferricin
LfR	Lactoferrin Receptor
LRP	Low density Lipoprotein Receptor-related Protein
mAb	Monoclonal Antibody
MDR	Multi-Drug Resistant
MRP	Multi-drug Resistance-related Protein
NMR	Nuclear Magnetic Resonance
ONPG	Ortho-nitrophenyl-β-D-galactosidase
P-gp	P-glycoprotein
PAMAM	Polyamidoamine
PBS	Phosphate Buffered Saline
PCL	Poly ε-caprolactone
pCMV	Porcine Cytomegalovirus
pCMV β-Gal	Plasmid DNA encoding β-galactosidase
PEEP	polyethyl ethylene phosphate
PEG	Polyethylene glycol
PEI	Polyethyleneimine
PhAsO	Phenylarsine Oxide
PIC	Protease Inhibitor Cocktail
PLA	Poly-Lactic Acid

PLB	Passive Lysis Buffer
PLys	Poly-L-Lysine
PMSF	Phenyl Methyl Sulfonyl Fluoride
PO	Propylene Oxide
PPE	Polyphosphoester
PPI	Polypropylenimine
RMT	Receptor Mediated Transcytosis
RNA	Ribonucleic acid
RVG	Rabies Virus Glycoprotein
siRNA	Small Interfering RNA
SPION	Superparamagnetic Iron Oxide Nanoparticles
TAT	Transactivating-Transduction
TE	Tris-Ethylenediaminetetraacetic acid
TEM	Transmission Electron Microscopy
Tf	Transferrin
TfR	Transferrin Receptor
TJ	Tight Junction
TNF	Tumour Necrosis Factor
TRAIL	Tumour necrosis factor-Related Apoptosis-Inducing Ligand
TRIS	Tris-(hydroxymethyl) aminomethane
VEGF	Vascular Endothelial Growth Factor
WHO	World Health Organization
ZO	*Zonula Occludens*

Abstract

Disorders of the central nervous system such as brain tumours, Alzheimer's disease, Parkinson's disease, Huntington's disease and others lead to a worst decline in the quality of life of patients. The possibility of using gene therapy for the treatment of these disorders is hindered due to the presence of blood-brain barrier and due to the lack of safe and efficacious gene delivery systems that can cross this barrier and express exogenous genes in global areas of the CNS.

Various receptors such as transferrin receptors, lactoferrin receptors and low-density lipoprotein receptor-related proteins 1 & 2 are widely expressed on the blood-brain barrier for the transport of endogenous molecules. These endogenous transport systems could be exploited for transport of molecules across the blood-brain barrier. In this thesis, we demonstrated the synthesis and characterization of transferrin-, lactoferrin-, lactoferricin-, Angiopep-2-bearing diaminobutyric polypropylenimine (DAB) dendrimers and evaluated their brain targeting efficiencies *in vitro* and *in vivo.*

Transferrin- and lactoferrin- bearing DAB dendriplexes led to a 2-fold and 6.4-fold increase in gene expression in the brain respectively, as compared to unconjugated DAB dendriplex after intravenous administration in mice, while decreasing the gene expression in other major organs of the body. Lactoferricin-bearing dendriplex did not show any gene expression in the brain after intravenous administration, whereas unexpected results requiring

further investigation were obtained after intravenous administration of Angiopep-2-bearing dendriplex.

CHAPTER 1

Introduction

1. Brain neoplasms and neurodegenerative disorders

Disorders of the central nervous system currently stand at the staggering 11 % of the global burden of diseases (Dominguez *et al.,* 2013). Amongst all these disorders, brain tumours and neurodegenerative disorders, such as Alzheimer's disease, Parkinson's disease and Huntington's disease, are among the most debilitating conditions of the 21st century.

1.1. Brain tumours

The term "brain tumour" refers to a collection of neoplasms, each with its own biology, prognosis and treatment. They are also scientifically known as intracranial neoplasms, since some do not arise from brain tissue (eg. meningiomas, lymphomas). According to Cancer Research UK, brain, central nervous system (CNS) and other intracranial tumours are the 9th most common cancers in the UK (2011), and 17th most common type of cancer in Europe and worldwide, with survival rates of less than 2 years in 70% of the patients. There are more than 130 different types of brain tumours. The major risk factors identified for the development of brain neoplasms include ionizing radiations, such as X-rays and CT-scans, age, metastases of other cancers (lung, breast, kidney, melanoma and colorectal cancers), genetic, family history and obesity. Currently, the most common modalities utilized for the treatment of brain tumours are surgery, radiation therapy and chemotherapy.

1.2. Alzheimer's disease

Alzheimer's disease is a neurodegenerative disease causing dementia characterized by memory loss in early stages and severe problems of communication, reasoning, orientation and hallucinations in later stages. The brain changes that lead to the development of Alzheimer's disease is the accumulation of the β-amyloid protein outside neurons (β-amyloid plaques) and accumulation of the abnormal form of tau protein in the neurons. As a result, the information transfer between the neurons fails, leading to neuronal death. The precise biological changes leading to the disease, differences in the rates of progression among individuals and ways to prevent, slow or halt the progression of the disease are yet to be found (World Alzheimer's report, 2009). In 2010, the worldwide prevalence of Alzheimer's disease was 36 million, which is forecasted to be quadrupled by 2050 (1 in 85 persons will be suffering from this disease). The major risk factors are age, gender (women are at higher risk compared to men), lifestyle (smoking, alcohol and obesity) and family history (Brookmeyer *et al*., 2007). Currently, there is no cure for Alzheimer's disease. The medicines available are to treat the symptoms and to slow down the progression temporarily.

1.3. Parkinson's disease

Parkinson's disease is the second most common progressive neurodegenerative disorder characterized by both motor and non-motor symptoms. People suffering from Parkinson's disease display rest tremor, rigidity, bradykinesia and stooping posture. Neuropsychiatric symptoms

include depression, anxiety, dementia and mood disturbances. The pathophysiology of Parkinson's disease demonstrates loss or degeneration of the dopaminergic neurons and development of Lewy bodies in dopaminergic neurons. The major risk factors include ageing, genetic inheritance, pesticide exposure and environmental chemicals, such as polychlorinated biphenyls, lead and manganese. However, the ultimate cause that leads to Parkinson's disease is still unknown. Parkinson's disease worldwide affects an estimated 7-10 million people with a predicted increase in the prevalence in the future. Treatments include reduction of the motor symptoms by drug therapy utilizing dopamine alternatives (carbidopa, levodopa or dopamine receptor agonists) and surgical therapies (deep brain stimulation) (Beitz, 2014). In the last decade, number of genetic mutations leading to the sporadic Parkinson's disease has been identified (Davie, 2008).

1.4. Huntington's disease

Huntington's disease is an autosomal dominant, fully penetrant, progressive neurodegenerative disease, leading to disability and untimely death of the patient. Early symptoms of the disease include involuntary movements of the body parts, like quick, sudden, jerking movements of the arms, legs, face and other body parts, impaired balance and unsteady gait. It is caused by the cytosine-adenine-guanine trinucleotide repeat expansion in the huntingtin (HTT) gene that leads to the expanded polyglutamine stretch in the HTT protein. This defective protein damages the brain cells by mechanisms that

are not fully understood yet. The prevalence of Huntington's disease is relatively rare with 4-8 cases per 100,000 people. Currently, there is no cure available for Huntington's disease. The treatments available are to reduce the severity of some of the symptoms (Ross and Tabrizi, 2011, Gudesblatt and Tarsy, 2011).

2. The Blood-brain barrier

The blood-brain barrier (BBB) is a unique extracellular fluid environment within the central nervous system, allowing a precise control of its composition (Figure 1.1). The BBB is the key regulating site for drug access to the brain due to its large surface area and short diffusion distances from capillaries to neurons (typically less than10-15 um) (Schlageter *et al.*, 1999). It also acts as an entrance gateway for various nutrients to the brain and also protects it from potentially toxic compounds. The barrier function of BBB is a combination of physical barrier, transport barrier and metabolic barrier (Abbott & Romero, 1996). Although the multi-tasking BBB has played an essential role in the development of CNS as a complex integrated network, it poses a major problem for treatment strategies that require the delivery of drugs and other therapeutic molecules to the brain for the treatment of CNS disorders. The low and selective permeability of BBB can be credited to its unique biological properties:

(a) the lack of fenestrations, vesicular transport and pinocytosis in the endothelial cells (Stewart, 2000; Abbott, 2005)

(b) the physical barrier created by tight junctions between adjacent endothelial cells (Persidsky *et al.*, 2006)

(c) the transport barriers created by expression of various transporters including Glucose transporter 1 (GLUT 1) glucose carrier, L-type amino acid transporter (LAT1), transferrin receptors, insulin receptors, lipoprotein receptors and ATP family of efflux transporters such as P-glycoprotein (P-gp) and the multidrug resistance-related proteins (MRP). These transporters and receptors carry only specific molecules to the brain (Abbott *et al.*, 2006).

(d) the enzymatic barrier of degrading enzymes (γ-glutamyltranspeptidase, alkaline phosphatase) localized in the endothelial cells.

2.1. Cellular components

The BBB consists of various components that functionally make a neuro-vascular unit performing as a barrier.

2.1.1. Endothelial cells

Brain microvascular endothelial cells (BMVECs) are positioned at the interface between the blood and the brain (Figure 1.1). The endothelial cells lining the cerebral capillaries differ from the other vascular endothelium in their ability to control the movement of molecules and cells to and from the neural parenchyma (Ge *et al.*, 2005; Weksler *et al.*, 2005). The cerebral microvessels are 50-100 times tighter than peripheral microvessels leading

to severe restriction of the paracellular pathway for diffusion of hydrophilic solutes (Abbott, 2002).

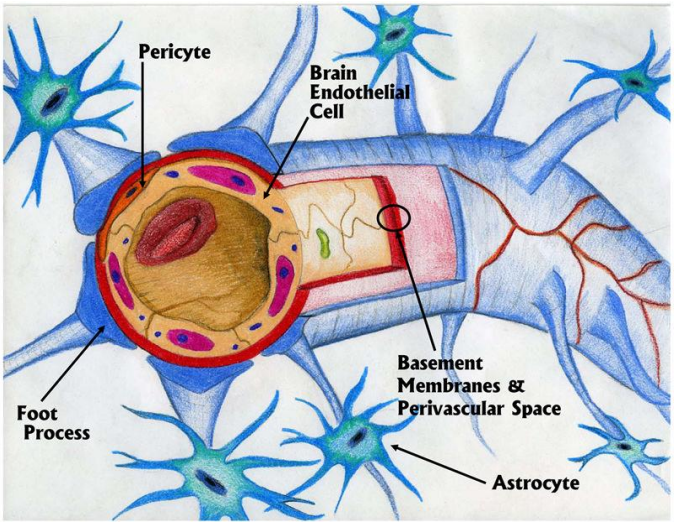

Figure 1.1 The Blood-brain barrier, or the neurovascular unit, showing endothelial cells, pericytes and astrocytes (Carvey, 2009)

Thus, they act as a barrier and also perform various functions such as the transport of nutrients, receptor-mediated signalling, leukocyte trafficking and osmoregulation (Persidsky *et al.*, 2006). These unique properties of the endothelial cells are due to their various structural elements:

(1) Tight junctions formed by various proteins like occludins, claudins and *zonula occludens*

(2) *Adherens* junctions composed of cadherins, catenins, vinculin and actinin

(3) Junctional adhesion molecules (Doolittle *et al.*, 2005).

The cytoplasm of endothelial cells of the brain has uniform thickness, no fenestrations, low pinocytic activity and a continuous basement membrane

(De Boer & Gaillard, 2006; Wong *et al.*, 2012). Endothelial cells of brain capillaries have larger volume and number of mitochondria than the endothelial cells of other parts of the body, that maintain ion differentials between blood plasma and brain extracellular fluid and also retain the unique structural characteristics of CNS capillaries. This facilitates the active transport of nutrients to the brain (Persidsky *et al.*, 2006; Cardoso *et al.*, 2010).

BMVECs also act as an enzymatic barrier that includes γ-glutamyl transpeptidase, alkaline phosphatase and aromatic acid decarboxylase. The concentration of these enzymes is higher in cerebral capillaries compared to the non-neuronal vessels. They are capable of metabolizing various drugs and nutrients (Pardridge, 2005).

The endothelial cells at the BBB have distinctive pattern of receptors and specific transport systems that facilitate the uptake of essential nutrients and hormones to facilitate brain homeostasis. Amongst the transporters, GLUT1 is of particular importance because glucose is the main energy source of the brain (Wolburg *et al.*, 2009). An important efflux transporter on the BBB is P-gp, which is an ATP-binding cassette transporter, is present on the apical surface of the endothelial cells. It is responsible for the active extrusion of non-polar molecules out of the endothelial cells (Ramakrishnan, 2003).

2.1.2. Astrocytes

The ability of endothelial cells to form a barrier depends on the neural environment in which they grow (Stewart and Wiley, 1981). Astrocytes/Astroglia encircle more than 99% of the microvascular endothelial cells of the BBB (Persidsky *et al.*, 2006). They play an important role in the development of unique brain microvascular endothelial cell phenotype which leads to its unique characteristic to function as a barrier (Hayashi *et al.*, 1997). The astrocytes induce and modulate many BBB features and their interaction with endothelial cells during biogenesis leads to the formation of tight junctions (Dehouck *et al.*, 1990; Rubin *et al.*, 1991).

In an *in vitro* study it was observed that enhanced tight junctions with markedly increased length, breadth and complexity, were observed in brain endothelial cells cultured with astrocytes as compared to endothelial cells alone (Tao-Cheng *et al*., 1987). Astrocyte-derived factors and second messenger levels, such as cyclic adenosine monophosphate (cAMP) levels, are found to be extremely important modulators in maintaining the functionality of BBB tight junctions (Wolburg *et al.*, 1994). Thus, astrocytes are believed to provide inductive influence to the endothelial cells of brain tissues, making them less leaky (Janzer & Raff, 1987).

Astrocytes play an important role in enhancing the trans-endothelial electrical resistance which is necessary for reducing cell permeability and tight junction organization (Rubin *et al.*, 1991). They are essential for adequate neuronal

function, and the close proximity of neuronal cell bodies to brain capillaries suggests that astrocytes-BMVEC interactions are crucial for a functional neurovascular unit (Abbott *et al.*, 2006).

2.1.3. Pericytes

Pericytes are polymorphic, elongated, multibranched peri-endothelial cells that vary in their degree of envelopment of endothelial cells in the vasculature (Shepro & Morel 1993). Pericytes show elevated contents of muscle and non-muscle actin (Herman & D'Amore, 1985), highlighting the contractile ability of pericytes both *in vitro* (Kelley *et al.*, 1987; Shepro & Morel, 1993) and *in vivo* (Peppiatt *et al.*, 2006).

The physical contacts between pericytes' cellular processes and the inter-endothelial junctions predict their role in maintaining the capillary diameter, ultimately leading to the control of blood flow (Peppiatt *et al.*, 2006), as well as in regulating the tight junction permeability (Edelman *et al.*, 2006).

Pericytes play specific roles in various angiogenesis and vascular endothelial barrier systems. *In vitro* studies demonstrated that endothelial cells associated with pericytes are more resistant to apoptosis than the isolated endothelial cells. This supports the role of pericytes on the structural integrity and genesis of the BBB (Ramsauer *et al.*, 2002).

Pericytes also contribute to the expression, maintenance and regulation of BBB properties (Lai & Kuo, 2005). A BBB co-culture of brain endothelial cells with pericytes supported the pericytes-induced up-regulation of the barrier property of the BBB (Dohgu *et al.*, 2005) .

2.2. Intercellular junctions

The stabilization of the BMVECs lining at the BBB occurs by specialized cell junctions between adjacent cells, tight junctions and *adherens* junctions and the signalling pathways involved in the regulation of their assembly.

2.2.1. Tight Junctions

Tight Junctions (TJ) are the major structures responsible for the barrier properties. They are located on the apical region of endothelial cells. They act as a seal, and control paracellular diffusion between the apical and basolateral plasma membrane (Figure 1.2 A) (Ge *et al.*, 2005; Hawkins & Davis, 2005; Cardoso *et al.*, 2010). They form an intricate complex of parallel, interconnected, trans-membrane and cytoplasmic strands of proteins arranged as a series of multiple barriers (Cardoso *et al.*, 2010). The TJ are composed of integral proteins (proteins permanently bound with the biological membrane), such as claudin, occludin and junctional adhesion molecules (JAM), and anchoring proteins such as *zonula occludens* (Persidsky *et al.*, 2006).

Claudin is a tight junction molecule weighing 20-24 kDa which establishes barrier properties and is responsible for permeability restriction (Morita & Furuse, 1999; Tsukita & Furuse, 1999; Tsukita *et al.*, 1999; Wolburg *et al.*, 2009).

Occludin is a highly expressed protein in BMVEC weighing 65-KDa and detected consistently along the cell margins (Wolburg & Lippoldt 2002; Hawkins & Davis 2005). High levels of occludin lead to decreased paracellular permeability (Huber *et al.*, 2001) and increased electrical resistance (Persidsky *et al.*, 2006), thus having an active role in BBB function (Yamamoto *et al.*, 2008).

Junctional adhesion molecules (JAMs) are 40-KDa proteins (JAM-1, JAM-2 & JAM-3) of the IgG superfamily (Persidsky *et al.*, 2006). They play an important role in developmental processes and also regulate the trans-endothelial migration of the leukocytes. The functions of JAMs are currently unknown in the mature BBB (Cardoso *et al.*, 2010).

Cytoplasmic proteins or anchoring proteins such as *Zonula Occludens* (ZO) proteins (ZO-1, ZO-2 and ZO-3) function as recognition proteins for TJ placement and as a support structure for signal transduction proteins (Huber *et al.*, 2001). Loss of ZO-1 from the junctional complexes leads to increased BBB permeability (Choi & Kim, 2008).

2.2.2. *Adherens* Junctions

Adherens Junctions (AJ) are located in the basal region of the lateral plasma membrane below the TJ (Figure 1.2 B). They are composed of trans-membrane glycoproteins linked to the cytoskeleton by cytoplasmic proteins, giving place to the adhesion belts (Cardoso *et al.*, 2010). They are responsible for the adhesion of the BMVEC to each other, giving rise to continuous adhesion belt (Petty & Lo, 2002), the initiation of cell polarity, regulation of paracellular permeability and thus contribute to the barrier function (Hawkins & Davis 2005; Carvey 2009) . AJ are constituted by cadherins and catenins (Perrière *et al.*, 2007).

Cadherins have cell-type specificity. Vascular endothelial VE-cadherin (cadherin-5), an integral membrane glycoprotein, is expressed exclusively in cells of vascular epithelial origin whereas neural (N)-cadherin is found in the cells of the nervous tissue, vascular smooth muscle cells and myocytes (Navarro *et al.*, 1998). It determines microvascular integrity both *in vitro* and *in vivo* (Vorbrodt & Dobrogowska, 2003). It mediates Ca^{2+}-dependent cell-cell adhesion, inhibits cell proliferation and decreases cell permeability (Cook *et al.*, 2008).

Catenins have a major role in anchoring cadherin complex to the actin cytoskeleton (Stamatovic *et al.*, 2008). Four types of catenins have been identified: α-, β-, δ- and γ- catenins. α- and β- catenins are expressed at inter-endothelial junctions of BBB type brain capillaries and are prime

requisite for cadherins to work as adhesion molecules (Vorbrodt *et al.*, 2008; Cook *et al.*, 2008).

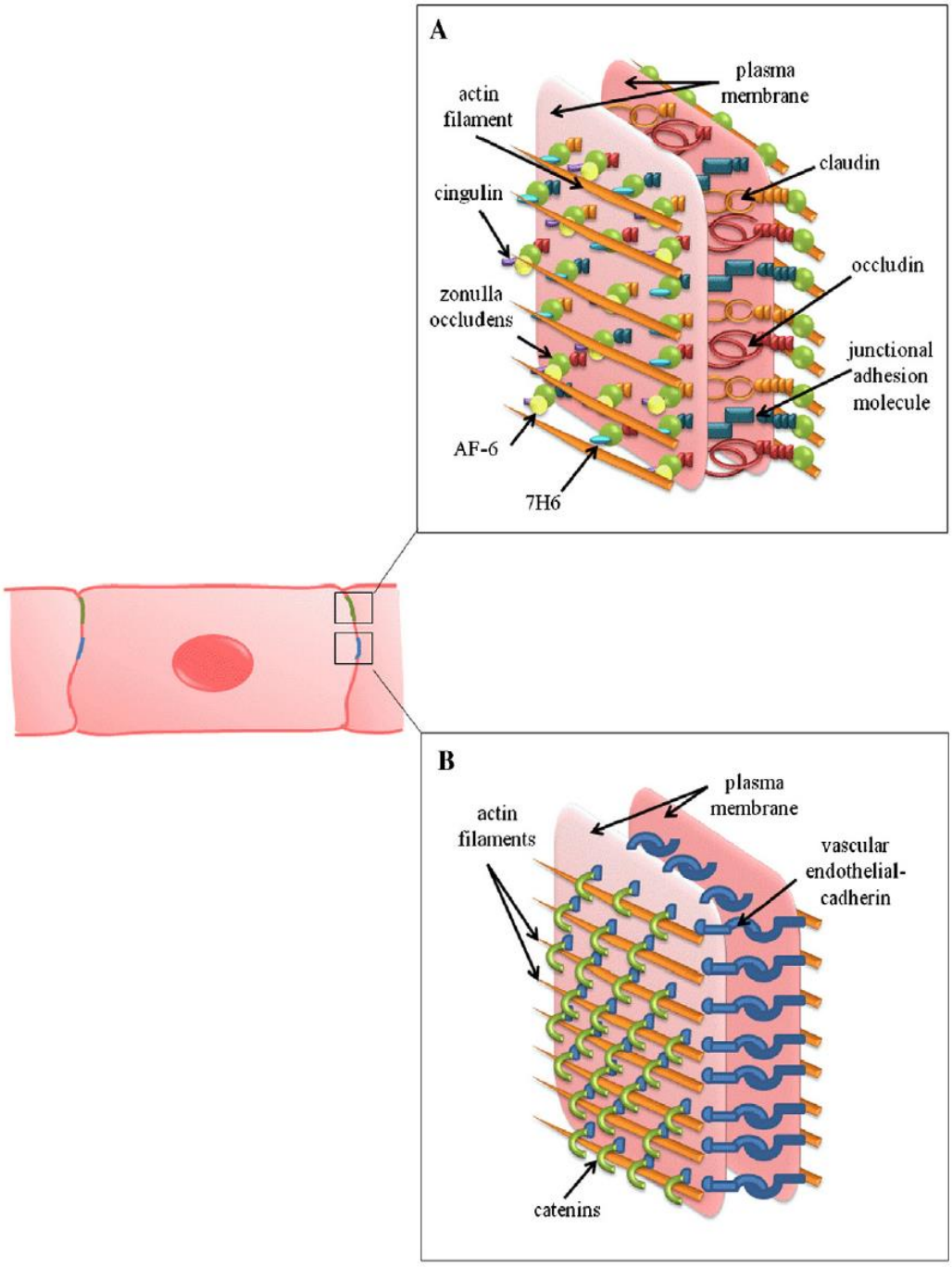

Figure 1.2 The endothelial cells at the BBB present tight junctions (TJ) (A) and *adherens* junctions (AJ) (B) (Cardoso *et al.*, 2010).

2.3. Transport mechanisms

The following organisational chart shows different transport mechanisms across the BBB that regulate the movement of various endogenous and exogenous substances across the BBB (Fig. 3).

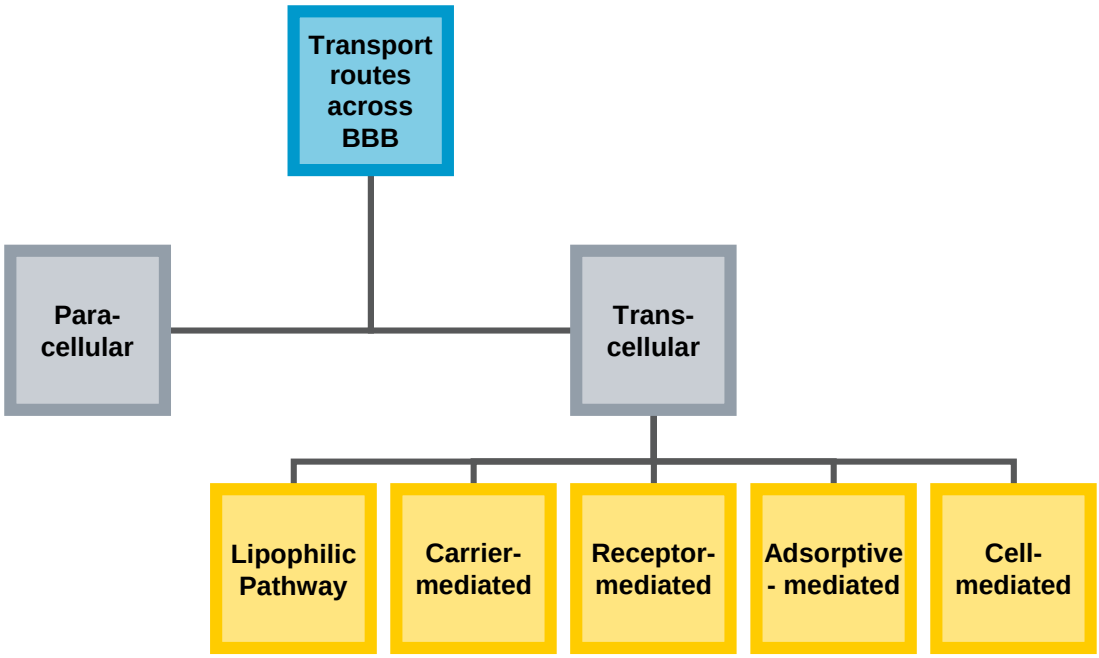

Figure 1.3 Different categories of transport across the BBB

2.3.1. Paracellular pathway

Small water-soluble molecules can diffuse through the tight junctions between the endothelial cells to a very low extent (Figure 1.4). This process is mediated through passive molecular diffusion from higher concentration to lower concentration (Chen & Liu, 2012).

2.3.2. Trans-cellular pathway

2.3.2.1. Lipophilic pathway

Small lipid-soluble substances can dissolve in the lipid plasma membrane of the brain capillary endothelial cells and penetrate through it. It is the case, for example, for alcohols and steroid hormones. (Figure 1.4) (Chen & Liu, 2012).

2.3.2.2. Carrier-mediated transport

Solutes such as glucose and amino acids can bind to a protein transporter on one side, which leads to conformational changes in the protein, resulting in the transport of the solutes to the other side of the membrane, according to the concentration gradient (Figure 1.4). If compounds need to be transported against the concentration gradient, ATP provides energy to allow this process (Chen & Liu, 2012). GLUT1 is expressed on the BBB that continuously maintains optimal levels of glucose in the CNS for its adequate functioning (Pardridge *et al*., 1990; McAllister *et al*., 2001). The transport of large amino acids that play an important role in brain amino acid metabolism, neurotransmitter synthesis and protein synthesis occurs through large amino acid transporters that are expressed on the endothelial cells of the BBB (Boado *et al*., 1999).

2.3.2.3. Receptor-mediated transcytosis

Receptor-mediated transcytosis (RMT) provides a means for selective uptake of macromolecules. Endothelial cells have receptors, such as transferrin receptors (TfR), insulin receptors and low density lipoprotein receptor-related

proteins (LRP 1 & 2), scavenger receptors class B type 1, diphtheria toxin receptors (DTR) and glutathione transporters for the selective uptake of many different types of ligands, including growth factors, enzymes and plasma proteins (Rip *et al*., 2009). Macromolecules bind to receptors in specialized areas of plasma membrane. Following this binding, the macromolecules invaginate into the cytoplasm to form endosomes. After acidification of the endosomes, the ligand will dissociate from the receptor and cross the other side of the membrane (Figure 1.4). RMT is being intensely studied for brain targeting (Shi & Pardridge 2000; Pardridge, 2005).

2.3.2.4. Absorptive-mediated transcytosis

Adsorptive-mediated transcytosis (AMT) is triggered by electrostatic interactions between the positively charged moieties of the proteins and negatively charged membrane surface regions (glycocalyx) on the brain endothelial cells. AMT-based drug delivery was performed using cationic proteins and cell-penetrating peptides, such as Tat-derived peptides and Syn-B vectors (Figure 1.4). It has high capacity compared to RMT, but has several limitations such as toxicity and immunogenicity (Hervé *et al*., 2008).

2.3.2.5. Cell-mediated transport

Since brain is under a constant immunological surveillance, cells of the innate immune system can be used as transporters of drugs to CNS. Cell-mediated transcytosis relies on immune cells, such as monocytes, to cross the BBB.

Serotonin, when conjugated to negatively charged liposomes, can actively cross the BBB with the help of circulating monocytes (Afergan *et al*., 2008).

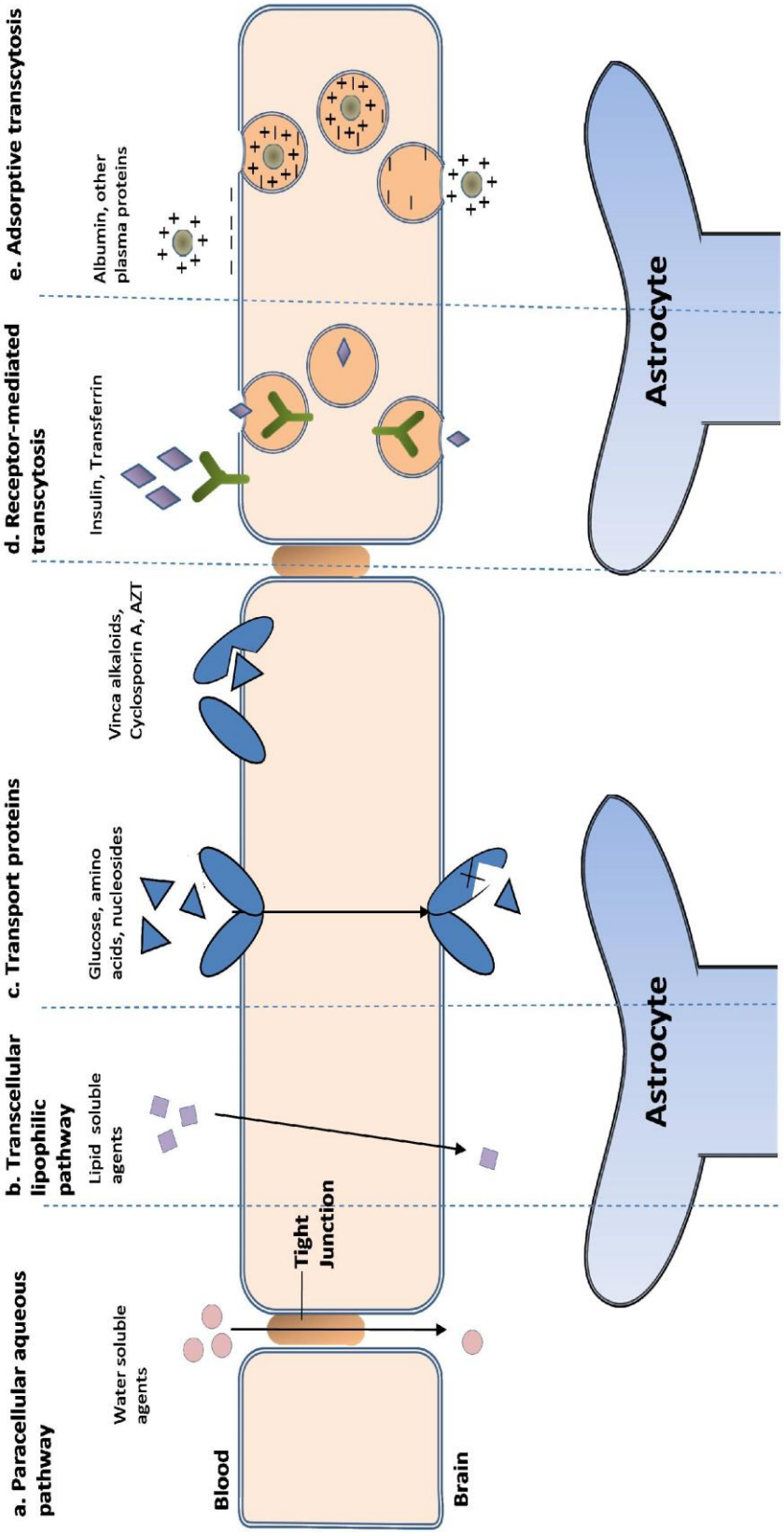

Figure 1.4 Transport routes across the BBB (adapted from Chen & Liu, 2012)

2.4. BBB under pathological conditions

The natural properties of the BBB neurovascular unit change under the pathological state of neurological disorders. Disorders such as cerebral ischemia and hypoxia lead to interference of blood flow to the brain, leading to the increase in BBB permeability. Inflammation of the neurons caused by various diseases such as Alzheimer's disease, multiple sclerosis, also leads to TJ opening and BBB disruption (Persidsky *et al*., 2006). The neurovascular unit is also compromised in brain tumours. There is functional reduction of endothelial tight junctions and overexpression of various receptors, such as folate, insulin and transferrin receptors, leading to increased permeability of the BBB (Doi *et al*., 2008; Maeda *et al*., 2009).

2.4.1. Changes in tight junctions and BBB permeability

The permeability of the BBB is highly influenced by the stimuli produced by physiological and pathological conditions, such as oxidative stress (nitric oxide, hydrogen peroxide), inflammatory mediators (interleukins, interferons), vasogenic agents (histamine, vascular endothelial growth factor), infective agents (bacteria, viruses, parasites, fungi), as well as physiological stimuli (intercellular Ca^{2+}) and immunological stimuli (leukocytes) (Stamatovic *et al*., 2008; Deli, 2009). There is strong evidence that BBB integrity is compromised, leading to higher permeability in disorders such as stroke, Alzheimer's disease, multiple sclerosis, Human immuno-deficiency virus (HIV), Parkinson's disease and brain tumours (Huber *et al*., 2001; Abbott *et al*., 2006; Holman *et al*., 2011).

In patients suffering from Alzheimer's disease, BBB disruption can be directly related to the increased rate of neurodegeneration. Activated astrocytes and microglial cells stimulated by the β-amyloid plaques lead to production of pro-inflammatory factors (McGeer *et al*., 2005). The deposition of neurotoxic β-amyloid on microvessels leads to the apoptosis of the BMVECs and to a compromised neurovascular unit. In addition, hyperhomocysteinemia (increased homocysteine in blood) leads to an increased filtration of peripheral immunoglobulin G (IgG) and neuroinflammation (Zlokovic, 2002; Zlokovic, 2008). Although the BBB impairment may be used for improved drug delivery and treatment, in Alzheimer's disease, however, restoring BBB integrity is more important. This is due to the fact that BBB impairment is directly proportional to neurodegeneration (Chen & Liu, 2012).

In diseases like Parkinson's disease and epileptic seizures, an increase in BBB permeability is observed due to neuroinflammation as a response to phagocyte activation, activation of microglia, increased synthesis and release of pro-inflammatory cytokines and release of reactive oxygen species (Whitton, 2007; Chung *et al*., 2010). In brain tumours, expression of tight junction proteins claudin 1 and claudin 5 was significantly down-regulated or lost, leading to a morphological change in the TJ and an increased BBB permeability (Liebner *et al*., 2000). The secretion of Vascular endothelial growth factor (VEGF), other growth factors and cytokines by the tumours, leads to the formation of blood vessels lacking tight junctions, further

resulting in TJ downregulation (Berkmann *et al.,* 1993, Plate *et al* 1993, Sato *et al*., 1994; Lamszus *et al*., 1999).

2.4.2. Changes in transport system

Under pathological conditions, the expression of various transporters P-gp, and processes like AMT and RMT drastically change.

P-gp is a member of the ATP-binding cassette superfamily of the multidrug resistant transporter (MDR) expressed on both luminal and abluminal sides of the BBB, where it functions as an efflux transporter. It plays a crucial role in preventing the entry of drugs and toxins in CNS and confers drug resistance by active ATP-dependent extrusion of xenobiotics from cells (Lee & Bendayan, 2004). In Alzheimer's disease, there is an inverse correlation between the expression of the P-gp transporter and deposition of β-amyloid plaques (Cirrito *et al*., 2005). Kortekas and colleagues (2005) demonstrated the decreased functional activity of P-gp in the brain of the patients with Parkinson's disease. The brain uptake of [^{11}C]-verapamil, which was normally extruded from brain by P-gp, was elevated in Parkinson's disease. The expression of P-gp varies in different types of brain tumours. Schwannomas and brain metastases from other cancers show a lower expression of P-gp compared to normal brain tissue. The levels of P-gp expression in malignant brain tumours, including both low-grade and high-grade gliomas, were similar to that of the normal brain, and meningiomas showed 7-10 times more P-gp expression (Demeule *et al*., 2001).

Variations in AMT and RMT have also been observed in BBB during pathological states. It has been shown that there is an increase in AMT in CNS disorders due to secretion of various inflammatory mediators (Chen & Liu, 2012). RMT is an important pathway for the transport of endogenous molecules, such as insulin, insulin-like growth factor, transferrin and lactoferrin (Roberts *et al*., 1993; Fillebeen *et al*., 1999). Various receptors on the BBB include TfR, insulin receptors, LRP1, LRP2 and DTR.

TfR, the most widely characterized receptor on BBB, mediates the transcytosis of transferrin-bound iron through BMVEC (Connor & Menzies, 1995). Its expression is decreased in cerebral inflammation, which occurs in neurodegenerative diseases such as Parkinson's disease and Alzheimer's disease. A transient reduction in TfR leads to decreased supply of iron to CNS, ultimately leading to neural dysfunction. Brain neoplasms demonstrate increased angiogenesis and proliferation that needs increased iron uptake through TfR. Tumour cells therefore show increased expression of TfR (Leitner & Connor, 2012). Insulin receptors are important for the regulation of the glucose metabolism in brain. Their expression is also altered in neurodegenerative diseases such as Alzheimer's disease. It was observed that insulin receptors are over-expressed in elderly individuals with Alzheimer's disease as compared to the controls of the same age group (Frölich *et al*., 1998). Low-density lipoprotein receptor (LDLR), LRP 1 and LRP 2, inhibit inflammatory process. Most diseases involving the process of inflammation, such as Alzheimer's disease and Parkinson's disease, affect

their expression. DTR is reported to be upregulated in many inflammatory conditions (Gaillard *et al*., 2005).

It can therefore be concluded that, while designing a delivery system for carrying drugs to brain, the impact of the diseases on the transport system should be taken into account. If the receptors are upregulated in a specific disease, there will be higher RMT, leading to higher intake of drugs into the brain.

2.4.3. Leukocyte trafficking

A number of neurodegenerative disorders cause CNS inflammation, which leads to the breakdown of BBB and causes increased migration of some immune cells such as leucocytes, including monocytes and macrophages (Huang *et al*., 2006). In brain tumours, histological analysis showed high levels of macrophage infiltration (Levy *et al*., 1972). It has been suggested that leucocytes naturally accumulate in the brain during pathology as part of the immune defence mechanism (Persidsky *et al*., 2006).

3. Strategies used to deliver therapeutics across the BBB

Rapid advances in the field of molecular biology have propelled the development of novel drug delivery systems. With a better understanding of BBB and brain disorders, the modern approaches utilize a multi-disciplinary

approach combining biology, nanotechnology and biophysics with a common goal of successful drug delivery to the brain.

3.1. Tight junctions opening

The emerging knowledge of the molecules involved in TJ and the discovery of modulators that can be used to temporary open the TJ and disrupt the BBB have been used as a strategy for drug transport to the brain. Various physical, chemical and biological stimuli can be used to modulate tight junctions.

Ultrasounds and microwaves have been widely researched as physical stimuli for the disruption of the tight junctions of the BBB. Ultrasounds were used as a diagnostic tool for many years. Due to the recent developments in the acoustics, focused ultrasounds can be used to concentrate acoustic energy at one focal spot deep in the body with minimal effect on the near-field tissue (Vykhodtseva *et al*., 2008). It was demonstrated that low power focused ultrasounds applied after the intravenous administration of the ultrasound contrast agent lead to consistent opening of the BBB without damaging the CNS tissue (Hynynen *et al*., 2001). Microwave energy has also been studied for the transport of drugs to the CNS. It leads to the reversible opening of the BBB TJ via microwave-induced hyperthermia (Chen & Liu, 2012).

There are various materials used as chemical stimuli for the modulation of the TJ and for the increase of the BBB permeability. It was observed that an intracarotid infusion of oleic acid, as well as sodium dodecyl sulphate, increased BBB permeability in a dose- dependent reversible manner (Sztriha & Betz, 1991; Saija *et al*., 1997). Most of the materials use intracarotid or arterial infusion for the BBB opening, which is considered as a highly invasive technique and requires expertise. In an *in vitro* model, it has been shown that cyclodextrins (α-, β-, and γ-) increase the BBB permeability by extracting the lipids from the plasma membrane (Monnaert *et al*., 2004). But no *in vivo* studies have been performed yet to determine the action of cyclodextrins on BBB.

Many biological compounds like Cereport™ (RMP-7) and some viruses can act on the TJ, leading to their opening and enhancement of the delivery of drugs to CNS. Cereport™ (RMP-7) is a selective bradykinin receptor agonist that increases the permeability of the BBB. It was shown to increase the delivery of chemotherapeutic agents to brain tumours (Emerich *et al*., 1999). Various viruses upregulate the chemokines that act as precursors to the infiltration of the immune cells in the CNS, and thus open the BBB (Kuang *et al*., 2009). The viruses used as biological stimuli for opening the BBB include the west-Nile virus and adeno-associated virus (Chen & Liu, 2012).

3.2. Drug delivery utilizing nanocarriers

Nanocarriers are entities in the size range of 10-1000 nm. They are used as vehicles for drug delivery to the targeted organs of the body, including brain. For drug delivery to the CNS, nanocarriers should ideally have the following characteristics (Bhaskar *et al.,* 2010):

- Particle size less than 100 nm
- Stable in blood (no degradation by proteins)
- No immune or inflammatory response
- Non-toxic, biodegradable and biocompatible
- CNS-targeted (use of targeting ligands, cell surface and receptor-mediated endocytosis)
- Easy scale-up in manufacturing process and cost effective
- Easily conjugated to small molecules, peptides, proteins and genes
- Bypass the reticulo-endothelial system
- Prolonged circulation time

Nano-carriers are unique due to their size, as well as due to the materials used to synthesize them. They are able to carry increased drug payload and to control its release. In addition, they can be loaded with a range of therapeutics, from small molecules to proteins and therapeutic genes. It has been possible to modify their surface characteristics for targeting and controlled release. Although various nanomaterials have been developed in the last decade, the most investigated nano-carriers for CNS targeting are liposomes and polymeric nano-particles (Garcia-Garcia *et al*., 2005).

Dendrimers have emerged as a new class of nanoparticles that are being studied for brain targeting. PEGylated liposomes carrying doxorubicin have already completed clinical trial Phase 2 for the treatment of glioma and have shown promising results. Brigger and colleagues (2002) used PEG-coated hexadecylcyanoacrylate nanospheres in a gliosarcoma model and showed that these nanoparticles exhibited retention in tumour tissue with satisfactory pharmacokinetic profile (Brigger *et al*., 2002). A polyamidoamine (PAMAM) dendrimer-based nano-carrier with dual targeting ligands on the surface and a drug inside the dendritic box was reported to cross the BBB and deliver the therapeutic drug to the tumour site. The targeting moieties used were transferrin and thiolated wheat germ agglutinin (He *et al*., 2011).

3.3. Drug delivery via Adsorptive-mediated transcytosis

AMT has emerged as a growing strategy for the transport of the drugs due to the fact that there are electrostatic interactions between the cationic moieties and negative charges of the plasma membrane. This leads to binding of cationic molecules, such as cationic proteins and cell-penetrating peptides (CPP), on the luminal side of the endothelial cells and exocytosis on the abluminal side (Hervé *et al*., 2008).

The transactivating-transduction (TAT) is the trans-activating protein of HIV type-1 and one of the cell-penetrating peptides investigated widely. TAT demonstrated that it can cross the BBB and accumulate in the CNS (Banks, 2012). TAT-modified cholesterol was utilized to formulate a liposome (TAT-

LIP) for enhanced brain delivery. TAT-LIP demonstrated improved uptake compared to the unmodified liposome *in vitro* and *in vivo*. Moreover, the mechanism of transport of TAT-LIP was confirmed as AMT (Qin *et al*., 2011). Ciprofloxacin-loaded polymeric micelles decorated by TAT molecules on the surface were able to cross the BBB. The TAT-conjugated micelles can be further investigated for the delivery of antibiotics to the brain for the treatment of brain infections (Liu *et al*., 2008).

The pegelin and penetratin peptides efficiently traverse the biological membranes and have provided the basis for the development of new peptide-conjugated drugs for transport through the BBB. Pegelin (SynB) and penetratin peptides belong to the family of CPP and successfully demonstrated the enhanced delivery of doxorubicin to the brain, which normally cannot cross the BBB. The CNS uptake of doxorubicin was enhanced by an average of 6 times when it was coupled to pegelin or penetratin compared to free doxorubicin (Rousselle *et al*., 2000). To further study this strategy, the same group coupled the enkephalin analog dalargin to SynB vector and demonstrated a significant enhancement in the brain uptake and analgesic activity of the drug (Rousselle *et al*., 2003).

AMT thus enables many poorly brain-penetrating drugs across the brain and holds potential for drug delivery to the brain, but the toxicity and the immunogenicity associated with the cationic proteins should be taken into

account (Saar *et al*., 2005; Lu *et al*., 2007). Moreover, AMT is a non-specific process, thus targeting capillaries of other organs along with the BBB.

3.4. Drug delivery via Receptor-mediated transcytosis

One of the biggest shortcomings of AMT is its lack of specificity. However, various receptors are expressed on the endothelial cells forming the BBB. These molecules can transport specific molecules across the BBB, thus facilitating active targeting of the BBB. RMT is also termed as “Trojan Horse Approach”. This approach exploits the binding of the drug conjugate to physiological transport receptor on the BBB, transports and delivers the drug to the brain. RMT occurs in 3 steps (Gabathuler, 2010):

1. Endocytosis of the compound through receptor at the luminal side
2. Movement across the endothelial cell cytoplasm
3. Exocytosis of the compound on the abluminal side

There are various receptors expressed on the brain capillary endothelial cells. These include insulin receptors, TfR, LRP1, LRP2 and DTR. Drug delivery through these receptors has been widely investigated.

3.4.1. Insulin Receptor

RMT via insulin receptor has been extensively studied for drug delivery. Using avidin-biotin technology, a peptide radiopharmaceutical was conjugated to a monoclonal antibody against human insulin receptor, 83-14 and delivered to the brain through RMT. This peptide radiopharmaceutical,

^{125}I-Aβ1-40, can be used for imaging amyloid plaques in Alzheimer's disease (Wu *et al*., 1997). The same mAb 83-14 was conjugated to liposomes and used to deliver genes across the BBB *in vitro* (Zhang *et al*., 2003). mAb 83-14 also allowed the complete knockdown of the specific gene expression by actively targeting siRNA and thus facilitating gene silencing *in vitro* (Xia *et al*., 2008). As the insulin receptor is associated with the mechanism of glucose homeostasis in CNS, this approach of targeting insulin receptors for drug delivery involves a risk of instability in glucose homeostasis.

3.4.2. Transferrin Receptor

TfR is the most characterized receptor system on the BBB. TfR can be targeted in two ways for drug delivery to the brain, by using endogenous transferrin (Tf) as a targeting ligand or by using a monoclonal antibody against TfR.

Antibody-directed liposomes, also known as immunoliposomes, have been reported to be promising vectors for the site-specific, targeted delivery of drugs. Traditional immunoliposomes are rapidly cleared from the blood circulation by the reticulo-endothelial system, thus restricting their use *in vivo* (Aragnol & Leserman, 1986). However, this could be overcome by coating liposomes with polyethylene glycol (PEG). PEG-coated immunoliposomes were synthesized utilizing OX26 mAb, an antibody against TfR, and used for *in vivo* brain targeting and delivery of anti-cancer agent daunomycin, which has very low permeability through the BBB. It was found that brain uptake of

daunomycin through PEG-coated immunoliposomes was higher than conventional liposomes and free daunomycin (Huwyler *et al*., 1996).

Polyphosphoester (PPE) is biodegradable polymer that degrades at physiological conditions through enzymatic cleavage of phosphoester bonds. PPE are biocompatible with neuronal cells. Zhang and colleagues (2012) synthesized an amphiphilic block co-polymer poly (ε-caprolactone)-block-poly (ethyl ethylene phosphate) (PCL-PEEP) by co-polymerization of PEEP (a hydrophilic derivative of PPE) and poly (ε-caprolactone) (PCL). PCL-PEEP micelles were surface-modified with Tf. The authors encapsulated paclitaxel, an anticancer agent, in hybrid micelles designated as Tf-modified paclitaxel-loaded hybrid micelles. They successfully transported the targeted micelles through the BBB and demonstrated its therapeutic effect by an increase in survival time in glioma bearing mice when compared to non-targeted drug delivery system (Zhang *et al*., 2012).

3.4.3. Low-density lipoprotein receptor related proteins (LRP1 & LPR2)

LRP1 and LRP2 can interact with a variety of molecules such as lactoferrin (Lf), melanotransferrin and angiopeps. They have been exploited for years in a similar way as insulin receptors and TfR for drug delivery to brain.

Lf is a mammalian cationic binding glycoprotein belonging to the transferrin family. Lf has demonstrated its ability to cross the BBB via LRP-mediated transcytosis in an *in vitro* model of the BBB (Fillebeen *et al*., 1999). However

evidences showed the presence of specific lactoferrin receptors (LfR) on the BBB. A novel brain-targeted drug delivery system by conjugation of poly (ethylene glycol)-poly (lactide) (PEG-PLA) nanoparticles to the Lf had shown enhanced uptake to the brain compared to the unconjugated nanoparticles (Hu *et al*., 2009). Urocortin, a corticotrophin-releasing hormone-related peptide, has shown its efficacy as a cytoprotectant for cultured hippocampal neurons, cerebellar granule cells and GABAergic neurons. An intracerebral injection of urocortin led to inhibition of Parkinsonian-like features in the rat 6-hydroxidopamine (6-OHDA) and lipopolysaccharide paradigms of Parkinson's disease, demonstrating the therapeutic utility of urocortin. However, after intravenous administration, no therapeutic activity was observed, as this drug was unable to cross the BBB. Urocortin-loaded Lf-(PEG-PLA) nanoparticles after intravenous administration successfully crossed the BBB and produced therapeutic efficacy (Hu *et al*., 2011).

Melanotransferrin (p97) is another targeting ligand that can bind to the LRP1 receptor and undergo transcytosis. This iron-binding protein is closely related to transferrin and lactoferrin. Recombinant human melanotransferrin (p97) effectively accumulated in brain after intravenous injection without affecting the integrity of the BBB, through LRP1 and LRP2 receptor mediated transcytosis (Demeule *et al*., 2002). Melanotransferrin (p97) was exploited to deliver Adriamycin to the brain, which normally cannot cross the BBB. The conjugate p97-adriamycin traversed the BBB and the pharmacological effect

of the drug demonstrated a significant increase in the survival time against glioma in a mouse model (Gabathuler *et al*., 2005).

Another group of the highly effective LRP binding ligands are Angiopeps. This family of peptides, in particular Angiopep-2, have shown affinity for LRP receptors (Demeule *et al*., 2008). Amphotericin B, an antifungal drug, has poor penetration into the CNS. When it is encapsulated in polymeric micelles bearing Angiopep-2, they demonstrated higher BBB-penetrating capacity compared to the unmodified micelles and free amphotericin B (Shao *et al.,* 2010).

3.4.4. Diphtheria toxin receptor

DTR is the membrane-bound precursor of heparin-binding epidermal growth factor (HB-EGF), a new endogenous transport receptor for the delivery of drugs across the BBB. As diphtheria toxin is too toxic for *in vivo* use, its non-toxic mutant protein cross-reacting material CRM197 is utilized as a receptor-specific carrier protein. CRM197 utilizes DTR-mediated transcytosis and delivers its cargo molecules to the CNS. It has showed to exert *in vitro* and *in vivo* brain targeting efficiency. Conjugates of CRM197 and horseradish peroxidase were transported across an *in vitro* model (Fenart & Cecchelli, 2005) and *in vivo* model of BBB (Gaillard & de Boer 2005; Gaillard *et al*., 2005).

3.5. Drug delivery via inhibition of efflux pumps

The expression of efflux pumps such as P-gp and MRPs in the endothelial cells of the BBB prevents the entry and accumulation of many drugs in the brain. One strategy to deliver drugs efficiently to the brain would be to co-administer them with modulators that inhibit the efflux pumps in brain capillary endothelial cells. Kabanov and colleagues investigated the concept of using pluronic block copolymers for brain delivery by inhibition of P-gp efflux pumps. Pluronic block copolymers consist of hydrophilic ethylene oxide (EO) and hydrophobic propylene oxide (PO) arranged in a tri-block structure (EO-PO-EO), giving rise to their amphiphilic nature. Thus, these copolymers can act as a surfactant and interact with the biological membranes. At concentrations above the critical micelle concentration (CMC) in water, they can self-assemble to form micelles. Miller *et al*. (1997) studied the membrane interactions of Pluronic P85 in an *in vitro* model of the BBB using bovine brain microvessel endothelial cells (BBMEC) and potential mechanisms of drug absorption. Cellular accumulation of rhodamine 123 in the BBMEC, with and without the presence of Pluronic P85 was examined. At concentration below the CMC, P85 inhibits P-gp function, reducing the drug efflux out of the brain endothelial cells and at concentrations above CMC, it increases the vesicular transport of the drug in the brain microvessels (Miller *et al*., 1997). The inhibition mechanisms of the P85 on the BBB involve membrane fluidization after interactions with the endothelial cells and ATP depletion by the inhibition of the P-gp ATPase activity (Kabanov *et al.,* 2003). Another study demonstrated that *in vivo* co-administration of digoxin with 1 % P85,

increased the brain penetration of the drug by 3-fold in comparison to the control group (Batrakova *et al.,* 2001). P-gp is also expressed in certain cancers, especially the recurrent and the relapsed cancers as well as the one induced after initial chemotherapeutic treatment. P-gp also plays a major role in the development of the multiple drug resistance (MDR) by transporting the drugs out of the tumour cells. P85 has also been used to increase the effect of anticancer drugs such as doxorubicin in the MDR tumours, by inhibition of P-gp (Sharma *et al*., 2008). Doxorubicin incorporated Pluronic block co-polymers is in Phase 3 clinical trials as a first line treatment against oesophageal carcinoma showing high incidence of MDR. This treatment has also received an orphan drug status by the FDA for the treatment of gastric cancers (Chen and Liu 2012).

These studies demonstrated that the block co-polymers are not inert. They have the capability of interacting with the biological systems. Caution has to be taken, as these block co-polymers might be acceptable for the treatment of cancers, but not for the treatment of the chronic disorders requiring repeated administrations for a long term.

4. Gene Therapy

A number of human diseases have genetic origin (SoRelle, 2000). Thus, a novel therapeutic approach of replacing the faulty gene with the normal healthy gene could provide new horizons for the treatment of such diseases.

Gene therapy can be defined as the introduction of nucleic acids (DNA/RNA) into the cells for the purpose of altering the course of medical condition or disease.

4.1. Gene as “drug”

The idea of using “genes” as “drugs” originated from the United States in the 1970s. This was an outcome of the growing knowledge on the human gene function, its mutations and the development of effective technologies for the delivery of DNA into mammalian cells (Giacca, 2010).

Gene therapy has become one of the most intensively studied and emergent strategies for the treatment of various diseases. It provides a potential therapeutic alternative for diseases for which the current treatment strategies are ineffective or less effective. The target diseases that can be potentially treated by gene therapy have a diverse range: they can be monogenic (single gene defect) disorders, such as cystic fibrosis, or complex disorders such as cancer (Gardlík *et al*., 2005).

Gene therapy is a technique for repairing the faulty genes responsible for the development of the disease. It usually involves insertion of a functional gene that is missing to produce a new protein or to trigger a cell function, to replace a gene with incomplete sequence (Patil *et al*., 2012), or to shut off a gene (gene silencing). The common aim of all those strategies is to achieve stable expression of functional genes into target tissue, for as long as desired

and without causing any toxic effects. Figure 1.5 shows the basic process of gene therapy and the various hurdles encountered in gene delivery.

There are various biological barriers for the gene delivery system to reach the target cell of an organ or tumour. The gene delivery system needs to travel in the blood stream to the specific organ or the tumour site. It then needs to extravasate and distribute throughout the organ or tumour where it should be efficiently taken up by cells by endocytotic processes. The plasmid DNA is then released into the cytoplasm and needs to gain entry into the nucleus and express the transgene (Dufès *et al*., 2005).

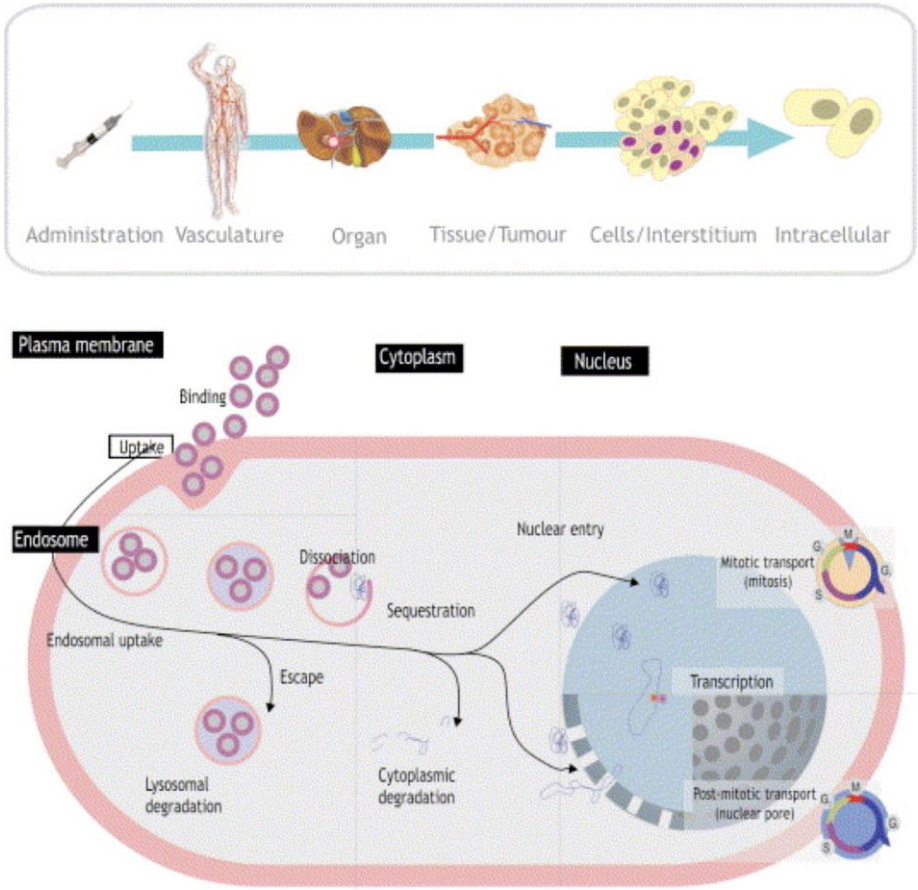

Figure 1.5 Gene delivery via systemic administration to the cells of the organs or the disease sites (Dufès *et al.*, 2005)

The prerequisite of development of any gene delivery system depends on parameters, such as the choice of the therapeutic gene, delivery system, route of administration and also a realistic assessment of the likelihood that a specific disease can be treated by gene therapy (Giacca, 2010). The current studies are aimed at developing effective and safe techniques and vectors to deliver genes to tissues, as well as improving the regulation of gene expression.

The naked DNA encoding the therapeutic protein cannot be delivered directly in the blood stream because it is degraded by endonucleases, leading to low efficiency. As a result, new delivery systems and methods for improving gene delivery are particularly needed. There are two major classes of vehicles used for the gene transfer:

(1) Viral vectors

(2) Non-viral vectors (Kay *et al*., 1997)

4.2. Viral Vectors

Viruses introduce their DNA into the cells with high efficiency. It has become possible to take advantage of this intrinsic property to utilize them for gene delivery (Walther & Stein, 2000). Viruses used for gene delivery are produced by genetic modification in such a way that their pathogenicity is eliminated and their gene transfer efficiency is retained. Unlike wild type viruses, viral vectors for gene delivery are made replication-deficient by deleting the genes

that allow replication, assembling or infection so that they are safe and non-pathogenic in the target cells. These genes can be replaced by the therapeutic or functional gene to be expressed in the host cell genome (Dando *et al*., 2001; Kootstra & Verma, 2003).

Viruses currently used as vectors can be divided in two types on the basis of their different strategies of replication and survival:

- Non-lytic viruses, including retrovirus and lentivirus, produce virions from the cellular membrane of an infected cell, leaving the host cell intact.

- Lytic viruses, including human adenovirus and herpes simplex virus, destroy the infected cells after production of virions and replication. Despite limitations of safety and reproducibility, they are the most used gene transfer vectors (Lundstrom, 2003).

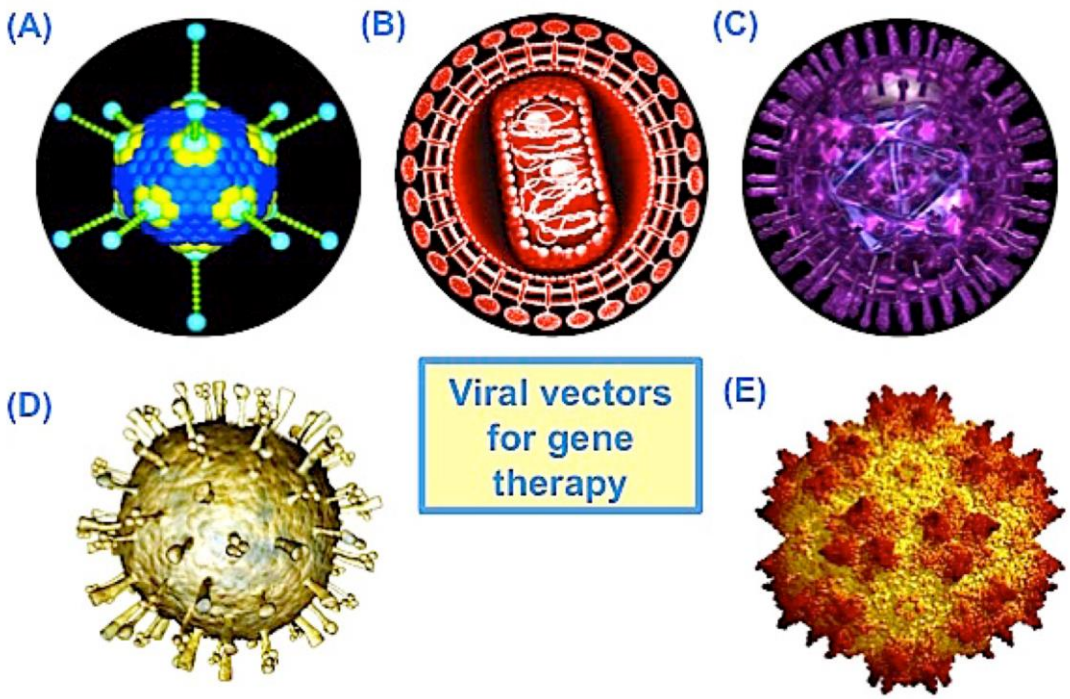

Figure 1.6 Different viral vectors used for gene therapy. (A) Adenovirus (National Cancer Institute, Dr. Richard Feldmann, 2001) (B) Retrovirus (Stanford School of Medicine) (C) Herpes-Simplex virus (Bryan Brandenberg blog) (D) Lentivirus (The value of virus, 2010) (E) Adeno-associated virus (International committee on taxonomy of viruses, 2008)

Table 1 describes the properties of some of the most commonly used viral vectors.

Table 2.1 Properties of the most widely used viral vectors (Thomas *et al*., 2003)

Vector	Tropism	Inflammatory potential	Advantages	Disadvantages
Retrovirus	Dividing cells only	Low	-Efficient transduction -Integration into host cell genome	-Low titres -Insertional mutagenesis -Silencing of gene expression -Exclusive transduction of actively replicating cells
Lentivirus	Broad	Low	- Transduc-tion of quiescent cells -Integration into the host cell genome	-Possible generation of replication-competent lentiviruses -Possible mobilization of vector in HIV-infected patients -Potential of insertional mutagenesis
Adenovirus	Broad	High	-Highly efficient transduction -High level transgene expression -Production of high titres -Transduc-tion of both quiescent and replicating cells -Broad host range	-Transient transduction -Stimulation of strong inflammatory and immune responses
Adeno-Associated virus	Broad, with the possible excep-tion of haematopoietic cells	Low	-Derived from non-pathogenic virus -Production at high titres -Infection of quiescent cells *in vivo* -Very long persistence and gene expression	-Limited cloning capacity (< 5 kb) -Lack of a packaging cell line -Tropism limited to specific cell types
Herpes Simplex Virus	Strong to neurons	High	-Persistence in latent form -Large cloning capacity -Tropism for neuronal cells	-Difficulty to manipulate -Poor knowledge of several biological features - Difficulty to identify and eliminate pathogenic genes

Viruses are efficient in transduction of genes in cells. But the safety concerns related to the use of viruses in humans create an opportunity for use of non-viral vectors for gene delivery.

4.3. Non-viral vectors

Non-viral vectors are particularly promising with regards to their simplicity to use, easy large scale production and quality control and non-immunogenicity (Li & Huang, 2000). The most commonly used non-viral vectors for gene therapy are liposomes, polymers and dendrimers.

4.3.1. Liposomes

Liposomes are generally formed by the self-assembly of dissolved lipid molecules in water, each lipid consisting of a hydrophilic head group and a hydrophobic tail group (Figure 1.7). Liposomes can exhibit a diverse range of sizes and morphologies depending upon the assembly of pure lipids or lipid mixtures in an aqueous medium. As liposomes are rapidly degraded after entering the circulation, they are conjugated with PEG for enhancement of stability and increased circulation times (Balazs & Godbey, 2011). Liposomes form complexes with DNA, called lipoplexes. These complexes have been used in several clinical trials for gene therapy (Nabel *et al*., 1993). They are non-pathogenic and can be used in several treatments. Their production is relatively cheap and easy compared to viral vectors, but their transfection efficiency is low compared to viruses (Robbins & Ghivizzani, 1998).

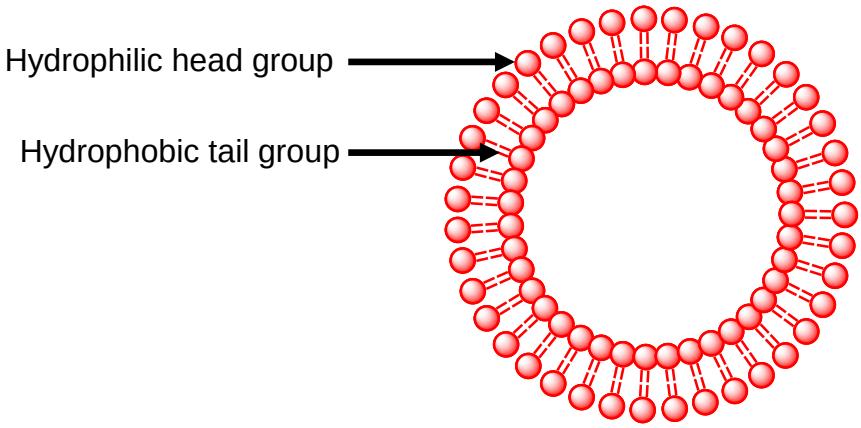

Figure 1.7 Schematic structure of a liposome

4.3.2. Polymers

Polymers are another class of non-viral vectors that have been extensively studied in gene delivery. They can be divided into three sub-classes depending on their structures: linear, branched and dendritic (Pack *et al*., 2005). They form complexes with DNA called polyplexes. Cationic polymers condense DNA more efficiently than cationic lipids (Li & Huang, 2000). Due to the flexibility of the polymer chemistry, it might be possible to provide multiple functionalities to the polymer for drug and gene delivery. Additional functionalities can also be added for maintaining biocompatibility and stability of the formulation. However, poor gene transfer efficiency of the polymers has limited their clinical applications (Pack *et al*., 2005). There are various classes of polymers widely investigated for gene delivery like polylysine, polyethyleneimine and chitosan. Polyethyleneimine (PEI) is found to be highly promising amongst all the polymers, with high gene delivery potential and low cytotoxicity (Boussif *et al*., 1995).

4.3.3. Dendrimers

Dendrimers are formed by a central core molecule from which a number of highly branched tree-like arms generate in a symmetrical and ordered fashion (Figure 1.8). The unique molecular structure of dendrimers leading to a number of original characteristics differentiates them from ordinary polymers. Dendrimers are synthesized by a stepwise method, which leads to a definite size and structure along with low polydispersity index. The multiple attachment sites on the surface of dendrimers provided due to the high density of terminal groups make them potential gene delivery vectors. Dendrimers are found to be non-toxic *in vitro* and have effective electrostatic interactions with cell membranes, which is important for DNA uptake by cells. It has been demonstrated that intravenous administration of polypropylenimine (PPI) dendrimer complexed with tumour necrosis factor (TNFα) under the control of specific promoter led to the intratumoural gene expression and regression of established tumours (Dufès *et al*., 2005). Tumour regression was further amplified after intravenous administration of Tf-bearing PPI dendrimer gene delivery system in mice, resulting in the complete disappearance of 90% of A431 subcutaneous tumours. (Koppu *et al*., 2010).

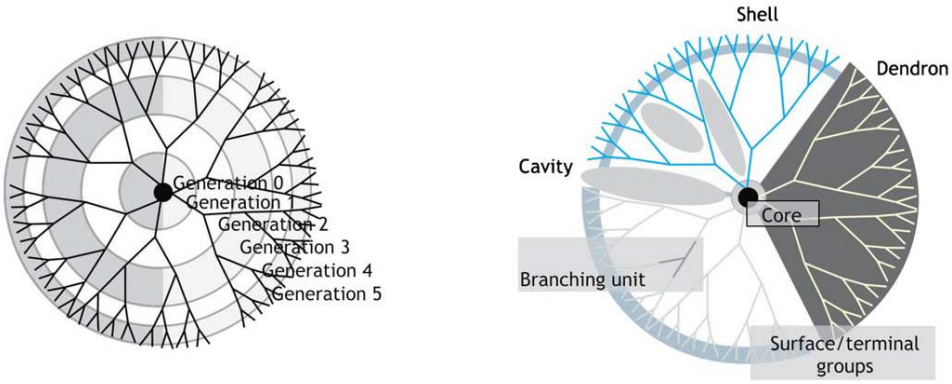

Figure 1.8 Schematic structure of a dendrimer (Dufès *et al.*, 2005)

4.4. Gene Therapy and the brain

In spite of the swift expansion of our knowledge about the molecular structure of the components of BBB and advancements in medical nanotechnology, small molecules still cannot cross the BBB nor treat most cerebral diseases (Chen & Liu, 2012). Gene therapy could provide a novel approach for the treatment of such diseases.

The preclinical studies on gene therapy for neurological disorders started with the utilization of viral vectors for gene transfer. Mainly herpes simplex virus, adenovirus, adeno-associated virus and retrovirus were explored as potential carriers for gene delivery to the brain in early 1990s (Suhr & Gage, 1993). However, in all these cases, highly invasive methods like craniotomy, intracarotid arterial infusion and stereotaxic injections were used as the routes of administration that cause disruption of the BBB (Shi & Pardridge, 2000). Moreover, viral vectors have been associated with tissue toxicity, immunologic and inflammatory reactions and other safety concerns that limit

their use for gene therapy. Several clinical trials utilized viruses as vectors but they did not succeed due to the safety concerns surrounding these vectors (Bansal & Engelhard, 2000).

Various receptors like insulin receptors, TfR, LfR, LRP1 and LRP2 receptors are expressed on brain capillary endothelial cells. Researchers have been targeting these receptors to allow DNA to cross the BBB via RMT. Insulin receptors that maintain the glucose metabolism in brain could be used for the gene delivery to the brain via RMT. However, this approach is considered hazardous as it targets the mechanism concerned with the glucose homeostasis in brain. TfR that maintain iron balance in the brain are the most characterized RMT system for gene delivery to CNS. These receptors can be utilized for transferring DNA across BBB either by using Tf as a targeting ligand or using an antibody (such as OX26) directed to TfR. LRP1 & LRP2 target a diverse range of molecules and so are called multifunctional, multi-ligand scavenger and signalling receptors. Lf, melanotransferrin and angiopeps have been used as targeting ligands for LRP1 and LRP2-mediated endocytosis (Chen & Liu, 2012).

Various non-viral vectors are investigated for CNS gene therapy, out of which the most popular ones are liposomes and dendrimers. Liposomes were the first ones to be investigated. Pardridge and co-workers utilized PEGylated liposomes conjugated with monoclonal antibody OX26 to target the transferrin receptors for gene delivery and brain targeting (Shi & Pardridge,

2000). The same group then used PEGylated immunoliposomes to target plasmid DNA to the brain with monoclonal antibody 8D3, targeting transferrin receptors on BBB. Tissue-specific gene expression in the brain was obtained after intravenous administration (Shi *et al*., 2001). Ko *et al*. (2009) used polyethylenimine (PEI) to form polyplexes with oligodeoxynucleotides (decoy ODN). These PEI/ODN polyplexes were encapsulated in PEG-stabilized liposomes containing biotin at the distal end of PEG chain. This biotinlylated-PEG-stabilized liposome encapsulating PEI/ODN polyplexes (bioPSL) was conjugated to 8D3, a monoclonal antibody targeting transferrin receptors for brain targeting and designated as antibody-targeted bioPSL. This delivery system delivers intact decoy ODN specifically to brain capillary endothelial cells through intravenous administration *in vivo* in mice. Polyamidoamine (PAMAM) dendrimers have emerged as a class of nano-constructs for CNS gene delivery. Tf-conjugated PEG-modified PAMAM (PAMAM-PEG-Tf) was synthesized and complexed with plasmid DNA and evaluated for gene delivery and expression in the brain (Huang *et al*., 2007). The same group used Lf as a brain targeting ligand. Lf was conjugated to PAMAM-PEG to form PAMAM-PEG-Lf. PAMAM-PEG-Lf/DNA complex had higher transfection efficiency than PAMAM-PEG-Tf/DNA complexes. After intravenous administration, the brain uptake and gene expression of PAMAM-PEG-LF/DNA was higher than that observed with PAMAM-PEG/DNA (Huang *et al*., 2008; Huang *et al*., 2009). Angiopep has also been used as a targeting ligand conjugated to PAMAM-PEG. Its complex with DNA formed PAMAM-PEG-Angiopep/DNA nanoparticles (NPs) able to target LRP-1 receptors on

the BBB. This gene delivery system efficiently crossed BBB, accumulated in the brain and exhibited gene expression. After achieving gene expression in the brain, this group targeted glioma as a model disease for gene therapy. They used again the high-branching dendrimer PAMAM as a main vector. They conjugated PAMAM with PEG to enhance its pharmacokinetics and biocompatibility. The targeting ligand used was Chlorotoxin (CTX) which has been showed to have an enhanced binding affinity to membrane-bound matrix metalloproteinase-2 (MMP-2), upregulated in gliomas, medulloblastomas and other tumours of neuroectodermal origin. In this study, pORF-TRAIL, a plasmid DNA expressing Tumour necrosis factor-related apoptosis-inducing ligand (TRAIL), led to selective killing of tumour cells without cytotoxic effect on normal cells. PAMAM-PEG-CTX/pORF-TRAIL demonstrated a highly efficient energy-dependent cellular uptake in brain via RMT and AMT. Biodistribution of gene expression was observed mainly in brain tumour, but also in liver and kidney (Huang *et al*., 2011).

Some researchers designed a novel gene delivery system Tat-magnetosome-PAMAM by modification of magnetosome with PAMAM dendrimer and Transactivating transcriptional (Tat) activator protein peptides. Magnetosome is a natural magnetic nanoparticle with a well-defined size (40-120 nm) derived from magnetotactic bacteria. It consisted of magnetic core and an envelope made of lipids and proteins, making them biocompatible. Tat-magnetosome-PAMAM readily formed polyplexes with the luciferase reporter plasmid and the inclusion of external magnetic field could

significantly improve transfection efficiency, transport across the BBB and accumulation in brain tissues (Han *et al*., 2011).

Some peptides have also emerged as a new class for brain targeted gene delivery. RVG29, which is a 29-unit peptide obtained from the rabies virus glycoprotein (RVG), selectively binds to neuronal cells expressing the nicotinic acetylcholine receptors (AchR). As AchR are widely present on the brain capillary endothelial cells, RVG29 efficiently crosses BBB. RVG-29-oligoarginine peptide (RVG29-9rR) complexed with plasmid DNA was utilized for brain targeting. High transfection efficiency was achieved *in vitro* and brain targeted gene expression was achieved *in vivo*. The main advantages of peptide-based DNA delivery systems are biocompatibility, biodegradability and low immunogenic response (Gong *et al*., 2012).

An emerging strategy using a combination of gene therapy and chemotherapy provides great hope for the treatment of brain tumours. The tumour-targeted, pH-triggered co-delivery system (DGDPT/pORF-hTRAIL) utilizing doxorubicin as chemotherapeutic drug and pORF-TRAIL as a therapeutic drug was developed. HAIYPRH (T7) peptide that can bind to TfR that are expressed on the BBB and also on the malignant brain tumour cells was used as a targeting ligand. This multifunctional co-delivery system shows potential synergistic effect of the chemotherapeutic drug doxorubicin and therapeutic gene TRAIL to induce tumour cell apoptosis, reducing toxicity in

healthy cells and increasing the median survival time of tumour-bearing mice (Liu *et al*., 2012).

5. Aims and Objectives

The presence of the BBB and the lack of safe and efficacious non-viral delivery systems are the major hurdles for the delivery of the therapeutic gene to the CNS. Various receptors like TfR , LfR, LRP1 and LRP2 are widely expressed on the BBB and serve as endogenous transport systems. DAB dendrimer has been investigated for the gene delivery to the cancer cells expressing transferrin receptors. Various studies demonstrated the targeted gene delivery efficacy of DAB dendrimer. Tf-bearing DAB dendrimer led to enhanced gene expression in the tumours over-expressing TfRs. In addition, tumour disappearance and regression was observed in the mice xenograft models without signs of toxicity (Koppu *et al*., 2010, Lemarie *et al*., 2012, Al Robaian *et al.,* 2014). Lf- and Lfc-bearing DAB dendrimer led to enhanced gene expression in the tumours (Yim *et al*., 2015). These studies demonstrate that DAB dendrimer is a safe and efficacious gene delivery system. It is therefore hypothesized that DAB could be exploited for targeted gene delivery to the brain by decorating it with Tf, Lf, Lfc and Angiopep-2 able to bind to specific receptors on the BBB, ultimately leading to gene expression in the brain. The main aims of this thesis are:

1. Synthesis and characterization of brain targeted gene delivery systems
2. *In vitro* evaluation of targeting efficiency in murine brain endothelial cells
3. *In vivo* evaluation of brain targeting efficiency in a mice model

CHAPTER 2

Materials and Methods

1. Materials

The following table lists the materials used for the experiments and their suppliers.

Table 3.1 List of materials and their suppliers

Material	Supplier
Ampicillin	Sigma Aldrich (Poole, UK)
Angiopep	DG peptides (Hangzhou, China)
Colchicine	Sigma Aldrich (Poole, UK)
DDAO-Gal	Invitrogen (Paisley, UK)
Deuterated water (D_2O)	Sigma Aldrich (Poole, UK)
Dextrose	Sigma Aldrich (Poole, UK)
Dimethylsuberimidate (DMSI)	Sigma Aldrich, (Poole, UK)
Dimethyl sulfoxide (DMSO)	Sigma Aldrich, (Poole, UK)
Dulbecco's Modified Eagle Medium	I Invitrogen (Paisley, UK)
Endotoxin-free Giga Prep Plasmid purification Kit	Qiagen (Hilden, Germany)

Material	Supplier
Expression plasmid encoding β-galactosidase (pCMV sport β-galactosidase)	Invitrogen (Paisley, UK)
Expression plasmid encoding tdTomato (pCMV tdTomato)	Clontech (Mountain view, CA)
Foetal bovine serum (FBS)	Invitrogen (Paisley, UK)
Filipin (Filipin complex from *Streptomyces filipinensis*)	Sigma Aldrich, (Poole, UK)
Generation 3-Diaminobutyric polypropylenimine dendrimer (DAB)	Sigma Aldrich (Poole, UK)
Glycine	Sigma Aldrich (Poole, UK)
Hydrochloric acid	Sigma Aldrich (Poole, UK)
L-Glutamine	Invitrogen (Paisley, UK)
Label IT® Cy3 Nucleic Acid Labelling kit	Cambridge Biosciences (Cambridge, UK)
Label IT® Fluorescein Nucleic Acid Labelling kit	Cambridge Biosciences (Cambridge, UK)
Lactoferricin	Sigma Aldrich (Poole, UK)

Material	Supplier
Lactoferrin	Sigma Aldrich (Poole, UK)
Luciferase assay reagent	Promega (Southampton, UK)
Lysine	Sigma Aldrich (Poole, UK)
Magnesium chloride	Sigma Aldrich (Poole, UK)
Maltose	Sigma Aldrich (Poole, UK)
Mercaptoethanol	Sigma Aldrich (Poole, UK)
Methanol	Sigma Aldrich (Poole, UK)
Ortho-nitrophenyl-β-D-galactosidase (ONPG)	Sigma Aldrich (Poole, UK)
Passive lysis buffer 5x (PLB)	Promega (Southampton, UK)
Penicillin-Streptomycin	Invitrogen, (Paisley UK)
Phenylarsine Oxide	Sigma Aldrich (Poole, UK)
Phenylmethyl sulfonyl fluoride (PMSF)	Sigma Aldrich (Poole, UK)

Material	Supplier
Phosphate buffered saline (PBS) tablets	Sigma Aldrich (Poole, UK)
Poly-Lysine	Sigma Aldrich (Poole, UK)
Protease Inhibitor cocktail (PIC)	Sigma Aldrich (Poole, UK)
Quanti-iT™ PicoGreen® dsDNA reagent	Invitrogen (Paisley, UK)
Sephadex G75	Sigma Aldrich (Poole, UK)
Sodium hydroxide	Sigma Aldrich (Poole, UK)
Tissue culture media	Invitrogen (Paisley, UK)
Human holo-Transferrin	Sigma Aldrich (Poole, UK)
Triethanolamine	Sigma Aldrich (Poole, UK)
Tris-(hydroxymethyl) aminomethane (TRIS) base	Sigma Aldrich (Poole, UK)
Trypsin	Invitrogen (Paisley, UK)
Tween 20	Sigma Aldrich (Poole, UK)

Material	Supplier
Vectashield® mounting medium with 4’,6-diamidino-2-phenylindole (DAPI)	Vector Laboratories (Peterborough, UK)

2. Methods

The following table summarizes the different methods and the chapters they were used in.

Table 2.2 Summary of methods and chapters they were used in

Methods		Used in
Synthesis	Synthesis	3,4,5
	Nuclear magnetic resonance (NMR) spectroscopy	4,5
Physico-chemical characterization	DNA condensation studies (Picogreen assay**)**	4,5
	Size and zeta potential measurements	4,5
	Transmission electron microscopy (TEM)	4
***In vitro* studies**	Transfection (B-galactosidase gene expression assay)	3,4,5
	Cellular uptake	3,4,5
	Mechanisms of cellular uptake	3,4,5
***In vivo* studies**	Biodistribution of gene expression	3,4,5
	Distribution of gene expression within the brain	3,4
Statistical Analysis	One-way analysis of variance and Tukey multiple comparison post-test	3,4,5

2.1. Synthesis and purification of targeted dendrimers

Transferrin (Tf) bearing-, Lactoferrin (Lf) bearing-, lactoferricin (Lfc) bearing- and Angiopep (Ang) bearing- generation 3- diaminobutyric polypropylenimine dendrimer (DAB) were synthesized in a similar manner to that previously reported for the preparation of other conjugates (Koppu *et al*., 2010; Aldawsari *et al*., 2011). DAB (24 mg) was added to Tf, Lf, Lfc or Ang (6 mg) and dimethylsuberimidate (12 mg) in triethanolamine HCl buffer (pH 7.4, 2 mL). The coupling reaction was allowed to take place for 2 h at 25^{o}C whilst stirring. The purification of conjugates was conducted by size exclusion chromatography using a Sephadex G75 column. Conjugates were then freeze-dried. The conjugation of Tf, Lf, Lfc and Ang to DAB was assessed by ^{1}H NMR spectroscopy at magnetic field strength of 400 MHz using a Jeol Oxford NMR AS 400 spectrometer. Deuterium oxide was used for the dissolution of DAB-Tf, DAB-Lf, DAB-Lfc and DAB-Ang for performing NMR.

2.2. Physico-chemical characterization

2.2.1 DNA condensation studies

The ability of the DNA to form complex with DAB-Lf, DAB-Lfc and DAB-Ang, was assessed by PicoGreen® assay, performed according to the supplier's protocol. The fluorescence of PicoGreen® significantly increases on intercalation with double stranded DNA. The electrostatic interaction between the anionic DNA and cationic group of the polymer on formation of the Tf-bearing DAB–DNA polyplex condenses the DNA and reduces the number of PicoGreen® binding sites, ultimately reducing the fluorescence intensity for

the PicoGreen® solution.

PicoGreen® reagent was diluted 200-fold in Tris–EDTA (TE) buffer (10 mM Tris, 1 mM EDTA, pH 7.5) on the day of the experiment. One mL of complex dendrimer–DNA at various dendrimer: DNA weight ratios (20:1, 10:1, 5:1, 2:1, 1:1, 0.5:1 and 0:1) was added to 1 mL PicoGreen® solution. The DNA concentration in the cuvette (10 µg/mL) was kept constant throughout the experiment. The fluorescence intensity of the complexes in the presence of PicoGreen® was analyzed at various time points with a Varian Cary Eclipse Fluorescence spectrophotometer (Palo Alto, CA) (λ_{exc}: 480 nm, λ_{em}: 520 nm). Results were represented as percentage of DNA condensation (= 100 − % relative fluorescence to DNA control) (n = 4) according to the following equation:

$$F_Y = (F_t – F_{PG})/ (F_0 - F_{PG})$$

where

F_t = fluorescence of the dendrimer / DNA complexes

F_0 = fluorescence of the DNA alone

F_{PG} = fluorescence of the Picogreen

Data was represented as a mean (n=4) (± S.E.M) and the values were plotted using Microcal Origin® v 12.0 software.

2.2.2. Size and Zeta potential measurements

Size and zeta potential of DAB-Lf, DAB-Lfc and DAB-Ang dendriplexes prepared at various dendrimer: DNA weight ratios (20:1, 10:1, 5:1, 2:1, 1:1,

0.5:1, 0:1) were measured by photon correlation spectroscopy and laser Doppler electrophoresis using a Malvern Zetasizer Nano-ZS (Malvern Instruments, Malvern, UK).

2.3. *In vitro* studies

2.3.1. Transfection

Transfection efficacy of the DNA carried by DAB-Tf, DAB-Lf, DAB-Lfc and DAB-Ang dendrimers was assessed by a β-galactosidase transfection assay, using a plasmid DNA encoding β-galactosidase (pCMV βgal). bEnd.3 cells were seeded at a density of 2000 cells/well in 96-well plates (n=15). After 72h incubation, the cells were treated with the DAB-Tf-DNA (dendrimer: DNA weight ratio 10:1), DAB-Lf-DNA and DAB-Lfc-DNA (dendrimer: DNA weight ratio 2:1) and DAB-Ang dendriplexes at the following dendrimer: DNA weight ratios: 20:1, 10:1, 5:1, 2:1, 1:1, 0.5:1, 0:1. DNA concentration (10 µg/mL) was kept constant for all the formulations tested. Naked DNA served as a negative control, DAB-DNA (dendrimer: DNA weight ratio 5:1) served as a positive control. After 72 h incubation, cells were lysed with 1X passive lysis buffer (PLB) (50 µL/well) and incubated for 20 min. The cell lysates were then analysed for β-galactosidase expression. Briefly, 50 µL of the assay buffer (2 mM magnesium chloride, 100 mM mercaptoethanol, 1.33 mg/mL o-nitrophenol-β-galactopyranoside, 200 mM sodium phosphate buffer, pH 7.3) were added to each well containing the lysates. After 2 h incubation at 37ºC, the absorbance of the samples was read at 405 nm with a Multiscan Ascent®

plate reader (Thermo Scientific, Waltham, MA). Results were compared with standard curve of recombinant β-galactosidase (0-5 mU).

2.3.2. Cellular uptake

Imaging of the cellular uptake of the DNA complexed to DAB-Tf, DAB-Lf, DAB-Lfc and DAB-Ang was carried out using epifluorescence microscopy. Labeling of the β-galactosidase-encoding plasmid DNA with the fluorescent probe fluorescein or Cy3 (for DAB-Tf) was performed using a Label IT® fluorescein or Cy3 Nucleic Acid Labeling kit, as described by the manufacturer. bEnd.3 cells were seeded on coverslips in 6-well plates (10^5 cells/well) (10^4 cells/well for DAB-Tf) and grown at 37 °C for 72 h. They were then incubated for different durations with fluorescein or Cy3-labelled DNA (2.5 µg DNA/well) complexed to DAB-Tf, DAB-Lf, DAB-Lfc and DAB-Ang, at the dendrimer: DNA weight ratio of 10:1, 2:1, 2:1 and 2:1 respectively. The cells were then washed three times with PBS and fixed with methanol for 10 min. Upon staining of the nuclei with DAPI, the cells were examined using an E600FN Upright Epifluorescence microscope (Nikon, Tokyo, Japan). DAPI was excited with the 405 nm CoolLED pE excitation system (bandwidth: 415-491 nm), whereas Cy3/fluorescein was excited with the 470 nm CoolLED pE excitation system (bandwidth: 515-555 nm).

Once the treatment duration allowing maximal DNA uptake was determined, a similar procedure was performed to compare the cellular uptake of fluorescein or Cy3-labelled DNA (2.5 µg/well) complexed to DAB-Tf, DAB-Lf,

DAB-Lfc, DAB-Ang and DAB (dendrimer: DNA weight ratios respectively of 10:1, 2:1, 2:1, 2:1 and 5:1) during the optimized treatment duration. Control samples were treated with naked DNA or remained untreated.

Quantification of cellular uptake was performed using flow cytometry. bEnd.3 cells were grown in 6-well plates (1.6×10^5 cells/ well) at 37 °C for 72 h. The cells were then treated with fluorescein-labelled DNA (5 µg DNA/well), alone or complexed to DAB-Tf, DAB-Lf, DAB-Lfc, DAB-Ang and DAB (dendrimer: DNA weight ratios respectively of 10:1, 2:1, 2:1, 2:1 and 5:1) and during the optimized treatment duration. Cells treated with DNA only or untreated cells served as negative controls. After optimized duration of incubation with the treatments, single cell suspensions were prepared, washed (2 mL PBS pH 7.4 per well) and pelleted (378 g/3000 rpm for 8 min) 3 times, before being analysed using a FACSCanto® flow cytometer (BD, Franklin Lakes, NJ). Ten thousand cells (gated events) were counted for each sample. Their mean fluorescence intensity was analysed with FACSDiva® software (BD, Franklin Lakes, NJ).

2.3.3. Mechanisms of cellular uptake

The mechanisms involved in the cellular uptake of DNA complexed to DAB-Tf, DAB-Lf, DAB-Lfc and DAB-Ang were investigated by pre-treatment of cells with uptake inhibitors- Phenylarsine oxide (Inhibitor of clathrin-dependent endocytosis), fillipin (Inhibitor of caveolae-mediated processes), colchicine (Inhibitor of macropinocytosis), polylysine (Inhibitor of the uptake

of cationic vectors) and endogenous ligands (Tf, Lf) (Visser *et al.,* 2004, Kim *et al.,* 2007, Liu & Shapiro 2003). Cells were seeded and grown as described above. After removal of the medium, they were then pre-treated with phenylarsine oxide (10 µmol/L), filipin (5 µg/mL), colchicine (10 µmol/L), poly-l-lysine (400 µg/mL) and free Tf (chapter 3) or free Lf and Lfc (chapter 4) or for 10 min at 37 °C. The cells were then treated with Cy3- or fluorescein-labelled DNA (respectively 2.5 and 5 µg/well for qualitative and quantitative analysis) complexed to DAB-Tf/Lf/Lfc/Ang for optimized treatment duration before being washed and processed for fluorescence microscopy and flow cytometer analysis as described above.

2.4. *In vivo* studies

2.4.1. Biodistribution of gene expression

The biodistribution of gene expression was visualized by bioluminescence imaging, using an IVIS Spectrum® (PerkinElmer, Waltham, MA).

To determinate the treatment duration leading to the highest gene expression, female BALB/c mice (n = 3, initial mean weight: 20 g) were injected intravenously with a single dose of DAB-Tf, DAB-Lf, DAB-Lfc and DAB-Ang carrying luciferase expression plasmid (50 µg of DNA) in dendrimer: DNA weight ratio of 10:1, 2:1, 2:1 and 2:1 respectively. They were then intraperitoneally injected with the luciferase substrate d-luciferin (150 mg/kg body weight) after various treatment durations and anesthetized by isoflurane inhalation. Light emission was measured 10 min after injection of the d-luciferin solution, for 2 min, using Living Image® software

(PerkinElmer, Waltham, MA). The resulting pseudo-color images represent the spatial distribution of photon counts within the animal. Identical illumination settings were used for acquiring all images.

A similar procedure was then performed at the optimum treatment duration to compare the distribution of gene expression resulting from the single intravenous injection of DAB-Tf, DAB-Lf or DAB-Ang, and DAB dendriplexes encoding luciferase (50 µg of DNA). Mice treated with DNA only served as negative control.

Biodistribution of gene expression was also quantified using a β-galactosidase reporter gene expression assay (Zinselmeyer *et al*., 2003). Groups of mice (n = 5) were injected intravenously with a single dose of DAB-Tf, DAB-Lf, DAB-Lfc or DAB-Ang and DAB dendriplexes encoding β-galactosidase (50 µg of DNA) (dendrimer: DNA weight ratio of 10:1, 2:1, 2:1 and 2:1 respectively). They were sacrificed at previously optimized duration after injection and their organs were removed, frozen in liquid nitrogen, before being analysed for their β-galactosidase levels. For the preparation of tissue homogenates, a homogenization / lysis buffer (25 mL) was prepared as below:

- 500 µL protease inhibitor cocktail
- 1000 µL PMSF 50 mM in methanol
- 5 mL PLB 5X
- 18.5 mL distilled water

Organs were weighed and 1 mL of freshly prepared homogenization buffer was added to each organ (except liver, where 2 mL was added). Organs were homogenized using a tissue homogenizer (PowerGen 125, Fischer Scientific) and the resultant tissue homogenates were incubated on ice.

Quantification of β-galactosidase enzymatic activity was performed by measurement of β-galactosidase enzymatic cleavage of its substrate 9H-(1,3-dichloro-9,9-dimethylacridin-2-one-7-yl) β-D-galactopyranoside (DDAO-Gal) to 7-hydroxy-9H-(1,3-dichloro-9,9-dimethylacridin-2-one) (DDAO) product.

A DDAO-Gal Reaction Mix was prepared for each tissue homogenate, as follows. For 1 sample:

- 15 µL DDAO-Gal in DMSO (5 mg/mL)
- 20 µL PMSF
- 100 µL maltose in PBS (20g / 100 mL)
- 15 µL protease inhibitor cocktail
- 150 µL PBS

To 100 µL tissue homogenates, 300 µL of DDAO-Gal reaction mix was added and incubated at 37^{o}C, with occasional mixing for the appropriate incubation time optimized for each organ (45 minutes for liver, 90 minutes for the other organs). A volume of 200 µL of the incubated reaction mixture was then transferred into another container and incubated in a heating block at

90º C for 2 minutes. The heated incubation was performed to stop the enzymatic cleavage of β-galactosidase on the DDAO-gal substrate and precipitate a large proportion of proteins. To extract the DDAO product, 800 µL isopropanol were added to dissolve the DDAO and the mixture was incubated for 20 minutes at 5º C. Subsequently, the mixtures were centrifuged (7 minutes at 15000 rpm or 1260g). 500 µL of the supernatant were mixed with 500 µL of 80% (v/v) water-isopropranol mixture and measured in a fluorescence spectrophotometer (Varian Cary Eclipse Fluorescence spectrophotometer, λ_{exc} = 630nm, λ_{em}= 650 nm, slit 5 nm). The fluorescence units were used to calculate the β-galactosidase activity based on a linear regression ($f(x) = a + b.x$) fitted to a β-galactosidase standard curve. The concentration of β-galactosidase in the organs was determined by using the following equations, given by a β-galactosidase standard curve (Zinselmeyer *et al*., 2003):

Concentration of β-galactosidase in 100 µL sample C1 (in mU):

C1 = (fluorescence intensity + Intercept) / Slope

Concentration of β-galactosidase per organ C2 (in mU):

C2 = C1 x (1+ weight sample (in g) / 0.1

2.4.2. Distribution of gene expression within the brain

Distribution of gene expression within the brain was qualitatively assessed by fluorescence microscopy imaging of the brain sections of mice treated with DAB-Tf or DAB-Lf dendriplex encoding tdTomato. Mice were intravenously injected with a single dose of DNA encoding tdTomato, naked or complexed

to DAB-Tf and DAB dendrimers (50 µg of DNA). They were sacrificed 24 h after injection. After this point, two different methods were used for Chapter 3 and Chapter 4.

For Chapter 3, the brains were removed, fixed in a solution of 10% formalin for 48 h. Following fixation, the brains were dehydrated through an ethanol gradient for 8.5 h, cleared in xylene for 2.5 h, before being embedded in paraffin wax. Coronal sections were cut at a thickness of 4 µm in different brain areas (anterior, median and posterior) and left in a 37 °C oven overnight before being stained with hematoxylin and eosin (H&E) according to standard procedures. The brain sections were then examined using an E600FN Upright Epifluorescence microscope. Positivity for tdTomato expression in the brain was assessed at excitation wavelengths of 530-635 nm and emission wavelengths of 605-655 nm.

For Chapter 4, the brains were removed, immediately frozen on dry ice, before being embedded in Tissue-Tek® optimal cutting temperature (OCT) compound. Coronal sections were cut at a thickness of 15 µm in different brain areas (anterior, median and posterior), fixed in ice-cold acetone for 5-10 min, in -20ºC methanol for 5-10 min. They were then washed and permeabilized in PBS/0.1% Tween-20 for 10 min before being mounted with Vectashield® medium containing DAPI. The brain sections were then examined using an E600FN Upright Epifluorescence microscope. Positivity

for tdTomato expression in the brain was assessed at excitation wavelengths of 530-635 nm and emission wavelengths of 605-655 nm.

CHAPTER 3

Transferrin-bearing polypropylenimine dendrimer for targeted gene delivery to the brain

1. Introduction

Receptor-mediated transcytosis (RMT) has been extensively studied for drug and gene delivery to the brain. Transferrin receptors (TfR) are widely expressed on the capillary endothelial cells of the BBB (Jefferies *et al*., 1984). The TfR, also widely referred to as TfR1 type II transmembrane glycoprotein, is involved in the iron metabolism. The iron uptake occurs by the RMT of the iron-loaded transferrin, also called holotransferrin. Transferrin (Tf) is part of a class of metal-binding glycoproteins whose major function is binding and transport of iron in the body. Tf molecule (apotransferrin) can bind up to 2 Fe^{3+} ions to form ferro-transferrin or holotransferrin. The conformational changes occurring in the molecule while binding to Fe^{3+} ions have been shown to play a key role in the selective recognition by TfR The iron loaded transferrin or holotransferrin has 10 to 100-times higher affinity for the TfR than that of apotransferrin at physiological pH (Richardson and Ponka 1997).

Various delivery systems targeting TfR on the BBB have been investigated for targeted gene delivery to the brain. Tf or anti-TfR antibodies (OX26, 8D3) were used as a targeting ligand. Pardridge and colleagues have investigated OX26- and 8D3- targeted pegylated immunoliposomes for enhanced gene expression in the brain (Shi and Pardridge 2000, Shi *et al*., 2001). Avidin-biotin technology has also been explored for the targeted delivery of the therapeutic nucleic acids to the brain. In one such study, biotinylated peptide

nucleic acid was bound to a conjugate of OX26 and streptavidin and was used for selective imaging of brain tumours (Suzuki *et al.,* 2004).

Dendrimers have recently been shown to be promising candidates for brain delivery, owing to their unique polymer architecture and easily modified surface groups. PAMAM has been studied as a vehicle to cross the BBB via TfR targeting (Huang *et al*., 2007). In this study, Tf was conjugated to PAMAM through bifunctional PEG and complexed to a plasmid DNA encoding green fluorescent protein (GFP). After intravenous administration to the mice, the Tf-bearing PAMAM-DNA complex was able to cross the BBB and led to the expression of GFP in several brain regions such as the hippocampus, *substantia nigra*, the 4th ventricle, the cortical layer and *caudate putamen*. This gene expression was about 2-fold higher than that observed following the administration of PAMAM and PAMAM-PEG complexes (Huang *et al*., 2007). All these gene delivery systems lead to an increase gene expression in brain, but non-specific gene expression was also found in other major organs of the body (Shi & Pardridge 2000, Shi *et al*., 2001, Huang *et al*., 2007).

Polypropylenimine (PPI) dendrimers have emerged as a novel nanoscopic carrier for targeted gene delivery. Dufes and colleagues recently demonstrated that transferrin (Tf)-bearing generation 3-diaminobutyric polypropylenimine dendrimer (DAB-Tf) was able to increase the uptake and gene expression of DNA by cancer cells overexpressing TfR compared to

non-targeted delivery systems, *in vitro* and *in vivo* (Koppu *et al*., 2010, Lemarie *et al*., 2012, Al-Robaian *et al*., 2014). Importantly, the treatment was well tolerated by the animals, with no apparent signs of toxicity.

2. Aims and Objectives

Based on the fact that iron can efficiently reach the brain via TfR-mediated transcytosis, we now hypothesize whether conjugation of Tf to DAB leads to increased gene expression in the brain. The main objectives of this chapter are:

- Synthesis and characterization of Tf bearing DAB dendrimer
- Evaluation of the brain targeting efficacy of DAB-Tf *in vitro* and *in vivo*

3. Results

3.1. Synthesis and characterization

The synthesis and physicochemical characterization of the DAB-Tf was done in a similar manner as described in Chapter 2. Dimethylsuberimidate (DMSI) act as a homobifunctional cross linker between DAB and Tf, forming covalent bonds to the primary amine groups of DAB and amino acids in the transferrin (Figure 3.1). The similar chemical reaction occurs when Lf, Lfc and Angiopep-2 is conjugated to DAB. The conjugation of Tf to DAB was confirmed by ^{1}H NMR spectrum. The ratio of the integrals of resonances at ca. 3.70 and 2.80 for methylene units (**d** and **a**) attached to the amino acid moiety via DMSI linkage and unbound free amine respectively is 1. This supports that 50 % of the surface primary amine groups on the DAB are conjugated to transferrin (Koppu *et al*., 2010). The proposed chemical reaction and the structure of the final product is shown in Figure 3.1.

The ability of the DAB-Tf to form complex with plasmid DNA through electrostatic interactions between positively charged DAB-Tf and negatively charged plasmid DNA was characterized using Pico Green® assay. DAB-Tf was able to condense more than 70% of DNA at all the dendrimer: DNA weight ratios. The condensation occurred almost instantaneously and was found to be stable for atleast 24 hours. It increased with the increasing dendrimer: DNA weight ratios. DAB-Tf displayed a mean diameter of 287 nm (PDI: 0.393). The conjugation of Tf on the periphery of the DAB led to the increase in the size. DAB dendriplex had the mean diameter of 196 nm (PDI:

0.683). The zeta potential of DAB-Tf dendriplex was 1.03 mV, which was less than the unmodified DAB dendriplex (6.42 mV).

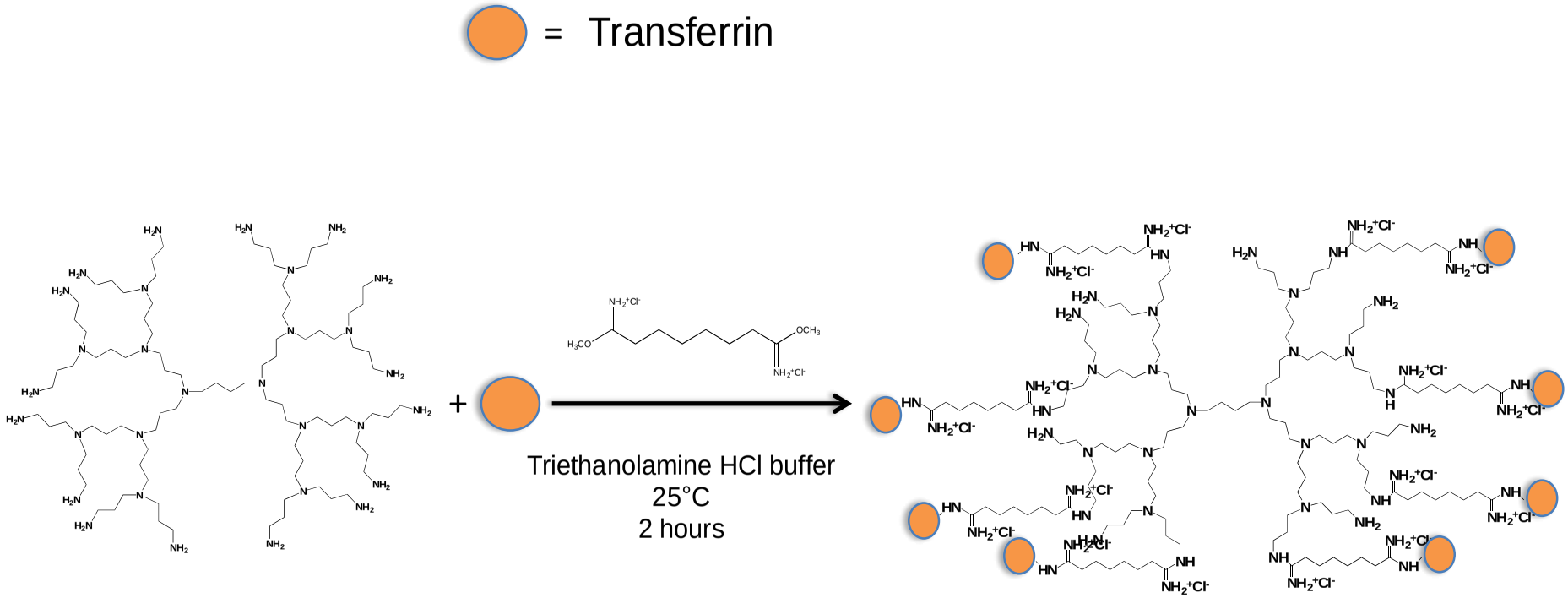

Figure 3.1 Chemical reaction of DAB dendrimer and Tf leading to the reaction product, DAB-Tf

3.2. *In vitro* studies

3.2.1. Transfection

The grafting of Tf to DAB dendriplex led to an increased transfection compared to DAB dendriplex on bEnd.3 cells (Figure 3.2). The treatment of bEnd.3 cells with DAB-Tf dendriplex led to a 1.3-fold increase in the gene expression compared to DAB dendriplex ($3.79x10^{-3} \pm 0.23x10^{-3}$ U/mL and $2.85x10^{-3} \pm 0.21x10^{-3}$ U/mL respectively for DAB-Tf and DAB dendriplexes. Gene expression following treatment with DAB-Tf dendriplex and DAB-dendriplex was 4.3-fold and 3.3-fold higher than that observed following treatment with naked DNA ($0.87x10^{-3} \pm 0.01x10^{-3}$ U/mL). The cells treated with naked DNA did not demonstrate any significant increase in the gene expression compared to untreated cells.

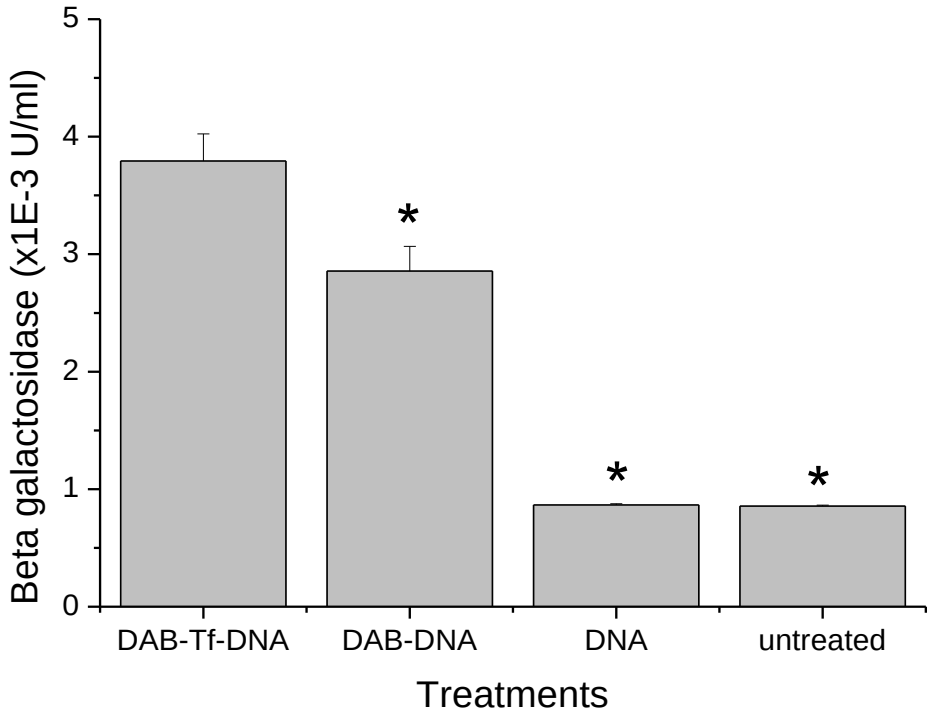

Figure 3.2 Transfection efficacy of DAB-Tf and DAB dendriplexes in bEnd.3 cells. DAB-Tf and DAB dendriplexes were dosed at their optimal dendrimer: DNA ratio of 10:1 and 5:1 respectively. Results are expressed as the mean ± SEM of three replicates (n=15). * : P <0.05 compared with DAB-Tf-DNA

3.2.2. Cellular uptake

The uptake of Cy3-labelled DNA complexed to DAB-Tf by bEnd.3 cells was qualitatively analysed by epifluorescence microscopy. Cellular uptake commenced as early as 15 minutes, as Cy3-labelled DNA could be visualized surrounding the nuclei. From all the durations tested, DNA uptake was most pronounced after treatment of bEnd.3 cells with DAB-Tf dendriplex for 2 hours (Figure 3.3).

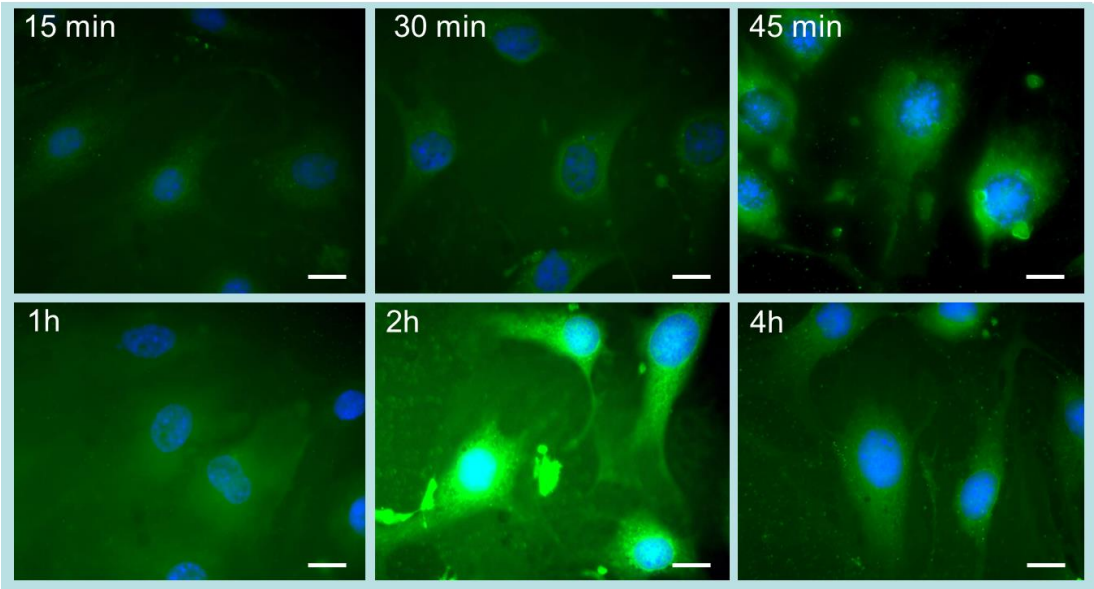

Figure 3.3 Epifluorescence microscopy imaging of the cellular uptake of Cy3- labelled DNA (2.5 µg/ well) complexed with DAB-Tf, after incubation for 15 min, 30 min, 45 min, 1 h, 2 h or 4 h with bEnd.3 cells (Blue: nuclei stained with DAPI (excitation: 405 nm, emission bandwidth: 415-491 nm), green: Cy3-labelled DNA (excitation: 543 nm, emission bandwidth: 550-620 nm) (Bar: 10 µm)

Following optimization of the duration of the maximum cellular uptake, bEnd.3 cells were treated with Cy3-labelled DNA complexed to DAB-Tf, DAB or in solution for 2 hours. Pronounced uptake of Cy3-labelled DNA complexed to DAB-Tf was observed. On the contrary, cells treated with DAB dendriplex or Cy3-labelled DNA solution did not show any Cy3-derived fluorescence (Figure 3.4).

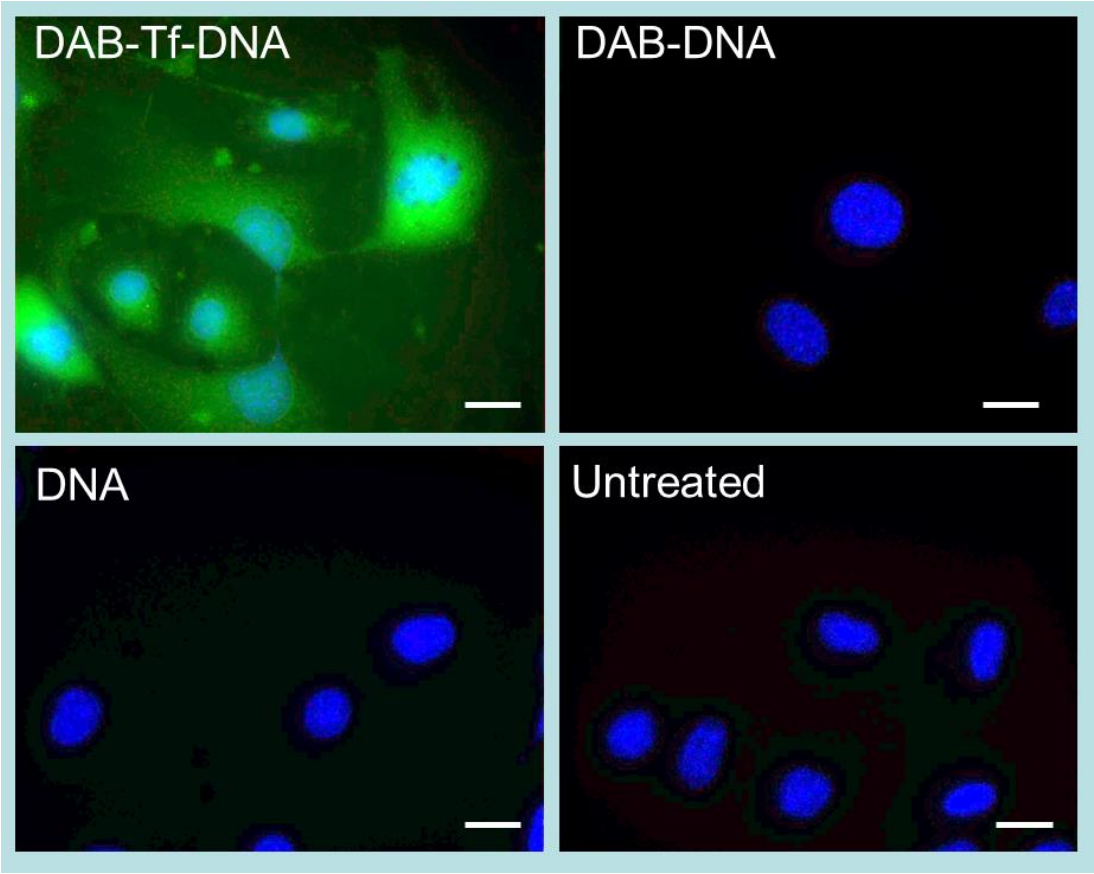

Figure 3.4 Epifluorescence microscopy imaging of the cellular uptake of Cy3- labelled DNA (2.5 µg/ well) either complexed with DAB-Tf, DAB or in solution, after incubation for 2 hours with bEnd.3 cells (Blue: nuclei stained with DAPI (excitation: 405 nm, emission bandwidth: 415-491 nm), green: Cy3-labelled DNA (excitation: 543 nm, emission bandwidth: 550-620 nm) (Bar: 10 µm)

The quantification of the cellular uptake was done utilizing flow cytometry. Figure 3.5). Cellular fluorescence was highest following treatment with DAB-Tf dendriplex (7682 ± 355 arbitrary units (a.u.)). It was respectively about 1.4-fold and 2.3-fold higher than the cellular fluorescence observed following treatment with DAB dendriplex (5531 ± 530 a. u.) and DNA solution (3370 ± 199 a. u.).

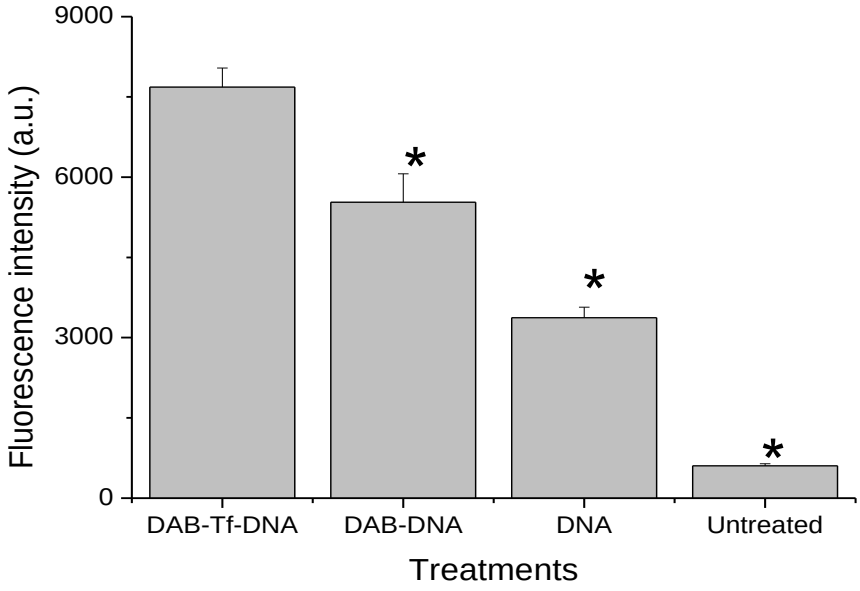

Figure 3.5. Flow cytometry quantification of the cellular uptake fluorescein-labelled DNA (2.5 µg/ well) either complexed with DAB-Tf, DAB or in solution, after incubation for 2 hours with bEnd.3 cells (n=5) * : P <0.05 compared with DAB-Tf-DNA.

3.2.3. Inhibitor studies

The mechanisms of cellular uptake of the DNA complexed to DAB-Tf were elucidated by utilizing cellular uptake inhibitors and escalating concentrations of Tf. Pre-treatment of the bEnd.3 cells with increasing concentrations of free Tf significantly decreased the cellular uptake of fluorescein-labelled DNA complexed to DAB-Tf to reach a plateau at Tf concentrations higher than 12.5 µM (Figure 3.6 and 3.7). At a Tf concentration of 20 µM, the cellular uptake of fluorescently-labelled DNA was 3.8-fold lower than that observed with DAB-Tf dendriplex without pre-Tf treatment (respectively 2010 ± 122 a. u. and 7682 ± 355 a. u.).

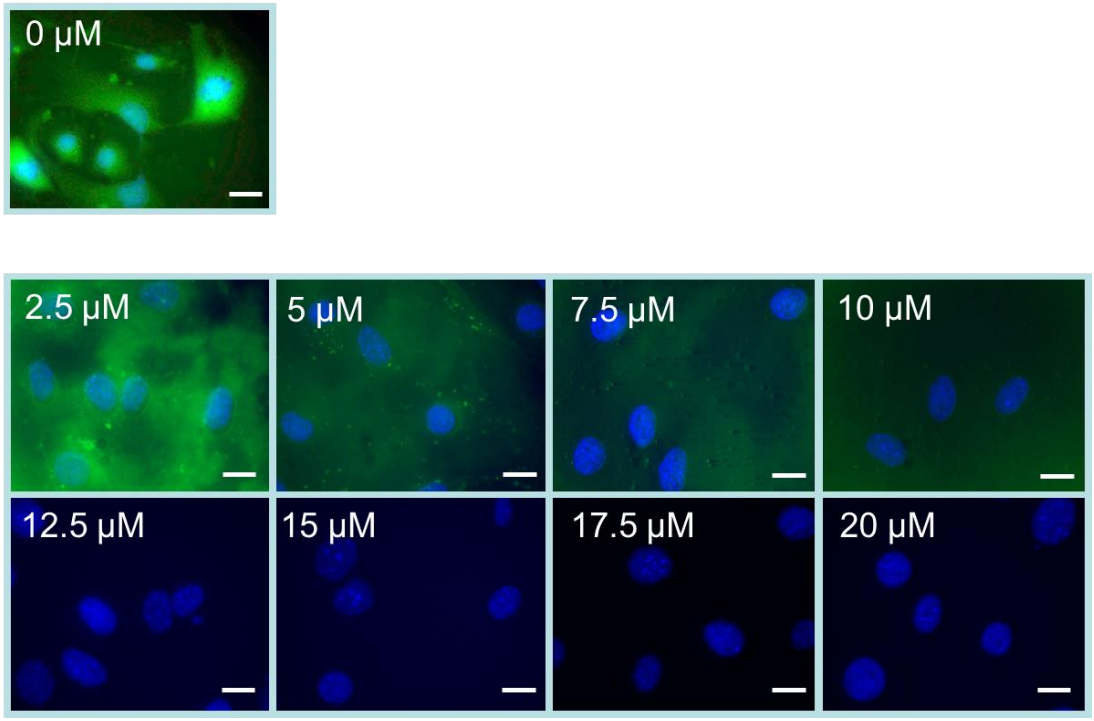

Figure 3.6 Epifluorescence microscopy imaging of the bEnd.3 cellular uptake of Cy3- labelled DNA (2.5 µg/ well) complexed with DAB-Tf, following pre-treatment with various concentrations of free Tf (ranging from 2.5 µM to 20 µM). (Blue: nuclei stained with DAPI (excitation: 405 nm, emission bandwidth: 415-491 nm), green: Cy3-labelled DNA (excitation: 543 nm, emission bandwidth: 550-620 nm) (Bar: 10 µm).

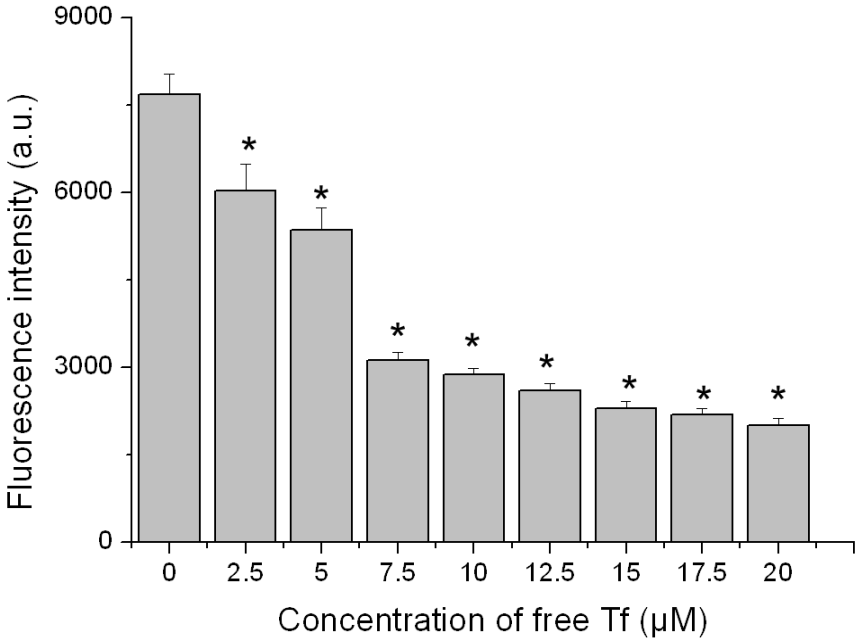

Figure 3.7 Flow cytometry quantification of the bEnd.3 cellular uptake of fluorescein- labelled DNA (2.5 µg/ well) complexed with DAB-Tf, following pre-treatment with various concentrations of free Tf (ranging from 2.5 µM to 20 µM) (n=5), * : P <0.05 compared with DAB-Tf-DNA.

The cellular uptake of fluorescein-labelled DNA complexed to DAB-Tf was also partially inhibited by phenylarsine oxide, filipin, colchicine and poly-L-lysine (Figure 3.8 and 3.9). Colchicine and phenylarsine oxide caused the most significant inhibition, with a cellular uptake respectively decreased by 2.3-fold and 2.1-fold compared to that observed with DAB-Tf dendriplex without inhibitory treatment (respectively 3316 ± 251 a. u. and 3614 ± 140 a.u. following pre-treatment with colchicine and phenylarsine oxide). Filipin and poly-L-Lysine appear to be less effective inhibitors, leading to a cellular uptake decreased by respectively 1.7-fold and 1.3-fold compared to DAB-Tf

dendriplex without pre-treatment (respectively 4532 ± 201 a. u. and 5974 ± 192 a.u. following pre-treatment with filipin and poly-L-Lysine).

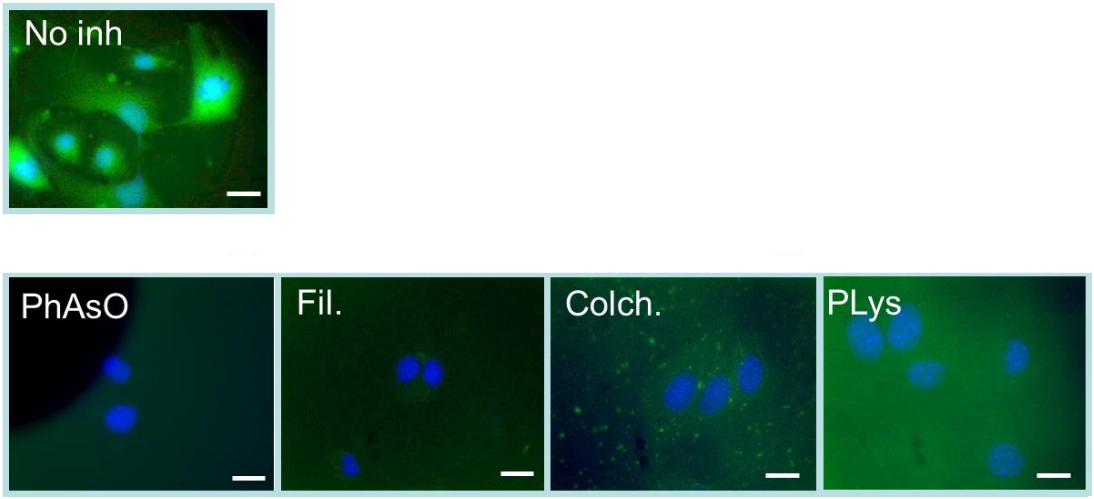

Figure 3.8 Epifluorescence microscopy imaging of the bEnd.3 cellular uptake of Cy3- labelled DNA (2.5 µg/ well) complexed with DAB-Tf, following pre-treatment with various cellular uptake inhibitors: phenylarsine oxide ("PhAsO"), filipin ("Fil."), colchicine ("Colch.") and poly-L-lysine ("PLys"). (Blue: nuclei stained with DAPI (excitation: 405 nm, emission bandwidth: 415-491 nm), green: Cy3-labelled DNA (excitation: 543 nm, emission bandwidth: 550-620 nm) (Bar: 10 µm)

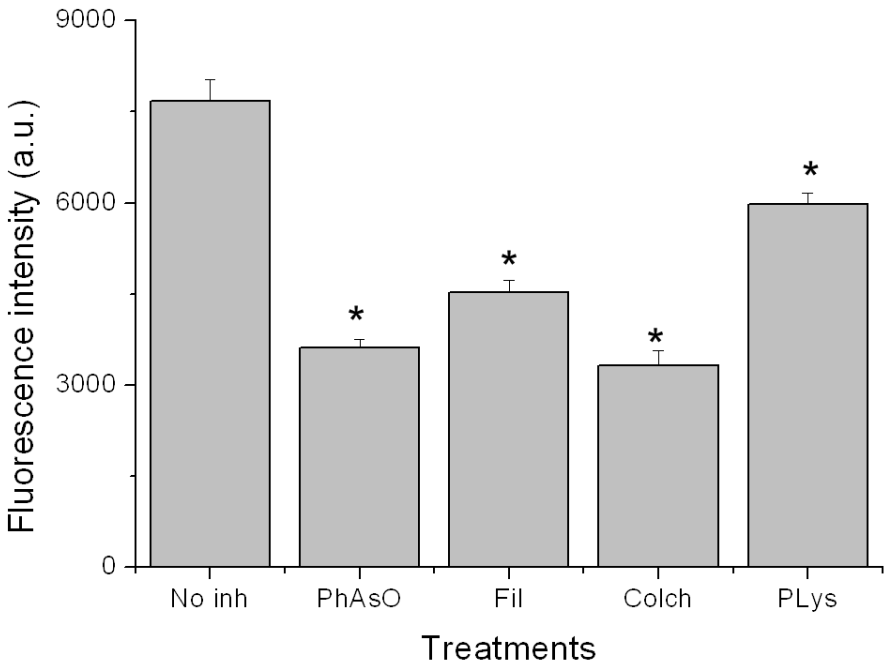

Figure 3.9 Flow cytometry quantification of the bEnd.3 cellular uptake of fluorescein- labelled DNA (2.5 µg/ well) complexed with DAB-Tf, following pre-treatment with various cellular uptake inhibitors: phenylarsine oxide ("PhAsO"), filipin ("Fil."), colchicine ("Colch.") and poly-L-lysine ("PLys"). (n=5), * : P <0.05 compared with DAB-Tf-DNA.

3.3. *In vivo* studies

3.3.1. Biodistribution of gene expression

The biodistribution of gene expression following intravenous injection of DNA encoding luciferase complexed to DAB-Tf was first qualitatively assessed by luminescence imaging, at various treatment durations. Gene expression appeared to be mainly located in the brain of the mice. The highest gene expression level was found 24 h following injection of the treatment (Figure 3.10).

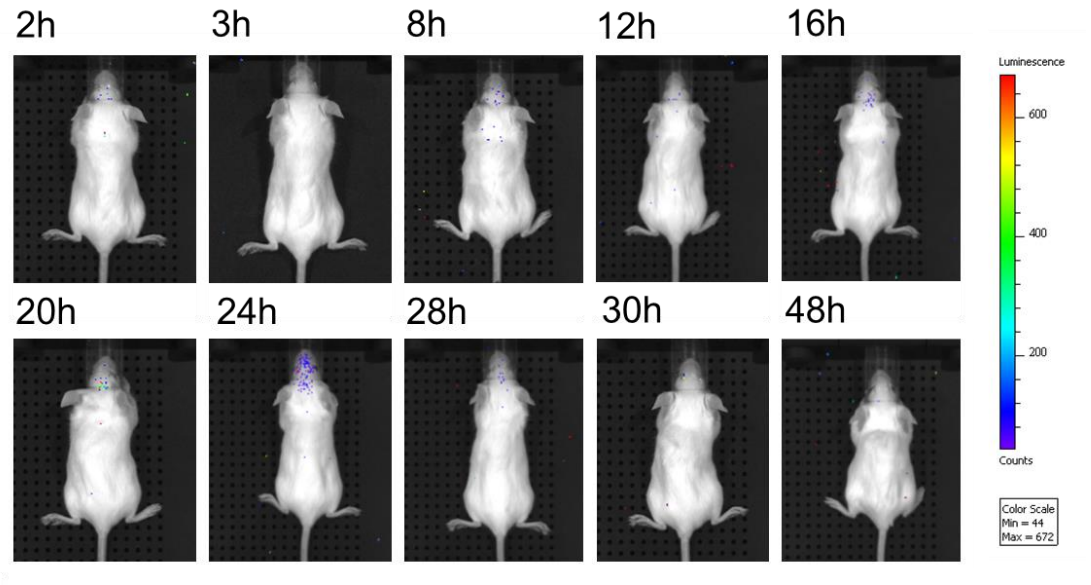

Figure 3.10 Bioluminescence imaging of gene expression after intravenous administration of DAB-Tf dendriplex (50 µg DNA administered). The mice were imaged using the IVIS Spectrum at various durations after injection of the treatment. The scale indicates surface radiance (photons/s/cm^2/steradian).

The gene expression following intravenous administration of DAB-Tf dendriplex was compared to that observed following administration of DAB-dendriplex and DNA only, 24 h after administration of the treatments. The level of gene expression in the brain appeared to be highest following treatment with DAB-Tf dendriplex (Figure 3.11).

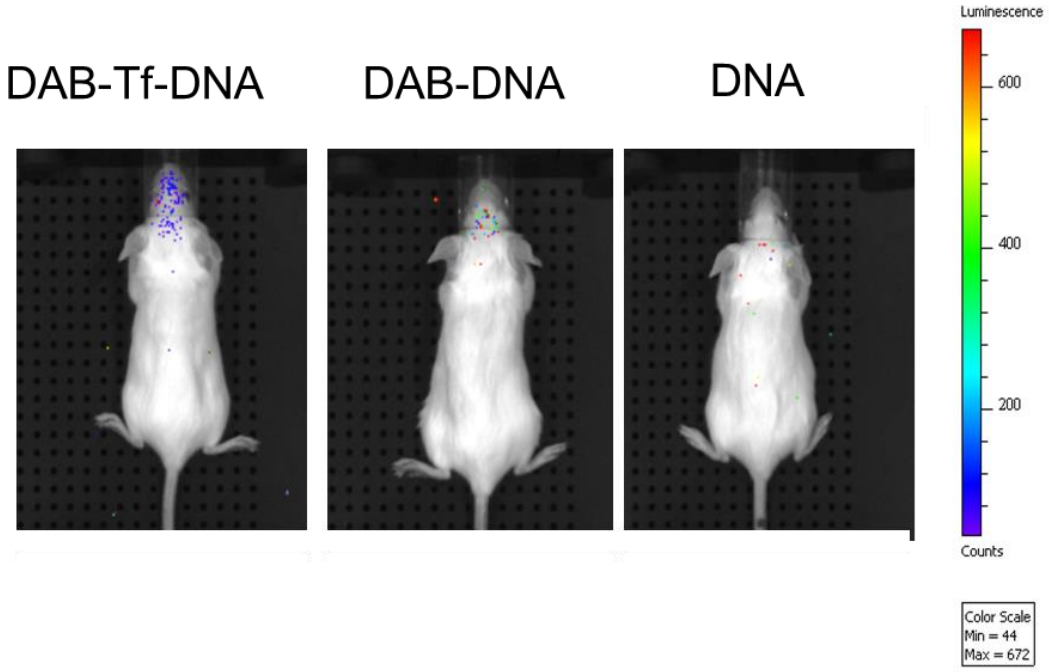

Figure 3.11 Bioluminescence imaging of gene expression after intravenous administration of DAB-Tf and DAB dendriplexes (50 µg DNA administered). (Controls: DNA solution, untreated cells). The mice were imaged using the IVIS Spectrum 24 h after injection of the treatments. The scale indicates surface radiance (photons/s/cm^2/steradian).

These results were confirmed by the quantification of gene expression in the major organs of the mice. After the intravenous administration of DAB-Tf dendriplex in mice, over 2-fold and 5-fold increase in the gene expression was observed compared to that of DAB dendriplex and DNA solution (37.3 ± 4.2 mU, 16.7 ± 7.6 mU and 7.7 ± 5.3 mU β-galactosidase per organ respectively for DAB-Tf , DAB dendriplexes and DNA solution) (Figure 3.12).

The levels of β-galactosidase expression in kidneys and heart following treatment with DAB-Tf dendriplex was similar to that observed after treatment with DAB-dendriplex and DNA solution (10.5 ± 6.1 mU, 12.1 ± 3.6 mU and

10.5 ± 7.2 β-galactosidase per organ in the kidneys for respectively DAB-Tf dendriplex, DAB dendriplex and DNA solution, 2.5 ± 1.6 mU, 0.9 ± 1.6 mU and 0.0 ± 3.0 mU β-galactosidase in the heart for respectively DAB-Tf dendriplex, DAB dendriplex and DNA solution). In liver, lung and spleen, a very little gene expression was observed following treatment with DAB-Tf dendriplex, whereas DAB dendriplex and DNA solution demonstrated high levels of β-galactosidase (except liver for DAB dendriplex) (0.0 ± 11.7 mU and 11.2 ± 8.2 mU β-galactosidase per organ in the liver for respectively DAB dendriplex and DNA solution, 6.6 ± 2.6 mU and 8.2 ± 2.8 mU β-galactosidase in the lung for respectively DAB dendriplex and DNA solution, 15.8 ± 2.6 mU and 15.9 ± 1.7 mU β-galactosidase in the spleen for respectively DAB dendriplex and DNA solution). B-galactosidase gene expression in the brain was at least 3-fold higher than in any peripheral organs tested in this study (Figure 3.12).

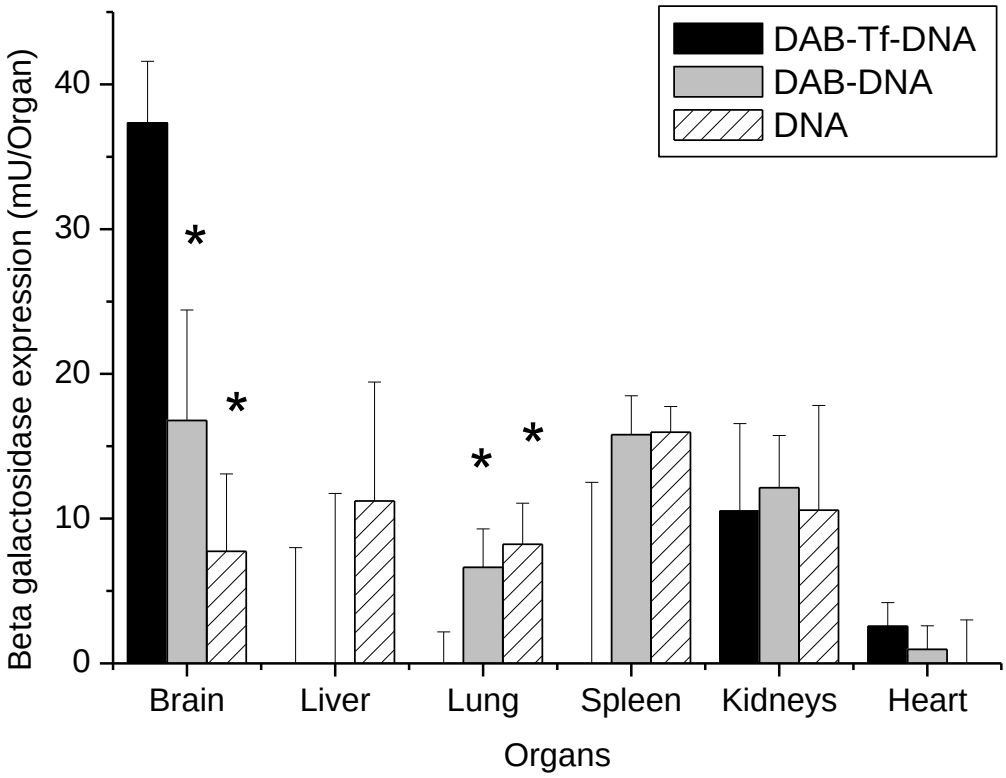

Figure 3.12 Biodistribution of gene expression after a single intravenous administration of DAB-Tf and DAB dendriplexes (50 µg DNA administered). Results were expressed as milliunits β-galactosidase per organ (n=5). * : P <0.05 compared with DAB-Tf-DNA for each organ

3.3.2. Distribution of gene expression in the brain

Within the brain, gene expression was the highest following administration of DAB-Tf dendriplex (Figure 3.13). It was homogenously distributed in the brain parenchyma in all the sections of the brain we observed, but did not appear to have reached the neurons and glial cells. By contrast, tdTomato gene expression was very limited in the brain following administration of DAB dendriplex. Some autofluorescence artefacts were visible in the brain treated with naked DNA or left untreated.

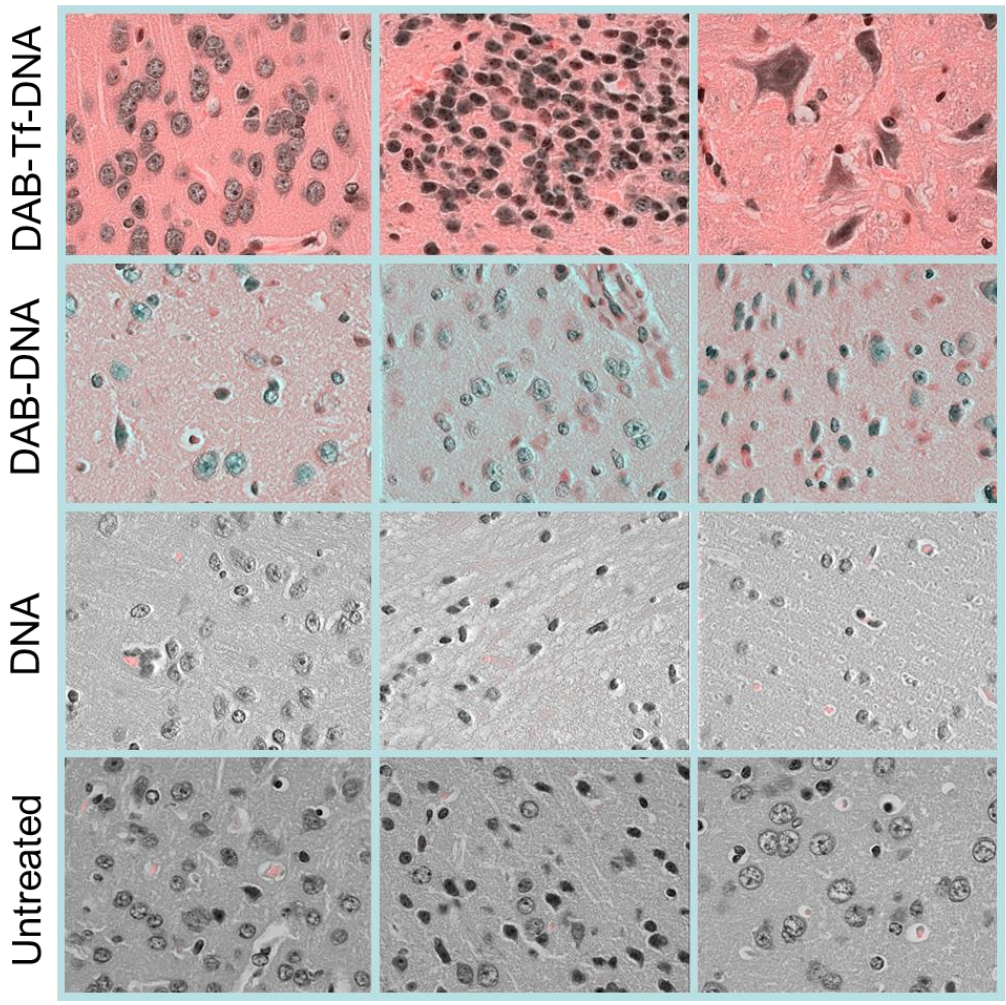

Figure 3.13 Epifluorescence microscopy imaging of the distribution of gene expression within the brain after a single intravenous injection of tdTomato-encoded DNA (50 µg) either complexed with DAB-Tf, DAB or in solution (Magnification: x 60)

4. Discussion

Transferrin receptors have been widely investigated for the drug and gene delivery to the brain. In this chapter, we demonstrated that conjugation of Tf to DAB, a highly efficient gene delivery system led to an increased gene delivery to the brain *in vitro* and *in vivo*. bEnd.3 cells showed an improved uptake of DNA (1.4-fold and 2.3-fold) following treatment with DAB-Tf dendriplex as compared to DAB dendriplex and DNA solution. Similar results were obtained when bEnd.5 cells were treated 8D3-biotinylated PEG-stabilized liposomes encapsulating PEI/ oligonucleotide targeting transferrin receptors and non-targeted liposomes. The cellular uptake was increased 3-fold (Ko *et al.,* 2009). However, cellular uptake of Tf bearing PAMAM-PEG dendrimers decreased by 2-fold compared to that of PAMAM-PEG dendrimers in brain capillary endothelial cells (Huang *et al*., 2007).

The inhibitor studies investigated the mechanism of cellular uptake of DNA complexed to DAB-Tf. The inhibitors used acted on the various endocytic mechanisms of cells. Phenylarsine oxide is an inhibitor of clathrin-mediated endocytosis (which is a requisite for receptor-mediated endocytosis) (Visser *et al.,* 2004). Filipin is known to block the caveolae-mediated process in non-specific adsorptive endocytosis (Ryoung Kim *et al*., 2007). Colchicine inhibits macropinocytosis (Liu and Shapiro 2003), which provides non-specific endocytosis of macromolecules, whereas cationic poly-L-Lysine can inhibit the uptake of cationic delivery systems. The cellular uptake of DNA complexed to DAB-Tf was therefore related to endocytosis processes mainly

to clathrin-mediated endocytosis and macropinocytosis, as phenylarsine oxide and colchicine demonstrated significant inhibition of the cellular uptake. Fillipin led to inhibition at a lesser extent displaying lower uptake of the DNA via caveolae-mediated endocytosis. The zeta potential of DAB-Tf dendriplex was slightly cationic (1.03 mV) (Koppu *et al*., 2010), which limited the possible inhibitory role of poly-L-lysine. These results suggested that both receptor- and adsorptive-mediated mechanisms might contribute to the cellular uptake of DNA complexed to DAB-Tf. Pre-treatment of cells with escalating amounts of free transferrin led to competition between DAB-Tf dendriplex and the free Tf for binding to TfR, demonstrating that the internalization mechanism of the DNA complexed to DAB-Tf is mainly via TfR-mediated endocytosis.

The enhanced β-galactosidase expression following transfection with DAB-Tf dendriplex resulted from increased cellular uptake after treatment. Both increases were of the same magnitude (1.4-fold for cellular uptake, 1.3-fold for gene expression compared to non-targeted DAB dendriplex treatment). Similar results were obtained when luciferase gene expression in the brain capillary endothelial cells was 1.8-fold higher after treatment with PAMAM-PEG-Tf/DNA as compared to that observed with PAMAM-PEG/DNA (Huang *et al*., 2007).

In vivo, intravenous administration of DAB-Tf dendriplex demonstrates higher luciferase gene expression in the brain compared to DAB dendriplex and

DNA, after 24 hours of injection. Gene expression is mainly observed in the brain and no other organs. The threshold of the technique that allowed only the most intensely luminescent organs to be analysed could explain this.

The biodistribution of the gene expression revealed that DAB-Tf dendriplex led to an improved β-galactosidase expression in brain after intravenous administration. The gene expression in the brain was significantly higher to that observed in the other major organs of the body. We have chosen to use a β-galactosidase expression assay for quantifying gene expression in the organs, as the spectrofluorimetric quantification of the reaction product 7-hydroxy-9H-(1, 3-dichloro-9, 9-dimethyl-acridin-2-one (DDAO) in the red part of the spectrum avoided interferences from haemoglobin which hamper many *in vivo* quantification assays (Colin *et al.,* 2000; Zinselmeyer *et al*., 2003). Various other studies have demonstrated higher gene expression in the brain following administration of Tf-bearing gene delivery systems as well as anti-TfR targeted monoclonal antibody targeted gene delivery systems. However gene expression was also observed in the other major organs of the body. After the intravenous administration of PAMAM-PEG-Tf/DNA complex in mice, Huang and colleagues demonstrated a 2-fold increase in the luciferase gene expression compared to that with PAMAM-PEG/DNA, but high levels of gene expression were also observed in heart, lung and kidney (Huang *et al*., 2007). Similarly, intravenous administration of 8D3-biotinylated PEG-stabilized liposomes encapsulating PEI/ oligonucleotide targeting transferrin receptors in mice led to a 10-fold increase in the brain

accumulation, but tracer activity was mainly found in spleen, liver and lungs. Pardridge and colleagues have demonstrated high levels of gene expression in brain in several studies. High level of luciferase gene expression was observed in the brain 48 hours after the administration of OX26-conjugated immunoliposomes. However, higher levels of gene expression were observed in liver, spleen and kidneys too (Shi and Pardridge, 2000). Additionally, the gene expression in these organs persisted over 6 days (Shi *et al*., 2001b). 8D3-conjugated immunoliposomes demonstrated similar results to that obtained for OX26-conjugated immunoliposomes (Shi *et al*., 2001a). In another study, they showed organ specific expression of the lacZ gene controlled by the opsin promoter after intravenous administration of 8D3-conjugated pegylated immunoliposomes carrying β-galactosidase expression plasmid. The gene expression was mainly observed in the brain and eye, but not in the peripheral organs like liver, spleen, lung and heart (Zhu *et al*., 2004).

We have chosen to use Tf as a targeting ligand over the anti-TfR antibodies (OX26, 8D3) due to three major reasons. Firstly, anti-TfR antibodies led to gene expression in all the TfR-rich organs like liver, lungs and spleen without distinguishing TfR1 and TfR2. TfR1 is expressed at low levels in most tissues, but highly expressed on the vascular endothelial cells of the brain capillaries that contribute to BBB (Jefferies *et al*., 1984). By contrast, α-transcript product of TfR2 is mostly expressed on hepatocytes, while its β-transcript is present on a wide range of tissues but at very low levels. In

addition, TfR1 has 25-fold higher affinity for Tf than TfR2, which will not be the case if anti-TfR antibodies were used (Kawabata *et al*., 2000). It has been argued that the high plasma concentration of endogenous Tf leads to the saturation of TfR on the brain microvessels, leading to inefficiency of Tf as a brain targeting ligand. In this study, the amount of Tf injected as DAB-Tf was much higher than the endogenous amount of Tf in the plasma (2.68 µg, corresponding to an endogenous plasma concentration of 25 µM (Seligman, 1983), which limited the risk of competition for binding to the TfR. Another reason is that it has been shown in various studies that anti-TfR antibodies are unable to mediate the actual crossing of the endothelial cell layer of the BBB, leading to capture of antibodies in the brain vasculature. Capillary depletion studies and morphological examinations of the brain section suggest that most of the OX26, an anti-TfR antibody was captured in brain capillaries throughout the parenchyma after intravenous administration (Moos and Morgan, 2001). Similar results were obtained using OX26 immunoliposomes and 8D3 anti-TfR antibody (Gosk *et al.,* 2004, Paris-Robidas, 2011). Moreover, there is a huge difference in the affinity of TfR towards antibody and Tf. The TfR-antibody is a high affinity receptor-antibody reaction that is not easily reversed however TfR-Tf reaction is readily reversible, depending on the pH and the iron content of the Tf. This questions the ability of the anti-TfR antibodies to get released from the receptor within endosomes to reach the post-capillary brain compartment (Morgan, 1996). Lastly, OX26 and 8D3 are mAbs originated from mice and rat respectively. They might have a completely different binding affinity to

human TfR and may generate an immunological response due to its animal origin.

In conclusion, we have demonstrated that Tf-bearing DAB polypropylenimine dendrimer led to an increased gene expression in the brain, which was at least 3-fold higher than in any tested peripheral organs. Tf-bearing DAB dendrimer is therefore a highly promising delivery system for gene delivery to the brain and will be further investigated to optimize its therapeutic potential.

CHAPTER 4

Lactoferrin- and Lactoferricin- bearing polypropylenimine dendrimers for targeted gene delivery to the brain

1. Introduction

Lactoferrin (Lf) belongs to the transferrin family of iron-binding glycoproteins weighing approximately 80 KDa. The three dimensional structure of Lf is similar to other proteins of the transferrin family, except a highly positive-charged N-terminal region. It is a globular protein consisting of two homologous iron-binding lobes. Each of these lobes can bind to one Fe^{3+} ion. Various biological functions of Lf include iron homeostasis, cell growth and differentiation, immunity against microbial infection, anti-inflammatory activity and protection against cancer (Ward *et al*., 2005). Lactoferricin (Lfc) is a peptide residue that can be produced by proteolysis of Lf by pepsin in acidic conditions. The two most investigated Lfc peptides are bovine Lfc (bLfc) and human Lfc (hLfc). Both these peptides are highly positive charged, but there are considerable differences in their structure. The primary structure of bLfc is a 25-residue peptide, obtained from bovine Lf (17-41 peptides) that forms a loop structure through a disulfide intramolecular bond, whereas the exact structure of hLfc is still controversial and is thought to be consisting of 47- to 49- residue peptide obtained from human Lf. Lfc is believed to have anti-microbial, antifungal, anti-parasitic, anti-viral, anti-tumour and immune-modulatory properties (Gifford *et al*., 2005).

Several studies demonstrate the presence of specific Lf receptors (LfR) in the brain. It has been documented *in vitro* and *in vivo* that receptor-mediated endocytosis is the major mechanism for the transport of Lf across the BBB. Huang and colleagues characterized LfR on the BBB, exhibiting two binding

sites, a high affinity (dissociation constant (K_d) = 6.8 nM) and low affinity (K_d = 4815 nM). The plasma concentration of the endogenous Lf is 5nM, which is much lower than the K_d of the LfR on the BBB. This makes Lf more interesting for delivering therapeutics across the BBB compared to Tf, which has a higher endogenous plasma concentration (Huang *et al*., 2007b).

LfR has recently been exploited for targeted delivery of therapeutics to the brain. Liposomes, polymerosomes, cyclodextrin nanocarriers and polylactic acid nanoparticles have been modified with Lf for targeted delivery of drugs to brain (Hu *et al*., 2009, Chen *et al*., 2010, Gao *et al*., 2010, Ye *et al*., 2013). Lf-conjugated PAMAM dendrimers have demonstrated targeted gene delivery to the brain after intravenous administration. The brain uptake of the Lf-conjugated PAMAM dendrimers and the subsequent gene expression was much higher to that observed with unconjugated PAMAM dendrimers (Huang *et al*., 2008).

We have recently demonstrated that Lf-bearing DAB dendrimer (DAB-Lf) was able to increase the cellular uptake and gene expression of DNA by cancer cells compared to non-targeted delivery systems, *in vitro* and *in vivo* (Lim *et al*., 2015). The treatment was well tolerated by the animals, with no apparent signs of toxicity.

2. Aims and Objectives

On the basis of the fact that LfR are highly expressed on the BBB, we now hypothesize whether conjugation of Lf to DAB dendrimer leads to increased gene expression in the brain. The main objectives of this chapter are:

- The synthesis and characterization of Lf-bearing DAB dendrimer
- The evaluation of the brain targeting efficacy of DAB-Lf *in vitro* and *in vivo*

3. Results

3.1. Synthesis and characterization

3.1.1. Conjugation of lactoferrin and lactoferricin to DAB

The synthesis of DAB-Lf and DAB-Lfc was confirmed by ^{1}H NMR (Figure 4.1). 1H NMR (D_2O): δ DAB (H_2N-C***H₂***-CH_2-) = 2.58; DAB (-N-C***H₂***-CH_2-) = 2.45; DAB (-CH_2-C***H₂***-CH_2-)=1.60; DAB-Lf/Lfc (Lf/Lfc-HN-**CH_2**-CH_2-) = 3.68 DAB-Lf/Lfc (H_2N-**C*H₂***-CH_2-CH_2-N-) = 2.78; DAB-Lf/Lfc (-N-**C*H₂***-CH_2-CH_2-) = 2.38-2.70; DAB-Lf/Lfc (-N-CH_2-C***H₂***-CH_2-) = 1.74. The characteristic triplet peak for the CH_2 adjacent to peripheral primary amino group of DAB at 2.58 was shifted to 3.68 ppm in the NMR spectrum of a conjugated DAB- Lf/Lfc analogue. The ratio of the integrals of resonances at ca. 3.68 and 2.78 for methylene units (**d** and **a**) attached to the amino acid moiety via DMSI linkage and unbound free amine, respectively is 1. This supports that 50 % of the surface primary amine groups on the DAB are conjugated to lactoferrin or lactoferricin. The proposed structure of the final product (DAB-Lf or DAB-Lfc) is shown in Figure 4.2.

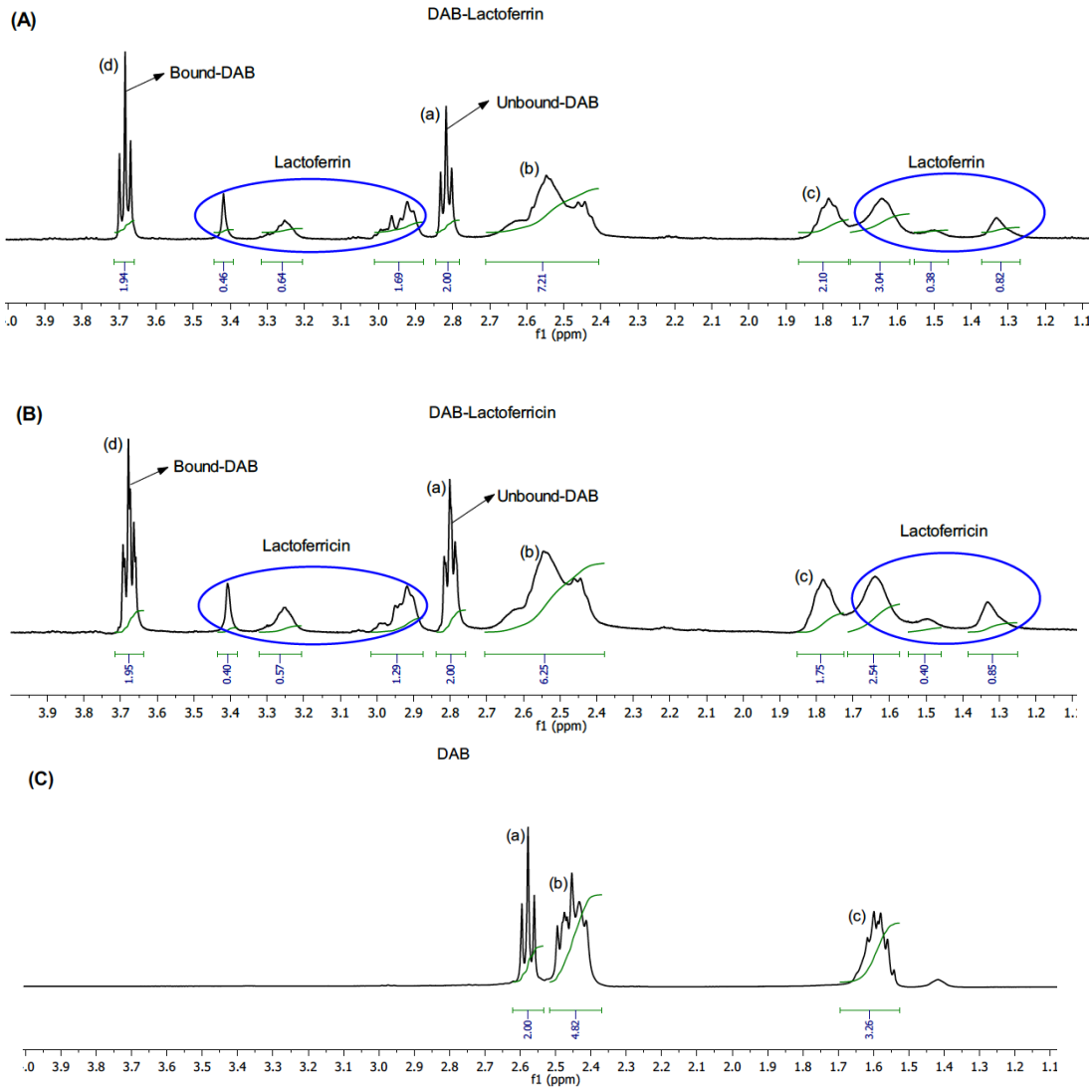

Figure.4.1 ^{1}H NMR spectra (400 MHz) of DAB-Lf (A), DAB-Lfc (B) and DAB (C) in D_2O.

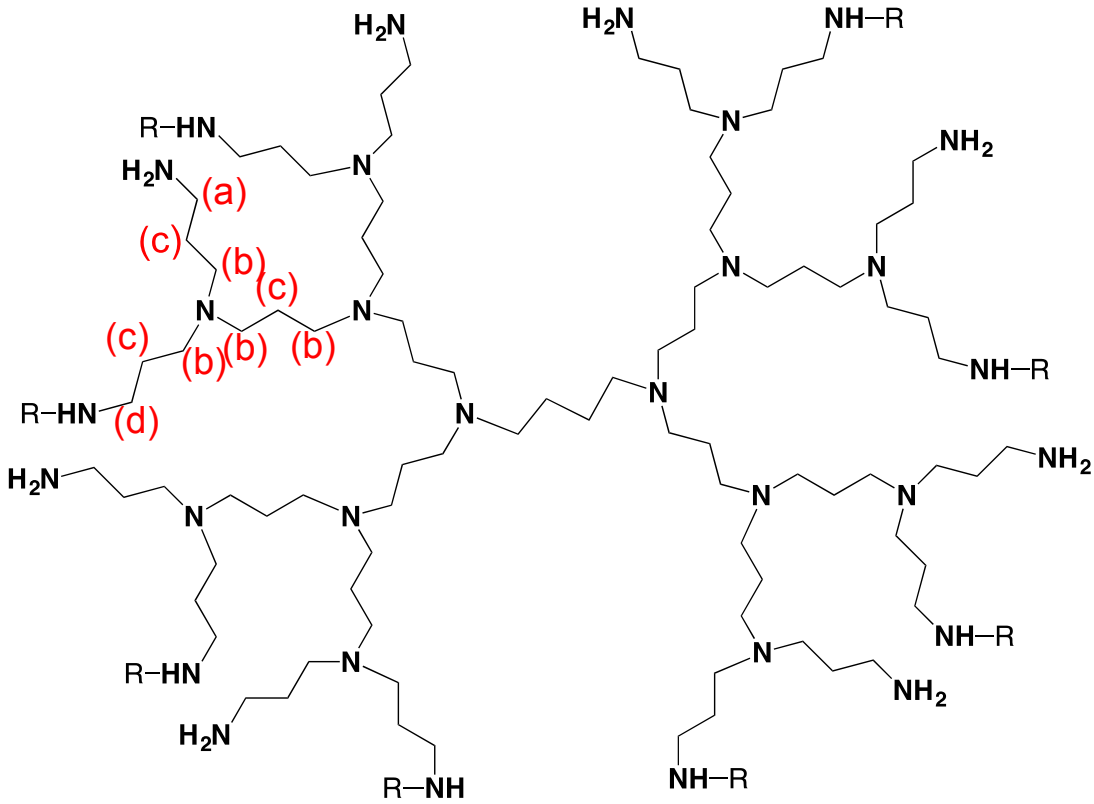

Figure.4.2 Protons of DAB conjugated to Lactferrin/ Lactoferricin (R=DMSI-Lactoferrin/Lactoferricin)

Table 4.1 Positions of various protons of DAB, DAB-Lf and DAB-Lfc in D_2O as depicted by ^1H NMR (400 MHz)

Positions of various protons	DAB	DAB-Lf	DAB-Lfc
(H_2N-C***H₂***-CH_2-) or (a)	2.58	2.78	2.78
(-N-C***H₂***-CH_2-) or (b)	2.45	2.38-2.70	2.38-2.70
(-CH_2-C***H₂***-CH_2-) or (c)	1.60	1.74	1.74
(Lf/Lfc-HN-**C*H₂***-CH_2-) or (d)	-	3.68	3.68

3.1.2. Characterization of dendriplex formation

DAB-Lf and DAB-Lfc were able to condense more than 80% and 90% of the DNA, respectively, at dendrimer: DNA weight ratios of 2:1 or higher (Figure 4.2). DNA condensation occurred almost instantaneously and was found to be stable over at least 24h. It increased with increasing weight ratios and was almost complete at a dendrimer: DNA weight ratio of 20:1 for DAB-Lfc dendrimer. The DNA condensation observed for dendrimer: DNA a weight ratio of 2:1 or higher was much higher than that observed for the unmodified dendrimer, which was of 60% at its best and decreasing with time.

The formation of spherical nanoparticles of DAB-Lf and DAB-Lfc dendriplexes was also demonstrated by transmission electron microscopy (Figure 4.3). These results demonstrated that DAB-Lf and DAB-Lfc could condense DNA via electrostatic interactions between the positively charged dendrimer and the negatively charged DNA. An excess of dendrimer was however required to ensure efficient DNA condensation.

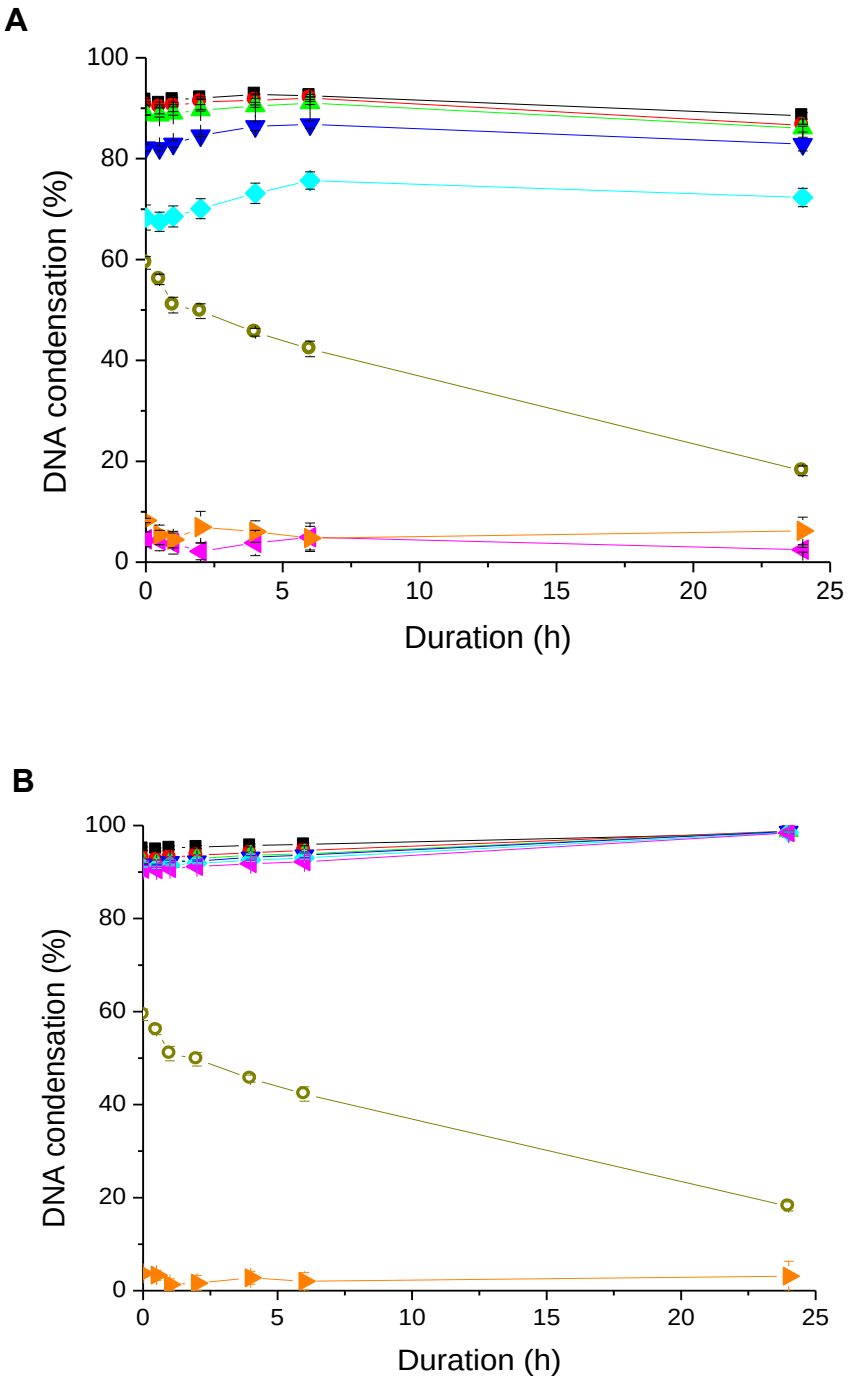

Figure 4.3 DNA condensation of DAB-Lf **(A)** and DAB-Lfc **(B)** dendriplexes using PicoGreen® reagent at various durations and dendrimer: DNA weight ratios : 20:1 (■, black), 10:1 (●, red), 5:1 (▲, green), 2:1 (▼, blue), 1:1 (♦, cyan), 0.5:1 (◄, pink), DNA only (►, orange) (empty symbol, dark yellow : DAB-DNA, dendrimer: DNA weight ratio: 5:1) . Results are expressed as mean ± SEM (n= 4)

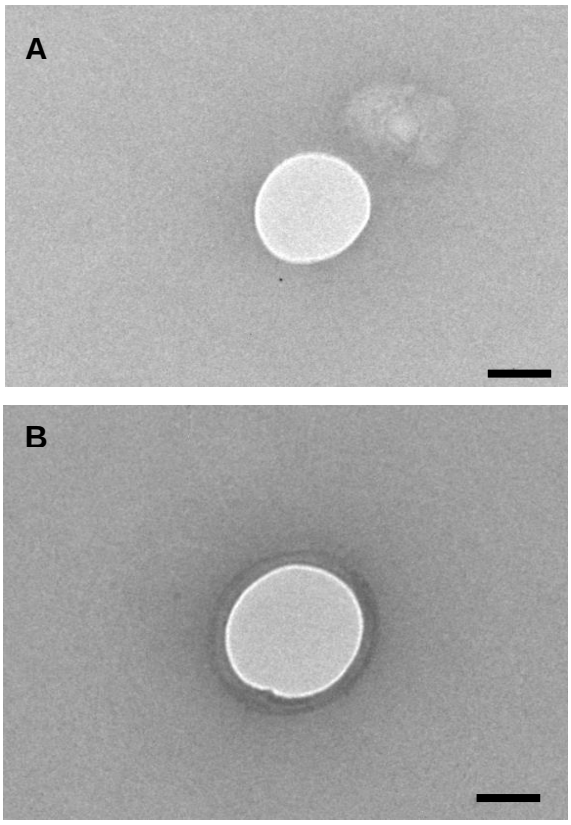

Figure 4.4 Transmission electron micrographs of a) DAB-Lf and b) DAB-Lfc dendriplexes (Bar: 100 nm).

3.1.3. Dendriplex size and zeta potential measurement

DAB-Lf and DAB-Lfc dendriplexes displayed average sizes less than 300 nm, at all weight ratios tested (Figure 4.4 A). The increase of dendrimer: DNA weight ratios did not have a significant impact on the dendriplexes size. Among the two tested targeted dendrimers, DAB-Lf dendriplex at a dendrimer: DNA weight ratio of 2:1 was found to be the largest, with an average size of 260 ± 18 nm. In contrast, DAB-Lf dendriplex at a dendrimer: DNA ratio of 0.5:1 was the smallest, with an average size of 208 ± 15 nm.

Zeta potential experiments demonstrated that DAB-Lf and DAB-Lfc dendriplexes were bearing a positive surface charge at all dendrimer: DNA weight ratios (Figure 4.4 B). The zeta potential values of DAB-Lf dendriplex reached their maximum (35 ± 2 mV) at a weight ratio of 2, before decreasing with increasing weight ratios and finally reaching their minimum (23 ± 1 mV) at a weight ratio of 20. The zeta potential values of DAB-Lfc followed a similar pattern, namely reaching a maximum (33 ±1 mV) at a weight ratio of 1 and then decreasing with increasing weight ratios to attain the same value as for DAB-Lf dendriplex (23 ± 6 mV at a weight ratio of 20).

A)

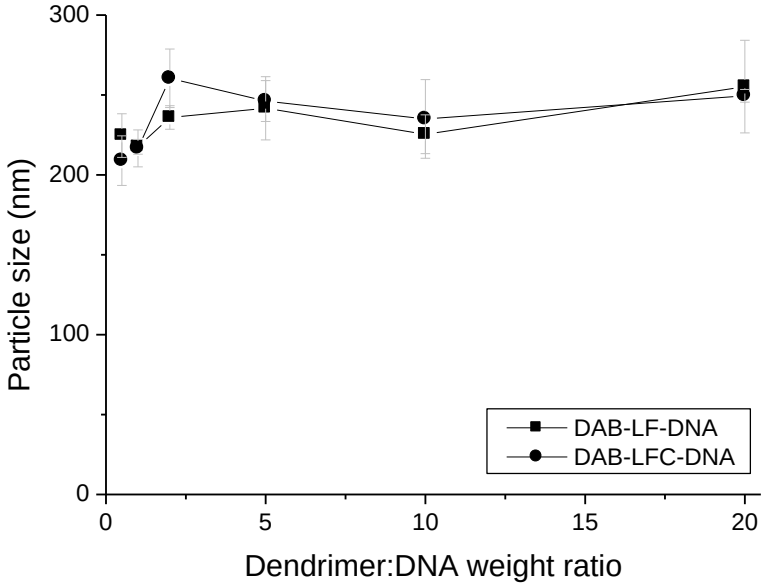

B)

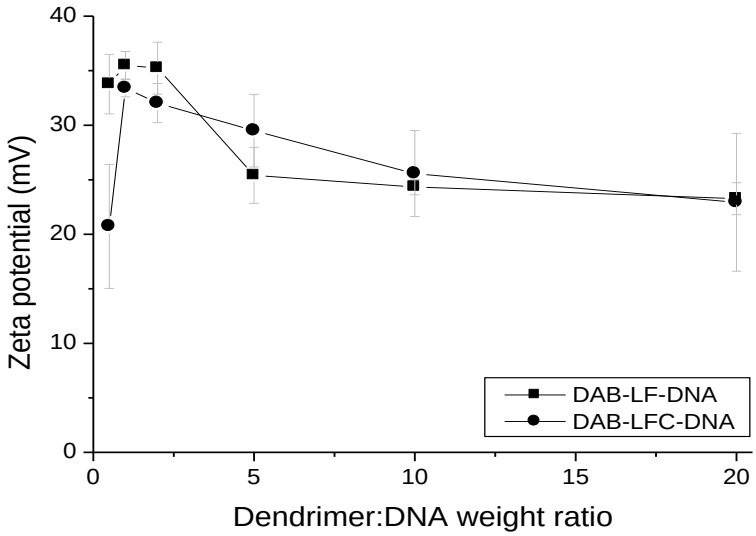

Figure 4.5 Size (A) and Zeta Potential (B) of DAB-Lf and Lfc dendriplexes at various dendrimer: DNA weight ratios: 20:1, 10:1, 5:1, 2:1, 1:1, and 0.5:1. Results are expressed as mean± SEM (n=4).

A)

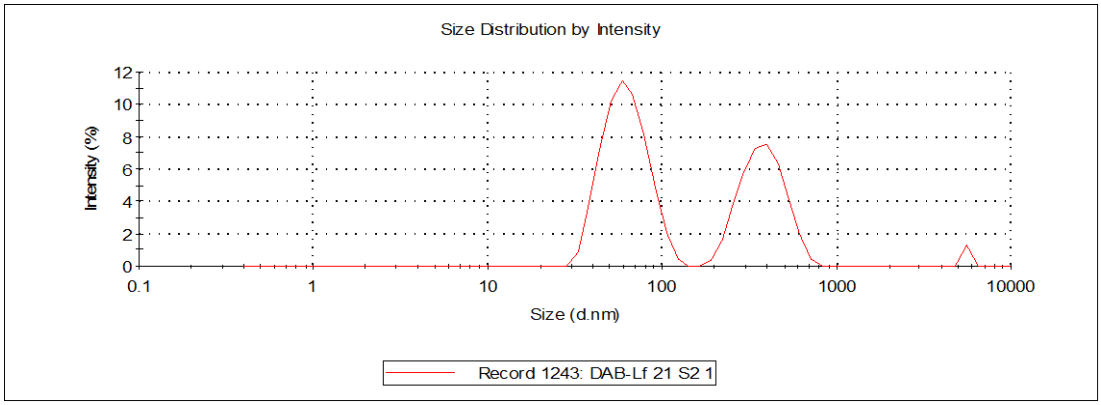

B)

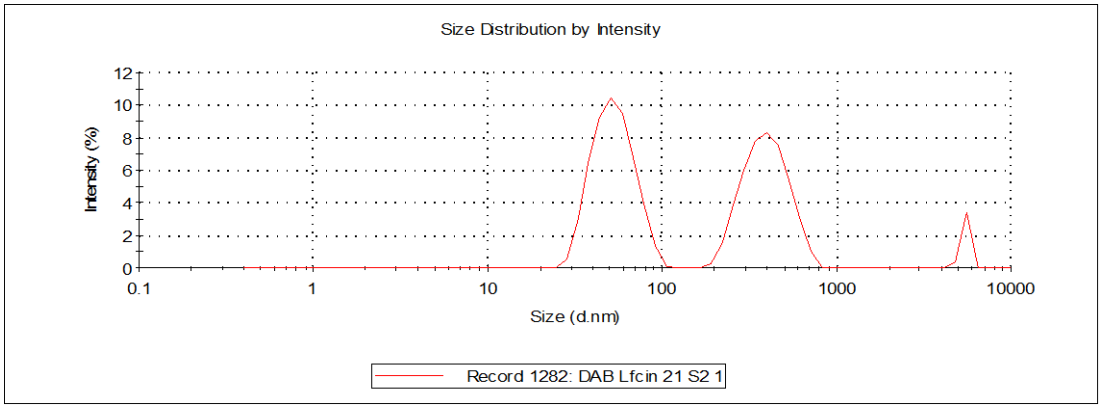

Figure 4.6 Size distribution by intensity of DAB-Lf (A) and DAB-Lfc dendriplexes at dendrimer:DNA weight ratios of 2:1.

3.2. *In vitro* studies

3.2.1. Transfection

The conjugation of Lf and Lfc to DAB dendriplex led to an increased transfection compared to DAB dendriplex on bEnd.3 cells (Figure 4.5). The treatment of bEnd.3 cells with DAB-Lf dendriplex and DAB-Lfc dendriplex led to a 2.1-fold and 1.5-fold increase in the gene expression compared to DAB dendriplex respectively ($6.01x10^{-3} \pm 0.42x10^{-3}$ U/mL, $4.45x10^{-3} \pm 0.33x10^{-3}$ and $2.85x10^{-3} \pm 0.21x10^{-3}$ U/mL respectively for DAB-Lf, DAB-Lfc and DAB dendriplexes). Gene expression following treatment with DAB-Lf dendriplex and DAB-Lfc dendriplex was 7-fold and 5.2-fold higher than that observed following treatment with naked DNA ($0.85x10^{-3} \pm 0.01x10^{-3}$ U/mL). The cells treated with naked DNA did not demonstrate any significant increase in the gene expression compared to untreated cells.

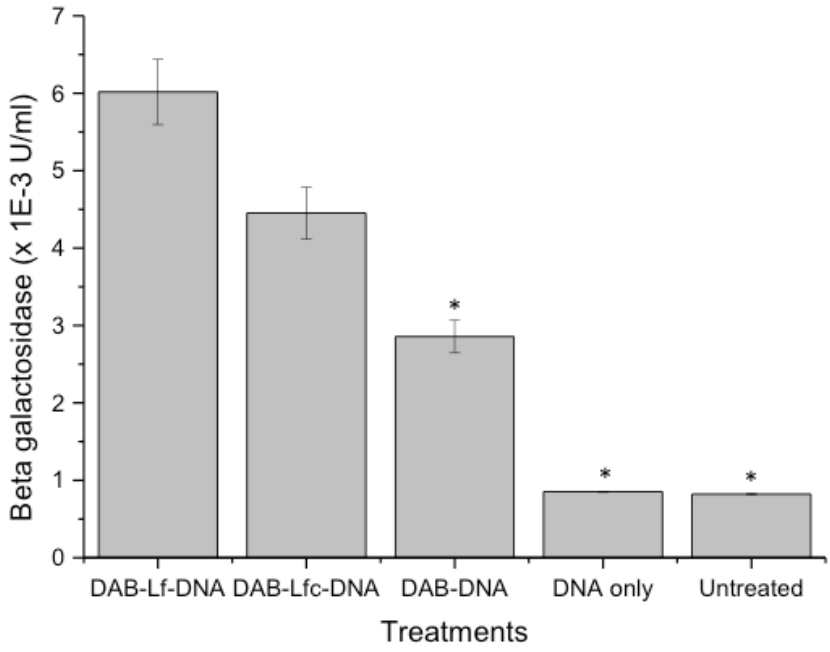

Figure 4.7 Transfection efficacy of DAB-Lf, DAB-Lfc and DAB dendriplexes in bEnd.3 cells. DAB-Lf, DAB-Lfc and DAB dendriplexes were dosed at their optimal dendrimer: DNA ratio of 2:1, 2:1 and 5:1 respectively. Results are expressed as the mean ± SEM of three replicates (n=15). * : P <0.05 compared with DAB-Lf-DNA and DAB-Lf-DNA.

3.2.2. Cellular uptake

The uptake of fluorescein-labelled DNA complexed to DAB-Lf and DAB-Lfc by bEnd.3 cells was qualitatively analysed by epifluorescence microscopy. Treatment with DAB-Lf and DAB-Lfc dendriplex did not demonstrate any cellular uptake of fluorescein-labelled DNA until 2 hours, when most pronounced uptake was observed (Figure 4.6 & 4.7).

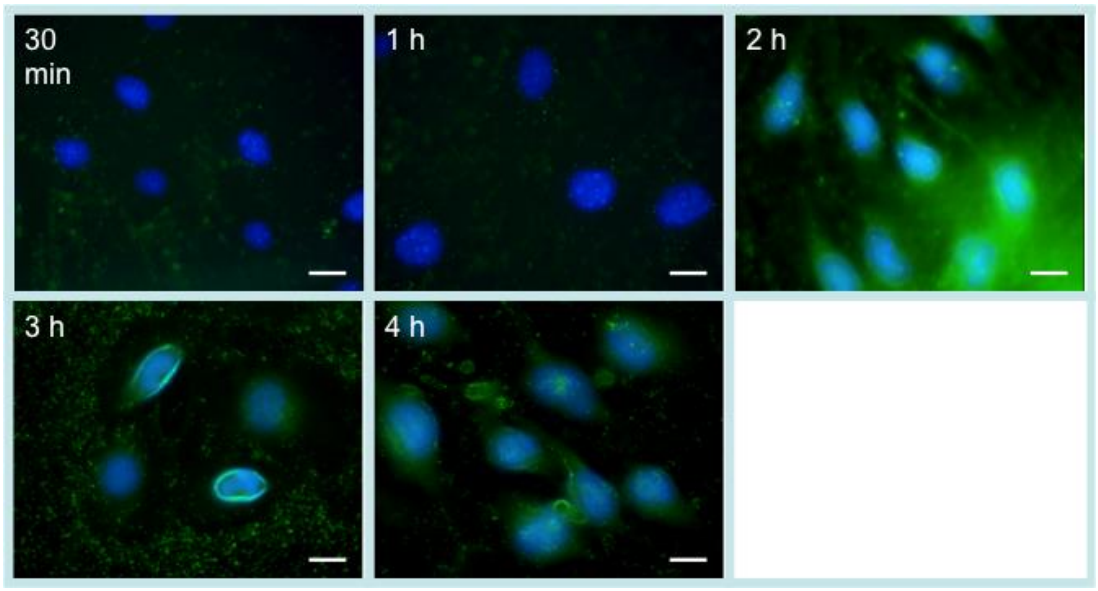

Figure 4.8 Epifluorescence microscopy imaging of the cellular uptake of Fluorescein- labelled DNA (2.5 µg/ well) complexed with DAB-Lf, after incubation for 30 min, 1 h, 2 h, 3 h or 4 h with bEnd.3 cells (Blue: nuclei stained with DAPI (excitation: 405 nm, emission bandwidth: 415-491 nm), green: Fluorescein-labelled DNA (excitation: 543 nm, emission bandwidth: 550-620 nm) (Bar: 10 µm)

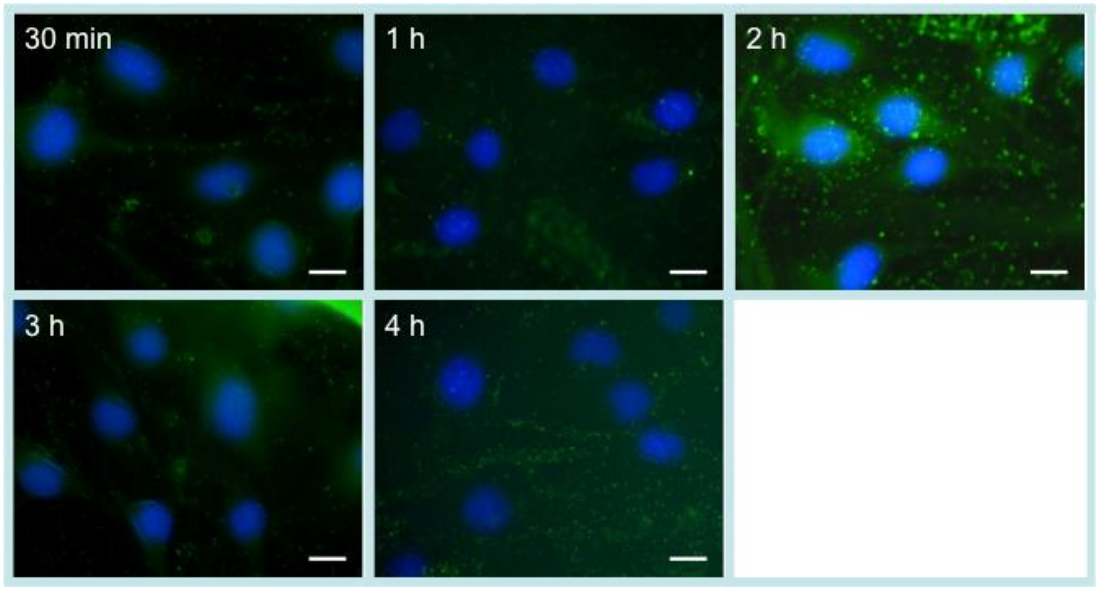

Figure 4.9 Epifluorescence microscopy imaging of the cellular uptake of fluorescein-labelled DNA (2.5 µg/ well) complexed with DAB-Lf, after incubation for 30 min, 1 h, 2 h, 3 h or 4 h with bEnd.3 cells (Blue: nuclei stained with DAPI (excitation: 405 nm, emission bandwidth: 415-491 nm), green: Fluorescein-labelled DNA (excitation: 543 nm, emission bandwidth: 550-620 nm) (Bar: 10 µm)

Following optimization of the duration of the maximum cellular uptake, bEnd.3 cells were treated with fluorescein-labelled DNA complexed to DAB-Lf, DAB-Lfc, DAB or in solution for 2 hours. Pronounced uptake of fluorescein-labelled DNA complexed to DAB-Lf and DAB-Lfc was observed. On the contrary, cells treated with DAB dendriplex or fluorescein-labelled DNA solution did not show any fluorescein-derived fluorescence (Figure 4.8).

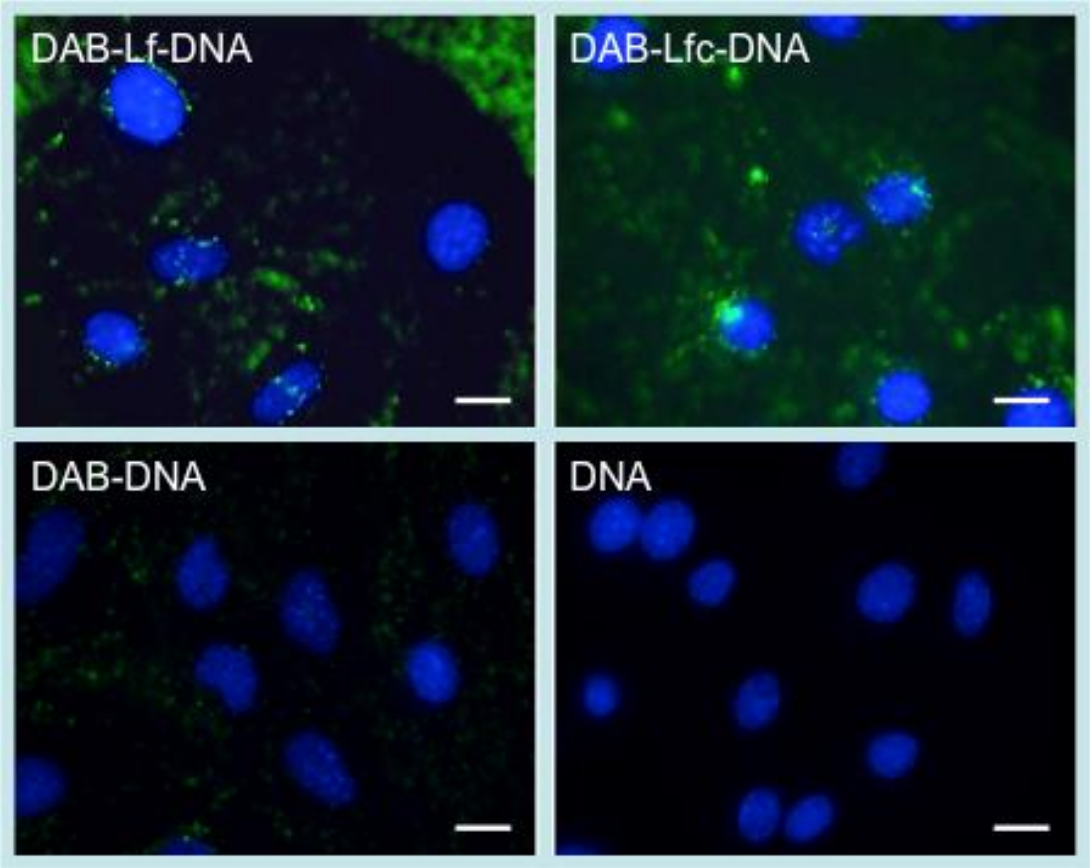

Figure 4.10 Epifluorescence microscopy imaging of the cellular uptake of fluorescein- labelled DNA (2.5 µg/ well) either complexed with DAB-Lf, DAB-Lfc, DAB or in solution, after incubation for 2 hours with bEnd.3 cells (Blue: nuclei stained with DAPI (excitation: 405 nm, emission bandwidth: 415-491 nm), green: Fluorescein-labelled DNA (excitation: 543 nm, emission bandwidth: 550-620 nm) (Bar: 10 µm).

The quantification of the cellular uptake was done utilizing flow cytometry (Figure 4.9). Cellular fluorescence following treatment with DAB-Lf dendriplex (20249 ± 649 arbitrary units (a.u.)) was 2.1-fold and 4.1-fold higher that that observed after treatment with DAB dendriplex (9368 ± 383 a.u.) and DNA solution (4839 ± 59 a.u.). It was 2-fold and 3.8-fold higher in case of DAB-Lfc dendriplex (18824 ± 1237 a.u.) when compared to DAB dendriplex and DNA solution.

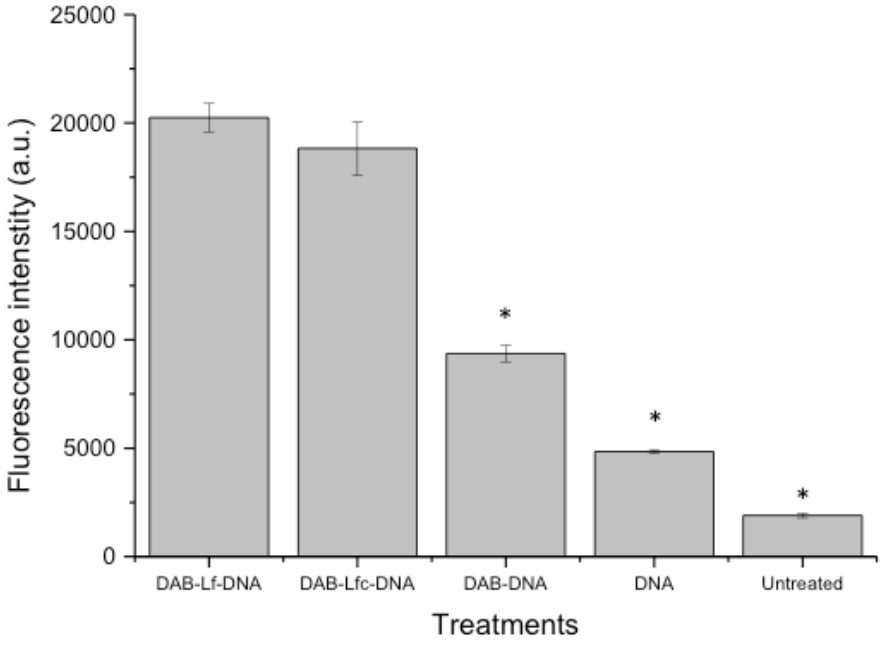

Figure 4.11 Flow cytometry quantification of the cellular uptake fluorescein-labelled DNA (5 µg/ well) either complexed with DAB-Lf, DAB-Lfc, DAB or in solution, after incubation for 2 hours with bEnd.3 cells (n=5) * : P <0.05 compared with DAB-Lf-DNA and DAB-Lfc-DNA

3.2.3. Inhibitor studies

The mechanisms of cellular uptake of the DNA complexed to DAB-Lf and DAB-Lfc were elucidated by utilising cellular uptake inhibitors and escalating concentrations of Lf or Lfc.

Pre-treatment of the bEnd.3 cells with increasing concentrations of free Lf (0 µM, 2.5 µM, 5 µM, 7.5 µM, 10 µM, 12.5 µM, 15 µM, 17.5 µM and 20 µM) significantly decreased the cellular uptake of fluorescein-labelled DNA complexed to DAB-Lf at concentrations as low as 2.5 µM and remained at similar levels up to 17.5 µM. (Figure 4.10 A & 4.11 A). At Lf concentration of 20 µM, the cellular uptake of fluorescein-labelled DNA was 4.3-fold lower than that observed with DAB-Lf dendriplex without pre-Lf treatment (respectively 4665 ± 96 a. u. and 20249 ± 649 a. u.).

The cellular uptake of fluorescein-labelled DNA complexed to DAB-Lf was inhibited by phenylarsine oxide, filipin, colchicine and poly-L-lysine (Figure 4.10 B & 4.11 B). Phenylarsine oxide caused the most significant inhibition, with a cellular uptake respectively decreased by 8.2-fold compared to that observed with DAB-Lf dendriplex without inhibitory treatment (2450 ± 71.56 a.u. following pre-treatment with phenylarsine oxide). Filipin and Colchicine appear to be partial inhibitors, leading to a cellular uptake decrease by respectively 2-fold and 2.1-fold compared to DAB-Lf dendriplex without pre-treatment (respectively 9773 ± 199 a. u. and 9579 ± 89 a.u. following pre-treatment with filipin and colchicine). Poly-L-Lysine caused the least inhibition

with 1.2-fold decrease in the cellular uptake (15764 ± 690 a.u following pre-treatment with poly-L-Lysine).

A)

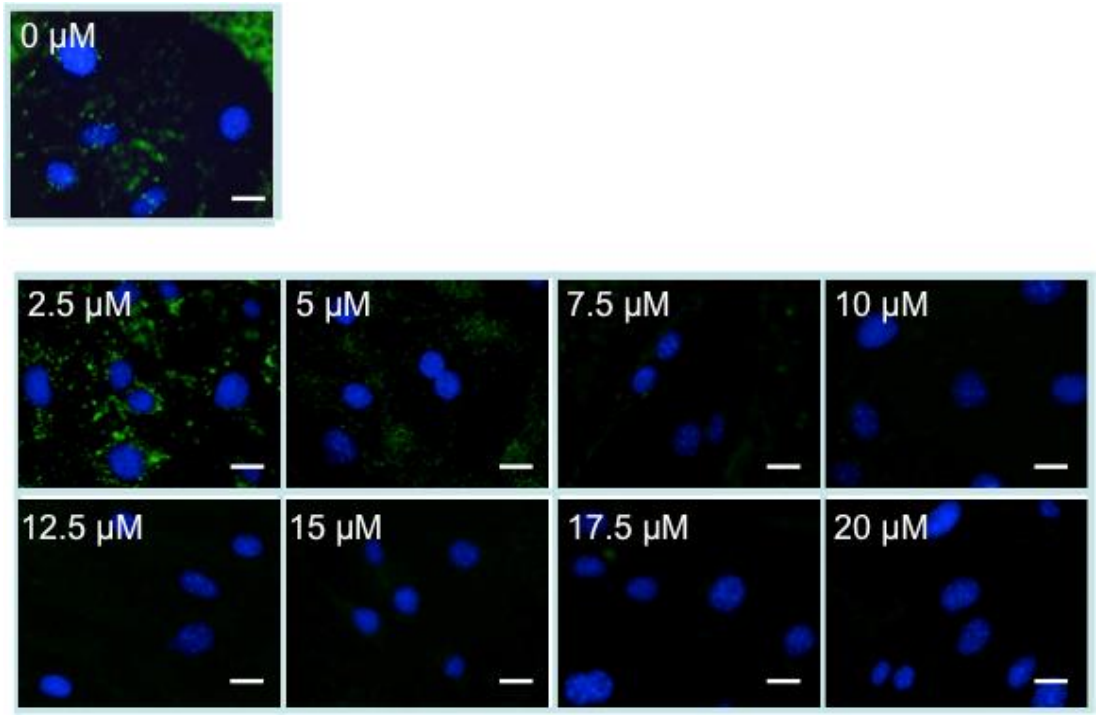

B)

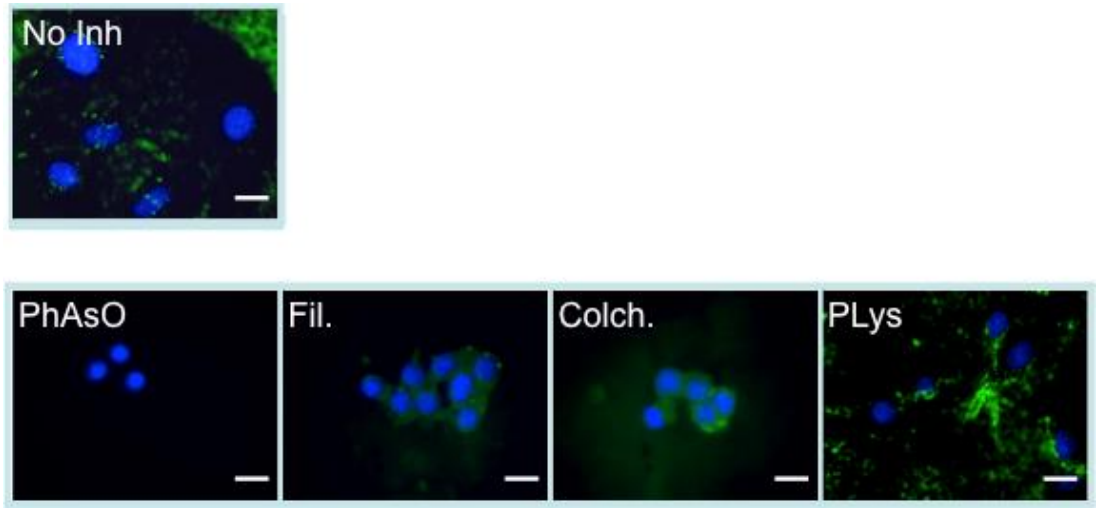

Figure 4.12. Epifluorescence microscopy imaging of the bEnd.3 cellular uptake of Fluorescein- labelled DNA (2.5 µg/ well) complexed with DAB-Lf **(A)** following pre-treatment with various concentrations of free Lf (ranging from 2.5 µM to 20 µM) and **(B)** following pre-treatment with various cellular uptake inhibitors: phenylarsine oxide ("PhAsO"), filipin ("Fil."), colchicine ("Colch.") and poly-L-lysine ("PLys"). (Blue: nuclei stained with DAPI (excitation: 405 nm, emission bandwidth: 415-491 nm), green: Cy3-labelled DNA (excitation: 543 nm, emission bandwidth: 550-620 nm) (Bar: 10 µm).

A)

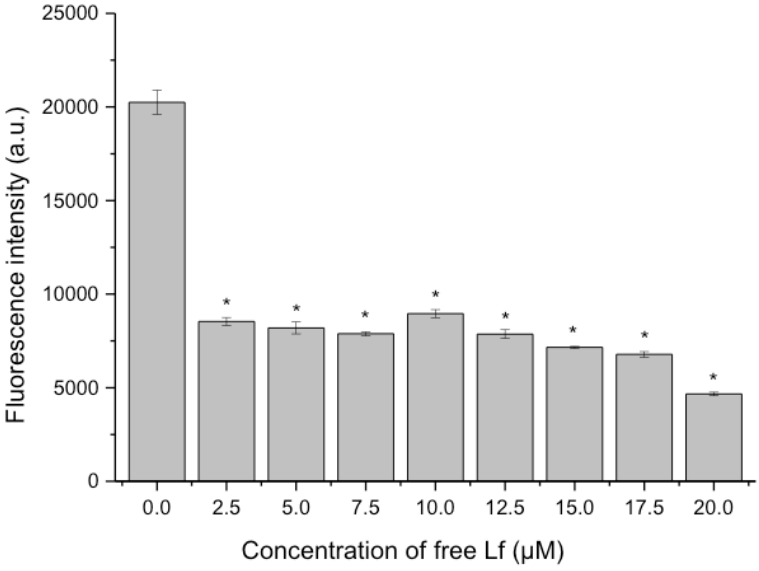

B)

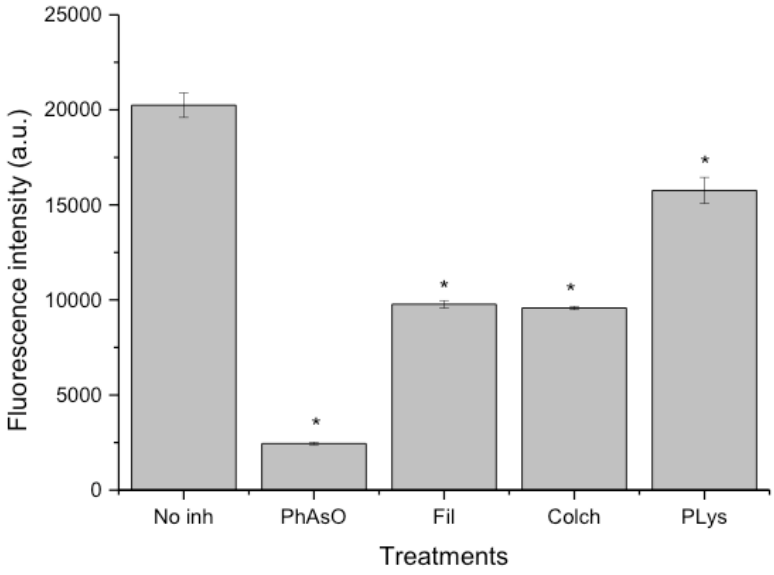

Figure 4.13 Flow cytometry quantification of the bEnd.3 cellular uptake of fluorescein- labelled DNA (5 μg/ well) complexed with DAB-Lf, **(A)** following pre-treatment with various concentrations of free Tf (ranging from 2.5 μM to 20 μM) and **(B)** following pre-treatment with various cellular uptake inhibitors: phenylarsine oxide ("PhAsO"), filipin ("Fil."), colchicine ("Colch.") and poly-L-lysine ("PLys") (n=5), * : P <0.05 compared with DAB-Tf-DNA.

The escalating concentration of the free Lfc (0 µM, 2.5 µM, 5 µM, 7.5 µM, 10 µM, 12.5 µM, 15 µM, 17.5 µM and 20 µM) significantly decreased the cellular uptake of fluorescein-labelled DNA complexed to DAB-Lfc in bEnd.3 cells. The decrease was inversely proportional to the concentration of free Lfc used for pre-treatment (Figure 4.12 A & 4.13 A). At a Lfc concentration of 20 µM, the cellular uptake of fluorescently-labelled DNA was 3.3-fold lower than that observed with DAB-Lfc dendriplex without pre-Lfc treatment (respectively 18824 ± 1237 a. u. and 5658 ± 245 a. u.).

Cellular uptake inhibitors, phenylarsine oxide, filipin, colchicine and poly-L-lysine also led to a significant decrease in the uptake of fluorescein-labelled DNA complexed to DAB-Lfc (Figure 4.12 B & 4.13 B). Most significant inhibition of the cellular uptake was caused by poly-L-Lysine as cellular uptake decreased by 6.9-fold compared to that observed without inhibitory treatment (2703 ± 87 a.u. following pre-treatment with poly-L-Lysine). Phenylarsine oxide and Colchicine appear to be partial inhibitors, leading to a decrease in cellular uptake by respectively 2.5-fold and 2.9-fold compared to DAB-Lfc dendriplex without pre-treatment (respectively 7374 ± 592 a. u. and 6304 ± 169 a.u. following pre-treatment with phenylarsine oxide and colchicine). Fillipin caused the least inhibition with 1.7-fold decrease in the cellular uptake (10943 ± 352 a.u following pre-treatment with poly-L-Lysine).

A)

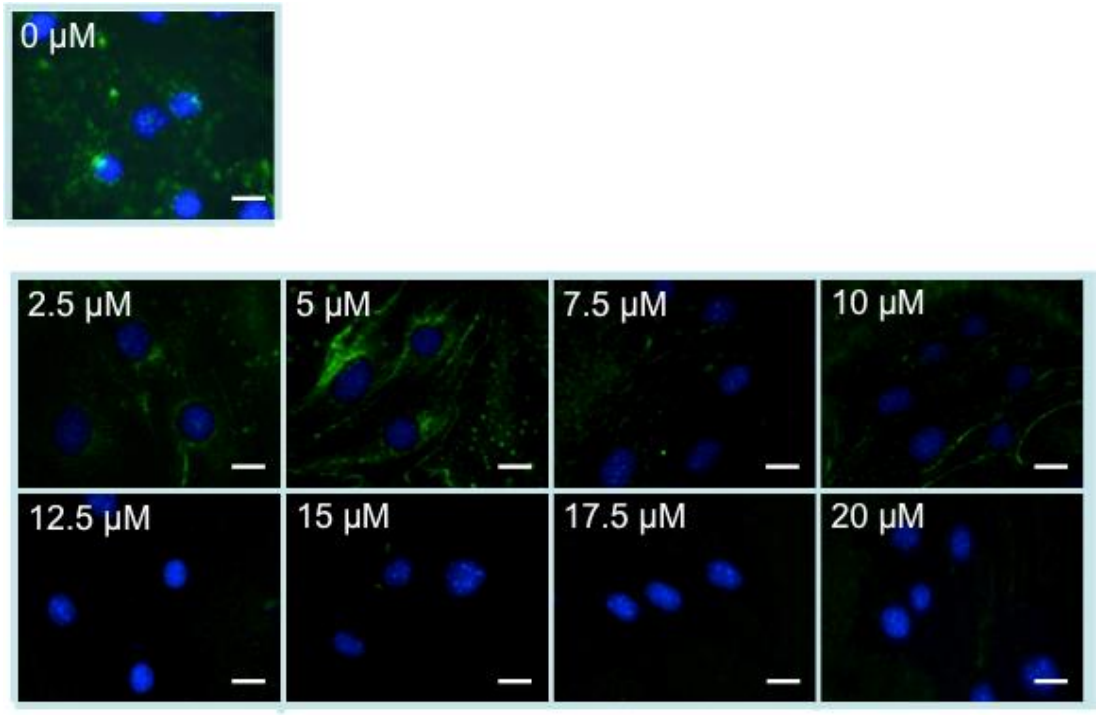

B)

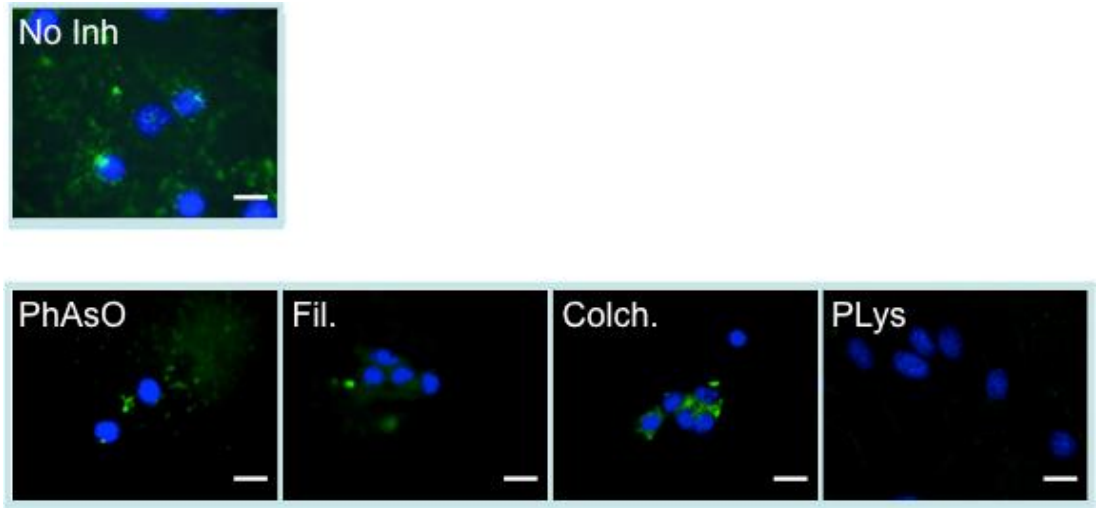

Figure 4.14 Epifluorescence microscopy imaging of the bEnd.3 cellular uptake of fluorescein-labelled DNA (2.5 µg/ well) complexed with DAB-Lfc **(A)** following pre-treatment with various concentrations of free Lfc (ranging from 2.5 µM to 20 µM) and **(B)** following pre-treatment with various cellular uptake inhibitors: phenylarsine oxide ("PhAsO"), filipin ("Fil."), colchicine ("Colch.") and poly-L-lysine ("PLys"). (Blue: nuclei stained with DAPI (excitation: 405 nm, emission bandwidth: 415-491 nm), green: Cy3-labelled DNA (excitation: 543 nm, emission bandwidth: 550-620 nm) (Bar: 10 µm)

A)

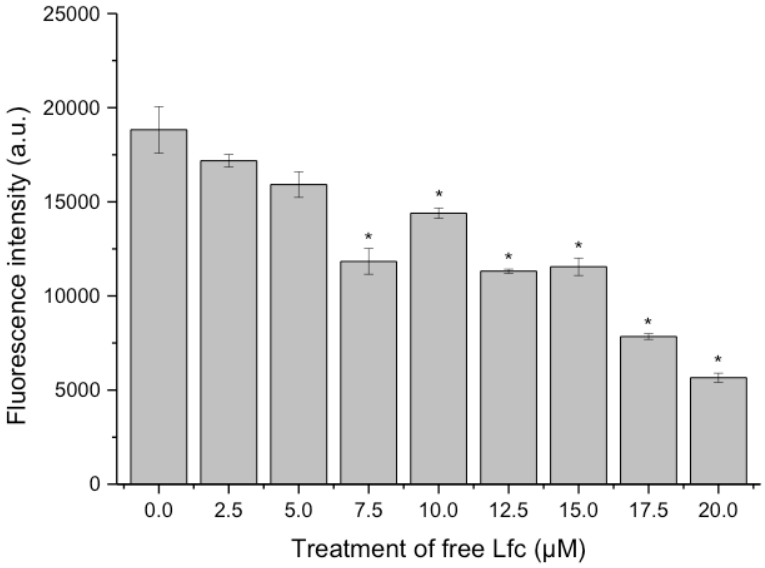

B)

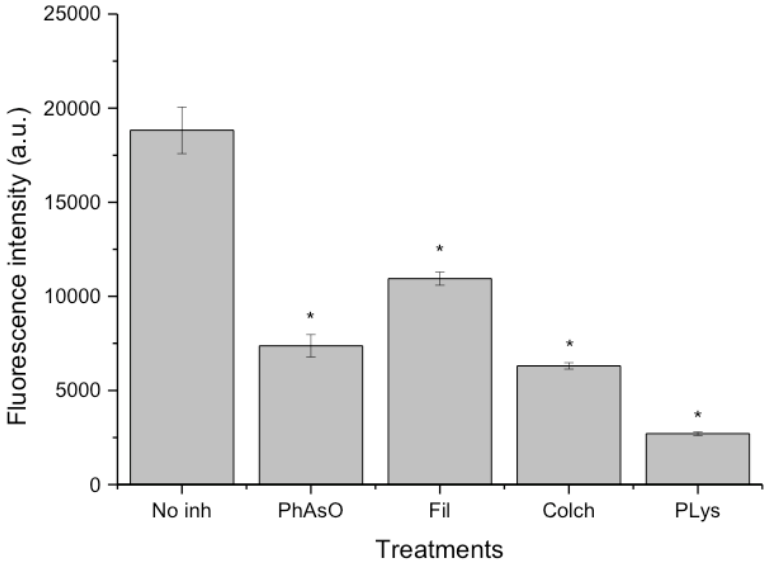

Figure 4.15. Flow cytometry quantification of the bEnd.3 cellular uptake of fluorescein- labelled DNA (5 μg/ well) complexed with DAB-Lf, **(A)** following pre-treatment with various concentrations of free Tf (ranging from 2.5 μM to 20 μM) and **(B)** following pre-treatment with various cellular uptake inhibitors: phenylarsine oxide ("PhAsO"), filipin ("Fil."), colchicine ("Colch.") and poly-L-lysine ("PLys") (n=5), * : P <0.05 compared with DAB-Tf-DNA.

3.3. *In vivo* studies

3.3.1. Biodistribution of gene expression

The biodistribution of gene expression following intravenous injection of DNA encoding luciferase complexed to DAB-Lf and DAB-Lfc was first qualitatively assessed by luminescence imaging, at various treatment durations. Gene expression appeared to be mainly located in the brain of the mice after treatment with DAB-Lf dendriplex. The highest gene expression level was found 24 h following injection of the DAB-Lf dendriplex (Figure 4.14). However no gene expression was observed after treatment with DAB-Lfc dendriplex (Figure 4.15).

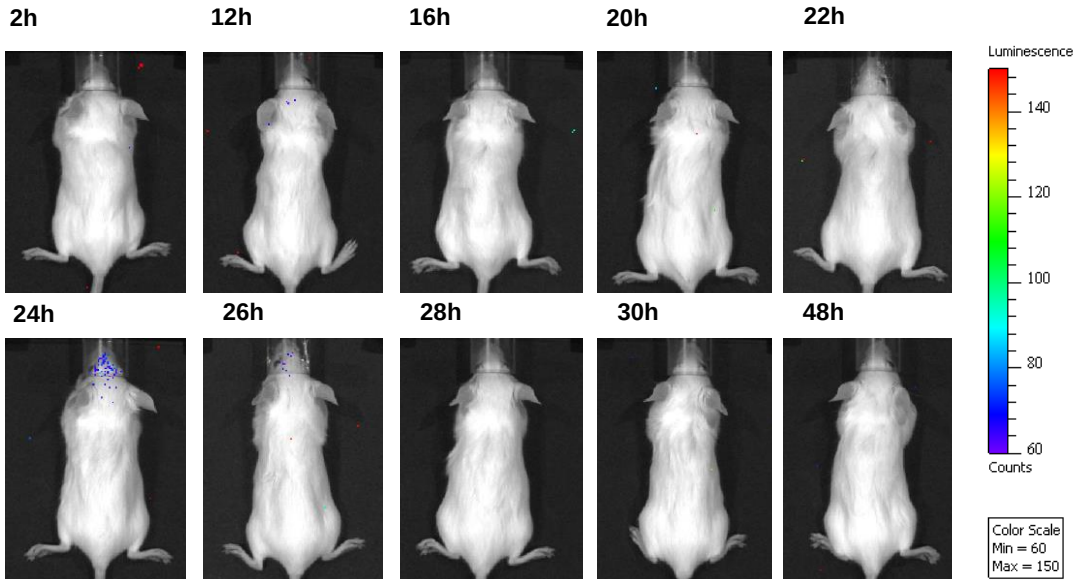

Figure 4.16 Bioluminescence imaging of gene expression after intravenous administration of DAB-Lf dendriplex (50 µg DNA administered). The mice were imaged using the IVIS Spectrum at various durations after injection of the treatment. The scale indicates surface radiance (photons/s/cm^2/steradian).

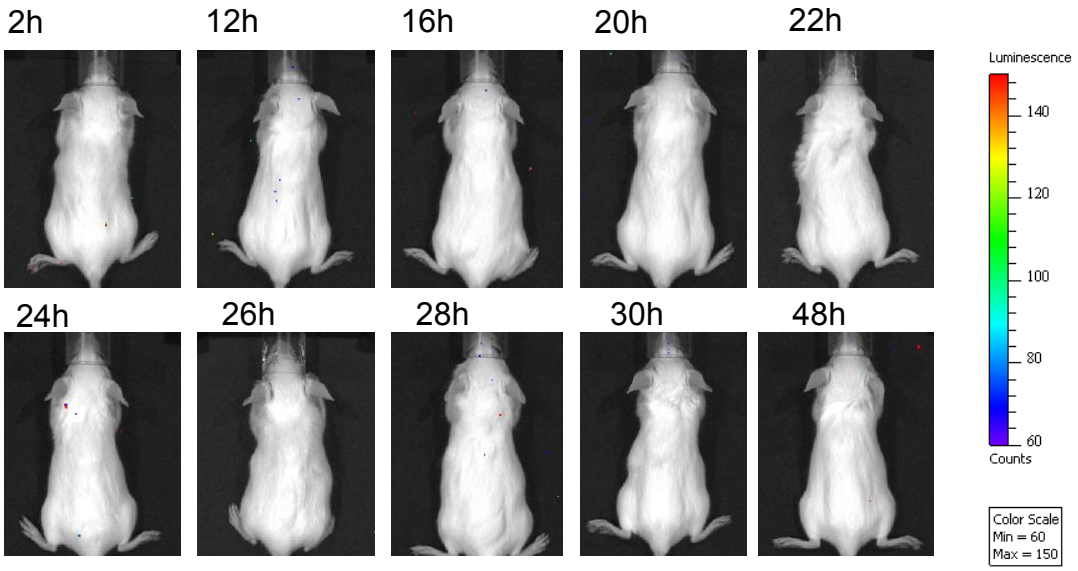

Figure 4.17 Bioluminescence imaging of gene expression after intravenous administration of DAB-Lfc dendriplex (50 µg DNA administered). The mice were imaged using the IVIS Spectrum at various durations after injection of the treatment. The scale indicates surface radiance (photons/s/cm^2/steradian).

Gene expression following intravenous administration of DAB-Lf dendriplex was compared to that observed following administration of DAB dendriplex and DNA only, 24 h after administration of the treatments. The level of gene expression in the brain appeared to be highest following treatment with DAB-Lf dendriplex (Figure 4.16).

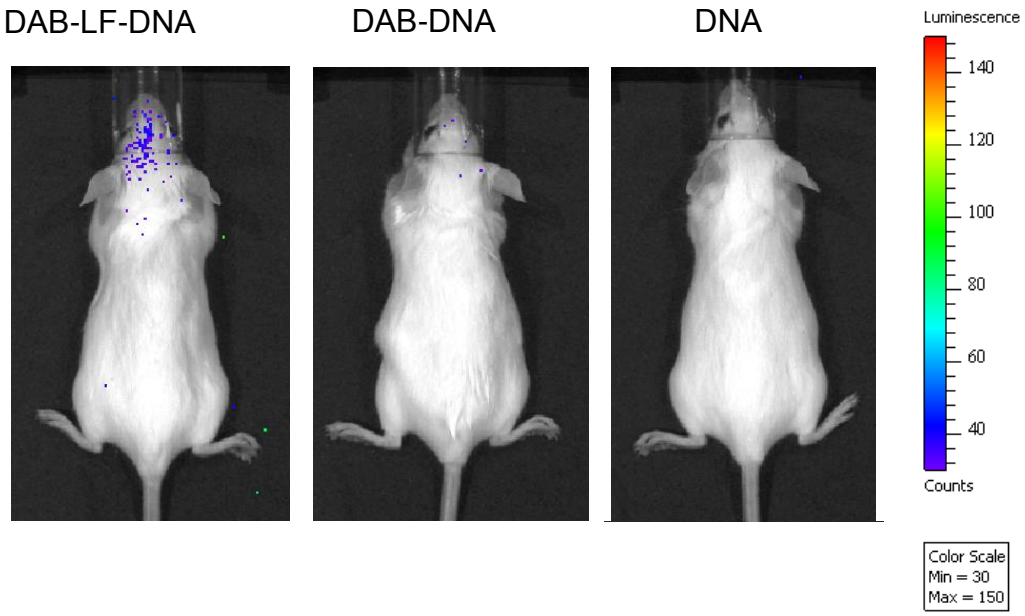

Figure 4.18 Bioluminescence imaging of gene expression after intravenous administration of DAB-Tf and DAB dendriplexes (50 µg DNA administered). (Controls: DNA solution, untreated cells). The mice were imaged using the IVIS Spectrum 24 h after injection of the treatments. The scale indicates surface radiance (photons/s/cm^2/steradian).

These results were confirmed by the quantification of gene expression in the major organs of the mice. After the intravenous administration of DAB-Lf dendriplex in mice, over 6.4-fold increase in gene expression in the brain was observed compared to that of DAB dendriplex (116.1 ± 9.0 mU and 17.9 ± 11.3 mU β-galactosidase per organ respectively for DAB-Lf and DAB dendriplexes) (Figure 4.17). On the contrary, very little gene expression was observed in the brain following intravenous administration of DAB-Lfc dendriplex (Figure 4.17).

There was no significant difference between the levels of β-galactosidase expression in liver and spleen following treatment with DAB-Lf dendriplex, DAB-dendriplex and DNA solution (70.9 ± 14.9 mU, 45.1 ± 9.0 mU and 45.1 ± 6.9 β-galactosidase per organ in the liver for respectively DAB-Lf dendriplex, DAB dendriplex and DNA solution, 17.6 ± 15.0 mU, 33.8 ± 24.3 mU and 10.5 ± 10.5 mU β-galactosidase in the spleen for respectively DAB-Lf dendriplex, DAB dendriplex and DNA solution). In lung, kidneys and heart, a very little amount of β-galactosidase expression was observed following treatment with DAB-Lf dendriplex, whereas DAB dendriplex and DNA solution demonstrated significantly high levels of expression (except heart) (46.30 ± 10.6 mU and 3.5 ± 3.6 mU β-galactosidase per organ in the lung for respectively DAB dendriplex and DNA solution, 28.9 ± 18.7 mU and 41.5 ± 29.1 mU β-galactosidase in the kidneys for respectively DAB dendriplex and DNA) (Figure 4.17).

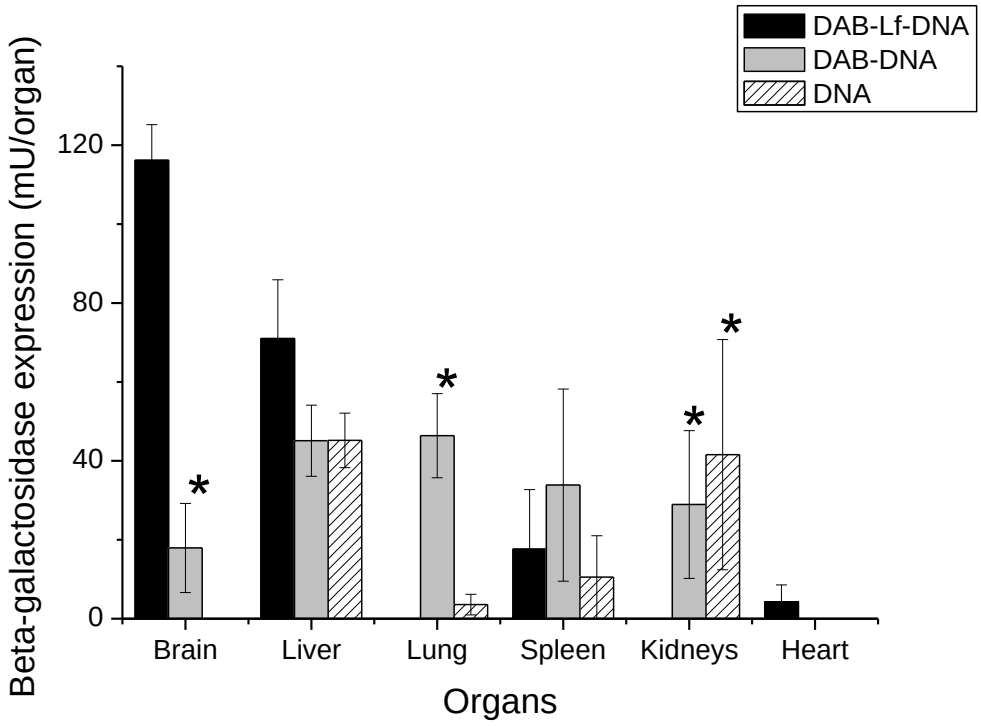

Figure 4.19 Biodistribution of gene expression after a single intravenous administration of DAB-Lf and DAB dendriplexes (50 µg DNA administered). Treatment duration was 24 hours. Results were expressed as milliunits β-galactosidase per organ (n=5). * : P <0.05 compared with DAB-Lf-DNA for each organ

3.3.2. Distribution of gene expression in the brain

Within the brain, tdTomato gene expression following administration of DAB-Lf dendriplex was visible in the dentate gyrus and in the granule cell layer of the hippocampus, in the median brain section (Figure 4.18). It appeared to be distributed in the cytoplasm of the cells rather than in their nuclei. By contrast, there was no gene expression visible in the median brain following injection of naked DNA, or in the anterior and posterior sections of the brain following any of these two treatments.

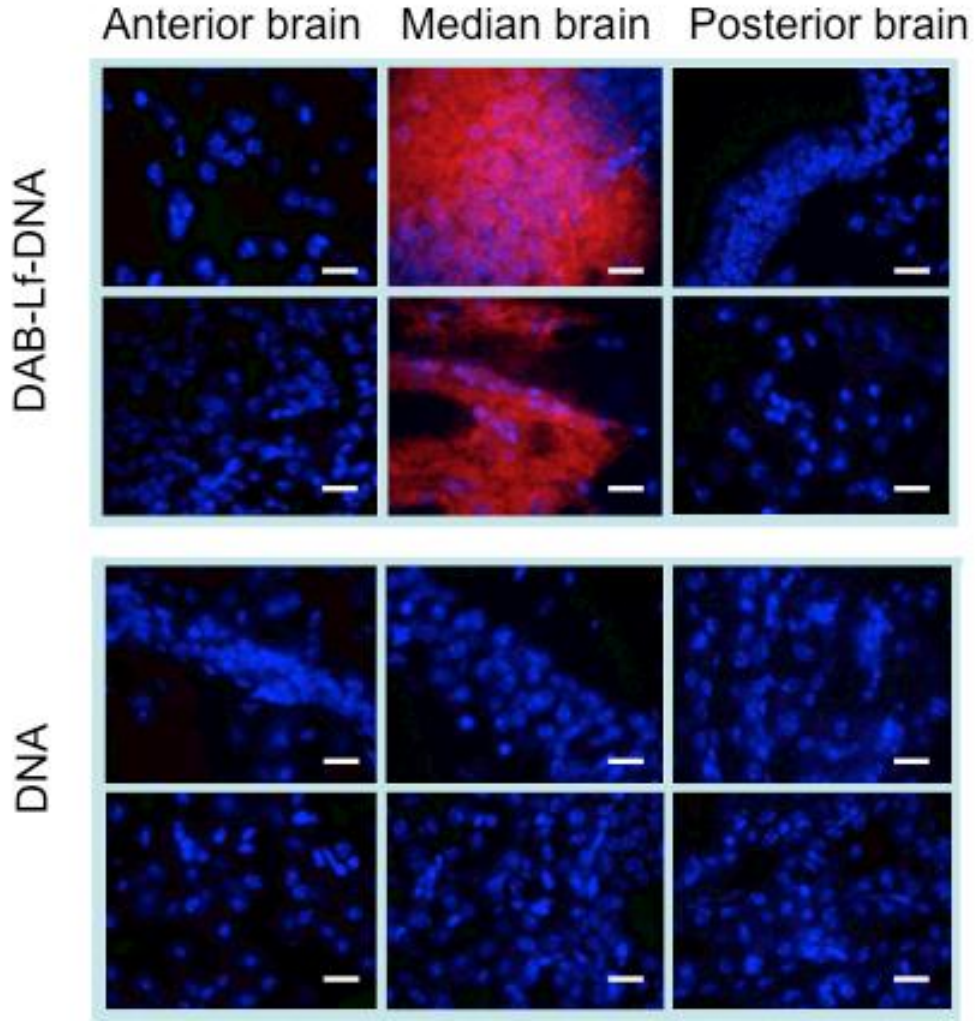

Figure 4.20 Epifluorescence microscopy imaging of the distribution of gene expression within the brain after a single intravenous injection of tdTomato-encoded DNA (50 µg) either complexed with DAB-Lf or in solution (Bar: 10 µm).

4. Discussion

Various studies demonstrate the presence of lactoferrin receptors (LfR) in the brain and the receptor-mediated uptake of Lf (Fillebeen *et al*., 1999, Talukder *et al*., 2003, Suzuki *et al*., 2005, Huang *et al*., 2007). In this chapter, we successfully synthesized Lf- and Lfc- bearing DAB dendrimers, and demonstrated an increased gene delivery to the brain *in vitr*o and *in vivo* (for DAB-Lf only). The NMR results showed that DAB has been successfully conjugated with Lf and Lfc. Percentage conjugation of the amino acids with the dendrimer was found to be 50% for both lactoferrin and lactoferricin, as previously observed when preparing amino acid- and transferrin -bearing DAB using the same simple one-step synthesis (Koppu *et al*., 2010; Aldawsari *et al*., 2011).

The conjugation of Lf and Lfc to DAB did not destabilize DNA condensation. However, an excess of DAB was required for an efficient DNA condensation. The ability of DAB-Lf and DAB-Lfc dendriplexes to condense DNA was measured using Picogreen® reagent at various durations and dendrimer: DNA weight ratios. That stability of DNA complexation is directly related to the increase in the dendrimer: DNA weight ratio.

The hydrodynamic diameter of both DAB-Lf and DAB-Lfc dendriplexes was higher compared to the unmodified DAB dendriplex, which had an average size of 196 nm (PDI: 0.683) (Aldawsari *et al*., 2011). This increase in size was due to the conjugation of Lf and Lfc on the periphery of DAB dendrimer.

Moreover, the conjugation of Lf and Lfc to DAB increased the overall positive charge of the dendriplexes compared to non-targeted DAB-DNA (6 mV) (Aldawsari *et al*., 2011) for weight ratios over 2:1. This zeta potential increase is most likely due to the presence of the positively charged amino acids of Lf and Lfc. It would eventually lead to an increase of the electrostatic interactions of the dendriplexes with negatively charged cellular membranes, resulting in an improved uptake by the BBB via receptor-mediated endocytosis and absorptive-mediated endocytosis jointly (Chen and Liu 2012).

bEnd.3 cells showed an improved uptake of DNA following treatment with DAB-Lf (2.1-fold and 4.1-fold) and DAB-Lfc dendriplex (2-fold and 3.8-fold) as compared to DAB dendriplex and DNA solution. Similar results were obtained when bEnd.3 cells were treated with Lf-bearing PEG-poly-(lactide) (PEG-PLA) nanoparticles encapsulating coumarin-6 targeting lactoferrin receptors and non-targeted PLA nanoparticles. The cellular uptake was increased 1.45-fold (Hu *et al*., 2009). Lf-conjugated polymersomes demonstrated similar effects, when their cellular uptake by bEnd.3 cells was 1.56-fold higher than the non-conjugated polymersomes (Gao *et al*., 2010). Similarly, the treatment of bEnd.3 cells with Lf-conjugated PEG-liposomes demonstrated a 3.4-fold increase in the cellular uptake to that observed with non-conjugated PEG-liposomes. The results can also be compared to Lf-bearing PAMAM-PEG dendrimer that demonstrated a 2-fold increase in the cellular uptake to that observed with Tf-bearing PAMAM-PEG dendrimer.

(Huang *et al*., 2008). However this is the first time Lfc has been investigated as a brain-targeting ligand.

Utilizing cellular uptake inhibitors and escalating concentration of the free ligands investigated the mechanism of cellular uptake of the DNA complexed to DAB-Lf and DAB-Lfc. The inhibitors act on the various endocytic mechanisms of cells. Phenylarsine oxide is an inhibitor of clathrin-mediated endocytosis (which is a requisite for receptor-mediated endocytosis) (Visser *et al*., 2004). Filipin is known to block the caveolae-mediated process in non-specific adsorptive endocytosis (Ryoung Kim et al., 2007). Colchicine inhibits macropinocytosis (Liu and Shapiro 2003), which provides non-specific endocytosis of macromolecules, whereas cationic poly-L-Lysine can inhibit the uptake of cationic delivery systems. The cellular uptake of DNA complexed to DAB-Lf was therefore related to endocytosis processes mainly to clathrin-mediated endocytosis as phenylarsine oxide led to significant inhibition of cellular uptake. Fillipin and colchicine demonstrated inhibition to a lesser extent, thus proving lower uptake of DNA via caveolae-mediated endocytosis and macropinocytosis. The cationic zeta potential of DAB-Lf dendriplex (35 mV) should demonstrate significant inhibition by poly-L-Lysine, but least inhibition was observed, owing to much stronger cellular uptake by receptor-mediated endocytosis. These results suggested that receptor-mediated endocytosis, adsorptive-mediated endocytosis and macropinocytosis might contribute to the cellular uptake of DNA complexed to DAB-Lf. Pre-treatment of cells with escalating amounts of free lactoferrin

led to competition between DAB-Lf dendriplex and free Lf for binding to LfR, demonstrating that the internalization mechanism of the DNA complexed to DAB-Lf is mainly via LfR-mediated endocytosis. Similar results were demonstrated when significant inhibition of the cellular uptake of Lf-bearing PAMAM-PEG dendrimer was observed when BCECs were pre-treated with phenylarsine oxide, fillipin, colchicine and excess free Lf (Huang *et al*., 2008). On the contrary, cellular uptake of DNA complexed to DAB-Lfc was mainly inhibited by poly-L-Lysine owing to the cationic zeta potential of DAB-Lfc dendriplex (32.5 mV). Phenylarsine oxide and colchicine demonstrated inhibition to a lesser extent, thus proving lower uptake of the DNA via clathrin-mediated endocytosis and macropinocytosis. The caveolae-mediated endocytosis contributed least to the cellular uptake of the DNA complexed to DAB-Lfc, as fillipin led to least inhibition. These results suggested that all receptor-mediated endocytosis and macropinocytosis contributed majorly to the cellular uptake of DNA complexed to DAB-Lf. Pre-treatment of cells with escalating amounts of free Lfc, led to competition between DAB-Lfc dendriplex and free Lfc for binding to TfR and LfR. It demonstrated that the internalization mechanism of the DNA complexed to DAB-Lf is mainly via TfR- and LfR-mediated endocytosis. It can be suggested that DAB-Lfc dendriplex acts on the lower affinity binding sites of both TfR and LfR.

The enhanced β-galactosidase expression following transfection with DAB-Lf and DAB-Lfc dendriplex resulted from increased cellular uptake after treatment. In case of DAB-Lf dendriplex, both increases were of the same

magnitude (2.1-fold for both cellular uptake and gene expression compared to non-targeted DAB dendriplex treatment). Similar results were obtained when luciferase gene expression in the brain capillary endothelial cells was 3.6-fold higher after treatment with PAMAM-PEG-Lf/DNA as compared to that observed with PAMAM-PEG/DNA.

The biodistribution of the gene expression revealed that DAB-Lf dendriplex led to an improved β-galactosidase expression in brain after intravenous administration. Gene expression in the brain was significantly higher than that observed in the other major organs. This results from the higher uptake of DAB-Lf dendriplex in the brain. Various other studies have demonstrated higher gene expression in the brain following administration of Lf-bearing gene delivery system, but non-specific gene expression was also observed in other major organs of the body. After intravenous administration of PAMAM-PEG-Lf/DNA complex in mice, Huang and colleagues demonstrated a 5.2-fold increase in the luciferase gene expression compared to that with PAMAM-PEG/DNA, but high levels of gene expression were also observed in liver, lung and kidney (Huang *et al.,* 2008). Similar results were obtained in the biodistribution studies of coumarin-6-loaded Lf-PEG-PLA nanoparticles, as the brain concentration was 3-fold higher than coumarin-6 loaded PEG-PLA nanoparticles. But high concentration was also observed in blood (Hu *et al*., 2009). The results can also be compared to Lf-conjugated PEG-liposomes encapsulating coumarin-6 that demonstrated a 1.4-fold increase in the brain uptake compared to that observed with PEG-liposomes, but non-

specific uptake in spleen also increased (Huang *et al*., 2013). Another study led to a 3.5-fold increase in the brain uptake of Lf-modified β-cyclodextrin nanocarrier, compared to that observed with β-cyclodextrin nanocarriers, but higher uptake was also found in liver, spleen and kidneys (Ye *et al*., 2013).

On the contrary, DAB-Lfc dendriplex demonstrated no gene expression in the brain. *In vitro* studies hinted that the cellular uptake of DAB-Lfc dendriplex may have occurred via receptor-mediated endocytosis. DAB-Lfc dendriplex might bind to the low affinity-binding site on the TfR or LfR that does not lead to its endocytosis on the abluminal site of the brain. The exact mechanism behind the discrepancy of the result needs to be investigated further.

In conclusion, the grafting of Lf and Lfc to DAB dendriplex has been shown to enhance DNA uptake in bEnd.3 murine brain capillary endothelial cells compared to the unmodified dendriplex *in vitro*. *In vivo*, the intravenous injection of Lf-bearing DAB dendriplex resulted in an enhanced gene expression in the brain, which was significantly higher than in any other major organs of the body. It also decreased gene expression in the lung and the kidneys, compared to that observed following treatment with DAB dendriplex. Lfc-bearing DAB dendriplex did not demonstrate gene expression in the brain. Lf-bearing DAB dendrimer is therefore a highly promising nanocarrier for gene delivery to the brain following intravenous administration.

CHAPTER 5

Angiopep-2-bearing polypropylenimine dendrimer for targeted gene delivery to the brain

1. Introduction

Low-density lipoprotein receptor related proteins 1 and 2 (LRP-1 and 2) are multifunctional receptors expressed on the endothelial cells of the BBB, neurons of the cerebrum and cerebellum and astrocytes (Dehouck *et al.,* 1997, Gabathuler, 2010). LRP1, which is also known as CD91 or α2macroglobulin receptor, is a multi-ligand scavenger and signalling receptor weighing 600-KDa and consisting of two associated polypeptide chains: membrane spanning C-terminal fragment weighing 85-KDa and an extracellular N-terminal fragment weighing 515-KDa. LRP1 can bind to more than 30 extracellular ligands. LRP2, also known as megalin is one of the largest cell surface transmembrane glycoprotein weighing 517-KDa. It is structurally very similar to LRP1. LRP2 is also widely expressed in neurons and astrocytes (Spuch *et al*., 2012).

Angiopeps are a family of peptides that were derived from the Kunitz domain of a protease inhibitor, Aprotinin, which is a LRP1 and LRP2 ligand. Demeule *et al.* (2008) derived 96 peptides from aprotinin and tested their endocytosis efficiency in an *in vitro* model of the BBB. Out of these, 8 peptides demonstrating the highest BBB transcytosis were radioiodinated and re-evaluated by *in situ* brain perfusion in mice followed by capillary depletion analysis. Peptide 67, also known as Angiopep-1 with an amino acid sequence TFFYGGCRGKRNNFKTEEY, was selected for further analysis due to its high level of transcytosis and higher brain parenchymal distribution volume compared to the other 7 peptides. For further analysis, amino acid

sequence of Angiopep-1 was modified to prevent peptide dimerization or disulfide bond formation with serum proteins. Cysteine at position 7 in the amino acid sequence was replaced by serine and the peptide was now designated as Angiopep-2. There was no significant difference observed in the brain parenchymal distribution of Angiopep-2 as compared to that of Angiopep-1. However, the brain uptake of Angiopep-2 was 5-fold higher than that of Aprotinin (Demeule *et al*., 2008).

Angiopep-2 was further investigated as a peptide vector for drug delivery to the brain. It was conjugated with the highly potent anti-cancer drugs paclitaxel, doxorubicin and etoposide. These conjugates demonstrated higher brain uptake compared to the drugs alone (Regina *et al*., 2008, Che *et al*., 2010). Jiang and colleagues demonstrated the first evidence of Angiopep-2 used as a ligand for targeted gene delivery to the brain. Angiopep-2 bearing PAMAM-PEG dendrimers demonstrated an increased brain uptake when compared to that of PAMAM-PEG. In the mouse brain, gene expression was observed in cortical layer, *caudate putamen*, hippocampus and *substantia nigra* (Ke *et al*., 2009). Angiopep-2 has also been exploited as a targeting ligand for drug delivery to the brain. Micelles encapsulating antifungal drug amphotericin B and electro-responsive hydrogels encapsulating the antiepileptic drug phenytoin sodium, decorated with angiopep-2 on the surface, led to a significantly higher brain penetration (Shao *et al*., 2010, Ying *et al*., 2014). PAMAM decorated with tumour vasculature targeting cyclic peptide and angiopep-2 led to an increased

penetration across the BBB and demonstrated a high imaging capability for experimental brain tumours (Yan *et al*., 2012).

2. Aims and Objectives

On the basis of the fact that LRP1 and LRP2 are highly expressed on the BBB, we now hypothesize whether conjugation of Angiopep-2 to a highly efficient gene delivery system, DAB dendrimer, leads to an increased gene expression in the brain. The main objectives of this chapter are:

- The synthesis and characterization of Angiopep-2 bearing DAB dendrimers (DAB-Ang)
- The evaluation of the brain targeting efficacy of DAB-Ang *in vitro* and *in vivo*

3. Results

3.1. Synthesis and characterisation of Angiopep- bearing DAB dendrimers

3.1.1. Conjugation of Angiopep-2 to DAB

^{1}H NMR confirmed the synthesis of DAB-Ang dendrimer. Figure 5.1 shows the peaks of the bound and the unbound DAB dendrimer. ^{1}H NMR (D_2O): δ DAB (H_2N-C***H₂***-CH_2-) = 2.58, DAB (-N-C***H₂***-CH_2-) = 2.45, DAB (-CH_2-C***H₂***-CH_2-)=1.60; DAB-Ang (Ang-HN-**CH_2**-CH_2-) = 3.70, DAB-Ang (H_2N-**C*H₂***-CH_2-CH_2-N-) = 2.84, DAB-Ang (-N-**C*H₂***-CH_2-CH_2-) = 2.42-2.68, DAB-Ang (-N-CH_2-C***H₂***-CH_2-) = 1.81. Multiple small peaks between 1.29 and 3.41 corresponded to the protons for Angiopep-2. The characteristic triplet peak for the C*H₂* adjacent to peripheral primary amino group of DAB at 2.58 was shifted to 3.70 ppm in the NMR spectrum of a conjugated DAB-Ang analogue. The ratio of the integrals of resonances at ca. 3.70 and 2.84 for methylene units (**d** and **a**) attached to the amino acid moiety via DMSI linkage and unbound free amine, respectively is 1. This supports that 50 % of the surface primary amine groups on the DAB are conjugated to Angiopep-2.

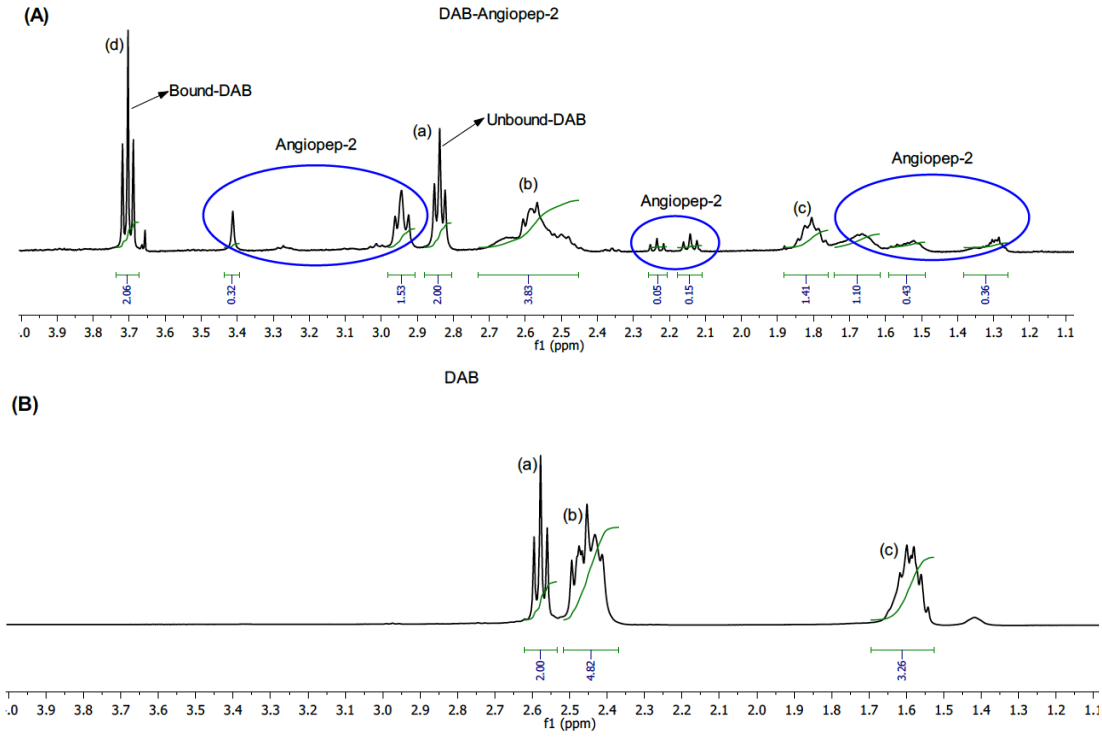

Figure 5.1 ^{1}H NMR spectra (400 MHz) of DAB-Ang (A) and DAB (B) in D_2O

3.1.2. Characterisation of dendriplex formation

DAB-Ang was able to condense more than 70 % of the DNA at all the dendrimer: DNA weight ratios (Figure 5.2). DNA condensation occurred almost instantaneously and was found to be stable over at least 24h. The condensation of DNA increased with the increasing dendrimer: DNA weight ratio. It was much higher than that observed for the unmodified dendrimer, which was of 60% at its best and decreasing with time.

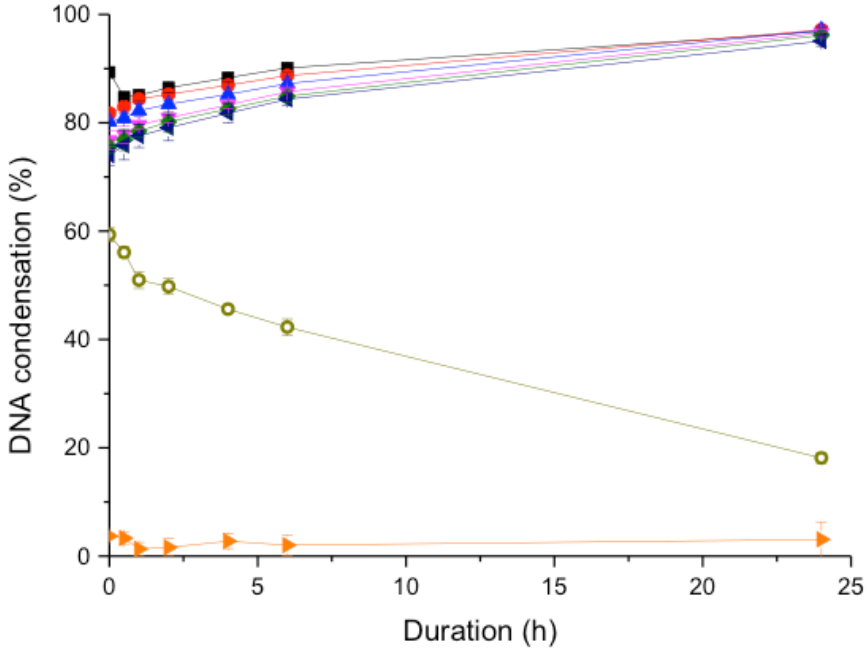

Figure 5.2 DNA condensation of DAB-Ang dendriplexes using PicoGreen® reagent at various durations and dendrimer: DNA weight ratios : 20:1 (■, black), 10:1 (●, red), 5:1 (▲, blue), 2:1 (▼, pink), 1:1 (♦, green), 0.5:1 (◄, black), DNA only (►, orange) (empty symbol, light green : DAB-DNA, dendrimer: DNA weight ratio: 5:1) . Results are expressed as mean ± SEM (n= 4)

3.1.3. Dendriplex size and zeta potential measurement

The average sizes of DAB-Ang dendriplexes at dendrimer: DNA weight ratios from 0.5:1 to 5:1 were less than 300 nm. At dendrimer: DNA ratio of 10:1 and 20:1 the size of the dendriplex increased and displayed a hydrodynamic diameter of 721 ± 339 nm an d 354 ± 89 nm respectively (Figure 5.3 A).The zeta potential of the dendriplexes remained close to neutral for all the tested ratios (Figure 5.3 B).

A)

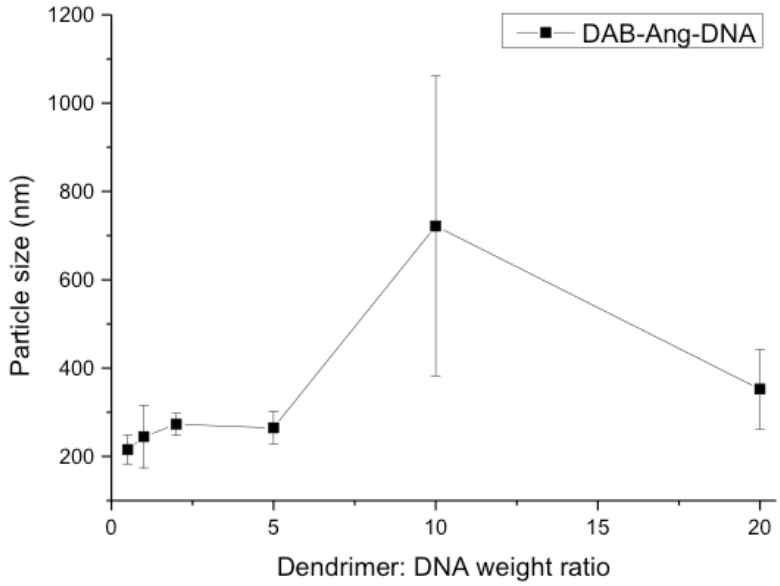

B)

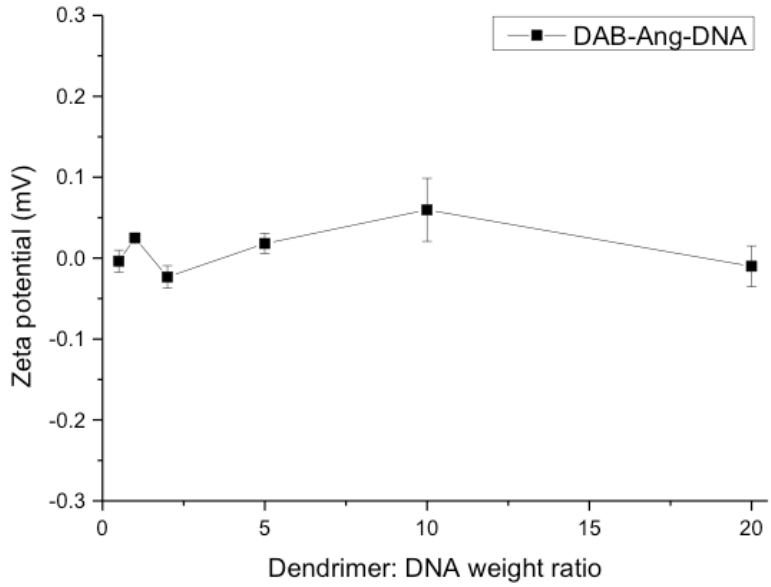

Figure 5.3 Size **(A)** and Zeta Potential **(B)** of DAB-Ang dendriplexes at various dendrimer: DNA weight ratios: 20:1, 10:1, 5:1, 2:1, 1:1, and 0.5:1. Results are expressed as mean ± SEM (n=4).

3.2. *In vitro* studies

3.2.1. Transfection

The conjugation of Ang to DAB dendriplex led to an increased transfection compared to DAB dendriplex on bEnd.3 cells (Figure 5.4). The highest level of transfection in bEnd.3 cells after treatment with DAB-Ang at various dendrimer: DNA weight ratios was obtained at DAB-Ang: DNA weight ratio of 2:1. The treatment of bEnd.3 cells with DAB-Ang dendriplex (2:1) led to a 1.9-fold increase in the gene expression compared to DAB dendriplex ($3.06x10^{-3} \pm 0.11x10^{-3}$ U/mL and $1.57x10^{-3} \pm 0.07x10^{-3}$ U/mL respectively for DAB-Ang and DAB dendriplexes. Gene expression following treatment with DAB-Ang dendriplex and DAB-dendriplex was 3.5-fold and 1.8-fold higher than that observed following treatment with naked DNA ($0.86x10^{-3} \pm 0.01x10^{-3}$ U/mL). The cells treated with naked DNA did not demonstrate any significant increase in the gene expression compared to untreated cells.

Taking into consideration the results of DNA condensation assay, size and zeta potential measurements and transfection, DAB-Ang dendriplex at a dendrimer: DNA weight ratio of 2:1 was chosen for further investigations.

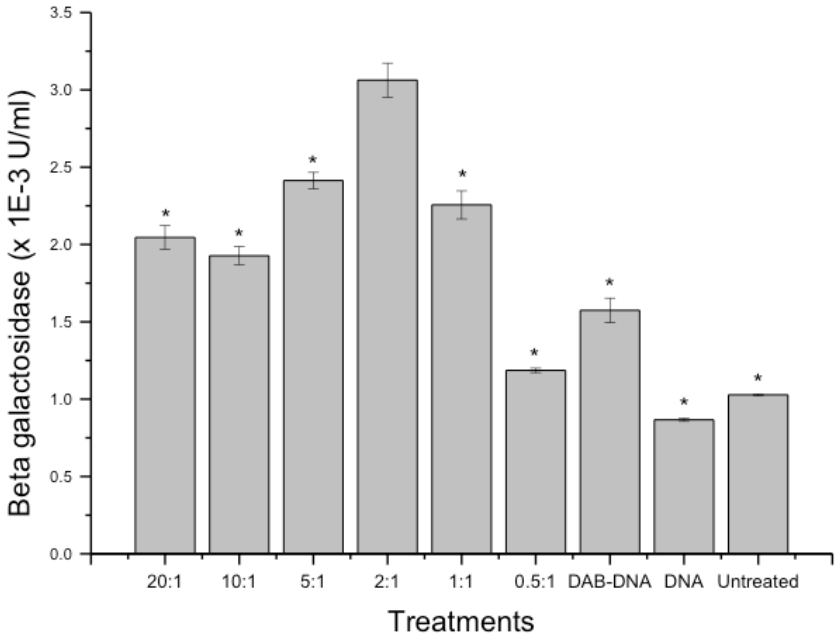

Figure 5.4 Transfection efficacy of DAB-Ang dendriplex at various dendrimer: DNA weight ratios and DAB dendriplex at dendrimer: DNA weight ratio of 5:1 in bEnd.3 cells. Results are expressed as the mean ± SEM of three replicates (n=15). * : P <0.05 compared with highest transfection treatment.

3.2.2. Cellular uptake

The uptake of fluorescein-labelled DNA complexed to DAB-Ang by bEnd.3 cells was qualitatively analysed by epifluorescence microscopy. Cellular uptake commenced at 1 h as fluorescein-labelled DNA could be visualized in the nuclei of the bEnd.3 cells. From all the durations tested, DNA uptake was most pronounced after treatment of bEnd.3 cells with DAB-Ang dendriplex for 3 hours (Figure 5.5).

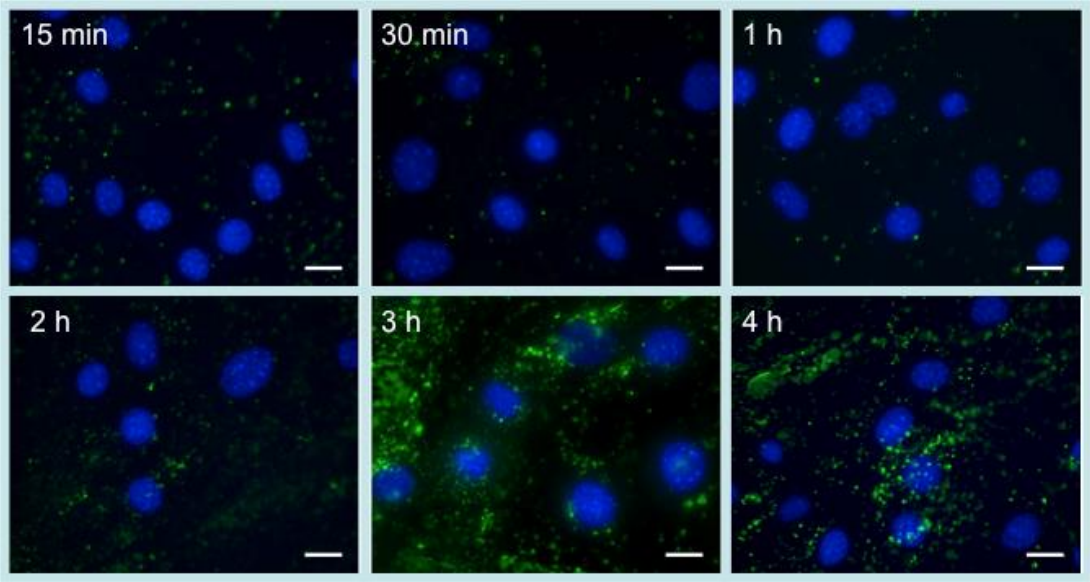

Figure 5.5 Epifluorescence microscopy imaging of the cellular uptake of fluorescein-labelled DNA (2.5 µg/ well) complexed with DAB-Ang, after incubation for 15 min, 30 min, 1 h, 2 h, 3 h or 4 h with bEnd.3 cells (Blue: nuclei stained with DAPI (excitation: 405 nm, emission bandwidth: 415-491 nm), green: Fluorescein-labelled DNA (excitation: 543 nm, emission bandwidth: 550-620 nm) (Bar: 10 µm)

Following optimization of the duration of the maximum cellular uptake, bEnd.3 cells were treated with fluorescein-labelled DNA complexed to DAB-Ang, DAB or in solution for 3 hours. Pronounced uptake of fluorescein-

labelled DNA complexed to DAB-Ang was observed. On the contrary, cells treated with DAB dendriplex demonstrated much less cellular uptake to that compared to DAB-Ang dendriplex. Fluorescein-labelled DNA solution did not show any cellular uptake (Figure 5.6).

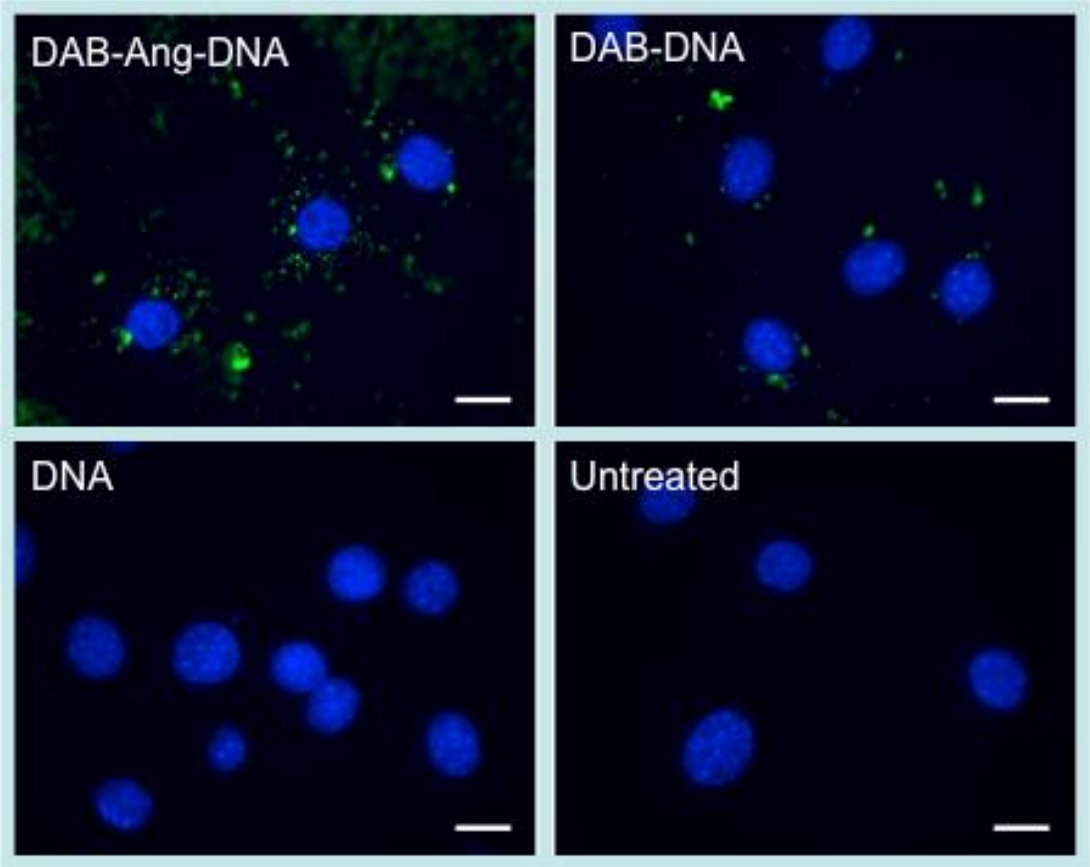

Figure 5.6 Epifluorescence microscopy imaging of the cellular uptake of fluorescein-labelled DNA (2.5 µg/ well) either complexed with DAB-Ang, DAB or in solution, after incubation for 3 hours with bEnd.3 cells (Blue: nuclei stained with DAPI (excitation: 405 nm, emission bandwidth: 415-491 nm), green: Fluorescein-labelled DNA (excitation: 543 nm, emission bandwidth: 550-620 nm) (Bar: 10 µm)

The quantification of the cellular uptake was done utilizing flow cytometry (Figure 5.7). Cellular fluorescence was highest following treatment with DAB-

Ang dendriplex (25567 ± 500 arbitrary units (a.u.)). It was respectively about 1.7-fold and 5.1-fold higher than the cellular fluorescence observed following treatment with DAB dendriplex (14473 ± 594 a. u.) and DNA solution (4999 ± 311 a. u.).

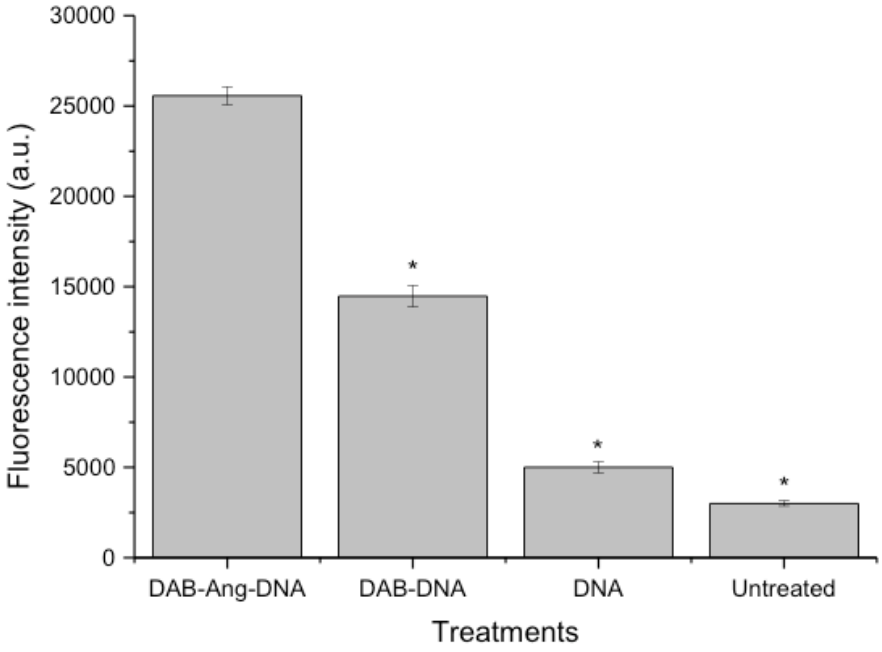

Figure 5.7 Flow cytometry quantification of the cellular uptake fluorescein-labelled DNA (5 µg/ well) either complexed with DAB-Ang, DAB or in solution, after incubation for 3 hours with bEnd.3 cells (n=15) * : P <0.05 compared with DAB-Tf-DNA.

3.2.3. Inhibitor studies

Utlilizing cellular uptake inhibitors elucidated the mechanisms of cellular uptake of the DNA complexed to DAB-Ang. Pre-treatment of the bEnd.3 cells

with phenylarsine oxide, fillipin, colchicine and poly-L-Lysine led to partial inhibition of the cellular uptake (Figure 5.8 & 5.9). Colchicine and phenylarsine oxide caused the most significant inhibition, with a cellular uptake respectively decreased by 1.7-fold and 1.6-fold compared to that observed with DAB-Ang dendriplex without inhibitory treatment (respectively 15000 ± 609 a. u. and 15040 ± 443 a.u. following pre-treatment with colchicine and phenylarsine oxide). Filipin and poly-L-Lysine appear to be less effective inhibitors, leading to a cellular uptake decrease by respectively 1.2-fold each compared to DAB-Ang dendriplex without pre-treatment (respectively 20766 ± 325 a. u. and 21228 ± 405 a.u. following pre-treatment with filipin and poly-L-Lysine).

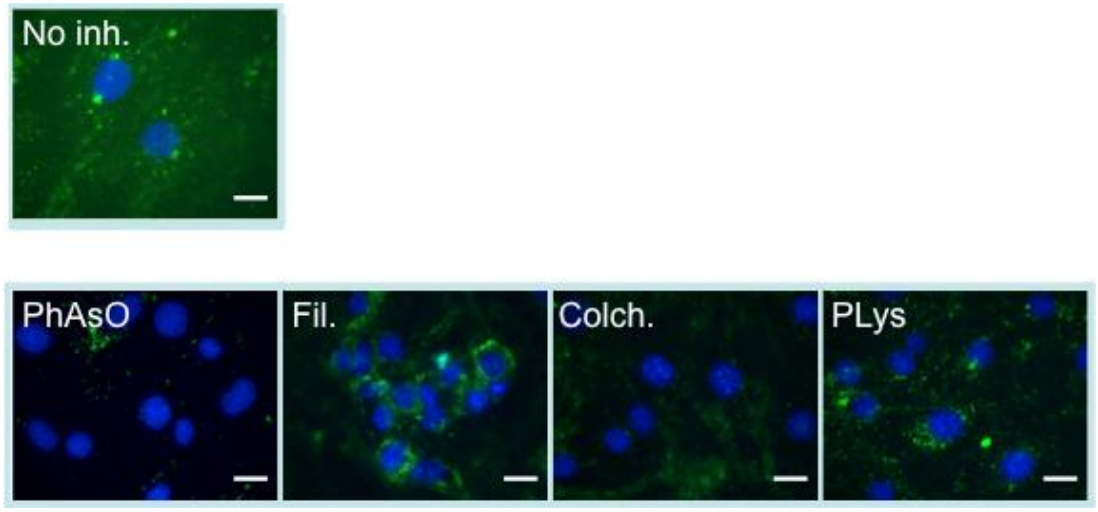

Figure 5.8 Epifluorescence microscopy imaging of the bEnd.3 cellular uptake of fluorescein- labelled DNA (2.5 µg/ well) complexed with DAB-Ang, following pre-treatment with various cellular uptake inhibitors: phenylarsine oxide ("PhAsO"), filipin ("Fil."), colchicine ("Colch.") and poly-L-lysine ("PLys"). (Blue: nuclei stained with DAPI (excitation: 405 nm, emission bandwidth: 415-491 nm), green: Fluorescein-labelled DNA (excitation: 543 nm, emission bandwidth: 550-620 nm) (Bar: 10 µm)

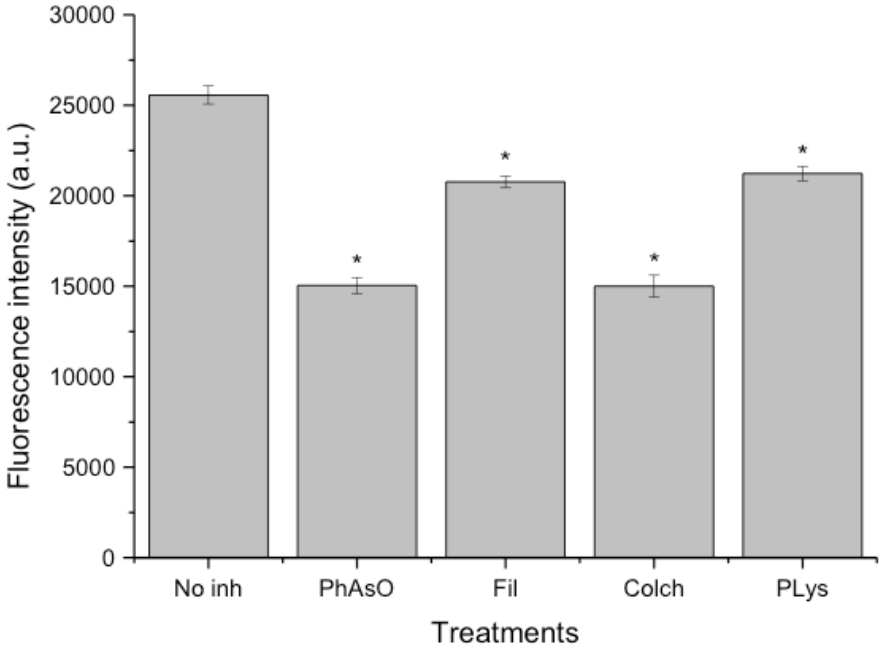

Figure 5.9 Flow cytometry quantification of the bEnd.3 cellular uptake of fluorescein- labelled DNA (5 µg/ well) complexed with DAB-Ang, following pre-treatment with various cellular uptake inhibitors: phenylarsine oxide ("PhAsO"), filipin ("Fil."), colchicine ("Colch.") and poly-L-lysine ("PLys"). (n=15), * : P <0.05 compared with DAB-Ang-DNA.

3.3. *In vivo* studies

3.3.1. Biodistribution of gene expression

The biodistribution of gene expression following intravenous injection of DNA encoding luciferase complexed to DAB-Ang was first qualitatively assessed by luminescence imaging, at various treatment durations. Gene expression appeared to be mainly located in the brain of the mice. The highest gene expression level was found 24 h following injection of the DAB-Ang dendriplex, but gene expression prevailed up to 11 days after treatment (Figure 5.10).

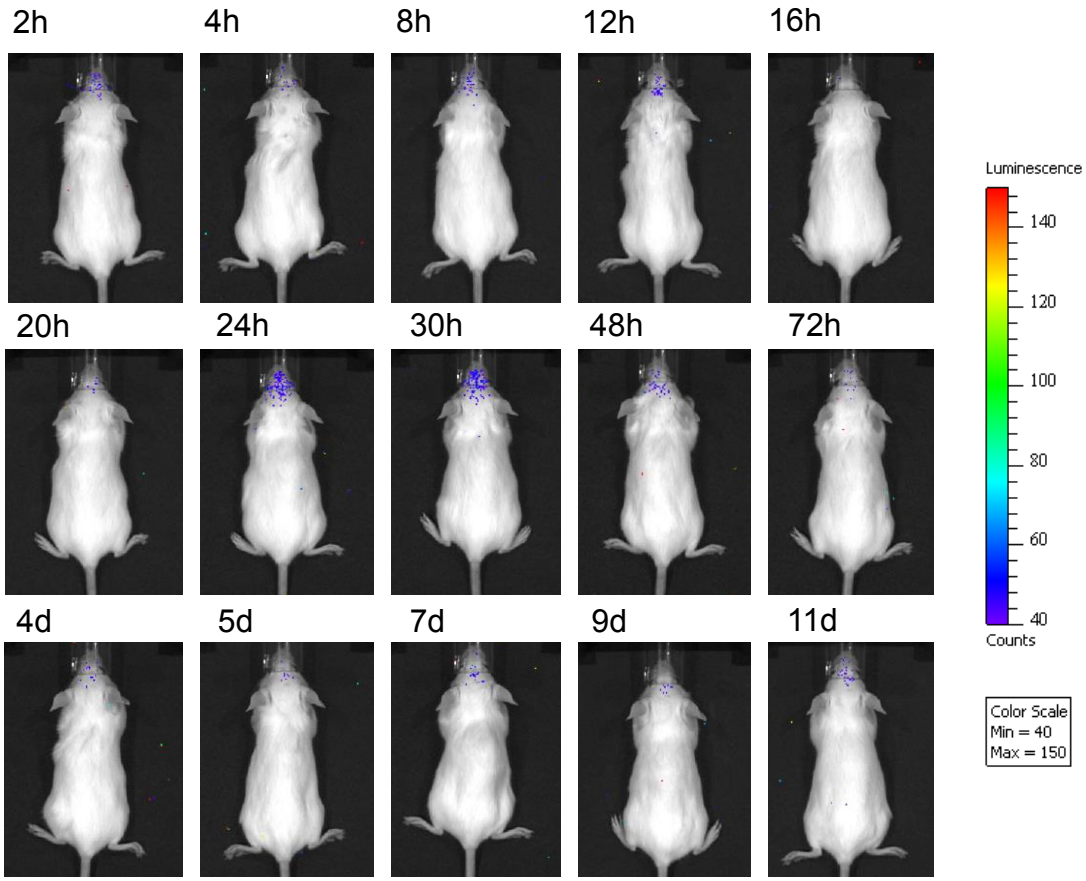

Figure 5.10 Bioluminescence imaging of gene expression after intravenous administration of DAB-Ang dendriplex (50 µg DNA administered). The mice were imaged using the IVIS Spectrum at various durations after injection of the treatment. The scale indicates surface radiance (photons/s/cm^2/steradian).

Gene expression following intravenous administration of DAB-Ang dendriplex was compared to that observed following administration of DAB-dendriplex and DNA only, 24 h after administration of the treatments. The gene expression in the brain appeared to be highest following treatment with DAB-Ang (Figure 5.11).

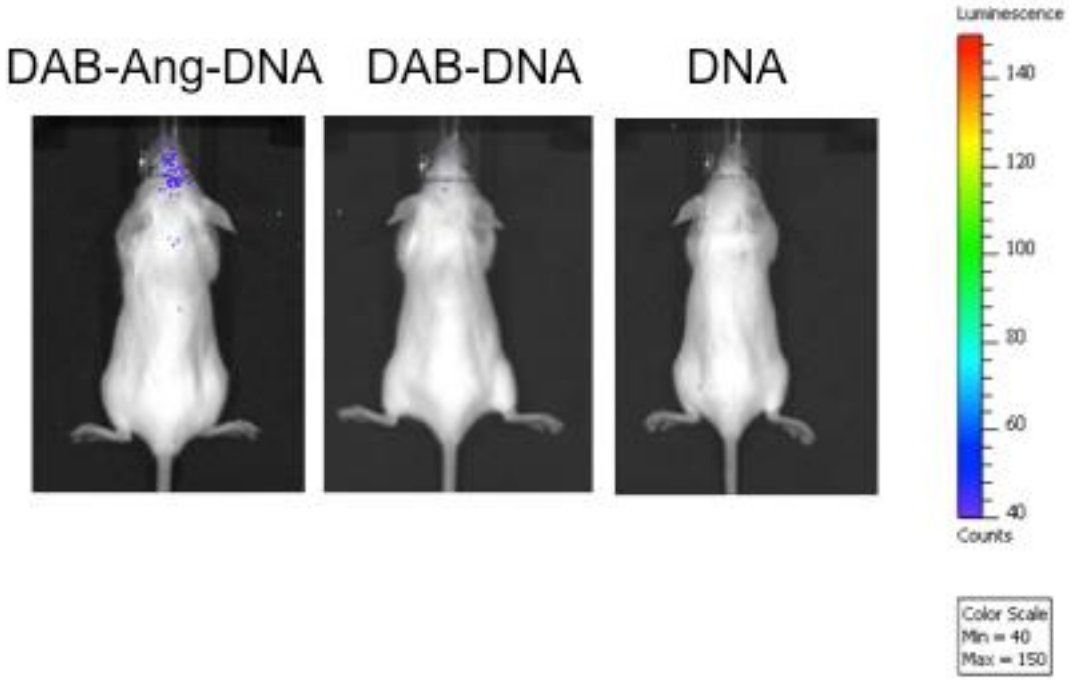

Figure 5.11 Bioluminescence imaging of gene expression after intravenous administration of DAB-Tf and DAB dendriplexes (50 µg DNA administered). (Controls: DNA solution, untreated cells). The mice were imaged using the IVIS Spectrum 24 h after injection of the treatments. The scale indicates surface radiance (photons/s/cm^2/steradian).

The quantification of biodistribution of gene expression showed unexpected results (Figure 5.12). After the intravenous administration of DAB-Ang dendriplex in mice, there was no significant difference in the gene expression in the brain as compared to DAB dendriplex (128.1 ± 14.3 mU and 163.9 ± 35.4 mU β-galactosidase per organ respectively for DAB-Ang and DAB dendriplexes). The gene expression in the spleen was significantly higher than DAB dendriplex and DNA solution (83.6 ± 2.1 mU, 0 ± 7.6 mU and 0 ± 26.8 mU β-galactosidase per organ for respectively DAB-Ang dendriplex, DAB dendriplex and DNA solution). The gene expression in kidneys and heart was at similar levels after treatment with DAB-Ang dendriplex and DAB dendriplex (223.2 ± 66.8 mU and 399.6 ± 114.3 mU β-galactosidase per

organ in the kidneys for respectively DAB-Ang dendriplex and DAB dendriplex, 146.83 ± 22.6 mU, and 150.6 ± 54.64 mU β-galactosidase in the spleen for respectively DAB-Ang dendriplex and DAB dendriplex).

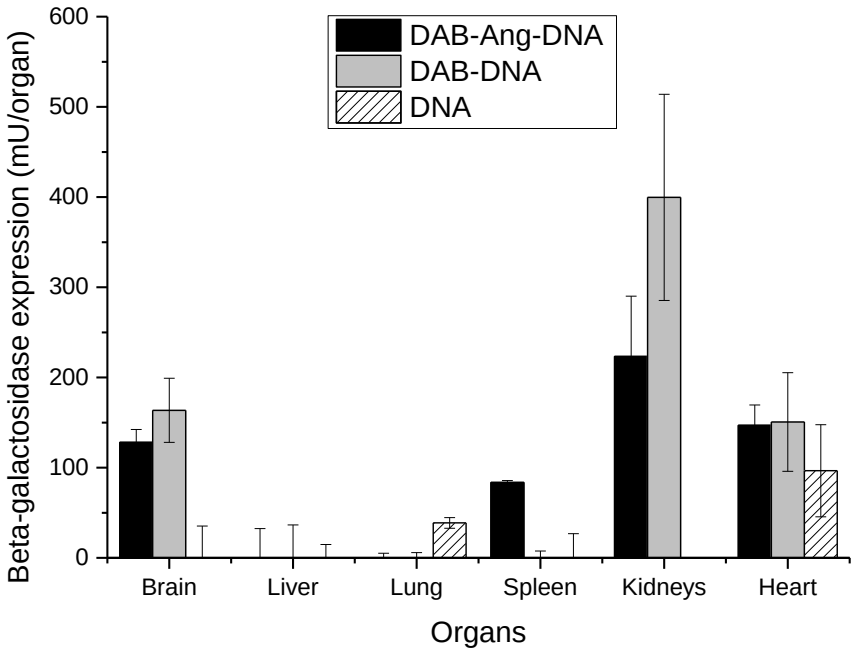

Figure 5.12. Biodistribution of gene expression after a single intravenous administration of DAB-Ang dendriplex, DAB dendriplex and DNA solution (50 µg DNA administered). Treatment duration is 24 hours. Results were expressed as milliunits β-galactosidase per organ (n=5). * : P <0.05 compared with DAB-Ang-DNA for each organ

4. Discussion

LRP1 and LRP2 receptors are multifunctional receptors expressed on the BBB that can bind to a variety of ligands, such as Apolipoprotein E, tissue plasminogen activator (tPA), amyloid precursor protein, melanotransferrin, plasminogen activator inhibitor 1, receptor associated protein, α2 macroglobulin, HIV-1 Tat protein, heat shock protein 96, heparin cofactor II , angiopeps and many others. These receptors are physiologically involved in controlling the permeability of the BBB and post-ischaemic lesion formation in response to active tPA (Herz 2003). Various ligands have demonstrated the increased uptake of the nanoparticles in the BBB via LRP1- and LRP2-mediated endocytosis. Polysorbate-80 coated nanoparticles have been investigated for a drug delivery of various drugs like dalargin, doxorubicin, loperamide and tubocurarine that normally do not circumvent the BBB (Schroder and Sable 1996, Blasi *et al*., 2007). Apolipoprotein E-conjugated albumin nanoparticles led to an increased uptake in the brain as compared to the unconjugated nanoparticles (Zensi *et al.,* 2009). Mellanotransferrin (P97), another protein of the Tf family, demonstrated an increased efficiency to cross BBB via LRP1- and LRP2-mediated endocytosis (Demeule *et al*., 2002, Gabathuler *et al*., 2005). Amongst all the ligands of the LRP, Angiopep-2 has shown an increased transcytosis across the brain (Demeule *et al*., 2008a, Demeule *et al*., 2008b, Ke *et al*., 2009). In this chapter, we exploited Angiopep-2 as a ligand for brain targeted gene delivery system.

The NMR results demonstrated that DAB has been successfully conjugated to Ang. The conjugation of Ang to DAB did not destabilize DNA condensation, but led to an increased condensation for a longer period of time. However, an excess of DAB was required for an efficient DNA condensation. The stability of the complexed DNA was directly related to the rise in the dendrimer: DNA weight ratio. There was an increase in overall size of the DAB-Ang dendriplex as compared to the unmodified DAB dendriplex that had an average size of 196 nm (PDI: 0.683) (Aldawsari *et al*., 2011). This was due to the conjugation of angiopep-2 on the periphery of the DAB dendrimer. However, this conjugation led to a decrease in the overall positive charge of the dendriplex compared to DAB dendriplex (6 mV) (Aldawsari *et al*., 2011). This zeta potential decrease was most likely due to the presence of the negatively charged amino acids (glutamic acid) of Angiopep-2.

The cellular uptake of the DNA in bEnd.3 cells showed a marked increase following treatment with DAB-Ang dendriplex as compared to that observed with DAB dendriplex and DNA solution. Similar results were obtained when BCEC cells were treated with BODIPY-labelled PAMAM-PEG-Ang dendrimer. The cellular uptake was increased by 4.8-fold compared to the control (Ke *et al.,* 2009). The formulation of 1, 2-Distearoyl-*sn*-glycero-3-phosphoethanolamine-N-[methoxy(polyethylene glycol)-2000] (PE-PEG)-based micelles loaded with an antimicrobial agent, amphotericin B, and surface-modified with angiopep-2 demonstrated similar effects, when their cellular uptake by BCECs was 1.5-fold and 6-fold higher than the non-

conjugated PE-PEG micelles loaded with amphotericin B and free amphotericin B respectively (Shao *et al*., 2010). The results can also be compared to the treatment of BCECs with Angiopep-targeted PEG-multiwalled carbon nanotubes (MWNTs), that led to a significantly higher cellular uptake compared to unconjugated PEG-MWNTs (Ren *et al*., 2012).

The inhibitor studies investigated the mechanism of cellular uptake of the DNA complexed to DAB-Ang. The inhibitors used act of the various endocytic mechanisms of cells. The cellular uptake of DNA complexed to DAB-Ang was related to endocytosis processes mainly to clathrin-mediated endocytosis and macropinocytosis as phenylarsine oxide and colchicine led to significant inhibition of cellular uptake. Fillipin demonstrated inhibition to a lesser extent, attesting the lower uptake of DNA via caveolae-mediated endocytosis. The zeta potential of DAB-Ang dendriplex was neutral, leading to much lesser inhibition by poly-L-lysine. This result suggested that receptor-mediated endocytosis and macropinocytosis might largely contribute to the cellular uptake of the DNA complexed to DAB-Ang, whereas adsorptive-mediated transcytosis may be a less favoured mechanism. Similar results were obtained when pre-treatment of cells with α2 macroglobulin, a LRP1 specific ligand, in an *in vitro* BBB model lead to a 26 % decrease in the passage of Angiopep-2 (Demeule *et al*., 2008a). All the inhibitors, phenylarsine oxide, fillipin, colchicine and poly-L-Lysine collectively inhibited the cellular uptake of the PAMAM-PEG-Ang/DNA nanoparticles in BCECs, but colchicine led to the most significant inhibition (Ke *et al*., 2009).

These results demonstrate that the uptake of DAB-Ang dendriplex was more selective and specific compared to the PAMAM-PEG-Ang/DNA. The increased cellular uptake following transfection with DAB-Ang dendriplex led to an enhanced β-galactosidase expression.

The qualitative analysis of the biodistribution of gene expression using IVIS revealed that there was an improved β-galactosidase expression in the brain following intravenous injection of DAB-Ang dendriplex, compared to DAB-dendriplex. The gene expression in the brain was visible for up to 11 days after treatment. However, the quantification of biodistribution of gene expression showed different results. After intravenous administration of DAB-Ang dendriplex, gene expression in the brain was similar to that observed after treatment with DAB dendriplex. Further investigations are needed to explain the difference in the contradictory results of these experiments. These results are not in line with Demeule and colleagues, who demonstrated a significantly higher uptake of Angiopep-2 in the brain as compared to transferrin (2.5-fold), lactoferrin and other ligands (Demeule *et al*., 2008a, Demeule *et al*., 2008b). When Angiopep-2 was conjugated to paclitaxel, doxorubicin and etoposide, the conjugates showed a much higher brain drug concentration (Paclitaxel: 5-fold, doxorubicin: 7-fold, etoposide: 10-fold) compared to the drug alone (Regina *et al*., 2008, Thomas *et al*., 2009, Che *et al*., 2010). The gene delivery system designed using PAMAM-PEG-Ang demonstrated a 3-, 5- and 8-fold increase in the brain uptake of the dendrimer depending on the amount of Angiopep-2 conjugated, compared to

that observed with PAMAM-PEG (Ke *et al*., 2009), The brain uptake of the Angiopep-conjugated micelles encapsulating amphotericin B was 1.6-fold higher than the non-conjugated micelles encapsulating amphotericin B (Shao *et al*., 2010). In an interesting study, van Rooy and colleagues demonstrated that Angiopep-2 conjugated liposomes have less brain uptake compared to the transferrin-conjugated liposomes and unconjugated liposomes. This study demonstrated that the type of nanoparticle (shape, size and surface properties) to which the ligand is conjugated has a major influence on the uptake of the nanoparticles (van Rooy *et al*., 2011).

In conclusion, we have successfully synthesized Angiopep-2 bearing DAB dendrimer that has enhanced efficiency of DNA uptake in bEnd.3 cells compared to that of DAB dendrimer *in vitro*. The *in vivo* results need further investigations.

CHAPTER 6

General Discussion

1. CNS disorders- prevalence and costs

According to the World Health Organization (WHO), around 25-30 % of the population in Europe is suffering from one or more CNS disorders (Olensen & Leonardi, 2003). Some other surveys put this figure to a whopping 38 %. These statistics also include the mental health disorders. The total economic costs for these disorders surmount to € 386 billion (2004 prices) for the most prevalent disorders, out of which only € 13 billion (3 %) accounted for drug-related costs (Andlin-Sobocki *et al*., 2005). Some of the disorders, such as depression, epilepsy, schizophrenia and pain, have responded well to the traditional small-molecule neuropharmaceuticals that cross the BBB, but others are still non-responsive or are heavily depended on pharmacotherapy. Some of these diseases are:

- Alzheimer's disease or other dementias
- Huntington's disease
- Parkinson's disease
- Brain cancer
- HIV infection of the brain
- Amyotrophic lateral sclerosis
- Stroke
- Brain and spinal cord injuries
- Ataxias
- Brain genetic disorders

The following table shows the prevalence of some of the most prevalent CNS disorders in UK, Europe and globally:

Table 6.1 Prevalence of most common CNS disorders in UK, Europe and globally (Andlin-Sobocki *et al*., 2005; Tanner *et al*., 2008; Beitz, 2009; Cancer Research UK; Parkinson's prevalence in the UK, 2009; World Alzheimer's report, 2009)

Disorder	UK	Europe	Global
Alzheimer's disease or other dementias	815,827	4.8 million	36 million
Huntington's disease	7,692	38,000-55,000	350,000-700,000
Parkinson's disease	127,000	1.2 million	7-10 million
Brain cancer	17,000	135,000	1.4 million
Stroke	133,000	1.1 million	33 million

The above mentioned numbers will rise in the future, not only due to the increase in the population, but also due to the increase in the median age of the people in UK and Europe and to the rising healthcare costs. In Europe, only 15 % of the total healthcare spending is allotted to the treatment of CNS disorders. The total economic cost of the brain disorders is higher than that of the diabetes and cancer together. The drugs that are used for the treatment of the CNS disorders only account for 8 % of the total drug sales (Andlin-Sobocki *et al*., 2005). These figures reflect a need for drastic

changes in the healthcare policies as well as an urgent necessity to develop novel therapies for the treatment of CNS disorders.

2. The neglected BBB problem in the CNS drug development process

The unprecedented rise in the number of the CNS disorders has generated enormous research activities in an attempt to develop new drugs for the treatment of these disorders. However, most of the research by industrial leaders is still focused on the traditional drug discovery programs that are based on the discovery of new therapeutic molecules, rather than developing new approaches to target the brain and circumvent the BBB, which is a major hurdle in the development of therapies for CNS disorders. For a traditional neuropharmaceutical molecule to cross the BBB, it has to be lipid-soluble and weigh less than 500 Da, which makes the CNS drug development quite limited. Figure 6.1 shows the graph representing the complexity of CNS drug development process. Around 40-60 % of the drugs/therapies for the treatment of CNS disorders remain in the pre-clinical or early phase of development. The percentage of CNS drugs in the clinical phases (Phase 1-3) of development ranges between 21-32 %, with less than 5 % of them reaching Phase 3 of clinical trials. Only less than 1-2 % of the total drugs are actually launched, demonstrating the complexity of the CNS drug development processes. Over 5-15 % of the drugs showed no development over a span of 18 months or more and 5-15 % of the drugs were discontinued at some phase of drug development (Kwon *et al*., 2004; Pogacic and Herrling, 2007; Kramp 2011). Majority of the drugs failed to

reach higher phases of clinical development, mainly due to their inability to cross the BBB. However, to date, there is not a single industrial leader having a freestanding BBB drug development platform. The 20th century drug development program was driven by a chemistry-driven platform by discovery of small molecules, however the 21st century shall be driven by a biology-driven pharmaceutics platform for drug development especially in the area of CNS disorders (Pardridge *et al*., 2002). More efficient design in the CNS drug development programs would be to merge the traditional drug discovery program and the novel drug delivery platform so that increased number of therapies could be actually brought from bench to bedside.

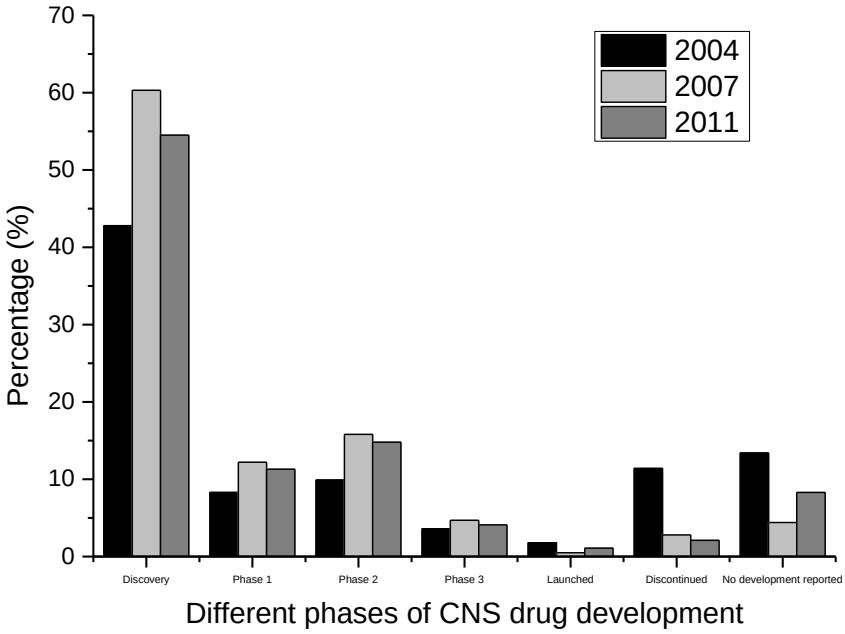

Figure 6.1 Percentage of CNS drugs in different stages of drug development in 2004, 2007 and 2011 (Kwon *et al*., 2004; Pogacic and Herrling 2007; Kramp 2011)

3. Novel platforms for non-invasive brain delivery

The major strategy in the development of novel strategies for the prevention, diagnosis and treatment of CNS disorders would be to design systems that are able to effectively cross the BBB and efficaciously treat the disorder. There are various nanomaterials that have been pre-clinically tested for the targeted delivery of diagnostics and therapeutics to the brain (Nunes *et al*., 2012). As an outcome of this thesis, we hereby provide a novel platform based on the DAB dendrimer for targeted gene delivery to the brain. The conjugation of Tf, Lf and Angiopep-2 to DAB dendrimer led to an enhanced exogenous gene expression in the brain *in vitro* and *in vivo* compared to the DAB dendrimer. However, further investigations will be required for DAB-Ang. Utilizing these novel brain targeted delivery systems will be even more advantageous in pathology, because the level of expression of many receptors that are targeted by these delivery systems will be significantly high in the brain during a pathological state compared to the normal brain.

There is a high expression of TfR in the brain with neoplasms compared to the normal brain tissue (Recht *et al*., 1990). In a study by Prior and colleagues (1990), the authors demonstrated that TfR is also highly expressed in 101 types of the tumours generating from human central and peripheral nervous system. The level of expression also depends on the type and grade of tumours. TfR type 2 is highly and frequently expressed in glioblastoma multiforme (GBM), which is the most common and aggressive brain tumour (Calzolari *et al*., 2010). TfR is also highly expressed in cerebral

ischemia, haemorrhage and stroke (Moos and Morgan, 2004). Several TfR-targeted delivery systems have demonstrated successful diagnostic and therapeutic effects in pre-clinical studies (Table 6.2). Tf-bearing DAB dendrimers could therefore provide an efficient means for the delivery of drugs, genes and other therapeutic and diagnostic agents in these pathologies.

Table 6.2 Various platforms for the TfR-targeted delivery of therapeutic and diagnostic agents to the CNS

Delivery system	Major findings	Reference
OX26-Brain-derived neurotrophic factor (BDNF) conjugate	• Increased uptake of BDNF in the brain • 243 % increase in the motor performance of rats presenting stroke symptoms	Pardridge *et al*., 1998 Zhang and Pardridge, 2006
OX26-Radiolabelled epidermal growth factor (EGF) conjugate	• Successful imaging of the experimental brain tumours in rats bearing human U87 glioma cells	Kurihara and Pardridge, 1999
8D3- $A\beta^{1-40}$ conjugate	• Visualization and quantification of β-amyloid plaques in a mouse model of Alzheimer's disease	Lee *et al*., 2002
OX26-Basic fibroblast growth factor (bFGF) conjugate	• Time dependent 80 % and 67 % reduction in the infarct volume in the brain with treatments administered immediately or 60 min respectively in cerebral ischaemia	Song *et al*., 2002
cTfRMAb-Glial-derived neurotrophic factor (GDNF) conjugate	• Increased brain uptake of GDNF • Therapeutic action in 3 experimental models of Parkinson's disease	Fu *et al*., 2010

Delivery system	Major findings	Reference
Tf- and Tamoxifen-modified liposomes encapsulating Epirubicin	• Inhibition of the tumour volume in a C6 glioma rat model • Longer survival time of the rats compared to the control treatments	Tian *et al*., 2010
Tf-modified *cyclo*-[Arg-Gly-Asp-d-Phe-Lys] (c[RGDfK])-paclitaxel conjugate (RP) loaded micelle (TRPM)	• Increased cellular uptake in brain microvascular endothelial cells • Anti-cancer activity in intracranial U-87 MG glioma mice model. • Mean survival time significantly longer compared to paclitaxel	Zhang *et al*., 2012
Tf- and p-aminophenyl-α-D-mannopyranoside-conjugated liposomes encapsulating daunorubicin	• Inhibition of the tumour volume in a C6 glioma rat model • Longer survival time of the rats compared to the control treatments	Ying *et al*., 2010
cTfRMAb-α-L-iduronidase fusion protein	• Reversal of Mucopolysaccharidosis type 1 or Hurlers syndrome in a mice model • Reduction of lysosomal inclusion bodies in the brain by 73 %	Boado *et al*., 2011
cTfRMAb-ScFv fusion protein	• $A\beta^{1-42}$ was reduced by 40 % in an Alzheimer's disease mice model, without elevation of $A\beta^{1-42}$ concentrations in the plasma • No cerebral microhemorrhage was observed in the treated mice.	Zhou *et al*., 2011
Tf-conjugated SPION	• Demonstrated capability as a MRI contrast agents in a C6 glioma rat model	Jiang *et al*., 2012

Delivery system	Major findings	Reference
Tf-modified paclitaxel-loaded polyphosphoester hybrid micelles	• Increased brain accumulation • Anti-tumour activity in intracranial U87 glioma mice model. • Prolonged survival time demonstrated compared to control groups	Zhang *et al*., 2012
T7-conjugated PEG-dendrigraft poly-L-Lysine covalently linked to doxorubicin and encapsulating pORF-hTRAIL	• Targeted drug and gene co-delivery system successfully synthesized • Synergistic increase in the anti-tumour activity in a U87 orthotropic glioma mice model. • Prolonged survival time compared to control groups.	Liu *et al*., 2012
Tf-modified PEG-graphene oxide encapsulating doxorubicin	• Increased uptake in the C6 rat glioma model • Longer survival time compared to the doxorubicin and other controlled treatment groups	Liu *et al*., 2013
Tf- and folate-modified liposomes encapsulating doxorubicin	• Antitumour-activity in C6 glioma rat model. Mean survival time significantly longer compared to doxorubicin and other treatment groups • Non-toxic on healthy cells compared to doxorubicin	Gao *et al*., 2013
Tf-conjugated magnetic silica PLGA nanoparticles encapsulating doxorubicin and paclitaxel	• Strongest tumour inhibition in an intracranial U87 MG glioma mice model	Cui *et al*., 2013
Tf- and TAT peptide-modified liposomes encapsulating doxorubicin	• Increased brain and tumour uptake • Anticancer-activity in orthotropic glioma model. Mean survival time was significantly longer compared to doxorubicin	Zong *et al*., 2014

Several lines of evidence suggest an increased LfR expression in Parkinson's disease. Iron accumulation in the *substantia nigra* of the Parkinson's disease occurs via lactoferrin receptors (Faucheux *et al*., 1995; Berg *et al*., 2001). Overexpression of LfR is also reported in Alzheimer's disease and other neurodegenerative disorders, owing to the fact that higher iron accumulation is observed in the neuronal cells of these disorders, ultimately leading to cell death (Qian and Wang, 1998). Lf-bearing DAB dendrimers can be a promising platform for the delivery of therapeutics in neurodegenerative disorders that overexpress LfR. We have recently demonstrated that Lf-bearing DAB dendrimers led to a substantial tumour regression in laboratory animals and that transport of these Lf-dendrimers occured through TfR on the tumour cells. (Lim *et al*., 2015). This delivery system can also be further investigated for the treatment of brain tumours. Various preclinical platforms that have already pre-clinically proven results have been mentioned in Table 6.3

Table 5.3 Various platforms for the LfR-targeted delivery of therapeutic and diagnostic agents to the CNS

Delivery system	Major findings	Reference
Lf-conjugated PAMAM encapsulating hGDNF gene	• Gene therapy for rotenone-induced chronic Parkinson rat model • Increased locomotor activity, reduced dopaminergic neuronal loss and enhanced monoamine neurotransmitter levels after repeated multiple dosing via intravenous injection	Huang *et al*., 2010

Delivery system	Major findings	Reference
Lf-conjugated polymersome encapsulating doxorubicin and tetrandrine	• Anticancer activity in C6 glioma rat model. Decreased glioma volume • Significantly longer mean survival time compared to control treatments	Pang *et al*., 2010
Lf-conjugated procationic liposome encapsulating doxorubicin	• Anticancer activity in C6 glioma rat model. Mean survival time was significantly longer compared to control treatments	Chen *et al.,* 2011
Lf-conjugated PEG-PLA nanoparticles encapsulating paclitaxel	• Co-administration with tLyp-1, a tumour penetration enhancement peptide led to enhanced anti-tumour activity in C6 glioma bearing mice model • Survival times were significantly longer compared to control treatments	Miao *et al*., 2013
Lf-conjugated micelles encapsulating super paramagnetic iron oxide nanoparticles	• MRI imaging of glioma in a rat model	Zhou *et al*., 2015

LRP1 and LRP2 are multifunctional receptors linked to many CNS pathologies. Increased expression of LRP1 and LRP2 is observed in stroke. They serve as a receptor for amyloid β precursor protein and ApoE, that are genetically linked to Alzheimer's disease. The expression of LRP1 and LRP2 significantly decreases with age, ultimately leading to AD development due to

the decrease in clearance of Aβ-anti-aβ complexes. As LRP1 and LRP2 inhibit inflammatory processes, they are linked with the majority of neurodegenerative disorders that has a neuroinflammatory process involved (Chen and Liu, 2012). Overexpression of LRP1 and LRR2 is also observed in brain tumours. Table 6.4 lists some of the Angiopep-2 targeted platforms pre-clinically evaluated for the CNS therapeutics. Angiopep-2 bearing DAB dendrimers can also be investigated further for pre-clinical testing.

Table 6.4 Various platforms for the Angiopep-2 targeted delivery of therapeutic and diagnostic agents to the CNS

Delivery system	Major findings	Reference
Angiopep-2-conjugated PAMAM-PEG loaded with pORF-TRAIL	• Anticancer-activity by gene therapy in C6 glioma mice model. Mean survival time was significantly longer compared to control treatments	Huang *et al*., 2011
Angiopep-2-conjugated liposome encapsulating pEGFP-hTRAIL and paclitaxel	• Synergistic increase in the anti-tumour activity in a U87 orthotropic glioma mice model. Decrease in the tumour volume • Prolonged survival time compared to the control treatment	Sun *et al*., 2011
Angiopep-2 functionalized PEGylated oxidized multi-walled carbon nanotubes encapsulating doxorubicin	• Anticancer-activity in C6 glioma mice model. Mean survival time was significantly longer compared to control treatments	Ren *et al*., 2012

Delivery system	Major findings	Reference
Angiopep-2-bearing polymeric micelles encapsulating Amphotericin B	• Increase brain penetration of Amphotericin B • Anti-fungal activity demonstrated in an intracerebral fungal infection murine model. Prolonged survival times reported compared to control treatments	Shao *et al*., 2012
Angiopep-2-conjugated PEG-polycaprolactone nanoparticles encapsulating Paclitaxel	• Anti-tumour activity in a U87 orthotropic glioma mice model • Decrease of tumour volume • Prolonged survival time compared to the control treatments	Xin *et al*., 2012
Angiopep-2- and tLyp-1-conjugated cationic liposomes encapsulating VEGF siRNA and docetaxel	• Synergistic increase in the anti-tumour activity in a U87 orthotropic glioma mice model • Decrease in the tumour volume	Yang *et al*., 2014
Angiopep-2- and Activatable cell penetrating peptide (ACP)-functionalized PEG-Polycaprolactone nanoparticles encapsulating docetaxel	• Anticancer activity in C6 glioma mice model. Mean survival time was significantly longer compared to control treatments	Gao *et al*., 2014
Angiopep-2-conjugated PEG-carbonaceous nanodots	• Non-invasive imaging agents in the C6 orthotropic glioma mice model	Ruan *et al*., 2014
Angiopep-2-decorated PEG-gold nanoparticles encapsulating doxorubicin	• Tumour microenvironment sensitive doxorubicin delivery in C6 glioma mice model • Anti-tumour activity and prolonged survival times compared to the control treatments	Ruan *et al*., 2015

Tf-, Lf- and Ang- bearing DAB dendrimers thus provide a safe and efficacious novel platform for the delivery of therapeutic and diagnostic agents to the brain, utilizing the endogenous receptor mediated transcytosis pathways that are already present at the BBB. These targeted dendrimers can be conjugated to different modalities like drugs, peptides, therapeutic genes and imaging agents, and customized for specific applications.

CHAPTER 7

Conclusion and Future work

1. Conclusion

The development of novel CNS targeted drug and gene delivery systems has been limited due to the presence of the BBB and due to the lack of safe and efficacious delivery systems. In this thesis, dendrimers modified with various targeting ligands were synthesized, characterized and evaluated for their efficiency for targeted gene delivery to the brain.

Chapter 1 provides a general introduction on the most common CNS disorders, the BBB and gene therapy. CNS disorders, such as brain neoplasms, Alzheimer's disease, Parkinson's disease and Huntington's disease, lead to the worst decline in the quality of life of the patient. BBB consists of specialized endothelial cells of the brain microvessels, supported by astrocytes and pericytes to form a functional neurovascular unit controlling the movement of molecules on either side. BBB is highly compromised in the CNS pathology. Various strategies, both invasive and non-invasive, have been investigated for the delivery of the therapeutics to the brain. Receptor-mediated transcytosis has emerged as the most promising solution for the delivery of the therapeutics to the brain. Gene therapy is a novel therapeutic approach that includes replacing a faulty gene with a functional or healthy gene. It is a highly promising approach for the treatment of CNS disorders, as the genetic basis of most of them is known. However, delivering gene to specific tissues or cells requires a gene delivery system. Viral delivery systems are efficient, but unsafe and unpredictable. Non-viral gene delivery

systems, such as liposomes, polymers and dendrimers have been investigated for gene delivery to the brain.

Chapter 2 describes the materials and methods used for experiments. Methods are broadly categorized in to three: Synthesis and characterization of targeted dendrimers, *in vitro* studies on immortalized murine brain capillary endothelial cells and *in vivo* studies in a mice model.

Chapter 3 describes the evaluation of transferrin-bearing DAB-polypropylenimine dendrimer for gene delivery to the brain. Transferrin, an iron-binding protein when grafted on a DAB dendrimer led to 2-fold increase in the gene expression in the brain to that observed with unconjugated DAB dendrimer *in vivo*. The non-specific gene expression in the other major organs was at least 3-fold lower to that observed in the brain.

Chapter 4 focuses on the synthesis, characterization, *in vitro* and *in vivo* evaluation of lactoferrin- and lactoferricin-bearing DAB-polypropylenimine dendrimers for targeted gene delivery to the brain. After intravenous administration, lactoferrin-bearing DAB dendrimer resulted in a 6.4-fold increase in gene expression compared to that observed with unconjugated DAB dendrimer. Lactoferricin-bearing DAB dendrimer exhibited an increased cellular uptake and gene expression *in vitro* compared to that observed with DAB dendrimer. However, no gene expression in the brain was observed *in vivo*.

Chapter 5 describes the synthesis, characterization, *in vitro* and *in vivo* evaluation of Angiopep-2-bearing DAB-polypropylenimine dendrimer for targeted gene delivery to the brain. *In vitro,* Angiopep-2-bearing DAB dendrimer led to a 1.7-fold and 1.9-fold increase in the cellular uptake and gene expression respectively, compared to DAB dendrimer. *In vivo,* bioluminescence imaging also demonstrated higher gene expression in the brain compared to the DAB dendrimer, but quantification of biodistribution showed different results. Further investigations will be needed to confirm both results.

Chapter 6 discusses the results obtained in this thesis, placed in the overall context of CNS drug development. It describes the prevalence of the CNS disorders in UK, Europe and globally and the healthcare costs related to these disorders. The pharmaceutical industry needs to revolutionize the way to develop CNS therapies by implementing novel strategies to circumvent the BBB in a non-invasive manner. Various platforms that have been pre-clinically tested for CNS disorders are described.

2. Future work

Due to their high efficiency to circumvent the BBB and enhance the exogenous gene expression in the brain, the dendrimers described in this thesis can be developed further in various ways, as described below.

Table 7.1 Possible future developments of brain-targeted dendrimers

Future work	Modality	Description
Bifunctional dendrimers	Dendrimers bearing 2 ligands on their surfaces: • Transferrin/lactoferrin/angio pep-2 and lysine • Transferrin/lactoferrin/Angio pep and arginine	• Lysine and Arginine are cell-penetrating peptides that can lead to Adsorptive-mediated transcytosis across the BBB, in addition to receptor-mediated transcytosis, resulting in higher brain penetration
	Dendrimers bearing 2 ligands on their surfaces • Transferrin/lactoferrin/angio pep-2 and epidermal growth factor • Transferrin/lactoferrin/angio pep-2 and vascular endothelial growth factor	• Brain tumour targeting • Higher targeting efficiency as receptors for all ligands are overexpressed on most brain tumours • Treatment using drugs that are unable to cross the BBB by themselves • Gene therapy using therapeutic genes
Targeted drug delivery	Dendrimer-drug conjugate	• Delivery of various drugs for various CNS disorders • Treatment of disorders by targeted drug therapy
Gene therapy	Dendrimer-therapeutic gene complexes	• Treatment of disorders by targeted gene therapy
Delivery of imaging agents	Dendrimer-superoxide iron oxide nanoparticles conjugate	• Targeted MRI imaging of brain tumours
Delivery of peptides, proteins and enzymes	Dendrimer-peptide/protein/enzyme conjugate	• Treatment of disorders by targeted peptide and protein therapy and enzyme replacement therapy

The targeted dendrimers developed in this thesis have shown to be highly efficient gene delivery systems for brain targeting and will be further investigated for the delivery of diagnostic and therapeutic agents in CNS disorders.

References

Abbott, N. J., Romero, I. A. (1996). Transporting therapeutics across the blood-brain barrier. *Molecular Medicine Today*, *2*(3), 106–13.

Abbott, N. J. (2002). Astrocyte-endothelial interactions and blood-brain barrier permeability. *Journal of Anatomy*, *200*(6), 629–38.

Abbott, N. J. (2005). Physiology of the blood–brain barrier and its consequences for drug transport to the brain. *International Congress Series*, *1277*, 3–18.

Abbott, N. J., Rönnbäck, L., Hansson, E. (2006). Astrocyte-endothelial interactions at the blood-brain barrier. *Nature reviews. Neuroscience*, *7*(1), 41–53.

Aldawsari, H., Edrada-Ebel, R., Blatchford, D., Tate, R., Tetley, L., Dufès, C. (2011). Enhanced gene expression in tumors after intravenous administration of arginine-, lysine- and leucine-bearing polypropylenimine polyplex. *Biomaterials, 32* (25), 5889-5899.

Al Robaian, M., Chiam, K. Y., Blatchford, D., Dufès, C. (2014). Therapeutic efficacy of intravenously administered transferrin-conjugated dendriplexes on prostate carcinomas. *Nanomedicine 9* (4), 421-434.

Andlin-Sobocki, P., Jonsson, B., Wittchen, H-U., Olesen, J. (2005). Cost of disorders of the brain in Europe. *European Journal of Neurology, 12*, 1-27.

Doi, E., Epstein, H., Dahan, R., Koroukhov, N., Rohekar, K., Danenberg, H. D., Golomb, G. (2008). Delivery of serotonin to the brain by monocytes following phagocytosis of liposomes. *Journal of Controlled Release*, *132*(2), 84–90.

Aragnol, D., Leserman, L. D. (1986). Immune clearance of liposomes inhibited by an anti-Fc receptor antibody *in vivo*. *Proceedings of the National Academy of Sciences of the United States of America*, *83*(8), 2699–703.

Balazs, D. A, Godbey, W. (2011). Liposomes for use in gene delivery. *Journal of Drug Delivery*, *2011*, 3264-97.

Banks, W. A. (2012). Drug delivery to the brain in Alzheimer's disease: consideration of the blood-brain barrier. *Advanced Drug Delivery Reviews*, *64*(7), 629–39.

Bansal, K., Engelhard, H. H. (2000). Gene therapy for brain tumors. *Current Oncology Reports*, *2*(5), 463–472.

Batrakova, E. V., Miller, D. W., Li, S., Alakhov, V. Y., Kabanov, A. V., Elmquist, W. F. (2001). Pluronic P85 Enhances the Delivery of Digoxin to the Brain: *In Vitro* and *in Vivo* Studies. *The Journal of Pharmacology and Experimental Therapeutics, 296* (2), 551-557.

Beitz, J. M. (2014). Parkinson's disease: a review. *Frontiers in Biosciences*, 6, 65-74.

Berkman, R. A., Merrill, M. J., Reinhold, W. C., Monacci, W. T., Saxena, A., Clark, W. C., Robertson, J. T., Ali, I. U., Oldfield, E. H. (1993). *The Journal of Clinical Investigation, 91*, 153-159 .

Bhaskar, S., Tian, F., Stoeger, T., Kreyling, W., De la Fuente, J. M., Grazú, V., Borm, P. (2010). Multifunctional Nanocarriers for diagnostics, drug delivery and targeted treatment across blood-brain barrier: perspectives on tracking and neuroimaging. *Particle and Fibre Toxicology*, *7*(3), 1-25.

Blasi, P., Giovagnoli, S., Schoubben, A., Ricci, M., Rossi, C. (2006). Solid lipid nanoparticles for targeted brain drug delivery. *Advanced Drug Delivery Reviews, 59*, 454-477.

Boado, R. J., Li, J. Y., Nagaya, M., Zhang, C., Pardridge, W. M. (1999) Selective expression of the large neutral amino acid transporter at the blood-brain barrier. *Proceedings of the National Academy of Sciences of the United States of America* 96 (21), 12079-12084.

Boado, R. J., Hui, E. K., Lu, J. Z., Zhou, Q. H., Pardridge, W. M. (2011). Reversal of lysosomal storage in brain of adult MPS-I mice with intravenous Trojan horse-iduronidase fusion protein. *Molecular Pharmaceutics, 8* (4), 1342-1350.

Boussif, O., Lezoualc'h, F., Zanta, M. A, Mergny, M. D., Scherman, D., Demeneix, B., Behr, J. P. (1995). A versatile vector for gene and oligonucleotide transfer into cells in culture and *in vivo*: polyethylenimine. *Proceedings of the National Academy of Sciences of the United States of America*, *92*(16), 7297–301.

Brigger, I., Morizet, J., Aubert, G., Chacun, H., Terrier-Lacombe, M., Couvreur, P., Vassal, G. (2002). Poly(ethylene glycol)-coated hexadecylcyanoacrylate nanospheres display a combined effect for brain tumor targeting. *Journal of Pharmacology and Experimental Therapeutics, 303* (3), 928-936.

Brookmeyer, R., Johnson, E., Ziegler-Graham, K., Arrighi, H.M. (2007). Forecasting the global burden of Alzheimer's disease. *Alzheimer's & Dementia*, 3, 186-191.

Bryan Brandenberg blog, assessed on 15th July 2015. http://bryanmbrandenburg.com/herpes-simplex-virus-gallery/

Cancer Research UK, Updated on 2nd Decemeber 2014, Assessed on 12th March 2015. http://www.cancerresearchuk.org/cancer-info/cancerstats/types/brain/uk-brain-and-cns-tumour-statistics

Cardoso, F. L., Brites, D., Brito, M. A. (2010). Looking at the blood-brain barrier: molecular anatomy and possible investigation approaches. *Brain Research Reviews*, *64*(2), 328–63.

Carvey, P. (2009). The blood–brain barrier in neurodegenerative disease: a rhetorical perspective. *Journal of Neurochemistry, 111*(2), 291–314.

Che, C., Yang, G., Thiot, C., Lacoste, M-C, Currie, J-C, Demeule, M., Regina, A., Beliveau, R., Castaigne, J-P. (2010). New Angiopep-Modified Doxorubicin (ANG1007) and Etoposide (ANG1009) Chemotherapeutics With Increased Brain Penetration. *Journal of Medicinal Chemistry, 53*, 2814-2824.

Chen, H., Tang, L., Qin, Y., Tang, J., Tang, W., Sun, X., Zhang, Z., Liu, J, He, Q. (2010). Lactoferrin-modified procationic liposomes as a novel drug carrier for brain delivery. *European Journal of Pharmaceutical Sciences, 14*, 94-102

Chen, Y., Liu, L. (2012). Modern methods for delivery of drugs across the blood-brain barrier. *Advanced Drug Delivery Reviews*, *64*(7), 640–65.

Choi, Y. K., Kim, K.W. (2008). Blood-neural barrier: its diversity and coordinated cell-to-cell communication. *BMB Reports*, *41*(5), 345–52.

Chung, Y. C., Ko, H. W., Bok, E., Park, E.S., Huh, S, H,. Nam, J. H., Jin, B. K. (2010). The role of neuroinflammation on the pathogenesis of Parkinson's disease. *BMB Reports,* 225-232

Cirrito, J. H., Deane, R., fagan, A. M., Spinner, M. L., Parsadanian, M., Fin, M. B., Jiang, H., Prior, J. L., Sagare, A., Bales, K. R., Paul, S. M., Zlokovic, B. V., Piwnica-Worms, D., Holtzman, D. M. (2005). P-glycoprotein deficiency at the blood-bain barrier increases amyloid- β deposition in an Alzheimer disease mouse model. *The Journal of Clinical Investigation*, 115, 3285-3290.

Colin, M., Moritz, S., Schneider, J., Capeau, C., Coutelle, C., Brahimi-Horn, M. C. (2000). Haemoglobin interferes with the *ex vivo* luciferase luminescence assay: consequence for detection of luciferase reporter gene expression *in vivo* , *Gene therapy, 7*, 1333-1336.

Calzolari, A., Larocca, L. M., Deaglio, S., Finisguerra, V., Boe, A., Raggi, C., Ricci-Vitani, L., Pierconti, F., Malavasi, F., De Maria, R., Testa, U., Pallini, R. (2010). Transferrin Receptor 2 Is Frequently and Highly Expressed in Glioblastomas. *Translational Oncology, 3* (2), 123-134.

Chen, H., Qin, Y., Zhang, Q., Jiang, W., Tang, L., Liu, J., He, Q. (2011). Lactoferrin modified doxorubicin-loaded procationic liposomes for the treatment of gliomas. *European Journal of Pharmaceutical Sciences, 44* (1-2), 164-173.

Computer Adenovirus by Dr. Richard Feldmann (2001), National Cancer Institute Visuals Online, assessed on 15th July 2015. https://visualsonline.cancer.gov/details.cfm?imageid=2132

Connor, J. R., Menzies, S. L. (1995). Cellular management of iron in the brain. *Journal of the Neurological Sciences*, *134* (12), 33–44.

Cook, B. D., Ferrari, G., Pintucci, G., Mignatti, P. (2008). TGF-beta1 induces rearrangement of FLK-1-VE-cadherin-beta-catenin complex at the adherens junction through VEGF-mediated signaling. *Journal of Cellular Biochemistry*, *105*(6), 1367–73.

Cui, Y., Xu, Q., Chow, P. K., Wang, D., Wang, C.H. (2013). Transferrin-conjugated magnetic silica PLGA nanoparticles loaded with doxorubicin and paclitaxel for brain glioma treatment. *Biomaterials,* 34 (33), 8511-8520.

Dando, J.S., Roncarolo, M.G., Bordignon, C., Aiuti, A., (2001). A novel human packaging cell line with haematopoetic supportive capacity increases gene transfer into early haematopoetic progenitors. *Human Gene Therapy* 12, 1979-1988

Davie, C.A. (2008). A review of Parkinson's disease. *British Medical Bulletin*, 86, 109-127

de Boer, A G., Gaillard, P. J. (2006). Blood-brain barrier dysfunction and recovery. *Journal of Neural Transmission*, *113*(4), 455–62.

Dehouck, B., Fenart, L., Dehouck, M. P., Pierce, A, Torpier, G., Cecchelli, R. (1997). A new function for the LDL receptor: transcytosis of LDL across the blood-brain barrier. *The Journal of Cell Biology*, *138*(4), 877–89.

Dehouck, M. P., Méresse, S., Delorme, P., Fruchart, J. C., Cecchelli, R. (1990). An easier, reproducible, and mass-production method to study the blood-brain barrier *in vitro*. *Journal of Neurochemistry*, *54*(5), 1798–801.

Deli, M. A. (2009). Potential use of tight junction modulators to reversibly open membranous barriers and improve drug delivery. *Biochimica et Biophysica Acta*, *1788*(4), 892–910.

Demeule, M., Shedid, D., Beaulieu, E., Del Maestro, R. F., Moghrabi, A., Ghosn, P. B., Moumdjian, R., Berthelet, F., Beliveau, R. (2001). Expression of multidrug-resistance P-glycoprotein (MDR1) in human brain tumors. *International Journal of Cancer,* 93, 62-66.

Demeule, M., Poirier, J., Jodoin, J., Bertrand, Y., Desrosiers, R. R., Dagenais, C., Nguyen, T., Lanthier, J., Gabathuler, R., Kennard, M., Jefferies, W. A., Karkan, D., Tsai, S., Fenart, L., Cecchelli, R., Beliveau, R. (2002). High transcytosis of melanotransferrin (P97) across the blood-brain barrier. *Journal of Neurochemistry*, *83*(4), 924–33.

Demeule, M., Re, A., Che, C., Poirier, J., Nguyen, T., Gabathuler, R., Castaigne, J. (2008). Identification and Design of Peptides as a New Drug Delivery System for the Brain, *Journal of Pharmacology and Experimental Therapeutics*, *324*(3), 1064–1072.

Demeule, M., Currie, J-P., Bertrand, Y., Che, C., Nguyen, T., Regina, A., Gabathuler, R., Castaigne, J-P., Beliveau, R. (2008). Involvement of the low-density lipoprotein receptor-related protein in the transcytosisof the brain delivery vector Angiopep-2. *Journal of Neurochemistry, 106*, 1534-1544

Dohgu, S., Takata, F., Yamauchi, A., Nakagawa, S., Egawa, T., Naito, M., Tsuruo, T. (2005). Brain pericytes contribute to the induction and up-regulation of blood-brain barrier functions through transforming growth factor-beta production. *Brain Research*, *1038*(2), 208–15.

Doi, A., Kawabata, S., Iida, K., Yokoyama, K., Kajimoto, Y., Kuroiwa, T., Shirakawa, T. (2008). Tumor-specific targeting of sodium borocaptate (BSH) to malignant glioma by transferrin-PEG liposomes: a modality for boron neutron capture therapy. *Journal of Neuro-oncology*, *87*(3), 287–94.

Domínguez, A., Álvarez, A., Hilario, E., Suarez-Merino, B., Goñi-de-Cerio, F. (2013). Central nervous system diseases and the role of the blood-brain barrier in their treatment. *Neuroscience Discovery*, 1(3), 1-11

Doolittle, N. D., Abrey, L. E., Bleyer, W. A., Brem, S., Davis, T. P., Dore-duffy, P., Drewes, L. R. (2005). New Frontiers in Translational Research in Neuro-oncology and the Blood-Brain Barrier: Report of the Tenth Annual Blood-Brain Barrier Disruption Consortium Meeting New Frontiers in Translational Research in Neuro-oncology and the Blood-Brain Barrier, *Clinical Cancer Research* 11, 421–428.

Dufès, C., Uchegbu, I. F., Schätzlein, A. G. (2005). Dendrimers in gene delivery. *Advanced Drug Delivery Reviews*, *57*(15), 2177–202.

Edelman, D. A., Jiang, Y., Tyburski, J., Wilson, R. F., Steffes, C. (2006). Pericytes and their role in microvasculature homeostasis. *The Journal of Surgical Research*, *135*(2), 305–11.

Emerich, D. F., Snodgrass, P., Dean, R., Agostino, M., Hasler, B., Pink, M., Xiong, H. (1999). Enhanced delivery of carboplatin into brain tumours with intravenous Cereport (RMP-7): dramatic differences and insight gained from dosing parameters. *British Journal of Cancer*, *80*(7), 964–70.

Fenart, P., Cecchelli, R., (2003). Protein transport in cerebral endothelium. *In vitro* transcytosis of transferrin. *Methods in Molecular Medicine, 89*, 277-290.

Fillebeen, C., Descamps, L., Dehouck, M. P., Fenart, L., Benaïssa, M., Spik, G., Cecchelli, R. (1999). Receptor-mediated transcytosis of lactoferrin through the blood-brain barrier. *The Journal of Biological Chemistry*, *274*(11), 7011–7.

Frölich, L., Blum-Degen, D., Bernstein, H. G., Engelsberger, S., Humrich, J., Laufer, S., Muschner, D. (1998). Brain insulin and insulin receptors in aging and sporadic Alzheimer's disease. *Journal of Neural Transmission*, *105*(4), 423.

Fu, A., Zhou, Q. H., Hui, E. K., Lu, J. Z., Boado, R. J., Pardridge, W. M. (2010). Intravenous treatment of experimental Parkinson's disease in the mouse with an IgG-GDNF fusion protein that penetrates the blood-brain barrier. *Brain Research, 1352*, 208-213.

Gabathuler, R. (2010). Approaches to transport therapeutic drugs across the blood-brain barrier to treat brain diseases. *Neurobiology of Disease*, *37*(1), 48–57.

Gabathuler, R., Arthur, G., Kennard, M., Chen, Q., Tsai, S., Yang, J., Schoorl, W. (2005). Development of a potential protein vector (NeuroTrans) to deliver drugs across the blood–brain barrier. *International Congress Series*, *1277*, 171–184.

Gaillard, P., de Boer, A. (2006). A novel opportunity for targeted drug delivery to the brain. *Journal of Controlled Release*, *116*(2), 58–60.

Gaillard, P. J., Brink, A., de Boer, A. G. (2005). Diphtheria toxin receptor-targeted brain drug delivery. *International Congress Series 1277*, 185–198.

Gao, H., Pang, Z., Fan, L., Hu, K., Wu, B., Jiang, X. (2010). Effect of lactoferrin- and transferrin-conjugated polymersomes in brain targeting: *in vitro* and *in vivo* evaluations. *Acta Pharmacologica Sinica*, *31*, 237–243.

Gao, J. Q., Lv, Q., Li, L. M,, Tang, X. J., Li, F. Z., Hu, Y. L., Han, M. (2013). Glioma targeting and blood-brain barrier penetration by dual-targeting doxorubicin liposomes. *Biomaterials, 34* (22), 5628-5639.

Gao, H., Zhang, S., Cao, S., Yang, Z., Pang, Z., Jiang, X. (2014). Angiopep-2 and activatable cell-penetrating peptide dual-functionalized nanoparticles for systemic glioma-targeting delivery. *Molecular Pharmaceutics*, 11 (8), 2755-2763.

Garcia-Garcia, E., Andrieux, K., Gil, S., Couvreur, P. (2005). Colloidal carriers and blood-brain barrier (BBB) translocation: a way to deliver drugs to the brain? *International Journal of Pharmaceutics*, *298*(2), 274–92.

Gardlík, R., Pálffy, R., Hodosy, J., Lukács, J., Turna, J., Celec, P. (2005). Vectors and delivery systems in gene therapy. *Medical Science Monitor: International Medical Journal of Experimental and Clinical Research*, *11*(4), 110–21.

Ge, S., Song, L., Pachter, J. S. (2005). Where is the blood-brain barrier ... really? *Journal of Neuroscience Research*, *79*(4), 421–7.

Giacca, M. (2010). *Gene Therapy*. Italy: Springer-Verlag Italia. 1-7.

Gifford, J. L., Hunter, H. N., Vogel, H. J. (2005). Lactoferricin: a lactoferrin-derived peptide with antimicrobial, antiviral, antitumor and immunological Properties. *Cellular and Molecular life Sciences, 62*, 2588-2598.

Gong, C., Li, X., Xu, L., Zhang, Y. H. (2012). Target delivery of a gene into the brain using the RVG29-oligoarginine peptide. *Biomaterials*, *33*(12), 3456–63.

Gosk, S., Vermehren, C., Storm, G., Moos, T. (2004). Targeting Anti–Transferrin Receptor Antibody (OX26) and OX26-Conjugated Liposomes to Brain Capillary Endothelial Cells Using *In Situ* Perfusion. *Journal of Cerebral Blood Flow and Metabolism, 24*, 1193-1204

Gudesblatt, M., Tarsy, D. (2011). Huntington's disease: A clinical review. *Supplement to Neurology reviews*, S1–S8.

Han, L., Zhang, A., Wang, H. (2011). Construction of novel brain targeting gene delivery system by natural magnetic nanoparticles. *Journal of Applied Polymer Science 121,* 3446-54.

Hawkins, B., Davis, T. (2005). The blood-brain barrier/neurovascular unit in health and disease. *Pharmacological Reviews*, *57*(2), 173–185.

Hayashi, Y., Nomura, M., Yamagishi, S., Harada, S., Yamashita, J., Yamamoto, H. (1997). Induction of various blood-brain barrier properties in non-neural endothelial cells by close apposition to co-cultured astrocytes. *Glia*, *19*(1), 13–26.

He, H., Li, Y., Jia, X. R., Du, J., Ying, X., Lu, W. L., Lou, J. N. (2011). PEGylated Poly(amidoamine) dendrimer-based dual-targeting carrier for treating brain tumors. *Biomaterials*, *32*(2), 478–87.

Herman, I. M., D'Amore, P. A. (1985). Microvascular pericytes contain muscle and non-muscle actins. *The Journal of Cell Biology*, *101*(1), 43–52.

Hervé, F., Ghinea, N., Scherrmann, J.-M. (2008). CNS delivery via adsorptive transcytosis. *The AAPS journal*, *10*(3), 455–72.

Herz, J. (2003). LRP: a bright beacon at the blood-brain barrier. *Journal of Clinical Investigation, 112*, 1483-1485.

Holman, D. W., Klein, R. S., Ransohoff, R. M. (2011). The blood-brain barrier, chemokines and multiple sclerosis. *Biochimica et Biophysica Acta*, *1812*(2), 220–30.

Hu, K., Li, J., Shen, Y., Lu, W., Gao, X., Zhang, Q., Jiang, X. (2009). Lactoferrin-conjugated PEG-PLA nanoparticles with improved brain delivery: *in vitro* and *in vivo* evaluations. *Journal of Controlled Release: 134*(1), 55–61.

Hu, K., Shi, Y., Jiang, W., Han, J., Huang, S., Jiang, X. (2011). Lactoferrin conjugated PEG-PLGA nanoparticles for brain delivery: preparation, characterization and efficacy in Parkinson's disease. *International Journal of Pharmaceutics*, *415*(1-2), 273–83.

Huang, J., Upadhyay, U. M., Tamargo, R. J. (2006). Inflammation in stroke and focal cerebral ischemia. *Surgical Neurology*, *66*(3), 232–45.

Huang, R. Q., Qu, Y. H., Ke, W. L., Zhu, J. H., Pei, Y. Y., Jiang, C. (2007a). Efficient gene delivery targeted to the brain using a transferrin-conjugated polyethyleneglycol-modified polyamidoamine dendrimer. *The FASEB Journal*, *21*(4), 1117–25.

Huang, R., Ke, W, Qu, Y., Zhu, J., Pei, Y., Jiang, C. (2007). Characterization of lactoferrin receptor in brain endothelial capillary cells and mouse brain*. Journal of Biomedical Sciences, 14*, 121-128.

Huang, R., Ke, W., Liu, Y., Jiang, C., Pei, Y. (2008). The use of lactoferrin as a ligand for targeting the polyamidoamine-based gene delivery system to the brain. *Biomaterials*, *29*(2), 238–246.

Huang, R., Ke, W., Han, L., Liu, Y., Shao, K., Ye, L., Lou, J. (2009). Brain-targeting mechanisms of lactoferrin-modified DNA-loaded nanoparticles. *Journal of Cerebral Blood Flow and Metabolism*, *29*(12), 1914–1923.

Huang, R., Ke, W., Han, L., Li, J., Liu, S., Jiang, C. (2011). Targeted delivery of chlorotoxin-modified DNA-loaded nanoparticles to glioma via intravenous administration. *Biomaterials*, *32*(9), 2399–2406.

Huang, R., Ke, W., Liu, Y., Wu, D., Feng, L., Jiang, C., Pei, Y. (2010). Gene therapy using lactoferrin-modified nanoparticles in a rotenone-induced chronic Parkinson model. *Journal of Neurological Sciences, 290* (1-2), 123-130.

Huang, S., Li, J., Han, L., Liu, S., Ma, H., Huang, R., Jiang, C. (2011). Dual targeting effect of Angiopep-2-modified, DNA-loaded nanoparticles for glioma. *Biomaterials, 32* (28), 6832-6838.

Huber, J. D., Egleton, R. D., Davis, T. P. (2001). Molecular physiology and pathophysiology of tight junctions in the blood-brain barrier. *Trends in Neurosciences*, *24*(12), 719–25.

Huwyler, J., Wu, D., Pardridge, W. M. (1996). Brain drug delivery of small molecules using immunoliposomes. *Proceedings of the National Academy of Sciences of the United States of America*, *93*(24), 14164–9.

Hynynen, K., McDannold, N. (2001). Noninvasive MR Imaging–guided Focal Opening of the Blood-Brain Barrier in Rabbits. *Radiology, 220*(3), 640-646.

International committee on taxonomy of viruses. (2008). Assessed on 15th July 2015. http://www.virology.wisc.edu/virusworld/ICTV8/aav-adeno-associated-ictv8.jpg

Janzer, R., Raff, M. (1987). Astrocytes induce blood–brain barrier properties in endothelial cells. *Nature*, *325*(6101), 253-257.

Jefferies, W. A., Brandon, M. R., Hunt, S. V., Williams, A. F., Gatter, K. C., Mason, D. Y. (1984). Transferrin receptors on endothelium of brain capillaries. *Nature, 312*, 162-163.

Jiang, W., Xie, H., Ghoorah, D., Shang, Y., Shi, H., Liu, F., Yang, X., Xu, H. (2012). Conjugation of functionalized SPIONs with transferrin for targeting and imaging brain glial tumors in rat model. *PLoS One, 7* (5).

Kabanov, A. V., Batrakova, E. V., Alakhov, V. Y. (2003). An essential relationship between ATP depletion and chemosensitizing activity of Pluronic® block copolymers. *Journal of Controlled Release*, 1 (2), 75-83.

Kawabata, H., Germain, R. S., Vuong, P. T., Nakamaki, T., Said, J. W., Koeffler, H. P. (2000). Transferrin receptor 2-alpha supports cell growth in iron-chelated cultured cells and *in vivo*. *Journal of Biological Chemistry, 275*, 16618-16625.

Kay, M., Liu, D., Hoogerbrugge, P. (1997). Gene therapy. *The National Academy of Sciences 94*, 12744–12746.

Ke, W., Shao, K., Huang, R., Han, L., Liu, Y., Li, J., Kuang, Y., Ye, L., Lou, J., Jiang, C. (2009). Gene delivery targeted to the brain using an Angiopep-conjugated polyethyleneglycol-modified polyamidoamine dendrimer. *Biomaterials, 30*, 6976-6985

Kelley, C., D'Amore, P., Hechtman, H. B., Shepro, D. (1987). Microvascular pericyte contractility *in vitro*: comparison with other cells of the vascular wall. *The Journal of Cell Biology*, *104*(3), 483–90.

Ko, Y. T., Bhattacharya, R., Bickel, U. (2009). Liposome encapsulated polyethylenimine/ODN polyplexes for brain targeting. *Journal of Controlled Release*, *133*(3), 230–7.

Kootstra, N.A.; Verma, I.M.; (2003). Gene therapy with viral vectors. *Annual Review of Pharmacology and Toxicology* 43, 413-439

Koppu, S., Oh, Y. J., Edrada-Ebel, R., Blatchford, D. R., Tetley, L., Tate, R. J., Dufès, C. (2010). Tumor regression after systemic administration of a novel tumor-targeted gene delivery system carrying a therapeutic plasmid DNA. *Journal of Controlled Release*, *143*(2), 215–21.

Kortekas, R., Leenders, K. L., van Oostrom, J. C. H., Vaalburg, W., Bart, J., Willemsen, A. T. M., Hendrikse, N. H. (2005). Blood-brain barrier dysfunction in Parkinsonian midbrain *in vivo*. *Annals of Neurology*, 176-179.

Kramp, V. P. (2011). List of Drugs in Development for Neurodegenerative Diseases: Update October 2011. *Neurodegenerative diseases, 9*, 210-283.

Kuang, Y., Lackay, S., Zhao, L., Fu, Z. (2009). Role of chemokines in the enhancement of BBB permeability and inflammatory infiltration after rabies virus infection. *Virus Research*, *144*, 18–26.

Kurihara, A., Pardridge, W. M. (1999). Imaging brain tumors by targeting peptide radiopharmaceuticals through the blood-brain barrier. *Cancer Research, 59* (24), 6159-6163.

Kwon, M-O., Fischer, F., Matthison, M., Herrling, P. (2004). List of Drugs in Development for Neurodegenerative Diseases. *Neurodegenerative Diseases, 1*, 113-152.

Lai, C. H., Kuo, K. H. (2005). The critical component to establish *in vitro* BBB model: Pericyte. *Brain Research Reviews*, *50*(2), 258–65.

Lamszus, K., Laterra, J., Westphal, M., Rosen, E. M. (1999). Scatter factor/ Hepatocyte growth factor (SF/HGF) content and function in human gliomas. *International Journal of Developmental Neuroscience*, 17 (5-6), 717-530.

Lee, H. J., Zhang, Y., Zhu, C., Duff, K., Pardridge, W.M. (2002). Imaging brain amyloid of Alzheimer disease *in vivo* in transgenic mice with an Abeta peptide radiopharmaceutical. *Journal of Cerebral Blood Flow and Metabolism. 22* (2), 223-231.

Lee, H. J., Boado, R. J., Braasch, D. A., Corey, D. R., Pardridge, W. M. (2002). Imaging gene expression in the brain *in vivo* in a transgenic mouse model of Huntington's disease with an antisense radiopharmaceutical and drug-targeting technology. *Journal of Nuclear Medicine, 43* (7), 948-956.

Lee, G., Bendayan, R. (2004). Functional expression and localization of P-glycoprotein in the central nervous system: relevance to the pathogenesis and treatment of neurological disorders. *Pharmaceutical Research*, *21*(8), 1313–30.

Leitner, D. F., Connor, J. R. (2012). Functional roles of transferrin in the brain. *Biochimica et Biophysica Acta*, *1820*(3), 393–402.

Lemarié, F., Croft, D. R., Tate, R. J., Ryan, K. M., Dufès, C. (2012). Tumor regression following intravenous administration of a tumor-targeted p73 gene delivery system. *Biomaterials 33* (9), 2701-2709.

Levy, N. L., Mahaley, M. S., Day, E. D. (1972). *In Vitro* Demonstration of Cell-mediated Immunity to Human Brain Tumors, *Cancer Research, 32,* 477–482.

Li, S., Huang, L. (2000). Nonviral gene therapy: promises and challenges. *Gene Therapy*, *7*(1), 31–4.

Liebner, S., Fischmann, A., Rascher, G., Duffner, F., Grote, E., Kalbacher, H., Wolburg, H. (2000). Claudin-1 and claudin-5 expression and tight

junction morphology are altered in blood vessels of human glioblastoma multiforme. *Acta Neuropathologica,* 100, 323-331.

Lim, L. Y., Koh, P. Y., Somani, S., Al Robaian, M., Karim, R., Yean, Y. L., Mitchell, J., Tate, R. J., Edrada-Ebel, R., Blatchford, D. R., Mullin, M. Dufès, C. (2014). Tumor regression following intravenous administration of lactoferrin- and lactoferricin-bearing dendriplexes. *Nanomedicine: Nanotechnology, Biology and Medicine* (in press).

Liu, J., Shapiro, J. I. (2003). Endocytosis and Signal Transduction: Basic Science Update. *Biological research for nursing, 5* (2), 117-128.

Liu, L., Venkatraman, S. S., Yang, Y. Y., Guo, K., Lu, J., He, B., Moochhala, S. (2008). Polymeric micelles anchored with TAT for delivery of antibiotics across the blood-brain barrier. *Biopolymers*, *90*(5), 617–23.

Liu, S., Guo, Y., Huang, R., Li, J., Huang, S., Kuang, Y., Han, L. (2012). Gene and doxorubicin co-delivery system for targeting therapy of glioma. *Biomaterials*, *33*(19), 4907–16.

Liu, G., Shen, H., Mao, J., Zhang, L., Jiang, Z., Sun, T., Lan, Q., Zhang, Z. (2013). Transferrin modified graphene oxide for glioma-targeted drug delivery: *in vitro* and *in vivo* evaluations. *ACS Applied Materials Interfaces, 5* (15), 6909-6914.

Lu, W., Wan, J., She, Z., Jiang, X. (2007). Brain delivery property and accelerated blood clearance of cationic albumin conjugated pegylated nanoparticle. *Journal of Controlled Release 118*(1), 38–53.

Lundstrom, K. (2003). Latest development in viral vectors for gene therapy. *Trends in biotechnology*, *21*(3), 117–22.

Maeda, H., Bharate, G. Y., Daruwalla, J. (2009). Polymeric drugs for efficient tumor-targeted drug delivery based on EPR-effect. *European journal of Pharmaceutics and Biopharmaceutics*, *71*(3), 409–19.

McAllister, M. S., Krizanac-Bengez, L., Macchia, F., Naftalin, R. J., Pedley, K. C., Mayberg, M. R., Marroni, M., Leaman, S., Stanness, K. A., Janigro, D. (2001) Mechanisms of glucose transport at the blood-brain barrier: an *in vitro* study. *Brain Research* 409, 20-30.

McGeer, E. G., Klegeris, A., McGeer, P. L. (2005). Inflammation, the complement system and the diseases of aging. *Neurobiology of Ageing* 265, S94-S97.

Miller, D. W., Batrakova, E. V., Waltner, T. O., Alakhov, V. Y., Kabanov, A. (1997). Interactions of Pluronic Block Copolymers with Brain Microvessel

Endothelial Cells: Evidence of Two Potential Pathways for Drug Absorption. *Bioconjugate Chemistry, 8* (5), 649–557.

Miao, D., Jiang, M., Liu, Z., Gu, G., Hu, Q., Kang, T., Song, Q., Yao, L., Li, W., Gao, X., Sun, M., Chen, J. (2014). Co-administration of dual-targeting nanoparticles with penetration enhancement peptide for antiglioblastoma therapy*. Molecular Pharmaceutics, 11* (1), 110-117

Monnaert, V., Tilloy, S., Bricout, H., Fennert, L., Ceccheli, R., Monflier, E. (2004). Behavior of alpha-, beta-, and gamma- cyclodextrins and their derivatives on an *in vitro* model of blood-brain barrier. *The Journal of Pharmacology and Experimental Therapeutics*, *310*(2), 745–751.

Morgan, E. H. (1996). Iron Metabolism and Transport. In Zakin, D., and Boyer, T. D. (eds.), *Hepatology. A Textbook of Liver Disease*, 1 (3), 526-554.

Morita, K., Furuse, M. (1999). Claudin multigene family encoding four-transmembrane domain protein components of tight junction strands. *Proceedings of the National Academy of Sciences of the United States of America*, *96*(1), 511–516.

Nabel, G. J., Nabel, E. G., Yang, Z. Y., Fox, B. a, Plautz, G. E., Gao, X., Huang, L. (1993). Direct gene transfer with DNA-liposome complexes in melanoma: expression, biologic activity, and lack of toxicity in humans. *Proceedings of the National Academy of Sciences of the United States of America*, *90*(23), 11307–11.

Navarro, P., Ruco, L., Dejana, E. (1998). Differential localization of VE- and N-cadherins in human endothelial cells: VE-cadherin competes with N-cadherin for junctional localization. *The Journal of Cell Biology*, *140*(6), 1475–84.

Nunes, A., Al-Jamal, K. T., Kostarelos, K. (2012). Therapeutics, imaging and toxicity of nanomaterials in the central nervous system. *Journal of Controlled Release, 161*, 290-306.

Olesen, J., Leonardi, M. (2003). The burden of brain diseases in Europe. *European Journal of Neurology, 10,* 471-477

Pack, D. W., Hoffman, A. S., Pun, S., Stayton, P. S. (2005). Design and development of polymers for gene delivery. *Nature Reviews. Drug Discovery*, *4*(7), 581–93.

Pang, Z., Feng, L., Hua, R., Chen, J., Gao, H., Pan, S., Jiang, X., Zhang, P. (2010). Lactoferrin-conjugated biodegradable polymersome holding doxorubicin and tetrandrine for chemotherapy of glioma rats. *Molecular Pharmaceutics, 7* (6), 1995-2005.

Pardridge, W. M., Boado R. J., Farell, C. R. (1990). Brain-type glucose transporter (GLUT-1) is selectively localized to the blood-brain barrier. *The Journal of Biological Chemistry*, 265 (29), 18035-18040.

Pardridge, W. M. (2002). Why is the global CNS pharmaceutical market so under-penetrated? *Drug Discovery Today, 7* (1), 5-7.

Pardridge, W. M. (2005). Molecular biology of the blood-brain barrier. *Molecular Biotechnology*, *30*(1), 57–70.

Paris-Robidas, S., Emond, V., Tremblay, C., Soulet, D., Caon, F. (2011). *In Vivo* Labeling of Brain Capillary Endothelial Cells after Intravenous Injection of Monoclonal Antibodies Targeting the Transferrin Receptor. *Molecular Pharmacology, 80*, 32-39.

Parkinson's prevalence in the United Kingdom (2009), Parkinson's UK assessed on 12th March 2015. http://www.parkinsons.org.uk/sites/default/files/parkinsonsprevalenceuk_0.pdf

Tanner, C. M., Brandabur, M., Dorsey, E. R. (2008). Parkinson Disease: A Global view. *Parkinson Report,* 1-3.

Patil, P., Chaudhari, P., Sahu, M., Durgakar, M. (2012). Review Article on Gene Therapy. *International Journal of Genetics, 4*(1), 74–79.

Peppiatt, C. M., Howarth, C., Mobbs, P., Attwell, D. (2006). Bidirectional control of CNS capillary diameter by pericytes. *Nature*, *443*(7112), 700–4.

Perrière, N., Yousif, S., Cazaubon, S., Chaverot, N., Bourasset, F., Cisternino, S., Declèves, X. (2007). A functional *in vitro* model of rat blood-brain barrier for molecular analysis of efflux transporters. *Brain Research*, *1150*, 1–13.

Persidsky, Y., Ramirez, S. H., Haorah, J., Kanmogne, G. D. (2006). Blood-brain barrier: structural components and function under physiologic and pathologic conditions. *Journal of Neuroimmune Pharmacology*, *1*(3), 223–36.

Petty, M. A., Lo, E. H. (2002). Junctional complexes of the blood-brain barrier: permeability changes in neuroinflammation. *Progress in Neurobiology*, *68*(5), 311–23.

Plate, K. H., Breuer, G., Millauer, B., Ullrich, A., Risau, W. (1993) Up regulation of vascular endothelial growth factor and its cognate receptors in a rat glioma model of tumor angiogenesis. *Cancer Reserch, 53*, 5822-5827.

Pogacic, V., Herrling, P. (2007). List of Drugs in Development for Neurodegenerative Diseases. *Neurodegenrative diseases, 4*, 443-486.

Prior, R., Reifenberger, G., Wechsler, W. (1990). Transferrin receptor expression in tumours of the human nervous system: relation to tumour type, grading and tumour growth fraction. *Virchows Archiv A Pathological Anatomy and Histopathology, 416*, 491-496.

Qin, Y., Chen, H., Yuan, W., Kuai, R., Zhang, Q., Xie, F., Zhang, L. (2011). Liposome formulated with TAT-modified cholesterol for enhancing the brain delivery. *International Journal of Pharmaceutics*, *419*(1-2), 85–95.

Ramakrishnan, P. (2003). The role of P-glycoprotein in the blood-brain barrier. *The Einstein Journal of Biology and Medicine, 19*, 160–165.

Ramsauer, M., Krause, D., Dermietzel, R. (2002). Angiogenesis of the blood–brain barrier *in vitro* and the function of cerebral pericytes. *The FASEB Journal*, 1274–1276.

Recht, L., Torres, C. O., Smith, T. W., Raso, V., Griffin, T.W. (1990). Transferrin receptor in normal and neoplastic brain tissue: implications for brain-tumor immunotherapy. *Journal of Neurosurgery, 72*, 941-994.

Regina, A., Demeule, M., Che, C, Lavallee, I, Poirier, J., Gabathuler, R., Beliveau, R., Castaigne, J-P. (2008). Antitumour activity of ANG1005, a conjugate between paclitaxel and the new brain delivery vector Angiopep-2. *British Journal of Pharmacology, 155*, 185–197.

Ren, J., Shen, S., Wang, D., Xi, Z., Liangran, G., Pang, Z., Qian, Y., Sun, X., Jiang, X. (2012). The targeted delivery of anticancer drugs to brain glioma by PEGylated oxidized multi-walled carbon nanotubes modified with angiopep-2. *Biomaterials, 33*, 3324-3333.

Richardson, D. R., Ponka, P. (1997). The molecular mechanisms of the metabolism and transport of iron in normal and neoplastic cells. *Biochimica et Biophysica Acta, 1331*, 1-40.

Rip, J., Schenk, G. J., de Boer, A.G. (2009). Differential receptor-mdiated drug targeting to the diseased brain. *Expert Opinions in Drug Delivery* 6, 227-237.

Robbins, P. D., Ghivizzani, S. C. (1998). Viral vectors for gene therapy. *Pharmacology & Therapeutics*, *80*(1), 35–47.

Roberts, R. L., Fine, R. E., Sandra, A. (1993). Receptor-mediated endocytosis of transferrin at the blood-brain barrier. *Journal of Cell Science*, *104*(2), 521–32.

Ross, C. A., Tabrizi, S. J. (2011). Huntington's disease: from molecular pathologenesis to clinical treatment. *Lancet Neurology*, 10, 83-98.

Rousselle, C, Clair, P., Lefauconnier, J. M., Kaczorek, M., Scherrmann, J. M., Temsamani, J. (2000). New advances in the transport of doxorubicin through the blood-brain barrier by a peptide vector-mediated strategy. *Molecular Pharmacology*, *57*(4), 679–86.

Rousselle, Christophe, Clair, P., Smirnova, M., Kolesnikov, Y., Pasternak, G. W., Rees, A. R., Scherrmann, J. (2003). Improved Brain Uptake and Pharmacological Activity of Dalargin Using a Peptide-Vector-Mediated Strategy, *Journal of Pharmacology and Experimental Therapeutics 306*(1), 371–376.

Ruan, S., Qian, J., Shen, S., Chen, J., Zhu, J., Jiang, X., He, Q., Yang, W., Gao, H. (2014). Fluorescent carbonaceous nanodots for noninvasive glioma imaging after angiopep-2 decoration. *Bioconjugate Chemistry, 25* (12), 2252-2259.

Ruan, S., Yuan, M., Zhang, L., Hu, G., Chen, J., Cun, X., Zhang, Q., Yang, Y., He, Q., Gao, H. (2015). Tumor microenvironment sensitive doxorubicin delivery and release to glioma using angiopep-2 decorated gold nanoparticles. *Biomaterials, 37*, 425-435

Rubin, L., Hall, D., Porter, S. (1991). A cell culture model of the blood-brain barrier. *The Journal of Cell Biology*, *115*(6), 1725-1735.

Ryoung Kim, H., Gil, S., Andrieux, K., Nicolas, V., Appel, M., Chacun, H., Desmaele, D., Taran, F., Georgin, D., Couvreur, P. (2007). Low-density lipoprotein receptor-mediated endocytosis of PEGylated nanoparticles in rat brain endothelial cells*. Cell and Molecular Life Sciences, 64*, 356-364.

Saar, K., Lindgren, M., Hansen, M., Eiríksdóttir, E., Jiang, Y., Rosenthal-Aizman, K., Sassian, M. (2005). Cell-penetrating peptides: a comparative membrane toxicity study. *Analytical Biochemistry*, *345*(1), 55–65.

Sato, H., Takino, T., Okada, Y., Shingawa, A., Yamamoto, E., Seiki, M. (1994). A matrix metalloproteinase expressed on the surface of invasive tumour cells. *Nature, 370* (6484), 61-65.

Saija, A, Princi, P., Trombetta, D., Lanza, M., De Pasquale, A. (1997). Changes in the permeability of the blood-brain barrier following sodium dodecyl sulphate administration in the rat. *Experimental Brain Research*, *115*(3), 546–51.

Schlageter, K. E., Molnar, P., Lapin, G. D., Groothuis, D. R. (1999). Microvessel organization and structure in experimental brain tumors: microvessel populations with distinctive structural and functional properties. *Microvascular Research*, *58*(3), 312–28.

Schroder, U., Sabel, B. A. (1996). Nanoparticles, a drug carrier system to pass the blood-brain barrier, permit central analgesic effects of i.v. dalargin injections. *Brain Research, 710*, 121-124.

Seligman, P. (1983). Structure and function of the transferrin receptor. *Programs of Haematology, 13,* 131-147.

Shao, K., Huang, R., Li J., Han L., Ye, L., Lou, J., Jiang, C. (2010). Angiopep-2 modified PE-PEG based polymeric micelles for amphotericin B delivery targeted to the brain. *Journal of Controlled Release, 147*, 118-126.

Shao, K., Wu, J., Chen, Z., Huang, S., Li, J., Ye, L., Lou, J., Zhu, L., Jiang, C. (2012). A brain-vectored angiopep-2 based polymeric micelles for the treatment of intracranial fungal infection. *Biomaterials, 33* (28), 6898-6907.

Sharma, A. K., Zhang, L., Li, S., Kelly, D. L., Alakhov, V. Y., Batrakova, E. V., Kabanov, A.V. (2008). Prevention of MDR development in leukemia cells by micelle-forming polymeric surfactant. *Journal of Controlled Release, 131*, 220-227.

Shepro, D., Morel, N. (1993). Pericyte physiology. *The FASEB Journal, 7*(11), 1031–1038.

Shi, N., Pardridge, W. M. (2000). Noninvasive gene targeting to the brain. *Proceedings of the National Academy of Sciences of the United States of America*, *97*(13), 7567–72.

Shi, N., Zhang, Y., Zhu, C., Boado, R. J., Pardridge, W. M. (2001a). Brain-specific expression of an exogenous gene after i.v. administration. *Proceedings of the National Academy of Sciences of the United States of America*, *98*(22), 12754–9.

Shi, N., Boado, R. J., Pardridge, W. M. (2001b). Receptor-mediated gene targeting to tissues *in vivo* following intravenous administration of pegylated immunoliposomes. *Pharmaceutical Research, 18* (8), 1091-1095.

Song, B. W., Vinters, H. V., Wu, D., Pardridge, W. M. (2002). Enhanced neuroprotective effects of basic fibroblast growth factor in regional brain ischemia after conjugation to a blood-brain barrier delivery vector.

Journal of Pharmacology and Experimental Therapeutics, 301 (2), 605-610.

SoRelle, R. (2000). Who Owns Your DNA? Who Will Own It? *Circulation*, *101*(5), 67–68.

Spuch, C., Ortolano, S., Navarro, C. (2012). LRP-1 and LRP-2 receptors function in the membrane neuron. Trafficking mechanisms andproteolytic processing in Alzheimer's disease. *Frontiers in Physiology, 3* (69), 1-14.

Stamatovic, S. M., Keep, R. F., Andjelkovic, A. V. (2008). Brain endothelial cell-cell junctions: how to "open" the blood brain barrier. *Current Neuropharmacology*, *6*(3), 179–92.

Stanford School of medicine, Care and handling of virus, assessed on 15th July 2015. http://med.stanford.edu/gvvc/retroviruses.html

Stewart, P. A., Wiley, M. J. (1981). Structural and histochemical features of the avian blood-brain barrier. *Journal of Comparative Neurology*, 202 (2), 157-167.

Stewart, P. A. (2000). Endothelial vesicles in the blood-brain barrier: are they related to permeability? *Cellular and Molecular Neurobiology*, *20*(2), 149–63.

Suhr, S. T., Gage, F. H. (1993). Gene therapy for neurologic disease. *Archives of Neurology* 50(11), 1252-1268.

Sun, X., Pang, Z., Ye, H., Qiu, B., Guo, L., Li, J., Ren, J., Qian, Y., Zhang, Q., Chen, J., Jiang, X. (2012). Co-delivery of pEGFP-hTRAIL and paclitaxel to brain glioma mediated by an angiopep-conjugated liposome. *Biomaterials, 33* (3), 916-924.

Suzuki, T., Wu, D., Schlachetzki, F., Li, J. Y., Boado, R. J., Pardridge, W. M. (2004). Imaging Endogenous Gene Expression in Brain Cancer *In Vivo* with ^{111}In-Peptide Nucleic Acid Antisense Radiopharmaceuticals and Brain Drug-Targeting Technology. *The Journal of Nuclear Medicine, 45* (10), 1766-1775.

Suzuki, Y. A., Lopez, V., Lönnerdal, B. (2005). Mammalian lactoferrin receptors: structure and function. *Cellular and Molecular Life Sciences, 62*, 2560-2575.

Sztriha, L., Betz, A. L. (1991). Oleic acid reversibly opens the blood-brain barrier. *Brain Research*, *550*(2), 257–62.

Talukder, J. M. R., Takeuchi, T., Harada, E. (2003). Receptor-Mediated Transport of Lactoferrin into the Cerebrospinal Fluid via Plasma in Young Calves. *Journal of Veterinary Medical Science, 65* (9), 957-964.

Tao-Cheng, J. H., Nagy, Z., Brightman, M. W. (1987). Tight Junctions of Brain Endothelium *in vitro* Are Enhanced by Astroglia, *The Journal of Neuroscience, 7*(10), 3293-9.

The Value of virus, (2008), Brainfacts.org. assessed on 15th July 2015. http://www.brainfacts.org/about-neuroscience/technologies/articles/2013/the-value-of-a-virus

Thomas, C. E., Ehrhardt, A., Kay, M. A. (2003). Progress and problems with the use of viral vectors for gene therapy. *Nature Reviews. Genetics*, *4*(5), 346–58.

Thomas, F. C., Taskar, K., Rudraraju, V., Goda, S., Thorsheim, H. R., Gaasch, J. A., Palmeiri, D., Steeg, P. S., Lockman, P. R., Smith, Q. R. (2009). Uptake of ANG1005, a Novel Paclitaxel Derivative, Through the Blood-Brain Barrier into Brain and Experimental Brain Metastases of Breast Cancer*. Pharmaceutical Research, 26* (11), 2486-2494.

Tian, W., Ying, X., Du, J., Guo, J., Men, Y., Zhang, Y., Li, R. J., Yao, H. J., Lou, J. N., Zhang, L. R., Lu, W. L. (2010). Enhanced efficacy of functionalized epirubicin liposomes in treating brain glioma-bearing rats. *European Journal of Pharmaceutical Sciences, 41* (2), 232-243.

Tsukita, S. Furuse, M. Itoh, M. (1999). Structural and signalling molecules come together at tight junctions, *Current Opinion in Cell Biology, 11*(5), 628–633.

Tsukita, S., Furuse, M. (1999). Occludin and claudins in strands: leading or supporting players?,*Trends in Cell Biology*, *9*(7), 87–92.

van Rooy, I., Mastrobattista, E., Storm, G., Hennink, W. E., Schiffelers, R. M. (2011). Comparison of five different targeting ligands to enhance accumulation of liposomes into the brain. *Journal of Controlled Release, 150*, 30-36.

Visser, C. C., Stevanović, S., Voorwinder, H., Gaillard, P. J., Crommelin, D. J., Danhof, M., De Boer, A. G. (2004). Validation of the transferrin receptor for drug targeting to brain capillary endothelial cells *in vitro*. *Journal of Drug Targeting, 12*, 145-150.

Vorbrodt, A., Dobrogowska, D. (2003). Molecular anatomy of intercellular junctions in brain endothelial and epithelial barriers: electron microscopist's view. *Brain Research Reviews*, *42*, 221–242.

Vorbrodt, A. W., Li, S., Brown, W. T., Ramakrishna, N. (2008). Increased expression of beta-catenin in brain microvessels of a segmentally trisomic (Ts65Dn) mouse model of Down syndrome. *Brain Cell Biology*, *36*(5-6), 203–11.

Vykhodtseva, N., McDannold, N., Hynynen, K. (2008). Progress and problems in the application of focused ultrasound for blood–brain barrier disruption. *Ultrasonics*, *48*(4), 279–296.

Walther, W., Stein, U. (2000). Viral vectors for gene transfer: a review of their use in the treatment of human diseases. *Drugs*, *60*(2), 249–71.

Ward, P. P., Paz, E., Conneely, O. M. (2005). Multifunctional roles of lactoferrin: a critical overview. *Cellular and Molecular Life Sciences*, 62, 2540-2548.

Weksler, B. B., Subileau, E. A, Perrière, N., Charneau, P., Holloway, K., Leveque, M., Tricoire-Leignel, H. (2005). Blood-brain barrier-specific properties of a human adult brain endothelial cell line. *FASEB Journal*, *19*(13), 1872–4.

Whitton, P. S. (2007). Inflammation as a causative factor in the aetiology of Parkinson's disease. *British Journal of Pharmacology,* 150, 963-976.

Wolburg, H, Neuhaus, J., Kniesel, U., Krauss, B., Schmid, E. M., Ocalan, M., Farrell, C. (1994). Modulation of tight junction structure in blood-brain barrier endothelial cells. Effects of tissue culture, second messengers and cocultured astrocytes. *Journal of Cell Science*, *107*, 1347–57.

Wolburg, Hartwig, Lippoldt, A. (2002). Tight junctions of the blood-brain barrier: development, composition and regulation. *Vascular Pharmacology*, *38*(6), 323–37.

Wolburg, Hartwig, Noell, S., Mack, A., Wolburg-Buchholz, K., Fallier-Becker, P. (2009). Brain endothelial cells and the glio-vascular complex. *Cell and Tissue Research*, *335*(1), 75–96.

Wong, H. L., Wu, X. Y., Bendayan, R. (2012). Nanotechnological advances for the delivery of CNS therapeutics. *Advanced Drug Delivery Reviews*, *64*(7), 686–700.

World Alzheimer's Report 2009, Alzheimer's Disease International. Assessed on 12th March 2015 . https://www.alz.co.uk/research/files/WorldAlzheimerReport.pdf

Wu, D., Yang, J., Pardridge, W. M. (1997). Drug targeting of a peptide radiopharmaceutical through the primate blood-brain barrier *in vivo* with

a monoclonal antibody to the human insulin receptor. *The Journal of Clinical Investigation*, *100*(7), 1804–12.

Xia, C.F., Boado, R. J., Pardridge, W. M. (2008). Antibody-mediated targeting of siRNA via the human insulin receptor using avidin-biotin technology. *Molecular Pharmaceutics*, *6*(3), 747–51.

Xin, H., Sha, X., Jiang, X,. Zhang, W., Chen, L., Fang, X. (2012). Anti-glioblastoma efficacy and safety of paclitaxel-loading Angiopep-conjugated dual targeting PEG-PCL nanoparticles. *Biomaterials, 33* (32), 8167-8176.

Yamamoto, M., Ramirez, S. H., Sato, S., Kiyota, T., Cerny, R. L., Kaibuchi, K., Persidsky, Y. (2008). Phosphorylation of claudin-5 and occludin by rho kinase in brain endothelial cells. *The American Journal of Pathology*, *172*(2), 521–33.

Yan, H., Wang, L., Wang, J., Lei, H., Wang, X., Jiang, L., Zhu, J., Lu, W., Wei, X., Li, C. (2012). Two-Order Targeted Brain Tumor Imaging by Using an Optical/Paramagnetic Nanoprobe across the Blood Brain Barrier. *ACS Nano, 6* (1), 410-420.

Yang, Z. Z., Li, J. Q., Wang, Z. Z., Dong, D. W., Qi, X. R. (2014). Tumor-targeting dual peptides-modified cationic liposomes for delivery of siRNA and docetaxel to gliomas. *Biomaterials, 35* (19), 5226-5239.

Ye, Y., Sun, Y., Zhao, H., Minbo, L., Gao, F., Song, C., Lou, K., Li, H., Wang, W. (2013). A novel lactoferrin-modified β-cyclodextrin nanocarrier for brain-targeting drug delivery. *International Journal of Pharmaceutics, 458*, 110-117.

Ying, X., Wen, H., Lu, W. L., Du, J., Guo, J., Tian, W., Men, Y., Zhang, Y., Li, R. J., Yang, T. Y., Shang, D. W., Lou, J. N., Zhang, L. R., Zhang, Q. (2010). Dual-targeting daunorubicin liposomes improve the therapeutic efficacy of brain glioma in animals. *Journal of Controlled Release, 141* (2), 183-192.

Ying, X., Wang, Y., Liang, J., Yue, J., Xu, C., Lu, L., Xu, Z., Gao, J., Du, Y., Zhong, C. (2014). Angiopep-Conjugated Electro-Responsive Hydrogel Nanoparticles: Therapeutic Potential for Epilepsy. *Angewandte Communications, 53*, 12436-12440.

Zensi, A., Begley, D., Pontikis, C., Legros, C., Mihoreanu, L., Wagner, S., Buchel, C., von Briesen, H., Kreuter, J. (2009). Albumin nanoparticles targeted with Apo E enter the CNS by transcytosis and are delivered to neurones*. Journal of Controlled Release, 137*, 78-96.

Zhang, Y., Boado, R. J., Pardridge, W. M. (2003). Marked enhancement in gene expression by targeting the human insulin receptor. *The Journal of Gene Medicine*, *5*(2), 157–63.

Zhang, Y., Pardridge, W.M. (2005). Delivery of β-galactosidase to mouse brain via the blood-brain barrier transferrin receptor. *The Journal of Pharmacology and Experimental Therapeutics*, 313 (3), 1075-1081.

Zhang, Y., Pardridge, W.M. (2006). Blood-brain barrier targeting of BDNF improves motor function in rats with middle cerebral artery occlusion. *Brain research, 1111* (1), 227-229.

Zhang, P., Hu, L., Yin, Q., Zhang, Z., Feng, L., Li, Y. (2012). Transferrin-conjugated polyphosphoester hybrid micelle loading paclitaxel for brain-targeting delivery: synthesis, preparation and *in vivo* evaluation. *Journal of Controlled Release, 159* (3), 429-434.

Zhang, P., Hu, L., Yin, Q., Feng, L., Li, Y. (2012). Transferrin-modified c[RGDfK]-paclitaxel loaded hybrid micelle for sequential blood-brain barrier penetration and glioma targeting therapy. *Molecular Pharmaceutics, 9* (6), 1590-1598.

Zhou, Q. H., Lu, J. Z., Hui, E. K., Boado, R. J., Pardridge, W. M. (2011). Delivery of a peptide radiopharmaceutical to brain with an IgG-avidin fusion protein. *Bioconjugate Chemistry, 22* (8), 1611-1618.

Zhou, Q., Mu, K., Jiang, L., Xie, H., Liu, W., Li, Z., Qi, H., Liang, S., Xu, H., Zhu, Y., Zhu, W., Yang, X. (2015). Glioma-targeting micelles for optical/magnetic resonance dual-mode imaging. *International Journal of Nanomedicine, 10*, 1805-1818.

Zhu, C., Zhang, Y., Zhang, Y. F., Yi Li, J., Boado, R. J., Pardridge, W. M. (2004). Organ-specific expression of the lacZ gene controlled by the opsin promoter after intravenous gene administration in adult mice. *The Journal of Gene Medicine, 6* (8), 906-912.

Zinselmeyer, B. H., Beggbie, N., Uchegbu, I. F., Schätzein, A. G. (2003). Quantification of β-galactosidase activity after non-viral transfection *in vivo*. *Journal of Controlled Release,* 91, 201-208.

Zlokovic, B. V. (2002). Vascluiar disorder in Alzheimer's disease: role in pathogenesis of dementia and therapeutic targets. *Advanced Drug Delivery Reviews*, 54. 1553-1559.

Zlokovic, B. V. (2008). The blood-brain barrier in health and chronic neurodegenerative disorders. *Neuron,* 57, 178-201.

Zong, T., Mei, L., Gao, H., Cai, W., Zhu, P., Shi, K., Chen, J., Wang, Y., Gao, F., He, Q. (2014). Synergistic dual-ligand doxorubicin liposomes improve targeting and therapeutic efficacy of brain glioma in animals. *Molecular Pharmaceutics, 11* (7), 2436-2457.

Appendix I List of Publications

Dufès, C., Al Robaian, M., Somani, S. (2013). Transferrin and the transferrin receptor for the targeted delivery of therapeutic agents to the brain and the cancer cells. *Therapeutic Delivery, 4*, 629-640.

Somani, S., Blatchford, D. R., Millington, O., Stevenson, M. L., Dufès, C. (2013). Transferrin-bearing polypropylenimine dendrimer for targeted gene delivery to the brain. *Journal of Controlled Release, 188*, 78-86.

Somani, S., Dufès, C. (2014). Applications of dendrimers for brain delivery and cancer therapy. *Nanomedicine, 9*, 2403-2414.

Lim, L. Y., Koh, P. Y., Somani, S., Al Robaian, M., Karim, R., Yean, Y. L., Mitchell, J., Tate, R. J., Edrada-Ebel, R., Blatchford, D. R., Mullin, M. Dufès, C. (2014). Tumor regression following intravenous administration of lactoferrin- and lactoferricin-bearing dendriplexes. *Nanomedicine: Nanotechnology, Biology and Medicine* (in press).

Somani, S., Robb, G., Pickard, B., Dufès, C. Enhanced gene expression in the brain following intravenous administration of lactoferrin-bearing polypropylenimine dendriplex (in press)

Transferrin and the transferrin receptor for the targeted delivery of therapeutic agents to the brain and cancer cells

The potential use of many promising novel drugs is limited by their inability to specifically reach their site of action after intravenous administration, without secondary effects on healthy tissues. In order to remediate this problem, the protein transferrin (Tf) has been extensively studied as a targeting molecule for the transport of drug and gene delivery systems to the brain and cancer cells. A wide range of delivery approaches have been developed to target the Tf receptor and they have already improved the specific delivery of Tf-bearing therapeutic agents to their site of action. This review provides a summary of the numerous delivery strategies used to target the Tf receptor and focuses on recent therapeutic advances.

Christine Dufès*, Majed Al Robaian‡ & Sukrut Somani‡

Strathclyde Institute of Pharmacy & Biomedical Sciences, University of Strathclyde, 161 Cathedral Street, Glasgow G4 0RE, UK
*Author for correspondence:
Tel.: +44 141 548 3796
Fax: +44 141 552 2562
E-mail: C.Dufes@strath.ac.uk
‡These authors contributed equally

Recent advances in the fields of pharmacology and chemistry have led to the discovery of numerous potential drugs with promising therapeutic effects on various pathologies. However, the clinical use of these drugs following intravenous administration is currently limited by the lack of specific delivery to the pathological site, resulting in toxicity and secondary effects to healthy tissues. In order to remediate this problem and enhance the therapeutic index of the drugs, it is crucial to target these drug candidates to their site of action.

For more than 20 years, the transferrin (Tf) protein has been extensively studied as a targeting moiety for drug- and gene-delivery systems as it is non-toxic, non-immunogenic and biodegradable [1]. Tf receptors (TfRs) are highly expressed on the brain capillary endothelium, which forms the **blood–brain barrier** (BBB) in conjugation with other cellular components, such as pericytes and astrocytes *in vivo* [2]. As intravenously administered Tf was observed to reach the brain by receptor-mediated transcytosis across the BBB [3,4], the TfR-targeting strategy quickly became the object of intense investigation for the brain delivery of CNS drug candidates: 100% of large-molecule drugs and more than 98% of small-molecule drugs are otherwise prevented from penetrating the brain by the BBB [5]. In addition, TfRs are present in abundance on the surface of cancer cells [6–9], thus, allowing a specific uptake of TfR-targeted therapeutic drugs and genes by cancer cells overexpressing TfRs.

The objective of this review was to present, in a succinct form, the numerous TfR-targeting strategies developed so far in laboratory settings, while focusing on recent promising breakthroughs in this research area.

Tf & the TfR: an introduction

■ Tf: structure & function

Tf is part of a family of ubiquitous iron-binding glycoproteins including ovotransferrin, lactoferrin and melanotransferrin, whose primary function is the binding and transport of iron [10,11]. It is a monomeric glycoprotein containing appoximately 700 amino acids, with a large molecular mass (approximately 80 kDa). The polypeptide chain is folded into two structurally similar globular domains, known as the N- and C-lobes, and connected by a short linear peptide linker [11]. Each lobe contains one binding site for Fe^{3+} with a very high affinity (10^{22} M^{-1} at pH 7.4) [12]. The iron-free Tf (apoTf) can, therefore, bind up to two Fe^{3+} ions to form ferro-Tf (also called holoTf). The conformational changes of the protein occurring during iron binding have been demonstrated to play a key role in the selective recognition by the TfR. Consequently, diferric Tf has a 10- to 100-times higher affinity for the TfR than that of apoTf at physiological pH [13] and is, therefore, preferred as a TfR ligand in targeting studies.

The principal biological function of Tf is to bind and distribute iron in the body. Tf is the main iron-transporting protein in the body. It binds circulating iron taken from the diet and transports it into the systemic circulation to various target tissues. This transport is extremely important as iron is required for various

FUTURE SCIENCE part of fsg

Key Term

Blood–brain barrier: Complex interface separating the peripheral circulation from the CNS. It is formed by brain microvascular endothelial cells connected by tight junctions. The resulting continuous endothelial wall is further reinforced by pericytes, astrocytic endfeet and vascular nerve endings surrounding the endothelial cells. This protective structure, therefore, prevents the delivery of most intravenously administered drugs to the brain.

Avidin/biotin technology: Glycoprotein obtained from egg white, known for its very high affinity for biotin, a vitamin that plays a role in numerous biological processes, such as cell growth and the production of fatty acids. The avidin–biotin complex is the strongest known interaction between a ligand and a protein in nature, and has been demonstrated to be resistant to extreme pH and temperature conditions.

biological processes, such as DNA synthesis, oxygen transport and electron transfer [11].

Due to its iron-binding mechanism, Tf also protects the cells against the toxic effects that could be generated by the presence of free iron in the circulation. It is only up to 30–40% iron-saturated under physiological conditions [14].

In addition to its key role as iron transporter, Tf has been observed to bind other cations such as copper, gallium, zinc, manganese and aluminium ions [10].

■ TfR

Cellular uptake of iron-loaded Tf occurs through receptor-mediated endocytosis. The TfR, referred to as TfR1 or CD71 in literature, is a type II transmembrane glycoprotein involved in iron uptake and cell growth regulation [15]. It consists of two identical monomers with an approximate molecular mass of 90 kDa each, linked by two disulfide bonds [1]. Each monomer is made of three distinct regions: a short N-terminal cytoplasmic domain, a hydrophobic transmembrane domain and a large, globular, extracellular C-terminal domain that contains the binding site for Tf [1,16]. As each monomer may bind a molecule of Tf, up to two molecules of Tf may bind one TfR and up to four Fe^{3+} ions within one Tf–TfR complex can be taken up by the cell. The recycling rate of TfR1 is very short (approximately 10–20 s) and can occur 100 times for each single receptor [17], making this receptor particularly efficient for the delivery of iron and therapeutics to cells.

Another member of the TfR family, referred to as TfR2, has been discovered. Although its extracellular domain has 66% similarity with TfR1, TfR2 has a much lower affinity for Tf than TfR1 (25-fold lower) [18]. In addition, its expression is not correlated to iron levels in the cells. Its α-transcript product is mostly expressed on hepatocytes, while its β-transcript is present on a wide range of tissues, but at very low levels [18]. TfR2 would, therefore, be a less efficient target for Tf-mediated drug and gene delivery to the brain or cancer cells.

TfR1 is expressed at low levels in most human tissues, but is highly expressed on the vascular endothelium of brain capillaries [2]. It is also expressed at levels up to 100-fold higher than those on normal cells on highly proliferative cells such as cancer cells [6–9]. Its increased expression on tumors is generally correlated with cancer progression and tumor stage [6–9].

This high expression of TfR on brain capillaries and cancer cells, together with the ability of the receptor to internalize with its ligand, make this receptor a highly promising target for the delivery of therapeutics to the brain and cancer cells.

TfR-mediated delivery of therapeutic agents to the brain

Most therapeutic molecules, including small-molecule drugs, proteins, peptides and genes, cannot reach the brain after intravenous administration due to their inability to cross the BBB [4,5]. As a result, various drugs with promising therapeutic effects *in vitro* are found to be ineffective for the treatment of neurological diseases such as Parkinson's and Alzheimer's diseases, as well as brain neoplasms.

Widely expressed on the BBB, the TfR has been widely investigated for the delivery of drugs and genes to the brain. The strategy employed would be to use Tf or antibodies directed against TfR as TfR-targeting moieties. Therapeutic agents entrapped in TfR-targeted delivery systems would then be able to cross the BBB and be delivered into the brain.

■ Targeted drug delivery

Many drugs are unable to cross the BBB. In order to overcome this problem, therapeutic molecules have been encapsulated in delivery systems able to recognize the TfR and to deliver their cargo to the brain. A wide range of delivery strategies, including the linkage of drugs to Tf/anti-TfR antibody, complexation with TfR-targeted quantum rods, entrapment of the drugs in TfR-targeted liposomes, lipid nanocapsules, nanoparticles and micelles, have been investigated for TfR-mediated delivery of drugs to the brain (**Figure 1**).

Linkage of drugs to Tf/anti-TfR antibody

Therapeutic agents can be delivered across the BBB following their linkage to either the Tf or a molecule able to specifically recognize the TfR.

OX26, a mouse monoclonal antibody against the rat TfR1, has been explored as a drug-delivery agent to the brain. It was used as an alternative to Tf itself in order to prevent any eventual vector failure linked to a saturation of TfRs [19]. This antibody presents the advantage of binding to an extracellular domain for the TfR different from the Tf-binding site and is, therefore, independent from Tf binding. It has been thoroughly studied for the brain delivery of numerous drugs following intravenous administration [1,4–5]. For example, it was conjugated to the hydrophilic anticancer drug methotrexate by a

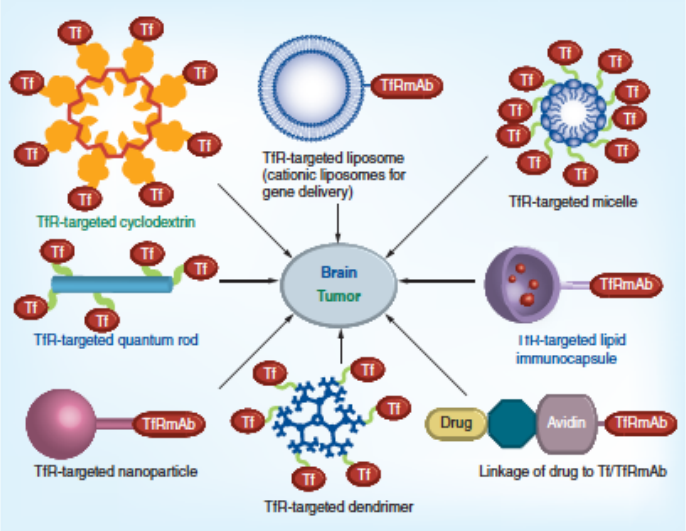

Figure 1. Formulation strategies used for the delivery of drugs and nucleic acids to the brain and tumor. TfR-targeted quantum rod [27,28]; TfR-targeted lipid immunonanocapsule [33,34]; Linkage of drug to Tf/TfRmAb [54–58]; TfR-targeted liposome [59–65,69]; TfR-targeted nanoparticle [66,67]; TfR-targeted cyclodextrin [70,71]; TfR-targeted micelle [72]; TfR-targeted dendrimer [73–78]. Formulation name in blue: delivery to the brain; formulation name in green: delivery to the tumor; formulation name in black: delivery to either brain or tumor.
Tf: Transferrin; TfR: Transferrin receptor; TfRmAb: Monoclonal antibody anti-transferrin receptor.

hydrazone bond. Approximately six molecules of methotrexate were attached per antibody. After intravenous injection to rats, the conjugate was demonstrated to be able to cross the BBB via TfR-mediated transcytosis and to deliver the drug to the brain, as confirmed by immunohistochemical detection of the conjugate in the brain parenchyma [20].

In another example, the BDNF, a neuroprotective agent, could not cross the BBB after intravenous administration and was unable to exert its neuroprotective effect in the first hours after regional brain ischemia because the BBB is still intact at this stage. However, the intravenous administration of OX26 conjugated to BDNF resulted in a 243% increase in motor performance of rats presenting stroke symptoms in comparison with the drug alone [21].

OX26 has also been used to deliver many other drugs, such as neuropeptides (vasoactive intestinal peptide) [22] and proteins (nerve growth factor) [23] to the rat brain after intravenous administration. As OX26 is specific to the rat TfR, another monoclonal antibody anti-mouse TfR, named 8D3, has been used as a TfR1-targeting vector in the mouse [19]. This antibody, conjugated to radiolabeled $A\beta^{1-40}$, has been used to visualize and quantify β-amyloid plaques in a mouse model of Alzheimer's disease [24]. A chimeric form of the 8D3 antibody was also conjugated to the GDNF, a neurotrophin with therapeutic potential on Parkinson's disease. The GDNF-antibody fusion protein was able to cross the BBB after intravenous injection and was found to be therapeutically active in three neurobehavioral models of experimental Parkinson's disease in mice [25].

Various approaches have been developed for the linkage of the drugs to Tf or anti-TfR antibodies. Among them, the **avidin/biotin technology** appears to be particularly promising for the delivery of drugs to the brain. The noncovalent binding between avidin and biotin is extremely strong (K_d ~10^{-15} M) and stable in the

Key Term

Stealth liposomes: Liposomes grafted with a polymer (generally polyethylene glycol), to prevent detection by the reticulo-endothelial system. This strategy therefore increases the circulating time of the delivery system compared with conventional liposomes.

circulation, but is labile in the tissues [26], thus, facilitating the release of the drug once it reaches the brain. The avidin/biotin strategy was, for example, used to link OX26 and the vasoactive intestinal peptide and resulted in an increase of cerebral blood flow following intravenous administration of this complex to rats [22].

This approach has also been successful in delivering high-molecular-weight enzymes to the brain. For example, the intravenous administration of 116-kDa β-galactosidase linked to the 8D3 monoclonal antibody via streptavidin–biotin binding resulted in a ten-fold increase in brain uptake of the enzyme, without loss of activity, in a mouse model [27]. In this study, brain delivery was confirmed by brain capillary depletion method and brain histochemistry.

TfR-targeted quantum rods

Quantum rods are semiconductor nanoparticles widely used as luminescent probes for various biological applications. In addition to their well-known optical properties, they can be functionalized and carry therapeutic molecules. For example, Tf-conjugated quantum rods complexed to the antiretroviral drug saquinavir were successfully transported across an *in vitro* BBB model through TfR-mediated transcytosis [28,29].

TfR-targeted liposomes & lipid nanocapsules

TfR-targeted liposomes are self-assembling vesicular structures based on one or more lipid bilayers encapsulating an aqueous core and able to recognize the TfR. They can encapsulate hydrophilic drugs in their aqueous core or entrap lipophilic drugs in the lipid bilayer membrane. The use of conventional liposomes for brain drug delivery was initially limited by their size (which has to be smaller than 200 nm in diameter to allow drug delivery across the BBB [30]) and by their rapid clearance by the reticuloendothelial system [31]. However, the latter problem was overcome by incorporating PEG-derivatized lipids in the lipid bilayer of the liposomes or by coating them with PEG, resulting in the formation of sterically stabilized (also called stealth) liposomes.

Tf-bearing liposomes have been used for the cerebral delivery of the anticancer drug 5-fluorouracil. The intravenous administration of this therapeutic system resulted in a 17-fold increase in the brain uptake of the drug compared with that observed with the free drug, as demonstrated by biodistribution studies with the radiolabeled drug [32].

Antibody-directed liposomes, or immunoliposomes, have also demonstrated to be promising vectors for the targeted delivery of drugs to the brain. OX26 antibody was conjugated to PEG-coated liposomes encapsulating the anticancer agent daunomycin, which has a very low permeability through the BBB. Brain delivery of OX26-bearing liposomes was higher than that of the non-targeted **stealth liposomes**, conventional liposomes or free daunomycin, following intravenous administration of the formulations to rats, as demonstrated by pharmacokinetic analysis [33].

Another lipid-based vector for brain targeting, the lipid nanocapsule, has recently been developed as a strategy to protect the entrapped drug from chemical and enzymatic degradation. This nanovector is made of a hydrophilic surfactant, Solutol® HS15 (BASF, Germany), surrounding an oily core [34]. The conjugation of OX26 antibody to the surface of the lipid nanocapsules doubled their concentration in the brain compared with non-targeted formulations, 24 h after intravenous administration to rats [35].

TfR-targeted nanoparticles

Nanoparticles are polymeric colloidal spheres made of natural or artificial polymers and range in size from 10 to 1000 nm. They can entrap drugs in their matrix, encapsulate them in their core or carry them on their surface. Like liposomes, they can be coated with PEG to prevent their clearance by the reticuloendothelial system.

Nanoparticles made of poly(butyl cyanoacrylate) or poly(D,L-lactide-*co*-glycolide acid) (PLGA) are among the most frequently used nanoparticle formulations for drug delivery to the brain [36–39]. For example, Tf-bearing PLGA nanoparticles entrapping the analgesic tramadol exhibited antinociceptive effects in rats for 24 h following their intravenous administration [39]. Similar results were obtained in rats following intravenous treatment with OX26-bearing PLGA nanoparticles entrapping endomorphins [38].

In another study, gold nanoparticles linked to the peptide CLPFFD had the capacity to destroy the aggregates of β-amyloid, similar to the ones found in the brains of patients suffering from Alzheimer's disease, but were unable to cross the BBB. Their conjugation to a peptide sequence recognizing the TfR allowed them to cross the BBB and to reach the brain of rats following

intravenous administration, as demonstrated by quantification of gold in brain tissue [40].

TfR-targeted hybrid micelles

Micelles are small spherical structures with a hydrophilic surface and a hydrophobic core region. They recently attracted a lot of interest for the delivery of drugs to the brain due to their small size and ease of preparation [41]. A polyphosphoester hybrid micelle, consisting of Tf-conjugated PEG-poly(ε-caprolactone) and the amphiphilic block copolymer poly (ε-caprolactone)-block-poly(ethyl ethylene phosphate), was used to encapsulate the BBB-impermeable anticancer drug, paclitaxel [42]. This Tf-bearing formulation enhanced intravenous delivery of the drug to the brain by 1.8-fold when compared with the non-targeted micelles and resulted in an improved antiglioma activity in mice bearing intracranial glioma [42,43]. In these studies, only Tf-bearing formulations entrapping paclitaxel led to significant therapeutic effects on orthotopic glioma, thus, rejecting the hypothesis that the delivery of the anticancer drug to the tumors may have been facilitated by the leakiness of tumor vessels.

It is also important to note that the therapeutic effect of a hydrophobic drug, which is often used as a measure for drug-delivery efficiency, may be explained by binding of the drug carrier system to the brain endothelium or its uptake by endothelial cells, followed by diffusion of the drug further into the brain parenchyma. It does not necessarily mean that the drug carrier system crossed the BBB. The use of non-targeted delivery systems as controls is, therefore, highly important to confirm the TfR-mediated BBB crossing.

■ Targeted gene delivery

Numerous brain-related diseases could be candidates for treatment by gene therapy. Unfortunately, the inability of the nucleic acids to cross the BBB limits their therapeutic applications. In addition, a widespread expression of the exogenous gene throughout the entire brain would be needed for the treatment of most cerebral disorders.

Viral delivery systems have been widely used for gene delivery as they facilitate highly efficient transfer and expression of exogenous genes, but they can be immunogenic, cytopathic or recombinogenic, thus, limiting their repeated administrations [44]. On the other hand, non-viral delivery systems have been explored as promising alternatives for gene delivery. Various approaches have been used to formulate TfR-targeted non-viral gene medicines able to transport nucleic acids to the brain following intravenous administration (FIGURE 1).

TfR-targeted liposomes

Various formulations of TfR-targeted liposomes have been investigated for the delivery of nucleic acids across the BBB.

Plasmid DNA encoding β-galactosidase has been delivered to the rat brain following its encapsulation in OX26-bearing stealth liposomes [45]. This delivery system crossed the BBB via TfR-mediated transcytosis and led to gene expression deep within brain parenchyma. Some levels of gene expression were also observed in the liver and the spleen [45].

This targeting strategy has also demonstrated efficacy in an experimental model of Parkinson's disease. In order to remediate the deficiency in striatal tyrosine hydoxylase characteristic of the disease, Parkinson's disease rat models were intravenously injected with TfR-targeted liposomes carrying a tyrosine hydoxylase expression plasmid. This administration led to a normalization of striatal tyrosine hydoxylase immunoreactivity. By contrast, rats treated with nontargeted liposomes did not show any improvement of their pathology, thus highlighting the importance of TfR for brain delivery [46].

TfR-targeting can also be used for the brain delivery of RNAi in brain cancer therapy. One of the therapeutic strategies used in this instance was to knockdown the human EGF receptor which has a pro-oncogenic function in tumor cell growth and is overexpressed on tumors. The plasmid used encoded a RNA antisense to a specific region of the human EGF receptor mRNA. The liposomes encapsulating the nucleic acid were conjugated to an antibody, anti-TfR, to cross the BBB and to an antibody anti-human insulin receptor to reach the tumor once inside the brain. Intravenous administration of the formulation every week in mice with U87 intracranial brain tumors resulted in a 100% increase in survival time of the animals [47].

Similar experiments were also carried out in mice, using the rat 8D3 monoclonal antibody against mouse TfR instead of OX26, which specifically recognizes rat TfR. 8D3-conjugated PEGylated liposomes encapsulating plasmid DNA encoding β-galactosidase were able to deliver their cargo to the brain of mice following intravenous administration. When the enzyme expression was driven by a brain-specific

Key Term

Dendrigraft: Dendrimeric-shaped polymer formed by stepwise conjugation of tree-shaped branches on a central core.

promoter, such as the glial fibrillary acidic protein promoter, gene expression was observed in the brain, especially in the astrocytes, but not in any peripheral organs [48].

TfR-targeted conjugates/complexes

Another strategy to deliver nucleic acid therapeutics to the brain is to attach them to TfR-targeting ligands with the use of the avidin/biotin technology. This approach allowed Suzuki and colleagues to image endogenous gene expression in the brain with sequence-specific antisense radiopharmaceutics [49]. In this study, the biotinylated peptide nucleic acids were antisense agents to the rat GFAP mRNA or the rat caveolin-1α (CAV) mRNA. They were chelated to a radionuclide and bound to a conjugate of streptavidin and OX26. The intravenous administration of TfR-targeted GFAP anti-sense to rats bearing brain glial tumors did not image brain cancer, due to the downregulation of GFAP mRNA in cancer. However, TfR-targeted CAV antisense did lead to selective imaging of brain cancer as a result of the administration of the delivery system, owing to the upregulation of CAV mRNA in brain glial tumors [49].

Using the same avidin/biotin approach, the intravenous administration of a TfR-targeted siRNA led to 69–81% decrease in luciferase gene expression in brain cancer [50].

Dendrimers have recently been demonstrated to be promising candidates for brain delivery, owing to their unique polymer architecture and easily modified surface groups. They are synthetic polymeric macromolecules of nanometer size composed of multiple branched monomers that emerge radially from the central core [51]. Due to their unusual structure, dendrimers are characterized by the following properties that differentiate them from other polymers and make them attractive for gene delivery: monodisperse size, modifiable surface functionality, multivalency, water solubility and available internal cavity eventually suitable for drug delivery [51].

So far, only one dendrimer, polyamidoamine (PAMAM), has been studied as a vehicle to cross the BBB via TfR targeting [52]. In this study, Tf was conjugated to PAMAM through bifunctional PEG and complexed to a plasmid DNA encoding GFP. After intravenous administration to mice, the Tf-bearing PAMAM–DNA complex was able to cross the BBB and led to the expression of GFP in several brain regions such as the hippocampus, *substantia nigra*, the fourth ventricle, the cortical layer and *caudate putamen*. This gene expression was approximately two-fold higher than that observed following the administration of PAMAM and PAMAM–PEG complexes [52].

In other studies, a **dendrigraft**, poly-L-lysine, was developed as a delivery system for the co-administration of the anticancer drug doxorubicin and a therapeutic plasmid DNA encoding TNF-related apoptosis-inducing ligand for brain tumor therapy. The combination of gene therapy and chemotherapy within one TfR-targeted delivery system was hypothesized to provide a synergistic therapeutic effect for the treatment of glioma. The peptide HAIYPRH (T7) was used as a TfR-targeting ligand. Doxorubicin was covalently conjugated to the dendrigraft via a pH-triggered hydrazine bond, while the DNA was complexed to the carrier. Following intravenous administration to mice bearing orthotopic glioma tumors, the TfR-targeted system was shortly detected in the brain and in the glioma (within 1 h post-administration). The combination treatment then resulted in a synergistic growth inhibition of the tumors, with a survival time increased by about 20 days compared with controls [30].

Most studies described above demonstrated that their TfR-targeted delivery systems were able to cross the BBB by TfR-mediated transcytosis, by showing that nontargeted delivery systems were not able to do so. The proof of such transport mechanism could also be obtained either by capillary depletion method or morphological investigation of brain tissue.

TfR-mediated delivery of therapeutic agents to cancer cells

Traditional chemotherapeutic drugs can successfully eradicate tumors, but often have their use limited due to their non-specific toxicity to normal cells. To overcome this major problem, many tumor-targeting strategies are currently under development [53]. Among them, TfR targeting has been the object of intense research in the field of cancer therapy, owing to the overexpression of this receptor on malignant cells that can be up to 100-fold higher than that observed in normal cells [6–9]. This overexpression of TfR on cancer cells is much higher than that observed on the BBB and therefore limits any delivery of chemotherapeutics to the brain, instead of tumors. Furthermore, TfR-targeted delivery systems were shown to be highly useful for the systemic treatment of brain

tumors, as they were able to transport therapeutic agents across the BBB and to increase their delivery to brain tumors following intravenous administration, as further described below [30,50].

■ Targeted drug delivery

A wide range of delivery strategies, including the linkage of drugs to Tf, entrapment of the drugs in TfR-targeted liposomes, vesicles and nanoparticles, have been investigated for TfR-mediated delivery of drugs to tumors (FIGURE 1).

Linkage of drugs to Tf

Many anticancer drugs have been conjugated to either Tf or an antibody against TfR. One of them, doxorubicin, is an effective and widely used anticancer anthracyclin drug that exhibits severe adverse effects, such as cardiotoxicity, nephrotoxicity by myelosuppression due to non-specific drug distribution and emergence of drug-resistant cancer cells. To overcome these limitations, doxorubicin was conjugated with Tf by glutaraldehyde crosslinking. This resulted in an increase of the *in vitro* cytotoxicity of the conjugate, with an IC_{50} decrease of up to 57-fold compared with the free drug in L929 murine fibrosarcoma cells [17]. *In vivo* studies on nude mice bearing H-MESO-1 tumors demonstrated that the intravenously administered Tf–doxorubicin conjugate significantly decreased the size of the tumors and consequently increased the life span of the animals by 69%, compared with 30% following administration of doxorubicin solution [54].

Conjugation of doxorubicin to Tf could also overcome the resistance of some cancer cells to doxorubicin solution, for example in KB human oral carcinoma cells and MCF-7 human breast cancer cells [55]. The resistance to free doxorubicin could be further overcome by conjugating Tf–doxorubicin conjugate with the antineoplastic drug gallium nitrate, which is a competitive inhibitor of the circulating holoTf. The Tf–doxorubicin–gallium nitrate conjugate was able to decrease the IC_{50} by 100-fold in doxorubicin-resistant MCF-7 human breast cancer cells [56].

Tf has also been conjugated to cisplatin, an alkylating agent used for treating testicular, ovarian and bladder cancers. The resulting conjugate was able to avoid metastatic growth of breast carcinoma cells in the lungs during *in vivo* experiments on rats. In addition, a clinical trial for advanced breast cancer has demonstrated a high response rate to the Tf–cisplatin conjugate in four out of 11 patients, including one complete response, with only minor side effects [57].

TfR-targeted liposomes & vesicles

Encapsulating an anticancer drug in Tf-bearing liposomes or other lipid-based vesicles can lead to an increase in antiproliferative efficacy and reduction of nonspecific adverse effects. The intravenous administration of Tf-bearing liposomes encapsulating doxorubicin in nude mice bearing HepG2 human hepatoma subcutaneous tumors resulted in an increase of drug concentration in tumors and a subsequent decrease of tumor growth, compared with doxorubicin solution [58].

Liposomes can also be conjugated to anti-TfR monoclonal antibodies instead of Tf. Such a strategy was used by Suzuki and colleagues, who reported the efficacy of doxorubicin-encapsulating liposomes conjugated to the anti-human TfR monoclonal antibody OKT9, on K562/ADM human leukemia cells resistant to free doxorubicin [59]. In this *in vitro* study, TfR-targeted doxorubicin was taken up by the cells, thus resulting in an increased cytotoxic activity compared with the drug solution.

Tf-bearing palmitoyl glycol chitosan-based vesicles were also tested for the delivery of doxorubicin to A431 human epidermoid carcinoma and the drug-resistant A2780AD human ovarian carcinoma cells [60]. Increased cellular uptake and cytotoxicity were observed for Tf-bearing formulations as compared with doxorubicin solution. *In vivo*, however, none of the vesicular formulations could significantly delay the growth of A431 tumors after a single administration and were less active than the drug solution.

Tf-bearing vesicles were also found to be extremely useful to evaluate the therapeutic efficacy of promising anticancer drugs unable to reach the tumors at therapeutic concentrations. This was the case for example for tocotrienol, a member of the vitamin E family of compounds. The authors have demonstrated that the entrapment of tocotrienol within Tf-bearing vesicles led to tumor regression and increase of the animal survival following intravenous administration to mice bearing A431 tumors [61]. In a follow-up study, the authors demonstrated that intravenously administered Tf-bearing multilamellar vesicles entrapping tocotrienol led to complete tumor eradication for 40% of B16-F10 murine melanoma and 20% of A431 tumors, as well as improvement of animal survival [62,63]. A similar strategy allowed

Key Term

Dendriplex: Complex of nucleic acids with a dendrimer.

the authors to demonstrate that treatment with the green tea extract, epigallocatechin gallate, encapsulated in Tf-bearing vesicles resulted in tumor suppression of 40% of A431 and B16-F10 tumors following intravenous administration of the targeted formulation [64].

TfR-targeted polymers & nanoparticles

Polymers and nanoparticles have become promising drug-delivery systems for cancer therapy, due to their multifunctional structure that allows the simultaneous transport of various drugs to cancer cells, leading to synergistic therapeutic effects *in vivo*. Polymers used as single polymeric systems or as part of nanoparticles are also biodegradable and nontoxic. They can be of natural origin, such as the polysaccharide chitosan, or synthetic, such as poly(lactic acid) and PLGA. TfR-targeting nanoparticles could be formulated to allow various kinetics of drug release depending of the pathology to be treated. For example, a slowly releasing polymer could be more advantageous for cancer treatment whereas a faster release may be required for acute brain disorders [65]. Tf-bearing PLGA-based nanoparticles loading the mitotic inhibitor paclitaxel increased the delivery of their cargo to C6 rat glioma subcutaneous tumors compared with the nontargeted vehicles, after 24 h of intravenous administration to rats [66]. In another study, 50% of treated S-180 tumor-bearing mice showed a complete tumor regression following the intravenous administration of Tf-bearing PEGylated poly(cyanoacrylate) nanoparticles entrapping paclitaxel. The life span of the animals was significantly increased, with three mice surviving over 60 days post-treatment with the TfR-targeting nanoparticles [67].

■ Targeted gene delivery

The possibility of using genes as medicines to treat patients suffering from cancer is still hampered by the lack of safe carrier systems able to specifically deliver the therapeutic nucleic acids to the tumors after intravenous administration. There is therefore an urgent need to develop efficacious gene-delivery systems that should be target-specific, nontoxic, noninflammatory, biodegradable and nonimmunogenic.

Among all the delivery systems currently being developed, non-viral delivery systems appear most suited to fulfill these requirements. Moreover, they have the advantages of being easy to prepare, flexible regarding the size of nucleic acid to be carried and suitable for repeated administrations as they are much safer than viral vectors [68]. TfR-mediated gene delivery using these vectors is a promising strategy since it provides an opportunity to achieve specific gene delivery to tumors while increasing the transfection efficiency in cancer cells (FIGURE 1).

TfR-targeted liposomes

Cationic liposomes complexed with DNA have been used extensively for the delivery of nucleic acids to cancer cells *in vitro* and *in vivo*. The negatively charged DNA can be complexed to the positively charged liposomes by electrostatic interactions to form lipoplexes. The intravenous injection of a Tf-bearing lipoplex encoding for the tumor-suppressor protein p53 resulted in high level of *p53* gene expression in tumors, contrarily to that observed with nontargeted lipoplexes, in mice bearing subcutaneous DU145 human prostate tumors [69]. In combination with radiotherapy, the TfR-targeting lipoplex encoding p53 exhibited complete tumor regression without recurrence 6 months after treatment [69].

TfR-targeted cyclodextrins

Cyclodextrins are a family of cyclic macromolecules consisting of 6–8 glucopyranoside units linked together by glycosidic bonds to form a ring. They are characterized by their toroidal molecular structure with hydroxyl groups orientated toward the outside. As a result, cyclodextrins are soluble in their aqueous environment while being able to host small hydrophobic drugs in their internal cavity to form inclusion complexes [70].

Cyclodextrins containing polycations have demonstrated efficacy in transporting nucleic acids such as plasmid DNA and siRNA. A TfR-targeting PEGylated imidazole-modified cyclodextrin was mixed with the siRNA targeting the EWS-FLI1 fusion protein known to be a transcription factor involved in tumorigenesis. Intravenous administration of this system in mice decreased gene expression of EWS-FLI1 in tumors and decreased the growth of tumors with short-term effect [71].

TfR-targeted micelles

TfR-targeting micelles have demonstrated efficacy to deliver nucleic acids to tumors intravenously. Micelles made of a copolymer of PEG–poly(ethylenimine) biotin were associated to biotinylated Tf by avidin/biotin noncovalent binding [72]. This micellar formulation was

demonstrated to enhance the tumor delivery of antisense oligonucleotides against the human multidrug resistance protein-1 (which plays a role in multidrug resistance) in MCF-7ADR human breast carcinoma as well as in KBV human oral epidermoid carcinoma [72].

TfR-targeted polymers & dendrimers

Many Tf-bearing polycationic polymers have been used to condense negatively charged DNA and to deliver it to cancer cells. Among them, polylysine and polyethylenimine (PEI) have been widely used for this purpose and both were found to be very efficient vectors for gene transfer to cancer cells. In the K-562 human erythroleukemic cell line, most of the cell population was found to express the transfected reporter genes following intravenous treatment with the Tf-bearing polylysine polyplex [73].

Similarly, Tf-bearing PEI was used to deliver a plasmid DNA encoding for TNFα, a cytokine with promising anticancer properties but also nonspecific toxicity limiting its potential use. Systemic treatment of mice bearing either subcutaneous Neuro2a neuroblastoma, MethA fibrosarcoma or M-3-melanoma cells with this targeted formulation resulted in anti-tumor effects on the three tumor models, with complete regression of MethA tumors [74,75]. The treatment was well tolerated by the animals.

In addition to their role as drug carriers, dendrimers have also been investigated as potential vehicles for nucleic acids. PAMAM dendrimer coated with PEG was targeted to TfR by conjugation with the peptide T7. It was able to co-deliver the drug doxorubicin together with a therapeutic plasmid encoding TNF-related apoptosis-inducing ligand [76]. A synergistic efficacy was observed between the two therapeutic agents following intravenous administration on mice bearing subcutaneous Bel-7402 human hepatoma tumors. The TfR-targeting system inhibited 77% of tumor growth, which was much higher than that obtained with non-targeted **dendriplex** or the free drug. The inhibition was also achieved using a smaller dose [76].

Recently, the authors have also demonstrated that an intravenously administered generation 3-diaminobutyric polypolypropylenimine dendrimer conjugated to Tf by crosslinking and complexed to plasmid DNA encoding TNFα led to complete disappearance of 90% of A431 human epidermoid carcinoma tumors, compared with the 40% complete tumor regression observed with the nontargeted dendriplex [77]. In another study, the authors used this targeted dendrimer to assess the therapeutic potential of p73, a member of the p53 family of transcription factors. We demonstrated that the intravenous administration of Tf-bearing, p73-encoding 3-diaminobutyric polypropylenimine dendrimer dendriplex led to a sustained inhibition of tumor growth and complete tumor suppression for 10% of A431 and B16-F10 tumors in mice [78]. The treatments with both dendriplexes were well tolerated by the animals.

Conclusion

A major challenge for the development of potential drugs with promising therapeutic effects resides in their inability to specifically reach the pathological site following intravenous administration, without generating secondary effects to healthy tissues.

In the past few decades, the protein Tf has been extensively explored as a targeting molecule for the transport of drug and gene delivery systems to the brain and cancer cells. A wide range of delivery approaches highlighted in this review are currently under investigation in laboratory settings and have already led to significant improvements in the systemic delivery of Tf-bearing therapeutic systems to their site of action. Clinical trials exploring the efficacy of Tf-bearing therapeutics are already under way. These advances therefore demonstrate that the targeting of TfR has a huge potential for the development of more specific and safer gene and drug-based therapeutics.

Future perspective

TfR targeting has demonstrated promise for the delivery of nucleic acids and drugs across the BBB and to tumors. The research area is expanding fully, and is currently the object of intense patenting worldwide.

In the future, it is likely that researchers will continue to develop novel TfR-targeted delivery systems or other techniques to further increase the specificity of the targeting to the pathological tissues. In addition, it will probably become important to focus on how to increase the transfection efficacy to optimize the therapeutic effect of potential gene medicines. One possibility would be to develop a strategy for facilitating the release of nucleic acids from the endosome to the cytoplasm of the cells.

Although highly promising, most current research on TfR-based targeted delivery of drugs and nucleic acids is still at an early stage

requiring more optimization. Some clinical trials are already under way. One of them, which aims to test the efficacy of a Tf–cisplatin conjugate for advanced breast cancer, has already reported highly positive results in a Phase I study [57] and will hopefully pave the way for many more trials to come.

More generally, targeting the delivery of a drug to its site of action can dramatically increase its therapeutic potential. Given the significant improvements already realized in the field of TfR targeting, it is likely that targeted delivery technologies will play a crucial role in the development of future therapeutics.

Financial & competing interests disclosure

The work in the authors' laboratory is currently supported by grants from the Medical Research Council, the Cunningham Trust and the University of Strathclyde. M Al Robaian is supported by a PhD studentship from the Saudi Cultural Bureau and Taif University (Kingdom of Saudi Arabia). S Somani is funded by The Cunningham Trust. The authors have no other relevant affiliations or financial involvement with any organization or entity with a financial interest in or financial conflict with the subject matter or materials discussed in the manuscript apart from those disclosed.

No writing assistance was utilized in the production of this manuscript.

Executive summary

Introduction

- The use of promising novel therapeutics is limited by their inability to specifically reach the pathological site after intravenous administration, resulting in toxicity to healthy tissues.
- Transferrin (Tf) has been extensively studied as a targeting moiety for drug- and gene-delivery systems, as its receptors are overexpressed on the blood–brain barrier and on cancer cells.

Tf receptor-mediated delivery of therapeutic agents to the brain & to cancer cells

- A wide range of delivery systems targeting the Tf receptor have been developed for the delivery of nucleic acids and drugs.
- Tf-bearing vehicles entrapping nucleic acids and drugs have been demonstrated to specifically deliver their cargo to their required site of action and to improve their therapeutic effects.

Conclusion

- Tf-bearing delivery systems are, therefore, highly promising for the delivery of therapeutics to the brain and tumors *in vitro* and *in vivo*, and should be further investigated.

References

Papers of special note have been highlighted as:
- • of interest
- •• of considerable interest

1 Qian ZM, Li H, Sun H, Ho K. Targeted drug delivery via the transferrin receptor-mediated endocytosis pathway. *Pharmacol. Rev.* 54, 561–587 (2002).

2 Jefferies WA, Brandon MR, Hunt SV, Williams AF, Gatter KC., Mason DY. Transferrin receptor on endothelium of brain capillaries. *Nature* 312, 162–163 (1984).

3 Fishman JB, Rubin JB, Handrahan JV, Connor JR, Fine RE. Receptor-mediated transcytosis of transferrin across the blood–brain barrier. *J. Neurosci. Res.* 18, 299–304 (1987).

4 Bickel U, Yoshikawa T, Pardridge WM. Delivery of peptides and proteins through the blood–brain barrier. *Adv. Drug Deliv. Rev.* 46, 247–279 (2001).

5 Pardridge WM. Drug targeting to the brain. *Pharm. Res.* 24, 1733–1744 (2007).

6 Yang DC., Wang F, Elliott RL., Head JF. Expression of transferrin receptor and ferritin H-chain mRNA are associated with clinical and histopathological prognostic indicators in breast cancer. *Anticancer Res.* 21, 541–549 (2001).

7 Seymour GJ, Walsh MD, Lavin MF, Strutton G, Gardiner RA. Transferrin receptor expression by human bladder transitional cell carcinomas. *Urol. Res.* 15, 341–344 (1987).

8 Kondo K, Noguchi M, Mukai K *et al.* Transferrin receptor expression in adenocarcinoma of the lung as a histopathologic indicator of prognosis. *Chest* 97, 1367–1371 (1990).

9 Prior R, Reifenberger G, Wechsler W. Transferrin receptor expression in tumours of the human nervous system: relation to tumour type, grading and tumour growth fraction. *Virchows Arch. A Pathol. Anat. Histopathol.* 416, 491–496 (1990).

10 Huebers HA, Finch CA. The physiology of transferrin and transferrin receptors. *Physiol. Rev.* 67, 520–582 (1987).

11 Brandsma ME, Jevnikar AM, Ma S. Recombinant human transferrin: beyond iron binding and transport. *Biotechnol. Adv.* 29, 230–238 (2011).

12 Aisen P, Leibman A, Zweier J. Stoichiometric and site characteristics of the binding of iron to human transferrin. *J. Biol. Chem.* 253, 1930–1937 (1978).

13 Richardson DR, Ponka P. The molecular mechanisms of the metabolism and transport of iron in normal and neoplastic cells. *Biophys. Acta* 1331, 1–40 (1997).

14 Baker HM, Anderson BF, Baker EN. Dealing with iron: common structural principles in proteins that transport iron and heme. *Proc. Natl Acad. Sci. USA* 100, 3579–3583 (2003).

15 Neckers LM, Trepel JB. Transferrin receptor expression and the control of cell growth. *Cancer Invest.* 4, 461–470 (1986).

16 Daniels TR, Delgado T, Rodriguez JA, Helguera G, Penichet ML. The transferrin receptor part I: biology and targeting with cytotoxic antibodies for the treatment of cancer. *Clin. Immunol.* 121, 144–158 (2006).

17 Lai BT, Gao JP, Lanks KW. Mechanism of action and spectrum of cell lines sensitive to a doxorubicin-transferrin conjugate. *Cancer Chemother. Pharmacol.* 41, 155–160 (1998).

18 Kawabata H, Germain RS, Vuong PT, Nakamaki T, Said JW, Koeffler HP. Transferrin receptor 2-alpha supports cell growth in iron-chelated cultured cells and *in vivo*. *J. Biol. Chem.* 275, 16618–16625 (2000).

19 Lee HJ, Engelhardt B, Lesley J, Bickel U, Pardridge WM. Targeting rat anti-mouse transferrin receptor monoclonal antibodies through blood–brain barrier in mouse. *J. Pharmacol. Exp. Ther.* 292, 1048–1052 (2000).

20 Friden PM, Walus LR, Musso GF, Taylor MA, Malfroy B, Starzyk RM. Anti-transferrin receptor antibody and antibody-drug conjugates cross the blood–brain barrier. *Proc. Natl Acad. Sci. USA* 88, 4771–4775 (1991).

21 Zhang Y, Pardridge WM. Blood–brain barrier targeting of BDNF improves motor function in rats with middle cerebral artery occlusion. *Brain Res.* 1111, 227–229 (2006).

22 Wu D, Pardridge WM. Central nervous system pharmacologic effect in conscious rats after intravenous injection of a biotinylated vasoactive intestinal peptide analog coupled to a blood–brain barrier drug delivery system. *J. Pharmacol. Exp. Ther.* 279, 77–83 (1996).

23 Li XB, Liao GS, Shu YY, Tang SX. Brain delivery of biotinylated NGF bounded to an avidin-transferrin conjugate. *J. Nat. Toxins.* 9, 73–83 (2000).

24 Lee HJ, Zhang Y, Zhu CN, Duff K, Pardridge WM. Imaging brain amyloid of Alzheimer disease *in vivo* in transgenic mice with an A beta peptide radiopharmaceutical. *J. Cereb. Blood Flow Metab.* 22(2), 223–231 (2002).

25 Fu A, Zhou QH, Hui EK, Lu JZ, Boado RJ, Pardridge WM. Intravenous treatment of experimental Parkinson's disease in the mouse with an IgG-GDNF fusion protein that penetrates the blood–brain barrier. *Brain Res.* 1352, 208–213 (2010).

26 Pardridge WM. Vector-mediated drug delivery to the brain. *Adv. Drug Delivery Rev.* 36, 299–321 (1999).

27 Zhang Y, Pardridge WM. Delivery of β-galactosidase to mouse brain via the blood–brain barrier transferrin receptor. *J. Pharmacol. Exp. Ther.* 313, 1075–1081 (2005).

28 Xu G, Yong KT, Roy I *et al.* Bioconjugated quantum rods as targeted probes for efficient transmigration across an *in vitro* blood–brain barrier. *Bioconjugate Chem.* 19, 1179–1185 (2008).

29 Mahajan SD, Roy I, Xu G, *et al.* Enhancing the delivery of anti-retroviral drug "Saquinavir" across the blood–brain barrier using nanoparticles. *Curr. HIV Res.* 8, 396–404 (2010).

30 Liu S, Guo Y, Huang R *et al.* Gene and doxorubicin co-delivery system for targeting therapy of glioma. *Biomaterials* 33, 4907–4916 (2012).

31 Aragnol D, Leserman LD. Immune clearance of liposomes inhibited by an anti-Fc receptor antibody *in vivo*. *Proc. Natl Acad. Sci. USA* 83, 2699–2703 (1986).

32 Soni V, Kohli DV, Jain SK. Transferrin-conjugated liposomal system for improved delivery of 5-fluorouracil to brain. *J. Drug Target.* 16, 73–78 (2008).

33 Huwyler J, Wu D, Pardridge WM. Brain drug delivery of small molecules using immunoliposomes. *Proc. Natl Acad. Sci. USA* 93, 14164–14169 (1996).

34 Béduneau A, Saulnier P, Hindré F, Clavreul A, Leroux JC, Benoit JP. Design of targeted lipid nanocapsules by conjugation of whole antibodies and antibody Fab' fragments. *Biomaterials* 28, 4978–4990 (2007).

35 Béduneau A, Hindré F, Clavreul A, Leroux JC, Saulnier P, Benoit JP. Brain targeting using novel lipid nanovectors. *J. Control. Release* 126, 44–49 (2008).

36 Kreuter J. Mechanism of polymeric nanoparticle-based drug transport across the blood–brain barrier. *J. Microencapsul.* 30, 49–54 (2013).

37 Olivier JC. Drug transport to brain with targeted nanoparticles. *NeuroRx* 2, 108–119 (2005).

38 Bao H, Jin X, Li L, Lv F, Liu T. OX26 modified hyperbranched polyglycerol-conjugated poly(lactic-co-glycolic acid) nanoparticles: synthesis, characterization and evaluation of its brain delivery ability. *J. Mater. Sci. Mater. Med.* 23, 1891–1901 (2012).

39 Lalani J, Raichandani Y, Mathur R *et al.* Comparative receptor based brain delivery of tramadol-loaded poly (lactic-co-glycolic acid) nanoparticles. *J. Biomed. Nanotechnol.* 8, 918–927 (2012).

40 Prades R, Guerrero S, Araya E *et al.* Delivery of gold nanoparticles to the brain by conjugation with a peptide that recognizes the transferrin receptor. *Biomaterials* 33, 7194–7205 (2012).

41 Kedar U, Phutane P, Shidhaye S, Kadam V. Advances in polymeric micelles for drug delivery and tumor targeting. *Nanomedicine* 6, 714–729 (2010).

42 Zhang P, Hu L, Yin Q, Zhang Z, Feng L, Li Y. Transferrin-conjugated polyphosphoester hybrid micelle loading paclitaxel for brain-targeting delivery: synthesis, preparation and *in vivo* evaluation. *J. Control. Release* 159, 429–434 (2012).

43 Zhang P, Hu L, Yin Q, Feng L, Li Y. Transferrin-modified c[RGDfK]-Paclitaxel loaded hybrid micelle for sequential blood–brain barrier penetration and glioma targeting therapy. *Mol. Pharm.* 9, 1590–1598 (2012).

44 Yang Y, Nunes FA, Berencsi K, Furth EE, Gonczol E, Wilson JM. Cellular-immunity to viral-antigens limits E1-deleted adenoviruses for gene-therapy. *Proc. Natl Acad. Sci. USA* 91, 4407–4411 (1994).

45 Shi N, Pardridge WM. Non-invasive gene targeting to the brain. *Proc. Natl Acad. Sci. USA* 97, 7567–7572 (2000).

46 Zhang Y, Schlachetzki F, Zhang YF, Boado RJ, Pardridge WM. Normalization of striatal tyrosine hydroxylase and reversal of motor impairment in experimental parkinsonism with intravenous nonviral gene therapy and a brain-specific promoter. *Human Gene Ther.* 15, 339–350 (2004).

47 Zhang Y, Zhu C, Pardridge WM. Antisense gene therapy of brain cancer with an artificial virus gene delivery system. *Mol. Ther.* 6, 67–72 (2002).

48 Shi NY, Zhang Y, Zhu CN, Boado RJ, Pardridge WM. Brain-specific expression of an exogenous gene after i.v. administration. *Proc. Natl Acad. Sci. USA* 98, 12754–12759 (2001).

• **Demonstrates that 8D3-conjugated PEGylated liposomes encapsulating plasmid DNA encoding β-galactosidase were able to deliver their cargo to the brain of mice following intravenous administration. When the enzyme expression was driven by a brain-specific promoter, gene expression was only observed in the brain.**

49 Suzuki T, Wu D, Schlachetzki F, Li JY, Boado RJ, Pardridge WM. Imaging endogenous gene expression in brain cancer *in vivo* with ^{111}In-peptide nucleic acid antisense radiopharmaceuticals and brain drug-targeting technology. *J. Nucl. Med.* 45, 1766–1775 (2004).

50 Xia CF, Zhang Y, Zhang Y, Boado RJ, Pardridge WM. Intravenous siRNA of brain cancer with receptor targeting and avidin-biotin technology. *Pharm. Res.* 24, 2309–2316 (2007).

51 Dufès C, Uchegbu IF, Schätzlein AG. Dendrimers in gene delivery. *Adv. Drug Deliv. Rev.* 57, 2177–2202 (2005).

52 Huang RQ, Qu YH, Ke WL, Zhu JH, Pei YY, Jiang C. Efficient gene delivery targeted to the brain using a transferrin-conjugated polyethyleneglycol-modified polyamidoamine dendrimer. *FASEB J.* 21, 117–1125 (2007).

53 Daniels TR, Bernabeu E, Rodriguez JA *et al.* The transferrin receptor and the targeted delivery of therapeutic agents against cancer. *Biochim. Biophys. Acta* 1820, 291–317 (2012).

•• **Very detailed description of transferrin (Tf), its receptor and all the Tf receptor-targeting delivery strategies attempted so far.**

54 Singh M, Atwal H, Micetich R. Transferrin directed delivery of Adriamycin to human cells. *Anticancer Res.* 18, 1423–1427 (1998).

55 Lubgan D, Jozwiak Z, Grabenbauer GG, Distel LV. Doxorubicin-transferrin conjugate selectively overcomes multidrug resistance in leukaemia cells. *Cell. Mol. Biol. Lett.* 14, 113–127 (2009).

56 Wang F, Jiang X, Yang DC, Elliott RL, Head JF. Doxorubicin-gallium-transferrin conjugate overcomes multidrug resistance: evidence for drug accumulation in the nucleus of drug resistant MCF-7/ADR cells. *Anticancer Res.* 20, 799–808 (2000).

57 Head JF, Wang F, Elliott RL. Antineoplastic drugs that interfere with iron metabolism in cancer cells. *Adv. Enzyme Regul.* 37, 147–159 (1997).

• **Describes that a clinical trial for advanced breast cancer has observed a high response rate to the Tf–cisplatin conjugate in four out of 11 patients, including one complete response, with only minor side effects.**

58 Li X, Ding L, Xu Y, Wang Y, Ping Q. Targeted delivery of doxorubicin using stealth liposomes modified with transferrin. *Int. J. Pharm.* 373, 116–123 (2009).

59 Suzuki S, Inoue K, Hongoh A, Hashimoto Y, Yamazoe Y. Modulation of doxorubicin resistance in a doxorubicin-resistant human leukaemia cell by an immunoliposome targeting transferrin receptor. *Br. J. Cancer* 76, 83–89 (1997).

60 Dufès C, Muller JM, Olivier JC, Uchegbu IF, Schätzlein AG. Anticancer drug delivery with transferrin targeted polymeric chitosan vesicles. *Pharm. Res.* 21, 101–107 (2004).

61 Fu JY, Blatchford DR, Tetley L, Dufès C. Tumor regression after systemic administration of tocotrienol entrapped in tumor-targeted vesicles. *J. Control. Release* 140, 95–99 (2009).

62 Fu JY, Zhang W, Blatchford DR, Tetley L, McConnell G, Dufès C. Novel tocotrienol-entrapping vesicles can eradicate solid tumors after intravenous administration. *J. Control. Release* 154, 20–26 (2011).

• **Describes that intravenously administered Tf-bearing multilamellar vesicles entrapping tocotrienol led to complete tumor eradication for 40% of B16-F10 murine melanoma and 20% of A431 tumors, as well as improvement of animal survival.**

63 Dufès C. Delivery of the vitamin E compound tocotrienol to cancer cells. *Ther. Deliv.* 2, 1385–1389 (2011).

64 Lemarié F, Chang CW, Blatchford DR *et al.* Anti-tumor activity of the tea polyphenol epigallocatechin gallate encapsulated in targeted vesicles after intravenous administration. *Nanomedicine (Lond.)* 8(2), 181–192 (2013).

65 Karatas H, Aktas Y, Gursoy-Ozdemir Y *et al.* A nanomedicine transports a peptide caspase-3 inhibitor across the blood-brain barrier and provides neuroprotection. *J. Neuroscience* 19, 13761–13769 (2009).

66 Shah N, Chaudhari K, Dantuluri P, Murthy RS, Das S. Paclitaxel-loaded PLGA nanoparticles surface modified with transferrin and Pluronic® P85, an *in vitro* cell line and *in vivo* biodistribution studies on rat model. *J. Drug Target.* 17, 533–542 (2009).

67 Pulkkinen M, Pikkarainen J, Wirth T *et al.* Three-step tumor targeting of paclitaxel using biotinylated PLA-PEG nanoparticles and avidin-biotin technology: formulation development and *in vitro* anticancer activity. *Eur. J. Pharm. Biopharm.* 70, 66–74 (2008).

68 Elsabahy M, Nazarali A, Foldvari M. Non-viral nucleic acid delivery: key challenges and future directions. *Curr. Drug Deliv.* 8, 235–244 (2011).

69 Xu L, Frederik P, Pirollo KF *et al.* Self-assembly of a virus-mimicking nanostructure system for efficient tumor-targeted gene delivery. *Hum. Gene Ther.* 13, 469–481 (2002).

70 Wenz G, Han BH, Muller A. Cyclodextrin rotaxanes and polyrotaxanes. *Chem. Rev.* 106, 782–817 (2006).

71 Hu-Lieskovan S, Heidel JD, Bartlett DW, Davis ME, Triche TJ. Sequence-specific knockdown of EWS-FLI1 by targeted, nonviral delivery of small interfering RNA inhibits tumor growth in a murine model of metastatic Ewing's sarcoma. *Cancer Res.* 65, 8984–8992 (2005).

72 Vinogradov S, Batrakova E, Li S, Kabanov A. Polyion complex micelles with protein-modified corona for receptor-mediated delivery of oligonucleotides into cells. *Bioconjug. Chem.* 10, 851–860 (1999).

73 Cotten M, Wagner E, Birnstiel ML. Receptor-mediated transport of DNA into eukaryotic cells. *Method Enzymol.* 217, 618–644 (1993).

74 Kircheis R, Ostermann E, Wolschek MF *et al.* Tumor-targeted gene delivery of tumor necrosis factor-alpha induces tumor necrosis and tumor regression without systemic toxicity. *Cancer Gene Ther.* 9, 673–680 (2002).

•• **Demonstrates that the systemically administered Tf-bearing polyethylenimine encoding TNFα resulted in antitumor effects on three tumor models, with complete regression of MethA tumors.**

75 Kursa M, Walker GF, Roessler V *et al.* Novel shielded transferrin-polyethylene glycol-polyethylenimine/DNA complexes for systemic tumor-targeted gene transfer. *Bioconjug. Chem.* 14, 222–231 (2003).

76 Han L, Huang R, Li J, Liu S, Huang S, Jiang C. Plasmid pORF-hTRAIL and doxorubicin co-delivery targeting to tumor using peptide-conjugated polyamidoamine dendrimer. *Biomaterials* 32, 1242–1252 (2011).

• **Demonstrates that a Tf receptor-targeted PEGylated polyamidoamine dendrimer was able to co-deliver the drug doxorubicin together with a therapeutic plasmid encoding TNF-related apoptosis-inducing ligand to tumors and to inhibit 77% of tumor growth.**

77 Koppu S, Oh YJ, Edrada-Ebel R *et al.* Tumor regression after systemic administration of a novel tumor-targeted gene delivery system carrying a therapeutic plasmid DNA. *J. Control. Release* 143, 215–221 (2010).

•• **Demonstrates that an intravenously administered Tf-bearing generation 3-diaminobutyric polypropylenimine dendriplex encoding TNFα led to complete disappearance of 90% of A431 human epidermoid carcinoma tumors in mice.**

78 Lemarié F, Croft DR, Tate RJ, Ryan KM, Dufès C. Tumor regression following intravenous administration of a tumor-targeted p73 gene delivery system. *Biomaterials* 33, 2701–2709 (2012).

Journal of Controlled Release 188 (2014) 78–86

Contents lists available at ScienceDirect

Journal of Controlled Release

journal homepage: www.elsevier.com/locate/jconrel

Transferrin-bearing polypropylenimine dendrimer for targeted gene delivery to the brain

Sukrut Somani [a], David R. Blatchford [a], Owain Millington [a], M. Lynn Stevenson [b], Christine Dufès [a,*]

[a] Strathclyde Institute of Pharmacy and Biomedical Sciences, University of Strathclyde, 161 Cathedral Street, Glasgow G4 0RE, UK
[b] School of Veterinary Medicine, University of Glasgow, Bearsden Road, Glasgow G61 1QH, UK

ARTICLE INFO

Article history:
Received 4 February 2014
Accepted 5 June 2014
Available online 14 June 2014

Keywords:
Brain delivery
Blood–brain barrier
Gene delivery
Dendrimer
Transferrin

ABSTRACT

The possibility of using genes as medicines to treat brain diseases is currently limited by the lack of safe and efficacious delivery systems able to cross the blood–brain barrier, thus resulting in a failure to reach the brain after intravenous administration.

On the basis that iron can effectively reach the brain by using transferrin receptors for crossing the blood–brain barrier, we propose to investigate if a transferrin-bearing generation 3-polypropylenimine dendrimer would allow the transport of plasmid DNA to the brain after intravenous administration.

In vitro, the conjugation of transferrin to the polypropylenimine dendrimer increased the DNA uptake by bEnd.3 murine brain endothelioma cells overexpressing transferrin receptors, by about 1.4-fold and 2.3-fold compared to that observed with the non-targeted dendriplex and naked DNA. This DNA uptake appeared to be optimal following 2 h incubation with the treatment.

In vivo, the intravenous injection of transferrin-bearing dendriplex more than doubled the gene expression in the brain compared to the unmodified dendriplex, while decreasing the non-specific gene expression in the lung. Gene expression was at least 3-fold higher in the brain than in any tested peripheral organs and was at its highest 24 h following the injection of the treatments.

These results suggest that transferrin-bearing polypropylenimine dendrimer is a highly promising gene delivery system to the brain.

1. Introduction

Gene therapy has emerged as a promising strategy to treat cerebral diseases such as glioma, Alzheimer's and Parkinson's diseases, which affect a large percentage of the world's population and hardly respond to intravenously administered, small molecule treatment [1–4]. Although the genetic basis for many of these diseases is known, the possibility of using genes as medicines is currently limited by the lack of safe and efficacious delivery systems able to cross the blood–brain barrier (BBB) and to deliver DNA to the brain after intravenous administration.

The BBB acts as an entrance gateway, restricting the movement of ions and nutrients to the central nervous system while protecting the brain against harmful blood-borne substances and invading organisms [2,5]. Its permeability properties prevent the delivery of more than 98% of drugs, including nucleic acids, to the brain [2,3]. In addition, locally administered treatments fail to achieve a widespread gene expression in the target cells throughout the entire brain, which is necessary for a successful treatment of most cerebral pathologies [2,3,6].

However, the BBB does possess specific receptor-mediated transport mechanisms that can potentially be exploited as a means to target drugs and genes to the brain. The transferrin receptor (TfR) is of particular interest because it is overexpressed on the brain capillary endothelial cells [7]. The antibodies that bind to the TfR have been shown to selectively target the brain microvascular endothelium due to the high levels of TfR expressed by these cells [8–10]. This strategy has been widely investigated for the delivery of drugs and genes to the brain [11].

Several strategies have been explored to formulate TfR-targeted delivery systems able to transport nucleic acids to the brain following intravenous administration [11]. Numerous non-viral gene delivery systems are currently under development, due to their low immunogenicity, stability, unrestricted plasmid size and versatility in types of modifications [12,13]. Among these delivery systems, generation 3-diaminobutyric polypropylenimine dendrimer (DAB) appears to be particularly promising. We recently prepared a transferrin (Tf)-bearing generation 3-diaminobutyric polypropylenimine dendrimer (DAB-Tf), able to increase the cellular uptake and gene expression of DNA by cancer cells overexpressing transferrin receptors compared to non-targeted delivery systems, *in vitro* and *in vivo* [14]. Importantly, the treatment was well tolerated by the animals, with no apparent signs of toxicity.

* Corresponding author. Tel.: +44 141 548 3796; fax: +44 141 552 2562.
E-mail address: CDufes@strath.ac.uk (C. Dufès).

http://dx.doi.org/10.1016/j.jconrel.2014.06.006
0168-3659/

Building on this study, we now would like to investigate if this Tf-bearing gene delivery system could improve the delivery of DNA to the brain, *in vitro* and *in vivo* following intravenous administration.

2. Materials and methods

2.1. Cell lines and reagents

Human holo-transferrin, generation 3-diaminobutyric polypropylenimine dendrimer (DAB), dimethylsuberimidate and all other chemicals and reagents that are not specifically mentioned below were obtained from Sigma-Aldrich (Poole, UK). The expression plasmids encoding β-galactosidase (pCMVsport β-galactosidase) and tdTomato (pCMV-tdTomato) were respectively purchased from Invitrogen (Paisley, UK) and Clontech (Mountain View, CA). They were propagated in *Escherichia coli* and purified using an Endotoxin-free Giga Plasmid Kit (Qiagen, Hilden, Germany). Vectashield® mounting medium with 4′,6-diamidino-2-phenylindole (DAPI) came from Vector Laboratories (Peterborough, UK). Passive lysis buffer, Label IT® Cy3- and fluorescein-Nucleic Acid Labeling kits were respectively obtained from Promega (Southampton, UK) and Cambridge Biosciences (Cambridge, UK). bEnd.3 murine brain capillary endothelial cell line was purchased from LGC Standards (Teddington, UK), while cell culture media were obtained from Invitrogen (Paisley, UK).

2.2. Synthesis and characterization of transferrin- bearing DAB dendrimer

Transferrin (Tf) was conjugated to generation 3-diaminobutyric polypropylenimine dendrimer (DAB) by using dimethylsuberimidate (DMSI) as a cross-linking agent, as previously reported [14,15]. DAB (24 mg) was added to transferrin (6 mg) and dimethylsuberimidate (12 mg) in triethanolamine HCl buffer (pH 7.4, 2 mL). The reaction took place for 2 h at 25 °C while stirring. The conjugate was purified by size exclusion chromatography using a Sephadex G75 column and freeze-dried. The conjugation of Tf to DAB was assessed by ^{1}H NMR spectroscopy using an Oxford NMR AS 400 spectrometer (Jeol, Peobody, MA).

2.3. In vitro biological characterization

2.3.1. Cell culture

Immortalized bEnd.3 cells overexpressing Tf receptors were grown as monolayers in Dulbecco's Modified Eagle Medium (DMEM) supplemented with 10% (v/v) fetal bovine serum, 1% (v/v) L-glutamine and 0.5% (v/v) penicillin-streptomycin. Cells were cultured at 37 °C in a humid atmosphere of 5% carbon dioxide.

2.3.2. Cellular uptake

Imaging of the cellular uptake of the DNA carried by DAB-Tf was carried out using epifluorescence microscopy. Labeling of the β-galactosidase-encoding plasmid DNA with the fluorescent probe Cy3 was performed using a Label IT® Cy3 Nucleic Acid Labeling kit, as described by the manufacturer. bEnd.3 cells were seeded on coverslips in 6-well plates (10^4 cells/well) and grown at 37 °C for 72 h. They were then incubated for different durations (15, 30, 45, 60, 120, 240 min) with Cy3-labeled DNA (2.5 μg DNA/well) complexed to DAB-Tf at the dendrimer:DNA weight ratio of 10:1. The cells were then washed three times with PBS and fixed with methanol for 10 min. Upon staining of the nuclei with DAPI, the cells were examined using an E600FN Upright Epifluorescence microscope (Nikon, Tokyo, Japan). DAPI was excited with the 365 nm CoolLED pE excitation system (bandwidth: 435-485 nm), whereas Cy3 was excited with the 470 nm CoolLED pE excitation system (bandwidth: 515-555 nm).

Once the treatment duration allowing maximal DNA uptake was determined, a similar procedure was performed to compare the cellular uptake of Cy3-labeled DNA (2.5 μg/well) complexed to DAB-Tf and DAB (dendrimer:DNA weight ratios respectively of 10:1 and 5:1) [14,16] during the optimized treatment duration. Control samples were treated with naked DNA or remained untreated.

Quantification of cellular uptake was performed using flow cytometry. Labeling of plasmid DNA with the fluorescent probe fluorescein was performed using a Label IT® Fluorescein Nucleic Acid Labeling kit, as described by the manufacturer. bEnd3 cells were grown in 6-well plates (1.6×10^5 cells/well) at 37 °C for 72 h. The cells were then treated with fluorescein-labeled DNA (5 μg DNA/well), alone or complexed to DAB-Tf and DAB (dendrimer:DNA weight ratios respectively of 10:1 and 5:1). Untreated cells served as a negative control. After 2 h incubation with the treatments, single cell suspensions were prepared, washed (2 mL PBS pH 7.4 per well) and pelleted (378 g for 8 min) 3 times, before being analyzed using a FACSCanto® flow cytometer (BD, Franklin Lakes, NJ). Ten thousand cells (gated events) were counted for each sample. Their mean fluorescence intensity was analyzed with FACSDiva® software (BD, Franklin Lakes, NJ).

2.3.3. Mechanisms of cellular uptake of DNA complexed to DAB-Tf dendriplex

The mechanisms involved in the cellular uptake of DNA complexed to DAB-Tf dendriplex were investigated by treatment with uptake inhibitors and escalating concentrations of free Tf. Cells were seeded and grown as described above. After removal of the medium, they were then pre-treated with phenylarsine oxide (10 μmol/L), filipin (5 μg/mL), colchicine (10 μmol/L), poly-L-lysine (400 μg/mL) and various concentrations of free Tf ranging from 2.5 to 20 μmol/L for 10 min at 37 °C. The cells were then treated with Cy3- or fluorescein-labeled DNA (respectively 2.5 and 5 μg/well for qualitative and quantitative analysis) complexed to DAB-Tf for 2 h, before being washed and processed for fluorescence microscopy and flow cytometer analysis as described above.

2.3.4. In vitro transfection

Transfection efficacy of the DNA carried by DAB-Tf dendrimer was assessed with a plasmid DNA encoding β-galactosidase (pCMV βgal), using a β-galactosidase transfection assay. bEnd.3 cells were seeded at a density of 2000 cells/well in 96-well plates (n = 15). After 72 h incubation, the cells were treated with the DAB-Tf dendriplex at the dendrimer:DNA weight ratio of 10:1, which has previously been shown to give the highest transfection on other cancer cell lines [14,15]. DNA concentration (10 μg/mL) was kept constant for all the formulations tested. Naked DNA served as a negative control, DAB-DNA (dendrimer:DNA weight ratio 5:1) served as a positive control. After 72 h incubation, cells were lysed with 1× passive lysis buffer (PLB) (50 μL/well) for 20 min. The cell lysates were subsequently analyzed for β-galactosidase expression. Briefly, 50 μL of the assay buffer (2 mM magnesium chloride, 100 mM mercaptoethanol, 1.33 mg/mL o-nitrophenol-β-galactopyranoside, 200 mM sodium phosphate buffer, pH 7.3) was added to each well containing the lysates. After 2 h incubation at 37 °C, the absorbance of the samples was read at 405 nm with a Multiscan Ascent® plate reader (Thermo Scientific, Waltham, MA).

2.4. In vivo study

2.4.1. Animals

Female BALB/c mice were housed in groups of five at 19 °C to 23 °C with a 12-h light-dark cycle. They were fed a conventional diet (Rat and Mouse Standard Expanded, B&K Universal, Grimston, UK) with mains water ad libitum. The *in vivo* experiments described below were approved by the local ethics committee and performed in accordance with the UK Home Office regulations.

2.4.2. Biodistribution of gene expression

The biodistribution of gene expression was visualized by bioluminescence imaging, using an IVIS Spectrum® (PerkinElmer, Waltham, MA).

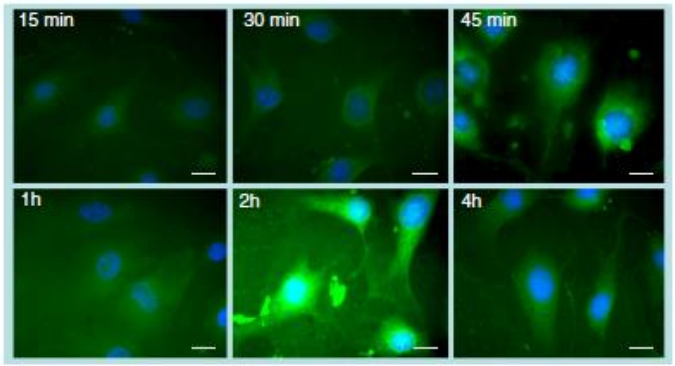

Fig. 1. Epifluorescence microscopy imaging of the cellular uptake of Cy3-labeled DNA (2.5 μg/well) complexed with DAB-Tf, after incubation for 15 min, 30 min, 45 min, 1 h, 2 h or 4 h with bEnd.3 cells. Blue: nuclei stained with DAPI (excitation: 365 nm, bandwidth: 435–485 nm), green: Cy3-labeled DNA (excitation: 470 nm, bandwidth: 515-555 nm) (Bar: 10 μm). (For interpretation of the references to color in this figure legend, the reader is referred to the web version of this article.)

To determinate the treatment duration leading to the highest gene expression, female BALB/c mice (n = 3, initial mean weight: 20 g) were injected intravenously with a single dose of DAB-Tf carrying luciferase expression plasmid (50 μg of DNA). They were then intraperitoneally injected with the luciferase substrate D-luciferin (150 mg/kg body weight) after various treatment durations and anesthetized by isoflurane inhalation. Light emission was measured 10 min after injection of the D-luciferin solution, for 2 min, using Living Image® software (PerkinElmer, Waltham, MA). The resulting pseudo-color images represent the spatial distribution of photon counts within the animal. Identical illumination settings were used for acquiring all images [17].

A similar procedure was then performed at the optimum treatment duration to compare the distribution of gene expression resulting from the single intravenous injection of DAB-Tf and DAB dendriplexes encoding luciferase (50 μg of DNA).

Biodistribution of gene expression was also quantified using a β-galactosidase reporter gene expression assay. Groups of mice (n = 5) were injected intravenously with a single dose of DAB-Tf and DAB dendriplexes encoding luciferase (50 μg of DNA). They were sacrificed 24 h after injection and their organs were removed, frozen in liquid nitrogen, before being analyzed for their β-galactosidase levels as previously described [18].

2.4.3. Distribution of gene expression within the brain

Distribution of gene expression within the brain was qualitatively assessed by fluorescence microscopy imaging of the brain sections of mice treated with DAB-Tf dendriplex encoding tdTomato. Mice were intravenously injected with a single dose of DNA encoding tdTomato, naked or complexed to DAB-Tf and DAB dendrimers (50 μg of DNA). They were sacrificed 24 h after injection and their brains were removed, fixed in a solution of 10% formalin for 48 h. Following fixation, the brains were dehydrated through an ethanol gradient for 8.5 h, cleared in xylene for 2.5 h, before being embedded in paraffin wax. Coronal sections were cut at a thickness of 4 μm in different brain areas (anterior, median and posterior) and left in a 37 °C oven overnight before being stained with hematoxylin and eosin (H&E) according to standard procedures. The brain sections were then examined using an E600FN Upright Epifluorescence microscope. Positivity for tdTomato expression in the brain was assessed at excitation wavelengths of 530-635 nm and emission wavelengths of 605-655 nm.

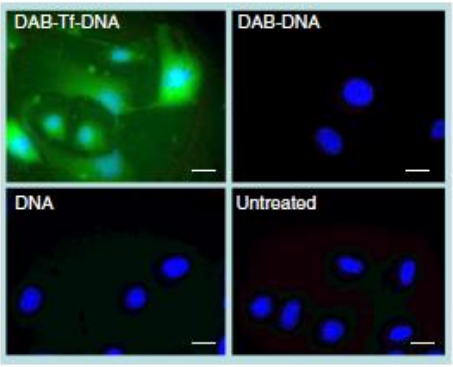

Fig. 2. Epifluorescence microscopy imaging of the cellular uptake of Cy3- labeled DNA (2.5 μg/well) either complexed with DAB-Tf, DAB or in solution, after incubation for 2 h with bEnd.3 cells. Blue: nuclei stained with DAPI (excitation: 365 nm, bandwidth: 435-485 nm), green: Cy3-labeled DNA (excitation: 470 nm, bandwidth: 515-555 nm) (Bar: 10 μm). (For interpretation of the references to color in this figure legend, the reader is referred to the web version of this article.)

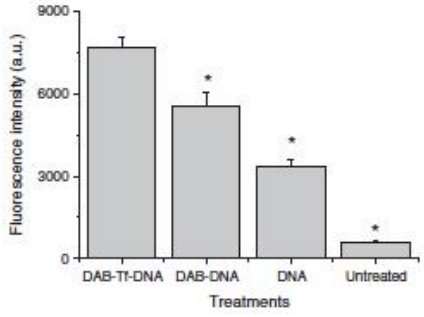

Fig. 3. Flow cytometry quantification of the cellular uptake of fluorescein-labeled DNA (2.5 μg/well) either complexed with DAB-Tf, DAB or in solution, after incubation for 2 h with bEnd.3 cells (n = 15). *: P < 0.05 compared with DAB-Tf-DNA.

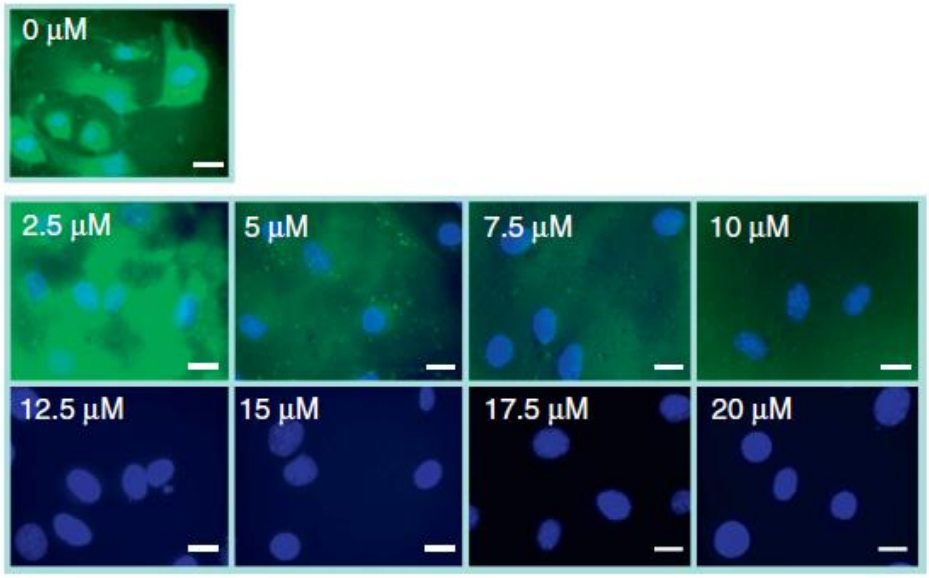

Fig. 4. Epifluorescence microscopy imaging of the bEnd.3 cellular uptake of Cy3-labeled DNA (2.5 µg/well) complexed with DAB-Tf, following pre-treatment with various concentrations of free Tf (ranging from 2.5 µM to 20 µM). Blue: nuclei stained with DAPI (excitation: 365 nm, bandwidth: 435–485 nm), green: Cy3-labeled DNA (excitation: 470 nm, bandwidth: 515–555 nm) (Bar: 10 µm). (For interpretation of the references to color in this figure legend, the reader is referred to the web version of this article.)

2.5. Statistical analysis

Results were expressed as means ± standard error of the mean (S.E.M.). Statistical significance was assessed by one-way analysis of variance (ANOVA) and Tukey multiple comparison post-test (Minitab® software, State College, PE). Differences were considered statistically significant for P values lower than 0.05.

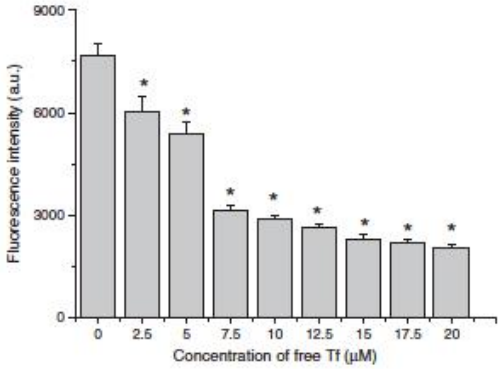

Fig. 5. Flow cytometry quantification of the bEnd.3 cellular uptake of fluorescein-labeled DNA (2.5 µg/well) complexed with DAB-Tf, following pre-treatment with various concentrations of free Tf (ranging from 2.5 µM to 20 µM) ($n = 15$). *: $P < 0.05$ compared with DAB-Tf-DNA.

3. Results and discussion

3.1. In vitro biological characterization

3.1.1. Cellular uptake

The uptake of Cy3-labeled DNA complexed to DAB-Tf by bEnd.3 cells was qualitatively confirmed by epifluorescence microscopy. Cy3-labeled DNA was disseminated in the cytoplasm from as early as 15 min after the start of the treatment. Following various treatment durations, the DNA uptake in cells appeared to be most pronounced after treatment with DAB-Tf dendriplex incubated with the cells for 2 h (Fig. 1).

We then evaluated the cellular uptake of Cy3-labeled DNA either administered as complexed to DAB-Tf and DAB, or as a solution, following 2 h incubation (Fig. 2). The treatment of the cells with DAB-Tf dendriplex resulted in a pronounced DNA uptake in the cytoplasm of the cells. By contrast, cells treated with DAB dendriplex or DNA solution did not show any Cy3-derived fluorescence, highlighting the need of a targeted delivery system to carry DNA to bEnd.3 cells. The diffuse Cy3-derived fluorescence may be due to the homogeneous distribution of the fluorescently-labeled DNA in the cytoplasm following the escape of the DAB-Tf dendriplex from the endosomes and the release of the DNA from its dendritic carrier.

These results were quantitatively confirmed by flow cytometry (Fig. 3). Cellular fluorescence was highest following treatment with DAB-Tf dendriplex (7682 ± 355 arbitrary units (a. u.)). It was respectively about 1.4-fold and 2.3-fold higher than the cellular fluorescence observed following treatment with DAB dendriplex (5531 ± 530 a. u.) and DNA solution (3370 ± 199 a. u.).

In this study, we successfully demonstrated that the conjugation of Tf on DAB improved DNA uptake by bEnd.3 murine brain capillary endothelial cells, compared to control dendriplex and naked DNA treatments. Tf receptor-mediated uptake of DNA has been widely

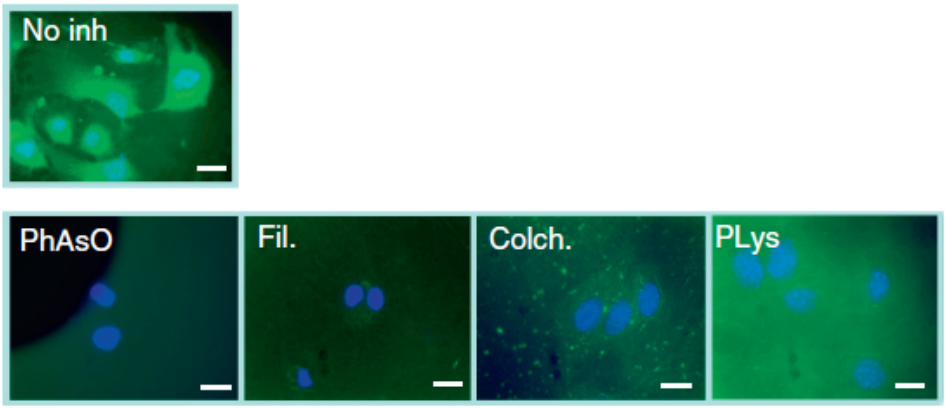

Fig. 6. Epifluorescence microscopy imaging of the bEnd.3 cellular uptake of Cy3-labeled DNA (2.5 μg/well) complexed with DAB-Tf, following pre-treatment with various cellular uptake inhibitors: phenylarsine oxide ("PhAsO"), filipin ("Fil."), colchicine ("Colch.") and poly-L-lysine ("PLys"). Blue: nuclei stained with DAPI (excitation: 365 nm, bandwidth: 435–485 nm), green: Cy3-labeled DNA (excitation: 470 nm, bandwidth: 515–555 nm) (Bar: 10 μm). (For interpretation of the references to color in this figure legend, the reader is referred to the web version of this article.)

studied on cancer cell lines and brain capillary endothelial cells [11,14,15,19–30]. Although the differences between treatments were less pronounced in our study, our results were in accordance with previous data obtained by Ko and colleagues [24], who revealed that the uptake of TfR-targeting biotinylated PEG-stabilized liposomes encapsulating PEI/oligodeoxynucleotide was about 3-fold higher compared to that of non-targeted nanoparticles, in the bEnd.5 mouse brain endothelial cell line. This outcome was also in line with our previous studies, in which we demonstrated that the conjugation of Tf to DAB increased the DNA uptake by T98G glioblastoma, PC-3M-luc-C6, DU145 and LNCaP prostate cells overexpressing Tf receptors [14,19].

3.1.2. Mechanisms of cellular uptake of DNA complexed to DAB-Tf dendriplex

Pre-treatment of the bEnd.3 cells with various concentrations of free Tf significantly decreased the cellular uptake of fluorescein-labeled DNA complexed to DAB-Tf with increasing concentrations of free Tf, to reach a plateau at Tf concentrations higher than 12.5 μM (Figs. 4 and 5). At a Tf concentration of 20 μM, the cellular uptake of fluorescently-labeled DNA was 3.8-fold lower than that observed with DAB-Tf dendriplex without pre-Tf treatment (respectively 2010 ± 122 a. u. and 7682 ± 355 a. u.).

The cellular uptake of fluorescein-labeled DNA complexed to DAB-Tf was also partially inhibited by phenylarsine oxide, filipin, colchicine and poly-L-lysine (Figs. 6 and 7). Colchicine and phenylarsine oxide caused the most significant inhibition, with a cellular uptake respectively decreased by 2.3-fold and 2.1-fold compared to that observed with DAB-Tf dendriplex without inhibitory treatment (respectively 3316 ± 251 a. u. and 3614 ± 140 a.u. following pre-treatment with colchicine and phenylarsine oxide). Filipin and poly-L-Lysine appear to be less effective inhibitors, leading to a cellular uptake decreased by respectively 1.7-fold and 1.3-fold compared to DAB-Tf dendriplex without pre-treatment (respectively 4532 ± 201 a. u. and 5974 ± 192 a.u. following pre-treatment with filipin and poly-L-Lysine).

These inhibitors act on various endocytic mechanisms on the BBB. Phenylarsine oxide is an inhibitor of clathrin-mediated endocytosis (which is a requisite for receptor-mediated endocytosis) [31]. Filipin is known to block the caveolae-mediated process in non-specific adsorptive endocytosis [32]. Colchicine inhibits macropinocytosis [33], which

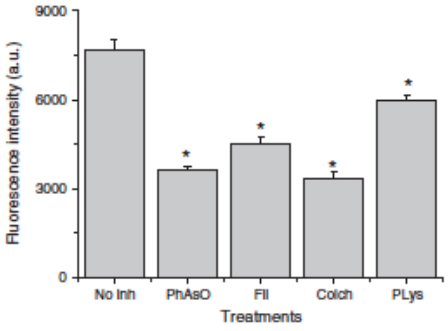

Fig. 7. Flow cytometry quantification of the bEnd.3 cellular uptake of fluorescein-labeled DNA (2.5 μg/well) complexed with DAB-Tf, following pre-treatment with various cellular uptake inhibitors: phenylarsine oxide ("PhAsO"), filipin ("Fil."), colchicine ("Colch.") and poly-L-lysine ("PLys"). (n = 15). *: P < 0.05 compared with DAB-Tf-DNA.

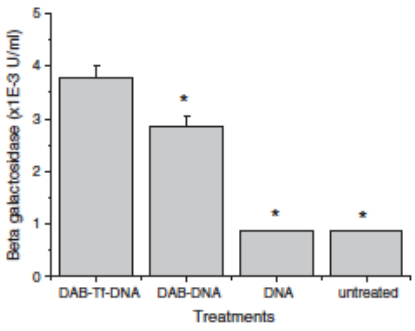

Fig. 8. Transfection efficacy of DAB-Tf and DAB dendriplexes in bEnd.3 cells. DAB-Tf and DAB dendriplexes were dosed at their optimal dendrimer:DNA ratio of 10:1 and 5:1 respectively. Results are expressed as the mean ± SEM of three replicates (n = 15). *: P < 0.05 compared with DAB-Tf-DNA.

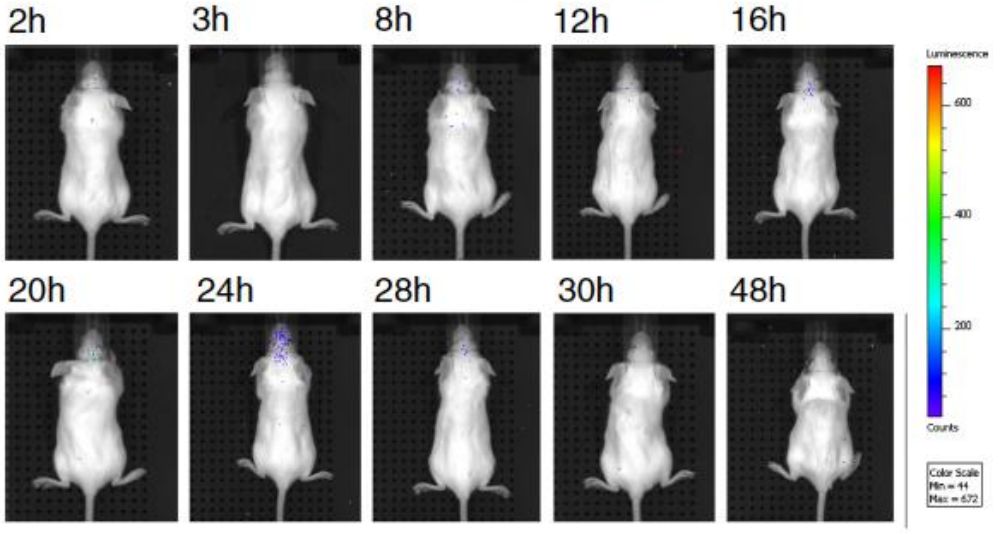

Fig. 9. Bioluminescence imaging of gene expression after intravenous administration of DAB-Tf dendriplex (50 μg DNA administered). The mice were imaged using the IVIS Spectrum at various durations after injection of the treatment. The scale indicates surface radiance (photons/s/cm^2/steradian).

provides non-specific endocytosis of macromolecules, whereas cationic poly-L-Lysine can inhibit the uptake of cationic delivery systems.

The cellular uptake of DNA complexed to DAB-Tf was therefore related to endocytosis processes, including clathrin-mediated endocytosis, macropinocytosis, and to a lesser extent caveolae-mediated endocytosis. The zeta potential of DAB-Tf dendriplex was slightly cationic (1.03 mV) [14], which limited the possible inhibitory role of poly-L-lysine. These results suggested that both receptor- and adsorptive-mediated mechanisms might contribute to the cellular uptake of DNA complexed to DAB-Tf.

Increasing amounts of Tf could significantly inhibit the cellular uptake of DNA complexed to DAB-Tf, suggesting that the Tf receptor-mediated mechanism might be the main mechanism of cellular internalization of DNA complexed to DAB-Tf.

3.1.3. *In vitro transfection*

The conjugation of Tf to DAB dendriplex led to an increased ransfection compared to unconjugated DAB dendriplex on bEnd.3 cells (Fig. 8). Gene expression following treatment with DAB-Tf dendriplex was 1.3-fold higher than following treatment with DAB dendriplex ($3.79 \times 10^{-3} \pm 0.23 \times 10^{-3}$ U/mL and $2.85 \times 10^{-3} \pm 0.21 \times 10^{-3}$ U/mL respectively for DAB-Tf and DAB dendriplexes).

The treatment of bEnd.3 cells with Tf-bearing and DAB dendriplexes resulted in an increase in gene expression by about 4.3-fold and 3.3-fold

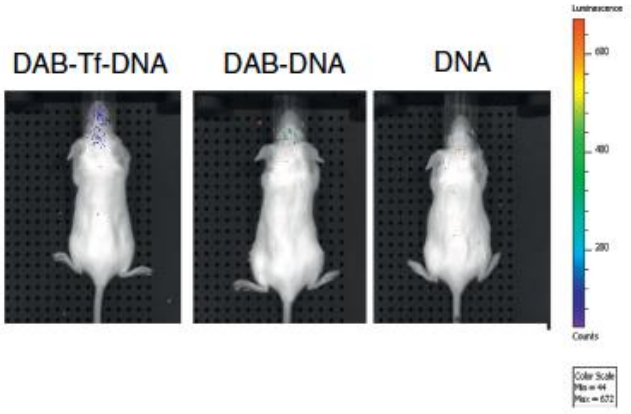

Fig. 10. Bioluminescence imaging of gene expression after intravenous administration of DAB-Tf and DAB dendriplexes (50 μg DNA administered). (Controls: DNA solution). The mice were imaged using the IVIS Spectrum 24 h after injection of the treatments. The scale indicates surface radiance (photons/s/cm^2/steradian).

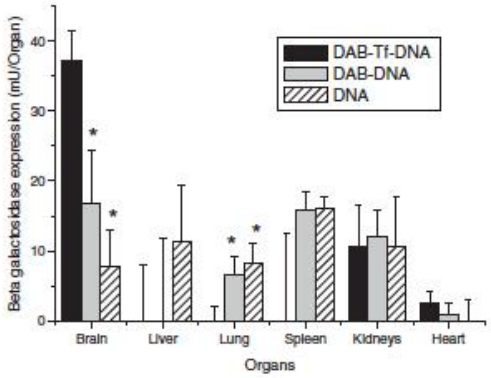

Fig. 11. Biodistribution of gene expression after a single intravenous administration of DAB-Tf and DAB dendriplexes (50 μg DNA administered). Results were expressed as milliunits β-galactosidase per organ (n = 5). *: P < 0.05 compared with DAB-Tf-DNA for each organ.

respectively, compared to that observed following treatment with naked DNA ($0.87 \times 10^{-3} \pm 0.01 \times 10^{-3}$ U/mL). The cells treated with naked DNA did not show any significant transfection increase compared to untreated cells.

The enhanced β-gal expression following DAB-Tf dendriplex treatment most likely resulted from the improved cellular uptake observed with this treatment. Both increases were of the same magnitude (1.4-fold for cellular uptake, 1.3-fold for gene expression compared to non-targeted DAB dendriplex treatment). These transfection results were in line with those described in the literature. For example, Huang and colleagues reported that the luciferase expression in brain capillary endothelial cells treated with Tf-bearing PEG-PAMAM dendriplex was 1.8-fold of that obtained with PAMAM dendriplex and PEG-PAMAM dendriplex [26]. In our previous experiments, the conjugation of Tf on DAB dendriplex already led to similar increases of gene expression, by 1.3-fold on both T98G and PC-3 cells, and by 2.2-fold on A431 cells, compared to that observed following treatment with DAB dendriplex [14, 19].

3.2. In vivo study

Distribution of gene expression following intravenous injection of DAB-Tf dendriplex encoding luciferase was first qualitatively assessed by luminescence imaging, at various treatment durations. Gene expression appeared to be mainly located in the brain of the mice. The highest gene expression level was found 24 h following injection of the treatment (Fig. 9).

Gene expression following administration of DAB-Tf dendriplex was then compared to that observed following administration of DAB dendriplex and DNA only, 24 h after administration of the treatments. The level of gene expression in the brain appeared to be highest

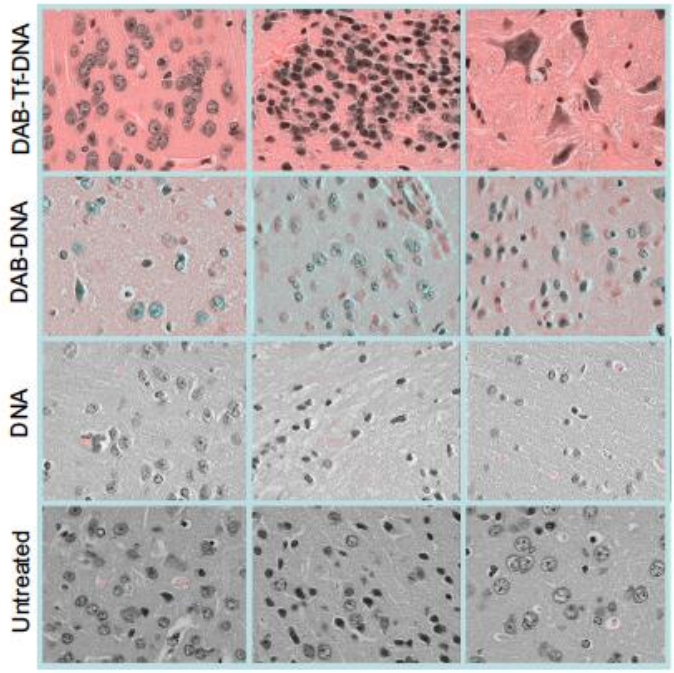

Fig. 12. Epifluorescence microscopy imaging of the distribution of gene expression within the brain after a single intravenous injection of tdTomato-encoded DNA (50 μg) either complexed with DAB-Tf, DAB or in solution (Magnification: ×60).

following treatment with DAB-Tf dendriplex (Fig. 10). In addition, luciferase expression appeared to be very limited in organs other than the brain. This might be explained by the threshold of the technique that probably allowed only the most intensely luminescent tissues to be analyzed.

These results were confirmed by quantification of gene expression in the major organs of the mice. The intravenous administration of DAB dendriplex led to gene expression mainly in the brain (16.7 ± 7.6 mU β-galactosidase per organ) and the spleen (15.8 ± 2.7 mU β-galactosidase per organ), followed by the kidneys (12.1 ± 3.6 mU β-galactosidase per organ) and then the lung (6.6 ± 2.6 mU β-galactosidase per organ) (Fig. 11).

By contrast, the conjugation of Tf to DAB significantly increased by more than 2-fold the gene expression in the brain (37.3 ± 4.2 mU β-galactosidase for DAB-Tf dendriplex), while there was very little β-galactosidase detected in the liver, the lung and the spleen. In the kidneys and the heart, gene expression reached similar levels to what was observed following treatment with DAB dendriplex (10.5 ± 6.1 mU and 12.1 ± 3.6 mU β-galactosidase per organ in the kidneys for respectively DAB-Tf dendriplex and DAB dendriplex, 2.5 ± 1.6 mU and 0.9 ± 1.6 mU β-galactosidase in the heart for respectively DAB-Tf dendriplex and DAB dendriplex). B-galactosidase gene expression in the brain was at least 3-fold higher than in any peripheral organs tested in this study.

The amount of Tf injected as DAB-Tf was much higher than the endogenous amount of Tf in the plasma (2.68 μg, corresponding to an endogenous plasma concentration of 25 μM [34], which limited the risk of competition for binding to the TfR.

We have chosen to use a β-galactosidase expression assay for quantifying gene expression in the organs, as the spectrofluorimetric quantification of the reaction product 7-hydroxy-9H-(1, 3-dichloro-9, 9-dimethyl-acridin-2-one (DDAO) in the red part of the spectrum avoided interferences from hemoglobin which hamper many *in vivo* quantification assays [18,35].

Within the brain, gene expression was the highest following administration of DAB-Tf dendriplex (Fig. 12). It was homogenously distributed in the brain parenchyma in all the sections of the brain we observed, but did not appear to have reached the neurons and glial cells. By contrast, tdTomato gene expression was very limited in the brain following administration of DAB dendriplex. Some autofluorescence artifacts were visible in the brain treated with naked DNA or left untreated.

This communication presents evidence that DAB-Tf dendriplex led to improved gene expression in the brain following intravenous administration. To our knowledge, it is the first time that the intravenous administration of a Tf-bearing non-viral delivery system resulted in such intense effects.

Other groups have already demonstrated gene transfer capabilities of Tf-bearing and TfR-targeting gene delivery systems following intravenous administration, but with much smaller gene expression in the brain and much larger non-specific expression in other organs. For example, the intravenous administration of liposomes encapsulating polyethylenimine/^{32}P-oligodeoxynucleotide polyplexes and conjugated to 8D3 anti-mouse Tf receptor monoclonal antibody, resulted in an increased brain uptake, but with the tracer activity being found mainly in liver, spleen and kidneys [24].

Similar gene expression levels and tissue expression patterns were seen when lipoplexes encoding luciferase were conjugated with the OX26 anti-rat Tf receptor monoclonal antibody. Following 48 h after intravenous administration of this lipoplex, the exogenous gene was expressed in the brain with levels as high as 0.2 pg/mg protein, but was also mainly found in peripheral tissues such as the liver, spleen and lung [36]. Another study using a similar lipoplex reported that the luciferase gene expression in brain was comparable to that of lung or spleen [22]. Similarly, the injection of 8D3-bearing PEGylated immunolipoplexes encoding β-galactosidase also led to a similar pattern of distribution, with gene expression being found in the brain, but mostly in the liver and spleen [20,22].

The differences in the biodistribution of gene expression may be explained by the targeting of different TfR and the use of Tf instead of anti-TfR antibodies as a targeting moiety. Both TfR1 and TfR2 are members of the Tf receptor family. TfR1 is expressed at low levels in most human tissues, but is highly expressed on the vascular endothelium of brain capillaries [7]. It is also expressed at levels up to 100-fold higher than those on normal cells on highly proliferative cells such as cancer cells [37], making this receptor a promising target for the delivery of therapeutics to the brain and cancer cells. By contrast, the α-transcript product of TfR2 is mostly expressed on hepatocytes, while its β-transcript is present on a wide range of tissues but at very low levels [38]. In addition, TfR1 has a much higher affinity for Tf than TfR2 (25-fold higher) [38], which is not the case for anti-TfR monoclonal antibodies. TfR1 would therefore be a more efficient target for transferrin-mediated gene delivery to the brain or cancer cells.

Previous studies using the dendrimer polyamidoamine (PAMAM) instead of DAB have shown that the gene expression of intravenously administered Tf-bearing PAMAM dendriplex was about 2-fold higher in the brain than that of non-targeted dendriplex. Gene expression of luciferase, however, was mainly found in the heart and lung [26].

In a previous study done on tumor-bearing mice, we demonstrated that the intravenous administration of DAB dendrimer conjugated to transferrin (Tf), whose receptors are also overexpressed on cancer cells, resulted in gene expression mainly in the tumors after intravenous administration [14]. Thus, DAB-Tf dendrimer complexed to a TNFα-encoding DNA led to a rapid and sustained tumor regression over one month, resulting in complete suppression of 90% of the tested A431 tumors and regression of the remaining 10% [14]. In this study, we wanted to investigate if the targeting properties of this dendrimer could lead to an enhanced delivery of DNA to the brain after intravenous administration, on mice without tumors. We demonstrated that this is indeed the case.

In conclusion, we have demonstrated that transferrin-bearing DAB polypropylenimine dendrimer led to an increased gene expression in the brain, which was at least 3-fold higher than in any tested peripheral organs. Transferrin-bearing DAB dendrimer is therefore a highly promising delivery system for gene delivery to the brain and will be further investigated to optimize its therapeutic potential.

Acknowledgments

This work was financially supported by a research grant from The Cunningham Trust (No. ACC/KWF/CT04).The IVIS was funded with an equipment grant (No. ME0442) from the Wellcome Trust.

References

[1] F. Schlachetzki, Y. Zhang, R.J. Boado, W.M. Pardridge, Gene therapy to the brain: the trans-vascular approach, Neurology 62 (8) (2004) 1285–1281.
[2] W.M. Pardridge, Brain drug targeting and gene technologies, Jpn. J. Pharmacol. 87 (2) (2001) 97–103.
[3] W.M. Pardridge, Drug targeting to the brain, Pharm. Res. 24 (9) (2007) 1733–1744.
[4] R. Gabathuler, Approaches to transport therapeutic drugs across the blood–brain barrier to treat brain diseases, Neurobiol. Dis. 37 (2010) 48–57.
[5] A.R. Jones, E.V. Shusta, Blood–brain barrier transport of therapeutics via receptor-mediation, Pharm. Res. 24 (9) (2007) 1759–1771.
[6] D.J. Begley, Delivery of therapeutic agents to the central nervous system: the problems and the possibilities, Pharmacol. Ther. 104 (1) (2004) 29–45.
[7] W.A. Jefferies, M.R. Brandon, S.V. Hunt, A.F. Williams, K.C. Gatter, D.Y. Mason, Transferrin receptor on endothelium of brain capillaries, Nature 312 (1984) 162–163.
[8] P.M. Friden, Receptor-mediated transport of therapeutics across the blood–brain barrier, Neurosurgery 35 (1994) 294–298.
[9] U. Bickel, T. Yoshikawa, E.M. Landaw, K.F. Faull, Pharmacological effects *in vivo* in brain by vector-mediated peptide drug delivery, Proc. Natl. Acad. Sci. U. S. A. 90 (1993) 2618–2622.
[10] T. Moos, E.H. Morgan, Restricted transport of anti-transferrin receptor antibody (OX26) through the blood–brain barrier in the rat, J. Neurochem. 79 (2001) 119–129.

[11] C. Dufès, M. Al Robaian, S. Somani, Transferrin and the transferrin receptor for the targeted delivery of therapeutic agents to the brain and cancer cells, Ther. Deliv. 4 (5) (2013) 629–640.
[12] S.D. Li, L. Huang, Non-viral is superior to viral gene delivery, J. Control. Release 123 (2007) 181–183.
[13] C. Dufès, I.F. Uchegbu, A.G. Schätzlein, Dendrimers in gene delivery, Adv. Drug Deliv. Rev. 57 (2005) 2177–2202.
[14] S. Koppu, Y.J. Oh, R. Edrada-Ebel, D.R. Blatchford, L. Tetley, R.J. Tate, C. Dufès, Tumor regression after systemic administration of a novel tumor-targeted gene delivery system carrying a therapeutic plasmid DNA, J. Control. Release 143 (2010) 215–221.
[15] F. Lemarié, D.R. Croft, R.J. Tate, K.M. Ryan, C. Dufès, Tumor regression following intravenous administration of a tumor-targeted p73 gene delivery system, Biomaterials 33 (2012) 2701–2709.
[16] C. Dufès, W.N. Keith, A. Bisland, I. Proutski, I.F. Uchegbu, A.G. Schätzlein, Synthetic anticancer gene medicine exploits intrinsic antitumor activity of cationic vector to cure established tumours, Cancer Res. 65 (2005) 8079–8084.
[17] H. Aldawsari, R. Edrada-Ebel, D.R. Blatchford, R.J. Tate, L. Tetley, C. Dufès, Enhanced gene expression in tumors after intravenous administration of arginine-, lysine- and leucine-bearing polypropylenimine polyplex, Biomaterials 32 (2011) 5889–5899.
[18] B.H. Zinselmeyer, N. Beggbie, I.F. Uchegbu, A.G. Schätzlein, Quantification of beta-galactosidase activity after non-viral transfection in vivo, J. Control. Release 91 (2003) 201–208.
[19] M. Al Robaian, K.Y. Chiam, D.R. Blatchford, C. Dufès, Therapeutic efficacy of intravenously administered transferrin-conjugated dendriplexes encoding TNF-α, TRAIL and interleukin-12 on prostate carcinomas, Nanomedicine 9 (4) (2014) 421–434.
[20] Y. Zhang, Y. Wang, R.J. Boado, W.M. Pardridge, Lysosomal enzyme replacement of the brain with intravenous non-viral gene transfer, Pharm. Res. 25 (2) (2008) 400–406.
[21] S. Liu, Y. Guo, R. Huang, J. Li, S. Huang, Y. Kuang, L. Han, C. Jiang, Gene and doxorubicin co-delivery system for targeting therapy of glioma, Biomaterials 33 (2012) 4907–4916.
[22] N. Shi, W.M. Pardridge, Noninvasive gene targeting to the brain, Proc. Natl. Acad. Sci. U. S. A. 97 (13) (2000) 7567–7572.
[23] N. Shi, Y. Zhang, C. Zhu, R.J. Boado, W.M. Pardridge, Brain-specific expression of an exogenous gene after i.v. administration, Proc. Natl. Acad. Sci. U. S. A. 98 (22) (2001) 12754–12759.
[24] Y.T. Ko, R. Bhattacharya, U. Bickel, Liposome encapsulated polyethylenimine/ODN polyplexes for brain targeting, J. Control. Release 133 (2009) 230–237.
[25] T. Suzuki, D. Wu, F. Schlachetzki, J.Y. Li, R.J. Boado, W.M. Pardridge, Imaging endogenous gene expression in brain cancer *in vivo* with ^{111}In-peptide nucleic acid antisense radiopharmaceuticals and brain drug-targeting technology, J. Nucl. Med. 45 (10) (2004) 1766–1775.
[26] R.Q. Huang, Y.H. Qu, W.L. Ke, J.H. Zhu, Y.Y. Pei, C. Jiang, Efficient gene delivery targeted to the brain using a transferrin-conjugated polyethyleneglycol-modified polyamidoamine dendrimer, FASEB J. 21 (4) (2007) 1117–1125.
[27] Y. Zhang, F. Schlachetzki, Y.F. Zhang, R.J. Boado, W.M. Pardridge, Normalization of striatal tyrosine hydroxylase and reversal of motor impairment in experimental parkinsonism with intravenous nonviral gene therapy and a brain-specific promoter, Hum. Gene Ther. 15 (4) (2004) 339–350.
[28] N. Shi, R.J. Boado, W.M. Pardridge, Receptor-mediated gene targeting to tissues *in vivo* following intravenous administration of pegylated immunoliposomes, Pharm. Res. 18 (8) (2001) 1091–1095.
[29] M.T. Girão da Cruz, S. Simões, M.C. Pedroso de Lima, Improving lipoplex-mediated gene transfer into C6 glioma cells and primary neurons, Exp. Neurol. 187 (2004) 65–75.
[30] C. Zhu, Y. Zhang, Y.F. Zhang, J.Y. Li, R.J. Boado, W.M. Pardridge, Organ-specific expression of the lacZ gene controlled by the opsin promoter after intravenous gene administration in adult mice, J. Gene Med. 6 (2004) 906–912.
[31] C.C. Visser, S. Stevanović, H. Voorwinden, P.J. Gaillard, D.J. Crommelin, M. Danhof, A. G. De Boer, Validation of the transferrin receptor for drug targeting to brain capillary endothelial cells *in vitro*, J. Drug Target. 12 (2004) 145–150.
[32] H.R. Kim, S. Gil, K. Andrieux, V. Nicolas, M. Appel, H. Chacun, D. Desmaële, F. Taran, D. Georgin, P. Couvreur, Low-density lipoprotein receptor-mediated endocytosis of PEGylated nanoparticles in rat brain endothelial cells, Cell. Mol. Life Sci. 64 (2007) 356–364.
[33] J. Liu, J.J. Shapiro, Endocytosis and signal transduction: basic science update, Biol. Res. Nurs. 5 (2003) 117–128.
[34] P. Seligman, Structure and function of the transferrin receptor, Prog. Hematol. 13 (1983) 131–147.
[35] M. Colin, S. Moritz, H. Schneider, J. Capeau, C. Coutelle, M.C. Brahimi-Horn, Haemoglobin interferes with the *ex vivo* luciferase luminescence assay: consequence for detection of luciferase reporter gene expression *in vivo*, Gene Ther. 7 (2000) 1333–1336.
[36] Y. Zhang, F. Schlachetzki, W.M. Pardridge, Global non-viral gene transfer to the primate brain following intravenous administration, Mol. Ther. 7 (2003) 11–17.
[37] R. Prior, G. Reifenberger, W. Wechsler, Transferrin receptor expression in tumours of the human nervous system: relation to tumour type, grading and tumour growth fraction, Virchows Arch. A Pathol. Anat. Histopathol. 416 (1990) 491–496.
[38] H. Kawabata, R.S. Germain, P.T. Vuong, T. Nakamaki, J.W. Said, H.P. Koeffler, Transferrin receptor 2-alpha supports cell growth in iron-chelated cultured cells and *in vivo*, J. Biol. Chem. 275 (2000) 16618–16625.

Review

Nanomedicine

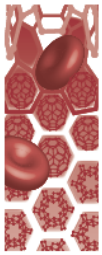

Applications of dendrimers for brain delivery and cancer therapy

Dendrimers are emerging as potential nonviral vectors for the efficient delivery of drugs and nucleic acids to the brain and cancer cells. These polymers are highly branched, 3D macromolecules with modifiable surface functionalities and available internal cavities that make them attractive as delivery systems for drug and gene delivery applications. This article highlights the recent therapeutic advances resulting from the use of dendrimers for brain targeting and cancer treatment.

Keywords: brain delivery • cancer therapy • dendrimer • gene therapy • tumor targeting

Sukrut Somani[1]
& Christine Dufès*,[1]
[1]Strathclyde Institute of Pharmacy & Biomedical Sciences, University of Strathclyde, 161 Cathedral Street, Glasgow, G4 0RE, UK
*Author for correspondence:
Tel.: +44 141 548 3796
Fax: +44 141 552 2562
c.dufes@strath.ac.uk

The treatment of brain diseases and cancer represent major therapeutic challenges in modern medicine. Cerebral diseases, such as Alzheimer's and Parkinson's diseases, affect a large percentage of the world's population and barely respond to intravenously administered, small-molecule treatments [1,2]. In addition, cancer remains one of the leading causes of mortality, accounting for 8.2 million deaths in 2012 [3].

Recent advances in multidisciplinary research have led to the discovery of numerous promising drugs against cerebral diseases and cancer. However, most of these drugs fail to specifically reach the pathological site, resulting in secondary effects on healthy tissues. In order to remedy this problem, it is therefore crucial to be able to deliver these drug candidates specifically to their site of action.

In this context, dendrimers are emerging as potential nonviral vectors for efficiently delivering drugs and nucleic acids to the brain and cancer cells. They are polymeric molecules with perfectly branched multiple monomers that emerge radially from a central core, similar to a tree (*dendron* in Greek) [4]. Their modifiable surface functionalities and available internal cavities make them attractive as delivery systems for drug and gene delivery applications (for comparison of the advantages and disadvantages of dendrimers with other delivery systems, please see [5]). These symmetrical molecules can be synthesized to a definite size in a reproducible manner in order to form spherical macromolecules, as initially described by the Vögtle group in the late 1970s [6], as well as the Tomalia group and the Newkome group in the 1980s [4,7–9]. The dendrimers can be synthesized mainly by two methods: Tomalia-type divergent synthesis, in which the dendrimer is formed in a stepwise manner from the core to the periphery [10]; and Fréchet-type convergent synthesis, in which the dendrons are synthesized first and then anchored to a multifunctional core [11].

Dendrimer can be divided into three structural domains:

- A multivalent surface, which has been largely exploited by many investigators as a means of achieving the conjugation of targeting moieties and the binding of drugs or nucleic acids for therapeutic applications;
- Dendrons delimiting the void spaces shielded by the surface – this domain has been used for the encapsulation of various chemically sensitive drugs;
- The core, which allows the attachment of the dendrons (Figure 1) [12].

Future Medicine part of fsg

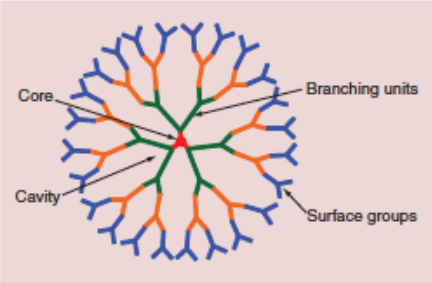

Figure 1. 2D representation of a dendrimer.

Each of these three parts can be tailored for a desired function of the dendrimers, such as drug delivery, molecular sensors, enzyme mimics and bioimaging (Figure 2). This article will mainly focus on the recent therapeutic advances that have been made using dendrimers for brain targeting and cancer therapy (for further reading regarding the therapeutic, imaging and diagnostic applications of dendrimers, please see [13–15]).

Dendrimers for brain delivery

Diseases of the CNS, such as Alzheimer's disease, Huntington's disease, Parkinson's disease and brain cancer, currently represent 11% of the global burden of disease. The number of new drugs that have been approved for the treatment of CNS disorders remains very low due to their inability to cross the blood–brain barrier (BBB), a key regulating site for drug access to the brain that acts as an entrance gateway for various nutrients to the brain while protecting it from potentially toxic compounds [1,2]. The barrier function of the BBB is a combination of a physical barrier, a transport barrier and a metabolic barrier [16]. The low and selective permeability of BBB can be credited to its unique biological properties:

- The lack of fenestrations, vesicular transport and pinocytosis in the endothelial cells [17,18];
- The physical barrier due to the presence of tight junctions between adjacent endothelial cells [19];
- The transport barriers resulting from the expression of various transporters, including GLUT-1, LAT1, transferrin receptors (TfRs), insulin receptors, LRP1, LRP2 and the ATP family of efflux transporters, such as P-glycoprotein and the multidrug resistance-related proteins. These transporters and receptors are expressed on the capillary endothelial cells of the BBB and only carry specific molecules to or from the brain [20];
- Although the multitasking BBB plays an essential role in the development of the CNS as a complex integrated network, it poses a major problem for treatment strategies that require the delivery of drugs and nucleic acids to the brain for the treatment of CNS disorders. However, this issue can be overcome by exploiting the specific transport systems expressed on the BBB for the transport of therapeutics to the brain. Various dendrimers based on this delivery strategy have been developed and preclinically evaluated. Among other nanomaterials, they appear to be particularly promising in this application due to the various advantages they offer, such as monodispersity, lack of immunogenicity, permeation through biological barriers, improved drug stability and maintenance of drug levels in the therapeutically desirable range [12].

Dendrimers for TfR targeting

Out of all of the tissues in the body, the expression of the TfRs is mainly found in the brain capillary endothelium that forms the BBB [21]. TfRs are responsible for the transport and distribution of iron in the body through an iron-binding glycoprotein, transferrin (Tf). Over the last two decades, Tf has been extensively investigated as a targeting ligand for drug and gene delivery systems in order to transport therapeutics to the brain [22].

Due to their unique physicochemical properties, dendrimers have been shown to be promising candidates for brain delivery. The polyamidoamide (PAMAM) dendrimer (Figure 3) is the most researched candidate for the delivery of therapeutics to the brain via TfR targeting. In a study by Huang and colleagues, PAMAM (G5) was conjugated to Tf through a bifunctional PEG spacer and complexed to a plasmid DNA encoding GFP [23]. After intravenous administration to mice, PAMAM–PEG–Tf/DNA was found to be able to cross the BBB, as demonstrated by a body distribution study of ^{125}I-labeled dendrimers. Qualitative analysis demonstrated GFP expression in several brain areas, such as the cortical layer, hippocampus, caudate putamen, substantia nigra and the fourth ventricle. This gene expression was approximately two-fold higher compared with the PAMAM/DNA and PAMAM–PEG/DNA complexes.

Following the discovery that WGA was a promising ligand for increasing drug uptake to the brain [24] and binding to cancer cells [25], a dual-targeting nanocarrier, PEGylated PAMAM (G4) conjugated to Tf and WGA on the periphery and loaded with doxorubicin (DOX) in its interior, was synthesized. Due to its dual-targeting effect, this delivery system led to an increased transport ratio of 13.5% in an *in vitro* model of the BBB compared with 8% for PAMAM–PEG–WGA, 7% for PAMAM–PEG–Tf

and 5% for free DOX. Moreover, this dual-targeted, dendrimer-based therapeutic system decreased the viability of C6 glioma cells in a brain microvascular endothelial cell/C6 glioma coculture model. The viability of C6 glioma cells was 14.5% in comparison with 21.3% for PAMAM–PEG–Tf–DOX, 23.7% for PAMAM–PEG–WGA–DOX and 22.4% for free DOX [26].

Multidrug resistance proteins, consisting of a family of ATP-binding cassette proteins such as P-glycoprotein, are expressed not only in the endothelial cells of the BBB, but also in glioma cells. They function as efflux transporters, restricting drug transport across the BBB and prohibiting cellular uptake by glioma cells [27,28]. Tamoxifen (TAM), an estrogen receptor antagonist, has the ability to inhibit the multidrug resistance proteins and thus improve BBB transport [29,30]. Based on this, Li *et al.* synthesized a pH-sensitive nanocarrier, consisting of PAMAM (G4) conjugated to Tf on the exterior and encapsulating TAM with a loading efficacy of 27 drug molecules per dendrimer molecule [31]. DOX was also peripherally linked to the peripheral amino groups of PAMAM through an acid-labile hydrazone bond, with a conjugation efficacy of seven to eight DOX molecules per dendrimer molecule. In an *in vitro* model of the BBB, PAMAM–DOX–PEG–Tf–TAM resulted in an increased DOX transport ratio of 6.1% compared with 4.9% for PAMAM–DOX–PEG–Tf and 4.6% for PAMAM–DOX–PEG. This targeted dendrimer-based therapeutic system also decreased the viability of C6 cells in a brain microvascular endothelial cell/C6 glioma coculture model. The viability of C6 glioma cells was 68.8% for PAMAM–DOX–PEG–Tf–TAM, which was reduced compared with that observed with other treatments (76.1% for PAMAM–DOX–PEG–Tf and 83.9% for PAMAM–DOX–PEG) [31].

Another dendrimer, polypropylenimine (PPI; Figure 3), is a promising alternative to PAMAM for gene delivery to the brain and cancer cells. Initial studies by Kabanov and colleagues demonstrated that this dendrimer binds to DNA via electrostatic interactions involving only the peripheral amine groups, allowing the tertiary amine

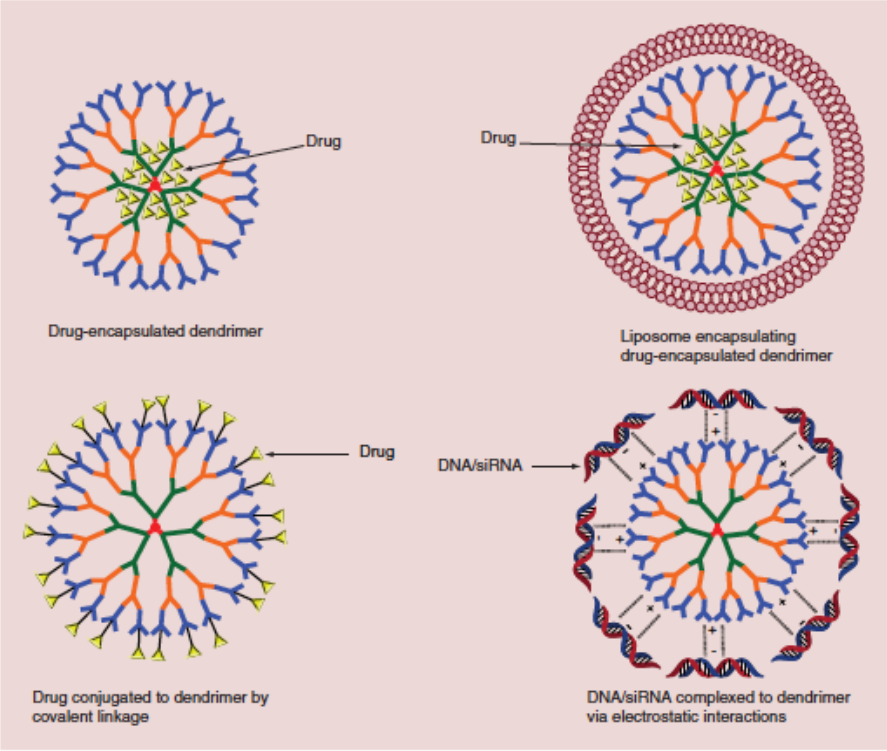

Figure 2. Dendrimer–drug/nucleic acid delivery systems.

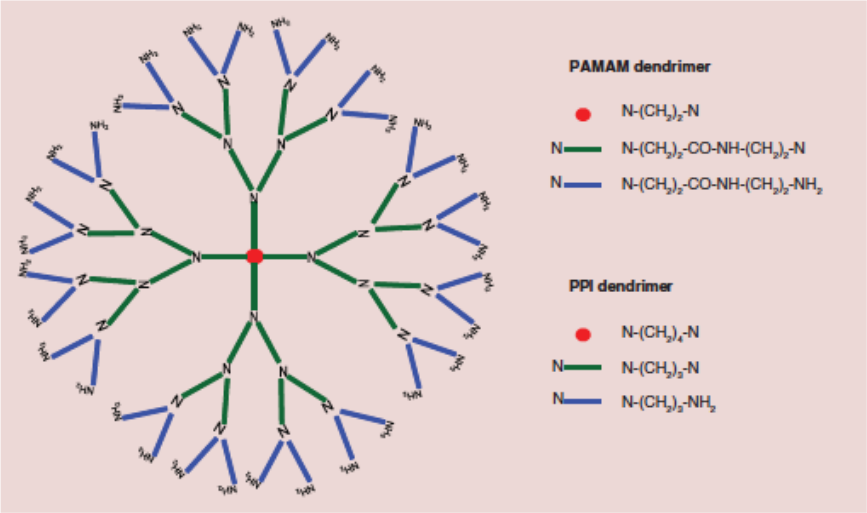

Figure 3. Chemical structure of polyamidoamine (G3) and polypropylenimine (G3) dendrimers.
PAMAM: Polyamidoamide; PPI: Polypropylenimine.

groups that are present inside the dendrimer to act as a 'proton sponge' in the endosome [32]. In a recent study, we demonstrated that the intravenous injection of the transferrin-bearing PPI dendriplex more than doubled the gene expression in the brain compared with the unmodified dendriplex while decreasing nonspecific gene expression in the lung. Gene expression was at least threefold higher in the brain than in any tested peripheral organs and was at its highest at 24 h following the injection of the treatments. These results suggest that the transferrin-bearing PPI dendrimer is a highly promising gene delivery system to the brain [33].

Dendrimer-based LRP1 & LRP2 targeting

LRP1 and LRP2 are multifunctional scavenger receptors expressed in the BBB. They have the ability to bind to a range of molecules, including proteinases, proteinase inhibitor complexes and lipoprotein lipase-enriched lipoproteins and make them cross the BBB [34].

Lactoferrin (Lf) is a single-chain, cationic, iron-binding protein belonging to the Tf family. Lf is capable of crossing the BBB through binding to low-density lipoprotein receptor-related protein (LRP) receptors [35]. Taking advantage of this ability, Huang and colleagues synthesized a nonviral brain-targeted gene delivery system consisting of PAMAM (G5) conjugated to Lf via a PEG spacer and complexed to a plasmid DNA encoding GFP [36]. Following intravenous administration of PAMAM–PEG–Lf/DNA in mice, GFP expression was observed in the cortical layer, hippocampus, caudate putamen, substantia nigra and fourth ventricle of the animals. This gene expression was 5.2-fold higher compared with that of PAMAM–PEG/DNA and PAMAM/DNA. In addition, the authors demonstrated that both LRP receptor and adsorptive-mediated mechanisms contributed to the higher uptake of the PAMAM–PEG–Lf/DNA in the brain capillary endothelial cells [37].

Angiopeps, a family of peptides derived from Kunitz domains of the drug aprotinin and other proteins, are highly effective brain-targeting ligands. They are transported across the BBB through LRP1-mediated transcytosis [38]. Angiopep-2 was conjugated to PAMAM through a specific reaction with the terminal N-hydroxysuccinimidyl of the bifunctional PEG derivative. After intravenous administration of PAMAM–PEG–angiopep complexed with a plasmid DNA encoding GFP, the brain uptake of DNA was up to 8.4-fold higher than with PAMAM/DNA in mice. Gene expression in the brain was observed in the cortical layer, caudate putamen, hippocampus and substantia nigra. Both LRP-mediated endocytosis and adsorptive endocytosis contributed to the mechanism of cellular uptake of PAMAM–PEG–angiopep [39]. In another study, angiopep was conjugated to the dendrigraft poly-L-lysine (DGL; G3) via a PEG linkage and complexed to a plasmid DNA encoding hGDNF in order to evaluate its neuroprotective effect in a Parkinson's disease model. The DGL–PEG–angiopep/hGDNF

not only exhibited a higher cellular DNA uptake and gene expression in brain cells compared with the unmodified DGL, but also improved the locomotor activity and recovery of the dopaminergic neurons [40].

Dendrimer-based GLUT-1 targeting

The glucose transporter GLUT-1 is abundantly expressed in the BBB for transporting optimal levels of glucose to the brain for its normal functioning [41]. Based on this, Dhanikula and colleagues synthesized polyether–copolyester dendrimers (G2) conjugated to D-glucosamine via carbamate linkages and loaded with up to 20.8% w/w methotrexate (MTX) for the treatment of gliomas [42]. As GLUT-1 is also expressed in brain tumors, the glycosylation of the MTX-loaded polyether–copolyester dendrimers not only enhanced the drug transport across the BBB compared with the free MTX, but also enabled the accumulation of large amounts of MTX in the central necrotic regions of the avascular brain tumor spheroids.

Other dendrimer-based targeting strategies

Leptin, a 146-amino acid polypeptide, is secreted in the blood by the adipocytes in response to food intake and acts to regulate appetite and retard weight gain. Leptin receptors are present on the luminal side of the brain microvessels and in the choroid plexus [43]. Exogenous leptin cannot be used as a targeting ligand for brain uptake, as the leptin receptors are saturated at very low concentrations (0.15–5 ng/ml) of endogenous leptin. However, peptide fragments derived from leptin contain important sequences for leptin receptor binding on the BBB. Among them, sequence 61–90 (leptin 30) is taken up by the brain and shows equivalent brain concentrations as its parent molecule, leptin [44]. Based on this result, the dendrigraft poly-L-lysine (DGL) was conjugated to leptin 30 through a PEG spacer and evaluated for gene delivery to the brain. After intravenous administration of DGL–PEG–leptin 30 complexed to a plasmid DNA, the gene expression was higher than that of DGL–PEG/DNA and DGL/DNA. It was observed mainly in cortical layer, hippocampus, caudate putamen and substantia nigra [45].

Magnetic delivery systems have been widely investigated for the targeted delivery of therapeutics. Han and colleagues synthesized a novel brain-targeted bifunctional gene delivery system based on natural magnetic particles, called magnetosomes (MSs), and combined the brain delivery effects of an external magnetic field and a cell-penetrating peptide [46]. To this end, they conjugated MSs to PAMAM and to a cell-penetrating peptide, the Tat protein. After intravenous administration of radiolabeled Tat–MS–PAMAM and MS–PAMAM followed by the application of an external magnetic field for 25 min, Tat–MS–PAMAM exhibited a twofold brain uptake increase compared with MS–PAMAM. Without a magnetic field, this brain uptake fell by 1.88-fold. However, it was not possible to evaluate the direct role played by Tat grafting and the MSs in this brain delivery increase, due to the absence of PAMAM DNA testing in this study.

However, the use of overexpressed receptors/transporters on the BBB in order to facilitate the uptake of DNA or drugs into the brain can be limited by the nonspecific presence of receptors/transporters on other tissues. For example, Tf can recognize both TfR1 and TfR2, but has a much higher affinity for TfR1 (25-fold higher) [47]. TfR1 is expressed at low levels in most human tissues, but also at high levels on the vascular endothelium of brain capillaries [21]. In addition, its levels of expression on cancer cells are up to 100-fold higher than those on normal cells [48], making this receptor a promising target for the delivery of therapeutics to the brain and cancer cells. In comparison, TfR2 is mostly expressed on hepatocytes and on a wide range of tissues, but at very low levels [47]. Although the risk of the nonspecific delivery of therapeutics to the liver and other normal tissues exists, it is therefore very limited due to the higher affinity of Tf for TfR1.

Dendrimers for cancer therapy

Drug delivery

Dendrimer-based drug delivery systems have been developed in order to improve the biodistribution of a drug in the body and to enable the controlled release of the drug at its target site. Their high aqueous solubility, low toxicity, compact globular shape and controlled surface functionalities make them ideal carriers for anticancer drugs [12]. Dendrimers can also facilitate the passive targeting of anticancer drugs to tumor tissues. This selective accumulation of macromolecules in tumors, termed the 'enhanced permeability and retention effect', is the consequence of the combination of reduced lymphatic drainage and increased permeability of the tumor vasculature to macromolecules [49]. Dendrimers can either noncovalently encapsulate drugs in the void spaces within the dendritic structure or carry them via covalent conjugation to the surface groups.

Encapsulation of drugs within the dendrimers

The internal cavity of the dendrimers could be used for the encapsulation of anticancer drugs, offering the advantage of subsequent controlled release of the drug to the tumors. Another less frequently used encapsulation strategy is to entrap anticancer drugs

by micellar formulation of dendrimers. Small hydrophobic anticancer drugs are generally entrapped in the dendrimers. Their solubility and toxicity against cancer cells have been shown to be increased by encapsulation within dendrimers (G4 to G6) [15]. Various anticancer drugs have been studied as dendrimer cargos, as described below.

Camptothecin

Camptothecin has its anticancer efficacy limited by its low water solubility and secondary effects on normal tissues, including bladder inflammation. In order to overcome this limitation, 10-hydroxycamptothecin has been encapsulated in a poly(glycerol-succinic acid) (G4) dendrimer at a concentration of 120 µM, which corresponded to a 20-fold increase in drug solubility in water compared with that of the unencapsulated drug (6 µM) [50]. Treatment of a panel of cancer cells with the drug-loaded dendrimers resulted in a decrease in the IC_{50} compared with free drug in DMSO for all of the cell lines that were tested by up to 7.1-fold in MCF-7 breast carcinoma [51]. This improved anticancer effect resulted from the faster internalization of the drug that was encapsulated in the dendrimer, with intracellular concentrations being 16-fold higher than the free drug after 2 h of treatment incubation. The retention time of the drug carried by the dendrimers was also longer compared with the free drug in solution (50 and 35%, respectively, at 10 h after the start of the treatment) [51].

Cisplatin

Another drug, cisplatin, also has its anticancer therapeutic effect limited by its poor water solubility, as well as the development of drug resistance by some cancer cell lines. The encapsulation of cisplatin in PAMAM dendrimers (dendrimer–platinum: 20–25 wt% platinum) resulted in an increased accumulation of the drug in B16F10 melanomas as a result of the passive targeting of tumor tissues due to the enhanced permeability and retention effect and decreased the toxicity towards normal tissues by three- to 15-fold compared with the free drug in solution in a murine model [52].

Doxorubicin

In order to increase DOX's drug solubility in water and decrease its secondary effects on healthy tissues, DOX was encapsulated in PEGylated PAMAM dendrimers (G3 and G4). The authors of this study demonstrated that dendrimer size and PEG chain length have a major impact on the encapsulation efficacy of the drug, with the PAMAM dendrimer (G4) and PEG_{2000} leading to the highest drug encapsulation of 6.5 DOX molecules per dendrimer molecule [53].

In another study, a PAMAM dendrimer (G4) loaded with DOX at a DOX:PAMAM molar ratio of 3.56 ± 0.04 was then encapsulated in liposomes. This 'PAMAM–DOX in liposomes' formulation presents the advantage of modulating the release and *in vivo* stability of DOX, which would otherwise leak very rapidly out of the liposomes. It resulted in an even slower release of the drug from the delivery system, which was necessary in order to increase its therapeutic index and reduce its side effects on healthy cells. This formulation was shown to be efficacious against various cancer cell lines, including DU145 human prostate carcinomas and MCF-7 human breast carcinomas [54].

Etoposide

Etoposide, an inhibitor of the enzyme topoisomerase II, is poorly water soluble. In order to remedy this issue, this drug was loaded into micelles made of a PAMAM (G2) block copolymer containing poly(γ-caprolactone) and PEG [55]. These polymeric micelles have been developed in order to overcome the stability limitations generally encountered with the classical micelle structures that may suddenly dissociate and cause serious toxicity issues. The covalent binding of the lipophilic poly(γ-caprolactone) and the PAMAM dendrimer as the core was shown to increase the stability of the polymeric micelle.

Etoposide was loaded in dendrimer-based polymeric micelles at a loading capacity of up to 22% (w/w). *In vitro*, the treatment of porcine kidney epithelial cells (LLC-PK) with this formulation showed a comparable cytotoxicity to that of the drug solution, which demonstrated that the drug was released from the polymer micelles and was able to exert its cytotoxic effects on cells [55].

5-fluorouracil

In order to improve its water solubility, the pyrimidine analog 5-fluorouracil was encapsulated in PEGylated PAMAM (G4), improving the drug loading by 12-fold compared with that achieved with the non-PEGylated dendrimer. Non-PEGylated PAMAM dendrimers suffer from drug leakage due to the relative unshielding of the void spaces containing the drug and hemolytic toxicity due to the presence of NH_2 groups on their surface. The coating on the surface of PAMAM dendrimers with PEG can therefore increase drug loading and overcome hemolytic toxicity. As a result, 5-fluorouracil displayed a sustained release from the delivery system over 6 days [56].

Methotrexate

In order to improve its bioavailability and its poor water solubility, MTX has been encapsulated in PEGylated PAMAM (G3 and G4) dendrimers. As with DOX, the encapsulation efficiency of this drug was highest with PAMAM (G4) and PEG_{2000}, resulting in the encapsulation of 26 MTX molecules per dendrimer molecule [53].

In another study, MTX has also been encapsulated in melamine-based dendrimers. These types of dendrimers have been shown to be able to solubilize hydrophobic drugs and to reduce their organ toxicity without altering their therapeutic efficacy. The intraperitoneal injection of the known hepatotoxic drug MTX loaded in melamine-based dendrimers resulted in a decrease of hepatotoxicity in mice, with a 27% decrease of the levels of alanine transaminase compared with those obtained with the free drug [57].

Paclitaxel

Similarly to the drugs mentioned above, the therapeutic use of the mitotic inhibitor paclitaxel is limited by its poor solubility in water. This problem has been overcome by the encapsulation of the drug in polyglycerol dendrimers, which led to the encapsulated drug's water solubility being 400-fold higher than that of the free drug [58].

However, the 'encapsulation of drugs within the dendrimer' approach is limited by the very small capacity of the void spaces within the dendrimers and the difficulty of effectively controlling the release of the encapsulated drugs. An alternative delivery approach for larger molecules is therefore to conjugate them to the surface of the dendrimers.

Conjugation of drugs to the dendrimers

Anticancer drugs can be covalently conjugated to the peripheral groups of the dendrimer. Owing to the multifunctional architecture of dendrimers, many drug molecules can be attached to one dendrimer, as well as the targeting moieties for enhanced tumor-delivery specificity. The release of the drug is controlled by the degradable chemical bonds linking the drug and the dendrimer. Various anticancer drugs have been studied as dendrimer–drug conjugates, as described below. This article will focus on the *in vivo* therapeutic data obtained with these conjugates.

Cisplatin

Cisplatin was conjugated to the PAMAM dendrimer (G3.5; dendrimer–cisplatin: 20–25 wt% platinum), which resulted in increased water solubility and the slow release of the drug [52,59]. The intravenous administration of the conjugate to mice bearing subcutaneous B16F10 tumors led to selective accumulation in tumors and antitumor efficacy, unlike the free drug solution. The conjugate also showed therapeutic efficacy against all of the tumors that were tested, including a platinum-resistant tumor model.

Doxorubicin

DOX was conjugated to one side of a 2,2-bis(hydroxymethyl)propionic acid dendrimer (G3), with the other side of the dendrimer being PEGylated, in order to form an asymmetric bow-tie dendrimer containing 8–10 wt% DOX [60]. The acyl hydrazine linkage that was used to conjugate the drug to the dendrimer was pH sensitive, thus releasing the drug after it reached its target. A single intravenous administration of this DOX conjugate in mice bearing subcutaneous DOX-insensitive C-26 colon carcinoma tumors resulted in the complete tumor regression and survival of all mice over 60 days. By contrast, no complete tumor regression was observed following treatment with the drug solution.

Methotrexate

MTX has been conjugated to folic acid- and fluorescein isothiocyanate-bearing PAMAM dendrimers (G5). This conjugate provided tumor targeting and inhibited cell growth of KB cells overexpressing folic acid receptors. By contrast, the MTX–dendrimer conjugate without folic acid did not succeed in inhibiting the growth of these cancer cells [61].

In addition, MTX was covalently linked to PAMAM (G5) as well, but this dendrimer was conjugated to cetuximab instead of folic acid [62]. Cetuximab is a monoclonal antibody that exerts its therapeutic effect as an EGF inhibitor. Cetuximab-bearing conjugates containing 12.6 molecules of MTX per unit of dendrimer were tested on rats bearing brain implants of a EGFR-expressing F98 rat glioma cell line, but unfortunately did not lead to a therapeutic improvement compared with the free drug. The median survival times of the rats receiving the conjugate, the monoclonal antibody alone or the free drug were 15, 17 and 19.5 days, respectively, which were not significantly different [62]. This may be due to the fact that the conjugation of the drug to PAMAM and a monoclonal antibody may have decreased the binding affinity of the drug for the dihydrofolate reductase, resulting in a loss of the antifolate activity of the drug. Another possibility is that the drug was not released from the conjugate and could not exert its therapeutic effect [62].

Gene delivery

The use of dendrimers as delivery systems for nucleic acids has been widely investigated for the treatment

of cancers. In this article, we will focus on the dendrimers used *in vivo* following intratumoral or intravenous administration, for which therapeutic effects have been obtained.

Intratumoral administration

PAMAM dendrimers have become widely used as nonviral carriers for gene delivery. The SuperFect® (Qiagen, Hilden, Germany) PAMAM dendrimer complexed to plasmid DNA encoding herpes simplex virus thymidine kinase at a dendrimer:DNA weight ratio of 3:1 resulted in growth delay [63]. This effect was even accentuated by the fact that the plasmid contained Epstein–Barr virus sequences conferring the capability to replicate and stay in the nucleus of the transfected cells.

Another study involved the same SuperFect® PAMAM dendrimer, but this time complexed to a 36-mer oligonucleotide that itself complexed the therapeutic plasmid DNA encoding the antiangiogenic peptide angiostatin or TIMP-2 [64]. The intratumoral administration of this dendrimer–plasmid–oligonucleotide complex led to growth delay of the tumor.

In addition, Bai and colleagues developed an arginine-bearing PAMAM dendrimer for the delivery of plasmid DNA encoding human IFN-β to mice bearing U87MG brain tumors [65]. Mice treated with the intratumoral administration of the dendriplex showed a decrease in their tumors and the induction of apoptosis compared with control animals.

Intravenous administration

PAMAM dendrimers

Wu and colleagues recently developed a PAMAM dendrimer (G5) with a triethanolamine core that was able to interact with siRNA in order to protect it from degradation and facilitate gene delivery to cells [66]. This dendriplex was able to deliver siRNA to prostate tumors, thus resulting in gene silencing of Hsp27 and anticancer effects against the tumors [67].

In another study, SuperFect PAMAM (G5) was complexed to Epstein–Barr virus-based plasmid vectors carrying the herpes simplex virus-1 thymidine kinase gene for suicide gene therapy against cancer in mice [63]. The intravenous administration of this complex led to the suppression of tumor growth and prolonged survival times of the tumor-bearing mice.

The PAMAM dendrimer has been used for the coadministration of a therapeutic DNA and an anticancer drug. This was the case in a study by Han and colleagues, where a PEGylated PAMAM carrying DOX was complexed to a plasmid DNA encoding human TRAIL and conjugated to the peptide HAIYPRH (T7), a TfR-specific peptide [68]. The peptide-conjugated dendriplex led to an enhanced cellular uptake of DNA and its accumulation in tumors over the nontargeted complex in the human liver cancer Bel-7402 cells overexpressing TfRs. This synergistic treatment resulted in a tumor decrease in mice compared with the nonmodified dendrimer [68].

The PAMAM dendrimer was also chosen as a delivery system for the treatment of glioma following intravenous injection. To this end, the PEGylated dendrimer was conjugated to angiopep-2, which can target the LRP-1 that is overexpressed on brain capillary endothelial cells and on glioma cells. Angiopep-2-bearing dendrimers were then complexed to a plasmid DNA encoding TRAIL and were able to specifically induce the cell apoptosis of brain tumors without secondary effects on normal cells [69]. The median survival time of the mice following intravenous administration of the angiopep-2-bearing dendriplex and temozolomide was 61 and 49 days, respectively, which demonstrated the ability of the dendriplex to target the glioma after intravenous administration [69].

The PAMAM dendrimer can also be used in conjunction with magnetic nanoparticles for gene therapy to brain tumors. Han and colleagues conjugated the PAMAM dendrimer to magnetic nanoparticles and Tat peptides [70]. This conjugate was then complexed to an siRNA-expressing plasmid that was able to downregulate the *EGFR* gene. The intravenous administration of this conjugate to mice bearing subcutaneous U251 tumors downregulated the expression of oncoproteins and slowed the growth rate of the tumors compared with controls [70].

PPI dendrimers

siRNA–PPI complexes were successively caged with a dithiol-containing cross-linker, PEG, and then conjugated with a synthetic analog of the LHRH peptide in order to deliver the siRNA specifically to LHRH receptor-positive cancer cells [71]. The administration of the LHRH-bearing PPI complex resulted in an increased siRNA accumulation in tumors, internalization by cancer cells and gene silencing.

The LHRH peptide was also used for the cancer-specific targeting of the PPI dendrimer (G5) complexed to superparamagnetic iron oxide nanoparticles and siRNA [72]. Superparamagnetic iron oxide nanoparticles have been widely studied as MRI contrast agents. Their integration into this therapeutic system was intended to allow MRI visualization of disease progression and therapeutic responses. This targeted delivery system enhanced the anticancer efficacy of the drug cisplatin by suppressing the antiapoptotic defense by siRNA targeted to *BCL2* mRNA in mice bearing

lung cancer xenografts. A result of this treatment was a tumor volume decrease by 75% in comparison with controls [72].

Dufès and colleagues have demonstrated that the intravenous administration of PPI (G3) complexed to plasmid DNA encoding TNF-α under the control of a tumor-specific promoter resulted in the regression of subcutaneous A431 epidermoid carcinomas and a survival rate of 100% in mice [73,74]. This treatment appeared to be well tolerated, as there was no weight loss compared with controls.

More recently, Dufès and colleagues demonstrated that a Tf-bearing PPI dendriplex resulted in gene expression mainly in the tumors after intravenous administration [75]. As a consequence of this improved distribution, the intravenous administration of the Tf-bearing PPI dendriplex encoding TNF-α led to a rapid and sustained tumor regression over 1 month (90% complete response and 10% partial response on A431 human epidermoid tumors). It also resulted in tumor suppression for 60% of PC-3 and 50% of DU145 prostate tumors [76]. In a parallel study by the same group, the Tf-bearing PPI dendriplex encoding p73, a member of the p53 family of transcription factors, led to complete tumor suppression for 10% of A431 and B16F10 tumors and long-term survival of the animals [77]. These treatments were well tolerated by the animals, demonstrating that Tf-bearing PPI is a promising delivery system for cancer therapy.

Conclusion & future perspective

Dendrimer-based delivery systems have been demonstrated to be highly promising carriers of therapeutic genes and drugs to the brain and cancer cells. Until recently, the full exploitation of this approach was hampered due to specific delivery and safety issues. This problem is now being overcome with the use of targeted strategies allowing intravenous delivery of these nanomedicines. Moreover, intensive study of the dendrimers has provided critical technological advances that will benefit the design of 'next-generation' dendrimers. Dendritic nanotechnology enables the synthesis of well-defined, globular structures incorporating specific chemical groups tailored for increasing the safe and effective delivery of a nucleic acid or a drug to its site of action in a controlled way. For example, the further development of dendrimers with environmentally sensitive linkages should improve the drug release from the dendrimer. Moreover, the exploitation of new targeting strategies should optimize the delivery of nucleic acids and drugs to the brain or tumors, and

Executive summary

Rationale for using dendrimers for brain delivery & cancer therapy

- The use of promising novel therapeutics is limited by their inability to specifically reach the brain and tumors after intravenous administration, resulting in toxicity to healthy tissues.
- Dendrimers are emerging as potential nonviral vectors for efficiently delivering drugs and nucleic acids to the brain and cancer cells.
- Dendrimers are well-defined, globular structures incorporating specific chemical groups that are tailored for increasing the safe and effective delivery of a nucleic acid or a drug to its site of action in a controlled way.
- Bioactive agents can be entrapped within the dendrimer structure or conjugated or complexed to the dendrimer surface, which allows for precise tailoring of the properties of the carriers to the specific needs of their cargos in terms of solubility, protection against degradation, release and delivery to the site of action.

Applications of dendrimers for brain delivery

- Dendrimers can deliver drugs and nucleic acids to the brain by exploiting the specific transport systems expressed on the blood–brain barrier.
- Various dendrimers targeting the transferrin receptor, the low-density lipoprotein receptor-related proteins, the glucose transporter GLUT-1 and the leptin receptors have been developed.
- Brain uptake of drugs and nucleic acids carried by targeted dendrimers was increased compared with nontargeted dendrimers.

Applications of dendrimers for cancer therapy

- Dendrimers can either noncovalently encapsulate anticancer drugs in the void spaces within the dendritic structure or carry them via covalent conjugation to the surface groups. A wide range of anticancer drugs have been studied as dendrimer cargos.
- The water solubility and therapeutic efficacy against tumors have been enhanced for anticancer drugs carried by dendrimers.
- Dendrimers have been used for the delivery of siRNA and plasmid DNA alone or associated with anticancer drugs to tumors following intratumoral or intravenous administration.
- Tumor regression has been obtained following intravenous administration of therapeutic nucleic acids carried by targeted dendrimers.

therefore improve their therapeutic efficacy. In addition, bioactive agents can be entrapped within the dendrimer structure or conjugated or complexed to the dendrimer surface, which allows for precise tailoring of the properties of the carriers to the specific needs of their cargos in terms of solubility, protection against degradation, release and delivery to the site of action. More generally, dendrimers are likely to be used in therapeutic strategies combining targeting, imaging, diagnostics and therapy due to their multifunctional architecture. Clinical trials using dendrimers in cancer therapy are still pending, but dendrimers have already been successfully introduced in the clinic as antiviral agents. Continued research in this area should therefore enable the preparation of highly specific, highly efficacious dendrimer-based nanomedicines for the treatment of cancer and brain diseases in the clinic.

Financial & competing interests disclosure

The work in this laboratory is currently supported by grants from the Medical Research Council, the Cunningham Trust and the University of Strathclyde. S Somani is funded by the Cunningham Trust. The authors have no other relevant affiliations or financial involvement with any organization or entity with a financial interest in or financial conflict with the subject matter or materials discussed in the manuscript apart from those disclosed.

No writing assistance was utilized in the production of this manuscript.

References

Papers of special note have been highlighted as:
** of considerable interest.

1 Pardridge WM. The blood–brain barrier: bottleneck in brain drug development. *NeuroRx* 2(1), 3–14 (2005).

2 Pardridge WM. Blood–brain barrier delivery. *Drug Discov. Today* 12(1–2), 54–61 (2007).

3 WHO. Cancer, Fact sheet no 297 (2014). www.who.int/mediacentre/factsheets/fs297/en/

4 Tomalia DA, Baker H, Dewald J *et al.* A new class of polymers: starburst–dendritic macromolecules. *Polym. J.* 17, 117–132 (1985).

** **One of the first publications regarding dendrimers by the pioneers in the field.**

5 Menjoge AR, Kannan RM, Tomalia DA. Dendrimer-based drug and imaging conjugates: design considerations for nanomedical applications. *Drug Discov. Today* 15(5–6), 171–185 (2010).

6 Buhleier E, Wehner W, Vögtle F. 'Cascade' and 'nonskid-chain-like' syntheses of molecular cavity topologies. *Synthesis* 2, 155–158 (1978).

** **One of the first publications regarding dendrimers by the pioneers in the field.**

7 Tomalia DA, Baker H, Dewald J *et al.* Dendritic macromolecules – synthesis of starburst dendrimers. *Macromolecules* 19, 2466–2468 (1986).

8 Newkome GR, Yao ZQ, Baker GR, Gupta VK. Micelles. Part 1. Cascade molecules – a new approach to micelles – a [27]-arborol. *J. Org. Chem.* 50, 2003–2004 (1985).

** **One of the first publications regarding dendrimers by the pioneers in the field.**

9 Newkome GR, Yao ZQ, Baker GR, Gupta VK, Russo PS, Saunders MJ. Cascade molecules. Part 2. Synthesis and characterization of a benzene [9]3-arborol. *J. Am. Chem. Soc.* 108, 849–850 (1986).

10 Esfand R, Tomalia DA. Poly (amidoamine) (PAMAM) dendrimers: from biomimicry to drug delivery and biomedical applications. *Drug Discov. Today* 6(8), 427–436 (2001).

11 Hawker CJ, Fréchet JMJ. Preparation of polymers with controlled molecular architecture – a new convergent approach to dendritic macromolecules. *J. Am. Chem. Soc.* 112, 7638–7647 (1990).

12 Liu M, Fréchet JMJ. Designing dendrimers for drug delivery. *Pharm. Sci. Technol. Today* 2(10), 393–401 (1999).

13 Mintzer MA, Grinstaff MW. Biomedical applications of dendrimers: a tutorial. *Chem. Soc. Rev.* 40(1), 173–190 (2011).

14 Xu L, Zhang H, Wu Y. Dendrimer advances for the central nervous system delivery of therapeutics. *ACS Chem. Neurosci.* 5(1), 2–13 (2014).

15 Wolinsky JB, Grinstaff MW. Therapeutic and diagnostic applications of dendrimers for cancer treatment. *Adv. Drug Deliv. Rev.* 60(9), 1037–1055 (2008).

16 Abbott NJ, Romero IA. Transporting therapeutics across the blood–brain barrier. *Mol. Med. Today* 2, 106–113 (1996).

17 Stewart PA. Endothelial vesicles in the blood–brain barrier: are they related to permeability? *Cell. Mol. Neurobiol.* 20, 149–163 (2000).

18 Abbott, NJ. Physiology of the blood–brain barrier and its consequences for drug transport to the brain. *Int. Congr. Ser.* 1277, 3–18 (2005).

19 Persidsky Y, Ramirez SH, Haorah J, Kanmogne GD. Blood–brain barrier: structural components and function under physiologic and pathologic conditions. *J. Neuroimmune Pharmacol.* 1, 223–236 (2006).

20 Abbott NJ, Rönnbäck L, Hansson E. Astrocyte–endothelial interactions at the blood–brain barrier. *Nat. Rev. Neurosci.* 7, 41–53 (2006).

21 Jefferies WA, Brandon MR, Hunt SV, Williams AF, Gatter KC, Mason DY. Transferrin receptor on endothelium of brain capillaries. *Nature* 312, 162–163 (1984).

22 Dufès C, Al Robaian M, Somani S. Transferrin and the transferrin receptor for the targeted delivery of therapeutic agents to the brain and cancer cells, *Ther. Deliv.* 4, 629–640 (2013).

23 Huang RQ, Qu YH, Ke WL, Zhu JH, Pei YY, Jiang C. Efficient gene delivery targeted to the brain using

a transferrin-conjugated polyethyleneglycol-modified polyamidoamine dendrimer. *FASEB J.* 21, 1117–1125 (2007).

•• **Demonstrates that the transferrin-bearing PEGylated polyamidoamide dendriplex can cross the blood–brain barrier following intravenous administration.**

24 Fisher D, Kissel T. Histochemical characterization of primary capillary endothelial cells from porcine brains using monoclonal antibodies and fluorescein isothiocyanate-labelled lectins: implications for drug delivery. *Eur. J. Pharm. Biopharm.* 52, 1–11 (2001).

25 Mo Y, Lim, L. Paclitaxel-loaded PLGA nanoparticles: potentiation of anticancer activity by surface conjugation. *J. Control. Release* 108, 244–262 (2005).

26 He H, Li Y, Jia XR *et al.* PEGylated poly(amidoamine) dendrimer-based dual-targeting carrier for treating brain tumors. *Biomaterials* 32(2), 478–487 (2011).

27 Cerveny L, Pavek P, Malakova J, Staud F, Fendrich Z. Lack of interactions between breast cancer resistance protein (BCRP/ABCG2) and selected antiepileptic agents. *Epilepsia* 47(3), 461–468 (2006).

28 Tian W, Ying X, Du J *et al.* Enhanced efficacy of functionalized epirubicin liposomes in treating brain glioma-bearing rats. *Eur. J. Pharm. Sci.* 41(2), 232–243 (2010).

29 Ferretti C, Blengio M, Ghi P, Racca S, Genazzani E, Portaleone P. Tamoxifen counteracts estradiol induced effects on striatal and hypophyseal dopamine receptors. *Life Sci.* 42(24), 2457–2465 (1988).

30 Kayyali R, Marriott C, Wiseman H. Tamoxifen decreases drug efflux from liposomes: relevance to its ability to reverse multidrug resistance in cancer cells? *FEBS Lett.* 344(2–3), 221–224 (1994).

31 Li Y, He H, Jia X, Lu WL, Lou J, Wei Y. A dual-targeting nanocarrier based on poly(amidoamine) dendrimers conjugated with transferrin and tamoxifen for treating brain gliomas. *Biomaterials* 33(15), 3899–3908 (2012).

32 Kabanov VA, Zezin AB, Rogacheva VB *et al.* Polyelectrolyte behavior of astramol poly(propyleneimine) dendrimers. *Macromolecules* 31(15), 5142–5144 (1998).

33 Somani S, Blatchford DR, Millington O, Stevenson ML, Dufès C. Transferrin-bearing polypropylenimine dendrimer for targeted gene delivery to the brain. *J. Control. Release* 188, 78–86 (2014).

•• **Demonstrates that the intravenous injection of the transferrin-bearing polypropylenimine dendriplex more than doubled the gene expression in the brain compared with the unmodified dendriplex while decreasing nonspecific gene expression in the lung.**

34 Herz J, Strickland DK. LRP: a multifunctional scavenger and signaling receptor. *J. Clin. Invest.* 108(6), 779–784 (2001).

35 Fillebeen C, Descamps L, Dehouck MP *et al.* Receptor-mediated transcytosis of lactoferrin through the blood–brain barrier. *J. Biol. Chem.* 274(11), 7011–7017 (1999).

36 Huang R, Ke W, Liu Y, Jiang C, Pei Y. The use of lactoferrin as a ligand for targeting the polyamidoamine-based gene delivery system to the brain. *Biomaterials* 29(2), 238–246 (2008).

37 Huang R, Ke W, Han L *et al.* Brain-targeting mechanisms of lactoferrin-modified DNA-loaded nanoparticles. *J. Cereb. Blood Flow Metab.* 29(12), 1914–1923 (2009).

38 Demeule M, Currie JC, Bertrand Y *et al.* Involvement of the low-density lipoprotein receptor-related protein in the transcytosis of the brain delivery vector angiopep-2. *J. Neurochem.* 106(4), 1534–1544 (2008).

39 Ke W, Shao K, Huang R *et al.* Gene delivery targeted to the brain using an angiopep-conjugated polyethyleneglycol-modified polyamidoamine dendrimer. *Biomaterials* 30(36), 6976–6985 (2009).

40 Huang R, Ma H, Guo Y *et al.* Angiopep-conjugated nanoparticles for targeted long-term gene therapy of Parkinson's disease. *Pharm. Res.* 30(10), 2549–2559 (2013).

41 Pardridge WM, Boado RJ, Farrell CR. Brain-type glucose transporter (GLUT-1) is selectively localized to the blood–brain barrier. studies with quantitative western blotting and *in situ* hybridization. *J. Biol. Chem.* 265(29), 18035–18040 (1990).

42 Dhanikula RS, Argaw A, Bouchard JF, Hildgen P. Methotrexate loaded polyether–copolyester dendrimers for the treatment of gliomas: enhanced efficacy and intratumoral transport capability. *Mol. Pharm.* 5(1), 105–116 (2008).

43 Golden PL, MacCagnan TJ, Pardridge WM. Human blood–brain barrier leptin receptor. binding and endocytosis in isolated human brain microvessels. *J. Clin. Invest.* 99(1), 14–18 (1997).

44 Barrett GL, Trieu J, Naim T. The identification of leptin-derived peptides that are taken up by the brain. *Regul. Pept.* 155(1–3), 55–61 (2009).

45 Liu Y, Li J, Shao K *et al.* A leptin derived 30-amino-acid peptide modified pegylated poly-L-lysine dendrigraft for brain targeted gene delivery. *Biomaterials* 31(19), 5246–5257 (2010).

46 Han L, Zhang A, Wang H, Pu P, Kang C, Chang J. Construction of novel brain-targeting gene delivery system by natural magnetic nanoparticles. *J Appl. Polym. Sci.* 121, 3446–3454 (2011).

47 Kawabata H, Germain RS, Vuong PT, Nakamaki T, Said JW, Koeffler HP. Transferrin receptor 2-alpha supports cell growth in iron-chelated cultured cells and *in vivo*. *J. Biol. Chem.* 275(22), 16618–16625 (2000).

48 Prior R, Reifenberger G, Wechsler W. Transferrin receptor expression in tumours of the human nervous system: relation to tumour type, grading and tumour growth fraction. *Virchows Arch. A Pathol Anat. Histopathol.* 416(6), 491–496 (1990).

49 Maeda H, Matsumura Y. A new concept in macromolecular therapeutics in cancer chemotherapy: mechanism of tumoritropic accumulation of proteins and the antitumor agent SMANCS. *Cancer Res.* 46(12 Pt 1), 6387–9392 (1986).

50 Morgan MT, Carnahan MA, Finkelstein S *et al.* Dendritic supramolecular assemblies for drug delivery. *Chem. Commun.* 34(14), 4309–4311 (2005).

51 Morgan MT, Nakanishi Y, Kroll DJ *et al.* Dendrimer-encapsulated camptothecins: increased solubility, cellular uptake, and cellular retention affords enhanced anticancer activity *in vitro*. *Cancer Res.* 66(24), 11913–11921 (2006).

52 Malik N, Evagorou EG, Duncan R. Dendrimer–platinate: a novel approach to cancer chemotherapy. *Anticancer Drugs* 10(8), 767–776 (1999).

** **Demonstrates that the conjugation of cisplatin to the polyamidoamide dendrimer results in increased water solubility and slower release of the drug. The intravenous administration of the conjugate to mice bearing subcutaneous B16F10 tumors led to selective accumulation in tumors and antitumor efficacy.**

53 Kojima C, Kono K, Maruyama K, Takagishi T. Synthesis of polyamidoamine dendrimers having poly(ethylene glycol) grafts and their ability to encapsulate anticancer drugs. *Bioconjug. Chem.* 11(6), 910–917 (2000).

54 Papagiannaros A, Dimas K, Papaioannou GT, Demetzos C. Doxorubicin–PAMAM dendrimer complex attached to liposomes: cytotoxic studies against human cancer cell lines. *Int. J. Pharm.* 302(1–2), 29–38 (2005).

55 Wang F, Bronich TK, Kabanov AV, Rauh RD, Roovers J. Synthesis and evaluation of a star amphiphilic block copolymer from poly(epsilon-caprolactone) and poly(ethylene glycol) as a potential drug delivery carrier. *Bioconjug. Chem.* 16(2), 397–405 (2005).

56 Bhadra D, Bhadra S, Jain S, Jain NK. A PEGylated dendritic nanoparticulate carrier of fluorouracil. *Int. J. Pharm.* 257(1–2), 111–124 (2003).

57 Neerman MF, Chen HT, Parrish AR, Simanek EE. Reduction of drug toxicity using dendrimers based on melamine. *Mol. Pharm.* 1(5), 390–393 (2004).

58 Wu G, Barth RF, Yang WL, Kawabata S, Zhang LW, Green-Church K. Targeted delivery of methotrexate to epidermal growth factor receptor-positive brain tumors by means of cetuximab (IMC-C225) dendrimer bioconjugates. *Mol. Cancer Ther.* 5(1), 52–59 (2006).

59 Ooya T, Lee J, Park K. Hydrotropic dendrimers of generations 4 and 5: synthesis, characterization, and hydrotropic solubilization of paclitaxel. *Bioconjug. Chem.* 15(6), 1221–1229 (2004).

60 Duncan R, Malik N. Dendrimers: biocompatibility and potential for delivery of anticancer agents. *Proc. Int. Symp. Control. Release Bioact. Mater.* 23, 105–106 (1996).

61 Lee CC, Gillies ER, Fox ME *et al.* A single dose of doxorubicin-functionalized bow-tie dendrimer cures mice bearing C-26 colon carcinomas. *Proc. Natl Acad. Sci. USA* 103(45), 16649–16654 (2006).

62 Thomas TP, Majoros IJ, Kotlyar A *et al.* Targeting and inhibition of cell growth by an engineered dendritic nanodevice. *J. Med. Chem.* 48(11), 3729–3735 (2005).

63 Maruyama-Tabata H, Harada Y, Matsumura T *et al.* Effective suicide gene therapy *in vivo* by EBV-based plasmid vector coupled with polyamidoamine dendrimer. *Gene Ther.* 7(1), 53–60 (2000).

64 Sato N, Kobayashi H, Saga T *et al.* Tumor targeting and imaging of intraperitoneal tumors by use of antisense oligo-DNA complexed with dendrimers and/or avidin in mice. *Clin. Cancer Res.* 7(11), 3606–3612 (2001).

65 Bai CZ, Choi S, Nam K, An S, Park JS. Arginine modified PAMAM dendrimer for interferon beta gene delivery to malignant glioma. *Int. J. Pharm.* 445(1–2), 79–87 (2013).

66 Shen XC, Zhou J, Liu X *et al.* Importance of size-to-charge ratio in construction of stable and uniform nanoscale RNA/dendrimer complexes. *Org. Biomol. Chem.* 5, 3674–3681 (2007).

67 Liu X, Liu C, Laurini E *et al.* Efficient delivery of sticky siRNA and potent gene silencing in a prostate cancer model using a generation 5 triethanolamine-core PAMAM dendrimer. *Mol. Pharm.* 9(3), 470–481 (2012).

68 Han L, Huang R, Li J, Liu S, Huang S, Jiang C. Plasmid pORF-hTRAIL and doxorubicin co-delivery targeting to tumor using peptide-conjugated polyamidoamine dendrimer. *Biomaterials* 32(4), 1242–1252 (2011).

69 Huang S, Li J, Han L *et al.* Dual targeting effect of Angiopep-2-modified, DNA-loaded nanoparticles for glioma. *Biomaterials* 32(28), 6832–6838 (2011).

70 Han L, Zhang A, Wang H *et al.* Tat-BMPs–PAMAM conjugates enhance therapeutic effect of small interference RNA on U251 glioma cells *in vitro* and *in vivo*. *Hum. Gene Ther.* 21(4), 417–426 (2010).

71 Taratula O, Garbuzenko OB, Kirkpatrick P *et al.* Surface-engineered targeted PPI dendrimer for efficient intracellular and intratumoral siRNA delivery. *J. Control. Release* 140(3), 284–293 (2009).

72 Taratula O, Garbuzenko O, Savla R, Wang YA, He H, Minko T. Multifunctional nanomedicine platform for cancer specific delivery of siRNA by superparamagnetic iron oxide nanoparticles–dendrimer complexes. *Curr. Drug Deliv.* 8(1), 59–69 (2011).

73 Dufès C, Keith WN, Bisland A, Proutski I, Uchegbu IF, Schätzlein AG. Synthetic anticancer gene medicine exploits intrinsic antitumor activity of cationic vector to cure established tumours. *Cancer Res.* 65(18), 8079–8084 (2005).

74 Dufès C, Uchegbu IF, Schätzlein AG. Dendrimers in gene delivery. *Adv. Drug Deliv. Rev.* 57(15), 2177–2202 (2005).

75 Koppu S, Oh YJ, Edrada-Ebel R *et al.* Tumor regression after systemic administration of a novel tumor-targeted gene delivery system carrying a therapeutic plasmid DNA. *J. Control. Release* 143(2), 215–221 (2010).

** **Demonstrates for the first time that the intravenous administration of the transferrin-bearing diaminobutyric polypropylenimine (DAB) dendriplex encoding TNF-α leads to the tumor suppression of 90% of A431 human epidermoid carcinoma tumors in mice.**

76 Al Robaian M, Chiam KY, Blatchford DR, Dufès C. Therapeutic efficacy of intravenously administered transferrin-conjugated dendriplexes on prostate carcinomas. *Nanomedicine* 9(4), 421–434 (2014).

77 Lemarié F, Croft DR, Tate RJ, Ryan KM, Dufès C. Tumor regression following intravenous administration of a tumor-targeted p73 gene delivery system. *Biomaterials* 33(9), 2701–2709 (2012).

Appendix II Conference Abstracts

UKICRS Annual Symposium 2013, University of Reading, Reading, UK, 16 April 2013

Contribution: Oral presentation and Poster presentation

Evaluation of transferrin-targeted dendrimers for gene delivery to the brain

Sukrut Somani, David R. Blatchford, Christine Dufès
University of Strathclyde, Glasgow, UK

Introduction: The treatment of cerebral disorders by gene therapy has been hindered by the presence of the blood-brain barrier that inhibits the entry of therapeutic DNA to the brain and by the lack of gene delivery systems able to efficiently cross this barrier. In order to remediate this problem, we propose to conjugate a highly efficient gene delivery system, polypropylenimine dendrimer, to transferrin, an iron transporter whose receptors are over-expressed on the blood-brain barrier. The objectives of this study are to evaluate the targeting efficacy of this novel transferrin conjugated gene delivery system *in vitro and in vivo*.

Methods: *In vitro* gene transfection efficiency of the transferrin-conjugated polypropylenimine dendrimer was determined on the cultured immortalized brain capillary endothelial cells. The cellular uptake of the transferrin-conjugated polypropylenimine dendrimer carrying plasmid DNA was observed after different durations of treatment by epifluorescence microscopy *in vitro*. After optimization of treatment duration, the same technique was utilized for comparison of transferrin-conjugated polypropylenimine dendrimer carrying plasmid DNA with the non-targeted dendrimer and naked DNA.

Results: Transferrin-conjugated polypropylenimine dendrimer led to an enhanced *in vitro* transfection efficiency 1.2 times higher compared to non-targeted dendrimer. The cellular uptake of the transferrin-conjugated dendrimer carrying plasmid DNA reached its maximum after 120 minutes. Transferrin-conjugated dendrimer carrying plasmid DNA exhibited a higher cellular uptake compared to non-targeted dendrimer and naked DNA.

Conclusion: Transferrin conjugated polypropylenimine dendrimer showed an improved DNA uptake by brain capillary endothelial cells *in vitro*. This delivery system is therefore promising and should be further investigated.

Nanomedicine 2014 Conference, Heriot-Watt University, Edinburgh, UK
26- 27 March 2014

Contribution: Poster presentation

Transferrin-bearing dendrimer for targeted gene delivery to the brain

Sukrut Somani, David R. Blatchford, Owain Millington, Christine Dufès
University of Strathclyde, Glasgow, UK

The possibility of using genes as medicines to treat brain disorders is currently limited by the lack of safe and efficacious delivery systems able to cross the blood-brain barrier, thus resulting in a failure to reach the brain after intravenous administration.
On the basis that iron can effectively reach the brain by using transferrin receptors for crossing the blood-brain barrier, we propose to investigate if a transferrin-bearing generation 3- polypropylenimine dendrimer would allow the transport of plasmid DNA to the brain after intravenous administration.
In vitro, the conjugation of transferrin to the polypropylenimine dendrimer increased the DNA uptake by bEnd.3 murine brain endothelioma cells overexpressing transferrin receptors, by about 1.4-fold and 2.3-fold compared to that observed with the non-targeted dendriplex and naked DNA.
In vivo, the intravenous injection of transferrin-bearing dendriplex more than doubled the gene expression in the brain compared to the unmodified dendriplex, while decreasing the non-specific gene expression in the liver, the lung and the spleen.
These results suggest that transferrin-bearing polypropylenimine dendrimer is a highly promising gene delivery system to the brain.

10th International Symposium on Polymer Therapeutics: From Laboratory to Clinical Practice, Centro de Investigación Príncipe Felipe Valencia, Spain, 19- 21 May 2014

Contribution: Oral presentation and Poster presentation

EVALUATION OF TRANSFERRIN-BEARING DENDRIMER FOR TARGETED GENE DELIVERY TO THE BRAIN

Sukrut Somani, David R. Blatchford, Owain Millington, Christine Dufès
University of Strathclyde, 161 Cathedral street, Glasgow, G4 0RE, UK

INTRODUCTION:

The treatment of central nervous system disorders by gene therapy has been hindered by the presence of the blood-brain barrier that inhibits the entry of therapeutic DNA to the brain and by the lack of gene delivery systems able to efficiently cross this barrier. In order to remediate this problem, we propose to conjugate a highly efficient gene delivery system, diaminobutyric polypropylenimine (DAB) dendrimer, to transferrin (Tf), an iron transporter whose receptors are over-expressed on the blood-brain barrier. This novel gene delivery system has previously demonstrated its gene delivery efficacy in cancers over-expressing transferrin receptors[1,2]. The objectives of this study are to evaluate the targeting efficacy of this novel transferrin-bearing gene delivery system (DAB-Tf) *in vitro* and *in vivo*.

RESULTS AND DISCUSSION

In vitro, the uptake of the fluorescently-labelled DNA, alone or complexed to DAB-Tf or DAB, by bEnd.3 murine brain capillary endothelial cells over-expressing transferrin receptors, was visualized by epifluorescence microscopy and quantified by flow cytometry. *In vitro,* the conjugation of transferrin to the polypropylenimine dendrimer increased the DNA uptake by bEnd.3 cells, by about 1.4-fold and 2.3-fold compared to that observed with the non-targeted dendriplex and naked DNA. *In vivo,* the gene expression in the brain and major organs after intravenous treatment with DAB-Tf-DNA, DAB-DNA and naked DNA, was visualized by bioluminescence imaging and quantified by a β-galactosidase reporter gene expression assay[3]. *In vivo,* the intravenous injection of transferrin-bearing dendriplex more than doubled the gene expression in the brain compared to the unmodified dendriplex, while decreasing the non-specific gene expression in the liver, the lung and the spleen. Gene expression was at least 3-fold higher in the brain than in any tested peripheral organs and was at its highest 24h following the injection of the treatments. These results suggest that transferrin-bearing polypropylenimine dendrimer is a highly promising gene delivery system to the brain.

REFERENCES

1. Koppu, S. *et al*. (2010). Tumor regression after systemic administration of a novel tumor-targeted gene delivery system carrying a therapeutic plasmid DNA. *Journal of Controlled Release, 143*(2), 215–21

2. Al Robaian, M. *et al*. (2013) Therapeutic efficacy of intravenously administered transferrin-conjugated dendriplexes encoding TNF-α, TRAIL and interleukin-12 on prostate carcinomas.Nanomedicine **(**In Press)
3. Zinselmeyer, B. H. *et al*. (2003). Quantification of β-galactosidase activity after non-viral transfection *in vivo*. *Journal of Controlled Release,* 91, 201-208

41st Annual Meeting & Exposition of the Controlled Release Society, in Chicago, Illinois, U.S.A, 13- 16 July, 2014

Contribution: Poster presentation

Transferrin-bearing Polypropylenimine Dendrimer for Targeted Gene Delivery to the Brain

S. Somani, D. Blatchford, G. Robb, O. Millington and C. Dufès

University of Strathclyde, Glasgow, G4 0RE, United Kingdom
sukrut.somani@strath.ac.uk

ABSTRACT SUMMARY

The possibility of using genes as medicines to treat brain diseases is currently limited by the lack of safe and efficacious delivery systems able to cross the blood-brain barrier, thus resulting in a failure to reach the brain after intravenous administration.

On the basis that iron can effectively reach the brain by using transferrin receptors for crossing the blood-brain barrier, we propose to investigate if a transferrin-bearing generation 3-polypropylenimine dendrimer (1) would allow the transport of plasmid DNA to the brain after intravenous administration.

In vivo, the intravenous injection of transferrin-bearing DAB-DNA more than doubled the gene expression in the brain compared to the unmodified DAB-DNA.

This gene delivery system can be further investigated for the treatment of the central nervous system disorders in future.

INTRODUCTION

The treatment of central nervous system (CNS) disorders by gene therapy has been hindered by the presence of the blood-brain barrier (BBB) that inhibits the entry of therapeutic DNA to the brain and by the lack of safe gene delivery systems able to efficiently cross this barrier. As transferrin (Tf) receptors are widely expressed on the BBB, they can be exploited for the delivery of therapeutics to the brain, via receptor-mediated transcytosis. We propose to conjugate a highly efficient gene delivery system, polypropylenimine dendrimer (DAB), to Tf for targeted gene delivery to the brain following intravenous administration. The objectives of this study are to evaluate the brain targeting efficacy of this novel transferrin-conjugated gene delivery system *in vitro* and *in vivo*.

EXPERIMENTAL METHODS

In vitro, the uptake of the fluorescently-labeled DNA, alone or complexed to DAB-Tf or DAB, by bEnd.3 murine brain capillary endothelial cells, was visualized by epifluorescence microscopy and quantified by fluorescence-activated cell sorting (FACS).

In vivo, the gene expression in the brain and major organs after intravenous treatment with DAB-Tf-DNA, DAB-DNA and naked DNA, was visualized by bioluminescence imaging and quantified by a β-galactosidase reporter gene expression assay (2).

RESULTS AND DISCUSSION

In vitro, the cellular uptake after the treatment with DAB-Tf-DNA resulted in a pronounced DNA uptake in the cytoplasm of bEnd.3 cells. By contrast, cells treated with DAB-DNA or naked DNA did not show any DNA uptake (Figure 1), highlighting the need of a receptor-specific delivery system to carry the DNA inside the cells.

In vivo, the distribution of gene expression following intravenous injection of DAB-Tf-DNA encoding luciferase was first qualitatively assessed by luminescence imaging, at various treatment durations. Gene expression appeared to be mainly located in the brain of the mice. The highest gene expression level was found 24 h following injection of the treatment.

Gene expression following administration of DAB-Tf-DNA was then compared to that observed following administration of DAB-DNA and naked DNA, 24h after administration of the treatments. The level of gene expression in the brain appeared to be highest following treatment with DAB-Tf-DNA (Figure 2).

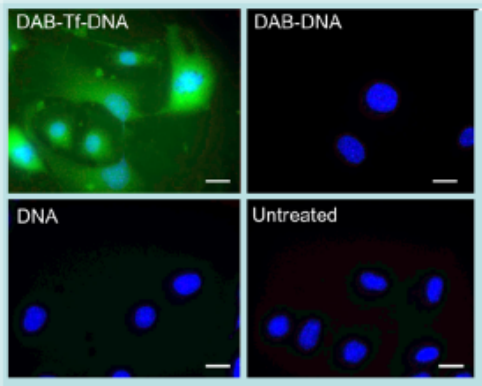

Figure 1. Epifluorescence microscopy imaging of the cellular uptake of Cy3- labeled DNA (2.5 µg/ well) either complexed with DAB-Tf, DAB or in solution, after incubation for 2 hours with bEnd.3 cells (Blue: nuclei stained with DAPI (excitation: 405 nm, laser line bandwidth: 415-491nm), green: Cy3-labeled DNA (excitation: 543 nm, laser line bandwidth: 550-620 nm) (Bar: 10 µm).

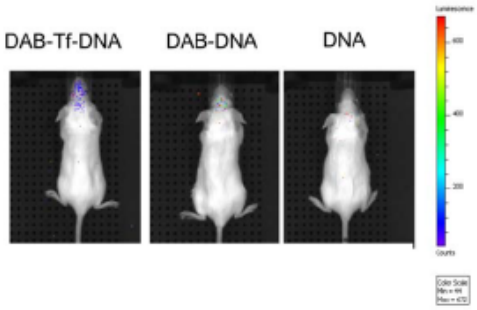

Figure 2. Bioluminescence imaging of gene expression after intravenous administration of DAB-Tf-DNA and DAB-DNA (50 µg DNA administered). (Controls: DNA solution, untreated cells). The mice were imaged using the IVIS Spectrum 24h after injection of the treatments. The scale indicates surface radiance (photons/s/cm^2/steradian).

The conjugation of Tf to DAB significantly increased by more than 2-fold the gene expression in the brain (37.3 ± 4.2 mU β-galactosidase for DAB-Tf-DNA), while there was no β-galactosidase detected in the liver, the lung and the spleen. In the kidneys and the heart, gene expression reached a similar level to that was observed following treatment with DAB-DNA (10.5 ± 6.1 mU and 12.1 ± 3.6 mU β-galactosidase per organ in the kidneys for respectively DAB-Tf-DNA and DAB-DNA, 2.5 ± 1.6 mU and 0.9 ± 1.6 mU β-galactosidase in the heart for respectively DAB-Tf-DNA and DAB-DNA).

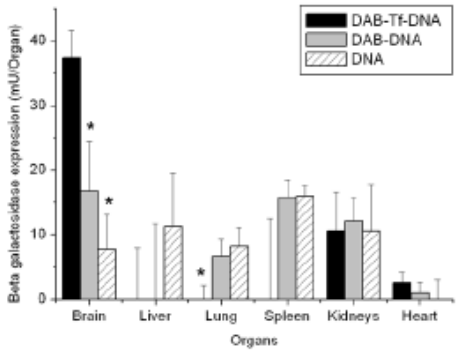

Figure 3. Biodistribution of gene expression after a single intravenous administration of DAB-Tf-DNA and DAB-DNA (50 µg DNA administered). Results were expressed as milliunits β-galactosidase per organ (n=5). * : P <0.05 : highest gene expression treatment vs. other treatments for each organ.

CONCLUSION

The intravenous administration of transferrin-conjugated polypropylenimine dendrimer DAB-Tf resulted in a 2-fold increase of gene expression in the brain compared to non-targeted dendrimer. This delivery system is therefore promising and should be further investigated for the treatment of CNS disorders by gene therapy.

REFERENCES

1. Koppu, S.; Oh, Y.J.; Edrada-Ebel, R.; Blatchford, D. R.; Tetley, L.; Tate, R. J.; Dufès, C. *J. Control. Release* **2010,** 143, 215-221.
2. Zinselmeyer, B. H.; Beggbie, N.; Uchegbu, I. F.; Schätzein, A. G. *J. Control. Release* **2003,** 91, 201-208.

ACKNOWLEDGEMENTS

This research project was funded by The Cunningham Trust.

42nd Annual Meeting & Exposition of the Controlled Release Society, in Edinburgh, U.K, 13- 16 July, 2014

Contribution: Oral presentation and Poster presentation

Lactoferrin-bearing Polypropylenimine Dendrimer for Targeted Gene Delivery to the Brain

S. Somani, G. Robb, B. Pickard and C. Dufès

University of Strathclyde, Glasgow, G4 0RE, United Kingdom
sukrut.somani@strath.ac.uk

ABSTRACT SUMMARY

The possibility of using genes as medicines to treat brain diseases is currently limited by the lack of safe and efficacious delivery systems able to cross the blood-brain barrier, thus resulting in a failure to reach the brain after intravenous administration.

Lactoferrin is a single chain iron-binding glycoprotein belonging to the transferrin family. Lactoferrin receptors are widely expressed in the brain and lactoferrin receptor mediated transcytosis in the brain has been demonstrated[1,2]. We propose to investigate whether lactoferrin-bearing generation 3-polypropylenimine dendrimer would allow the transport of plasmid DNA to the brain after intravenous administration.

In vivo, the intravenous injection of lactoferrin-bearing DAB-DNA led to a 7-fold increase in the gene expression in the brain compared to the unmodified DAB-DNA.

This gene delivery system can be further investigated for the treatment of the central nervous system disorders in future.

INTRODUCTION

The treatment of central nervous system (CNS) disorders by gene therapy has been hindered by the presence of the blood-brain barrier (BBB) that inhibits the entry of therapeutic DNA to the brain and by the lack of safe gene delivery systems able to efficiently cross this barrier. Intracerebral injection is the most frequently used method to transfer exogenous genes in the brain. However, it is highly invasive and is unable to deliver genes to the global areas of the brain. Various receptors are located on the luminal side of the blood-brain barrier (BBB). Receptor mediated transcytosis can be one of the options for efficient transfer of exogenous gene across the BBB after intravenous injection. As lactoferrin (Lf) receptors are widely expressed on the BBB, they can be exploited for the delivery of therapeutics to the brain, via receptor-mediated transcytosis. We propose to conjugate a highly efficient gene delivery system, polypropylenimine dendrimer (DAB), to Lf for targeted gene delivery to the brain following intravenous administration. The objectives of this study are to evaluate the brain-targeting efficacy of this novel lactoferrin-conjugated gene delivery system *in vitro* and *in vivo*.

EXPERIMENTAL METHODS

In vitro, the uptake of the fluorescently labeled DNA, alone or complexed to DAB-Lf or DAB, by bEnd.3 murine brain capillary endothelial cells, was visualized by epifluorescence microscopy and quantified by fluorescence-activated cell sorting (FACS).

In vivo, the gene expression in the brain and major organs after intravenous treatment with DAB-Lf-DNA, DAB-DNA and naked DNA, was visualized by bioluminescence imaging and quantified by a β-galactosidase reporter gene expression assay.

RESULTS AND DISCUSSION

In vitro, the cellular uptake after treatment with DAB-Lf-DNA resulted in a pronounced DNA uptake in the cytoplasm of bEnd.3 cells. By contrast, cells treated with DAB-DNA or naked DNA did not show any DNA uptake (Figure 1), highlighting the need of a receptor-specific delivery system to carry the DNA inside the cells.

In vivo, the distribution of gene expression following intravenous injection of DAB-Lf-DNA encoding luciferase was first qualitatively assessed by luminescence imaging. Gene expression following administration of DAB-Lf-DNA was compared to that observed following administration of DAB-DNA and naked DNA,

24h after administration of the treatments. The level of gene expression in the brain appeared to be highest following treatment with DAB-Lf-DNA (Figure 2).

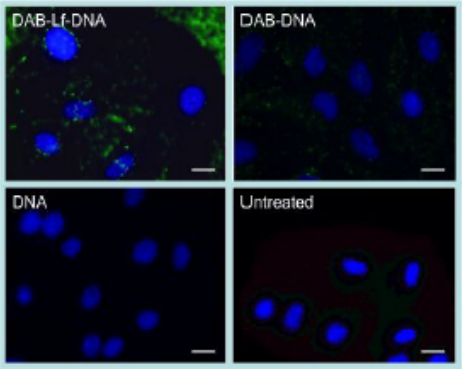

Figure 1. Epifluorescence microscopy imaging of the cellular uptake of Fluorescein- labeled DNA (2.5 µg/well) either complexed with DAB-Lf, DAB or in solution, after incubation for 2 hours with bEnd.3 cells (Blue: nuclei stained with DAPI (excitation: 405 nm, laser line bandwidth: 415-491nm), green: Fluorescein-labeled DNA (excitation: 543 nm, laser line bandwidth: 550-620 nm) (Bar: 10 µm).

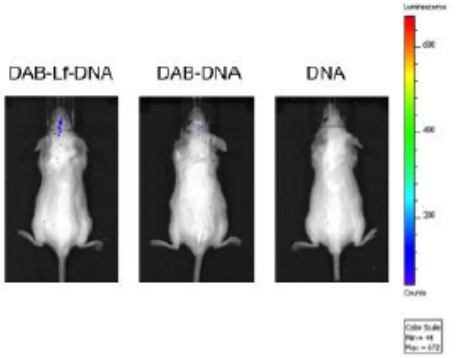

Figure 2. Bioluminescence imaging of gene expression after intravenous administration of DAB-Lf-DNA and DAB-DNA (50 µg DNA administered). (Controls: DNA solution,). The mice were imaged using the IVIS Spectrum 24h after injection of the treatments. The scale indicates surface radiance (photons/s/cm^2/steradian).

The conjugation of Lf to DAB significantly increased by more than 7-fold the gene expression in the brain (116.16 ± 9.07 mU β-galactosidase for DAB-Lf-DNA), followed by liver (70.97 ± 14.07 mU) and spleen (17.61 ± 15.07 mU), while there was no β-galactosidase detected in the lung and the kidneys. The gene expression in the brain (DAB-Lf-DNA) is also 3-fold higher than transferrin-bearing polypropylenimine dendrimer previously reported by our group[3].

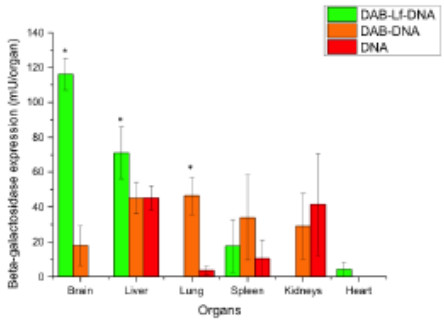

Figure 3. Biodistribution of gene expression after a single intravenous administration of DAB-Lf-DNA and DAB-DNA (50 µg DNA administered). Results were expressed as milliunits β-galactosidase per organ (n=5). * : P ≤0.05 : highest gene expression treatment vs. other treatments for each organ.

CONCLUSION

The intravenous administration of lactoferrin-conjugated polypropylenimine dendrimer DAB-Tf resulted in a 7-fold increase of gene expression in the brain compared to non-targeted dendrimer. This delivery system is therefore promising and should be further investigated for the treatment of CNS disorders by gene therapy.

REFERENCES

1. Huang R, Ke W, Liu Y, Jiang C, Pei Y; *Biomaterials* **2008**, 29, 238-246.
2. Huang R, Ke W, Qu Y, Zhu J, Pei Y, Jiang C; *J. Biomed. Sci* **2007**, 14, 121-128.
3. Somani S, Blatchford DR, Stevenson ML, Millington O, Dufès C; *J. Control. Release* **2014**, 188, 78-86.

Others

- “Best Poster” award at Nanomedicine 2014 conference.
- University of Strathclyde PGR travel award for poster presentation at 41st Controlled Release Society annual meeting, Chicago, US.
- Strathclyde Institute of Pharmacy and Biomedical sciences travel award for oral and poster presentation at 10th International Symposium on Polymer Therapeutics: From Laboratory to Clinical Practice, Centro de Investigación Príncipe Felipe Valencia, Spain.